University of Miskolc
Faculty of Earth Science and Engineering
Department of Hydrogeology and Engineering Geology
Institute of Water Resources and Environmental Management

MIKOVINY SÁMUEL DOCTORAL SCHOOL OF EARTH SCIENCES

Head of the Doctoral School: Prof. Dr. Péter Szűcs

Multi-Scale Simulation for Contaminants Transport in Organic Enriched Water Infiltration Process

Doctoral Thesis

Prepared By:

Abdalkarim S. S. Gharbia

Thesis Supervisors: Dr. Zákányi Balázs, Associate Professor

&

Dr. Tóth Márton, Associate Professor

A PhD Thesis submitted in Partial Fulfilment of Requirements for the Degree of Doctor in Philosophy in the Department of Hydrogeology and Engineering Geology.

MISKOLC – HUNGARY

2024

Dedication

To my dearest father, whose unwavering support and encouragement have been my guiding light throughout this journey. Your wisdom and strength have shaped my path, and I am grateful for your constant belief in me.

To my loving mother, whose boundless love and sacrifices have nurtured my dreams. Your unwavering faith in my abilities has given me the courage to persevere, and I am forever indebted to you.

To my brothers and sisters, your camaraderie and encouragement have been a source of strength and inspiration. Together, we have shared laughter, challenges, and triumphs that have enriched my life.

To my beloved wife, your unwavering faith in me and your steadfast love have been my anchor in times of uncertainty. Your sacrifices and understanding have allowed me to pursue this endeavor wholeheartedly.

To my two precious daughters, you are the heartbeats of my existence. Your innocence and boundless joy remind me of the purpose behind every endeavor. I dedicate this achievement to you, hoping it sets an example of perseverance and determination.

With love and gratitude

Acknowledgement

I am profoundly grateful to my supervisor, Dr. Zákányi Balázs, for his unwavering support and mentorship. His expertise, insightful feedback, and encouragement to explore innovative ideas have shaped my research journey, transforming challenges into growth opportunities.

I extend special gratitude to my co-supervisor, Dr. Tóth Márton, for his exceptional insights, meticulous attention to detail, and steadfast encouragement throughout this endeavor. Your mentorship in lab work and the entirety of my PhD journey has provided a unique and enriching perspective. Your willingness to discuss intricate concepts, offer constructive critique, and share your extensive knowledge has been invaluable.

I would like to express my heartfelt gratitude to Dr. Madarász Tamás and Prof. Dr. Szűcs Péter for their unwavering support and encouragement throughout my study. Their efforts in creating a comfortable and conducive work environment in the lab and study places have been instrumental in fostering my research journey.

I am deeply thankful to Dr. Balázs Kovács, Dr. Tamás Kántor, Dr. Viktória Mikita, Dr. Andrea Tóth, Dr. Rita Miklós, and Dr. Gábor Nyiri for their invaluable support, encouragement, and guidance throughout my study. Their insightful advice, teaching, and assistance have played a significant role in shaping my research journey.

Abdalkarim S. S. Gharbia

Abstract

My doctoral research conducts an in-depth exploration of pollutant removal in soil aquifer treatment (SAT) systems, with a particular focus on understanding the intricate interactions between infiltrated pollutants, soil media, and operational environmental conditions. The study aims to unravel the mechanisms governing pollutant behavior within SAT systems, shedding light on their diverse capabilities for pollutant removal.

Examining the performance of sand and sandy loam soils within SAT systems, reveals significant variations in efficiency and pollutants removal capabilities. Utilizing a multifaceted approach, the analysis incorporates static adsorption behavior through Freundlich and Langmuir isothermal models. Freundlich models indicate that sandy loam has a higher adsorption capacity for specific pollutants, while sand excels in others. The supportive Langmuir models underscore sandy loam's overall superior efficiency in pollutant removal. Dynamic breakthrough curve analysis further emphasizes sand's proficiency in handling certain pollutants, as evidenced by higher area under the curve values, while sandy loam exhibits higher efficiency for different pollutants. Concentration levels in sandy loam generally lower values for NH_4^+, PO_4^{3-}, Cu^{2+}, Mn^{2+}, MoO_4^{2-}, Zn^{2+}, Co^{2+}, and BO_3^{3-} whereas sand exhibits lower concentrations for NO_3^-, NO_2^-, SO_4^{2-}, and Fe^{2+}. These disparities underscore the diverse capabilities of the two soil types in adsorbing and retaining pollutants.

Simultaneously, the infiltration rates meticulously examine at 0.5 mL/min and 10 mL/min, drawing on experimental, modeling, and statistical analyses. Breakthrough curves under these infiltration rates reveal distinct trends for various pollutants. The slower infiltration rate of 0.5 mL/min demonstrates heightened removal efficiency for specific pollutants, attributed to extended contact times fostering enhanced adsorption and biogeochemical reactions. Conversely, the 10 mL/min high infiltration rate excels in removing different pollutants, indicating greater pollutant release and reduced interaction with the sand matrix. Modeling results reinforce these experimental findings, capturing pollutant behavior over time and depth profiles. Statistical analyses, specifically t-tests, robustly compare the two infiltration rate scenarios, underscoring the significance of differences in pollutant removal. Furthermore, the interplay of wetting and drying conditions in a SAT system emerges as a critical determinant of pollutant removal and performance within the sand column. These cycles operate through physical filtration, adsorption, and biological degradation during wet periods and facilitate retention and immobilization during drying periods, significantly influencing pollutant transport, solubility, and sorption capacity. The treatment performance of the sand column displays inherent variability due to these cycles, impacting factors such

as pH, dissolved oxygen levels, and redox conditions. Continuous exposure induces long-term changes in the sand's physical structure, affecting porosity, permeability, and adsorption capacity, all crucial to sustained system performance. Moreover, infiltrated synthetic wastewater with varying concentrations through SAT systems can have profound impacts on pollutant interactions and treatment efficiency. The interplay between pollutants involves competitive sorption, complex formation, redox reactions, microbial activity, and pH fluctuations. Concentration levels influence the competitive nature of pollutant removal mechanisms.

In conclusion, my doctoral research provides a comprehensive understanding of the diverse capabilities of pollutant removal within SAT systems. The nuanced insights into pollutant interactions, infiltration rates, wetting and drying conditions, and pollutant concentration levels emphasize the complexity of designing effective soil aquifer treatment systems.

Table of Contents

List of Tables

List of Figures

List of abbreviations

SAT	Soil aquifer treatment
MAR	Managed aquifer recharge
RBF	Riverbank filtration
ARR	Artificial recharge and recovery
WWTPs	Wastewater treatment plants
PE	Primary effluent
HLR	Hydraulic loading rate
TWW	Treated wastewater
ASR	Aquifer storage and recovery
SOM	Soil organic matter
CEC	Cation exchange capacity
$CH_3COONa.3H_2O$	Sodium acetate
NH_4Cl	Ammonium chloride
KH_2PO_4	Potassium dihydrogen phosphate
$MgSO_4.7H_2O$	Magnesium sulfate heptahydrate
$CaCl_2.2H_2O$	Calcium chloride dihydrate
$NaHCO_3$	Sodium hydrogen carbonate
KCl	Potassium chloride
EDTA	Ethylenediaminetetraacetic acid
$FeCl_3.6H_2O$	Iron chloride hexahydrate
H_3BO_3	Boric acid
$CuSO_4.5H_2O$	Copper sulfate pentahydrate
KI	Potassium iodide
$MnSO_4.4H_2O$	Manganese sulfate tetrahydrate
$(NH_4)6Mo_7O_{24}.4H_2O$	Ammonium molybdate tetrahydrate
$ZnSO_4.7H_2O$	Zinc sulfate heptahydrate
$CoCl_2.6H_2O$	Cobalt chloride hexahydrate
EC	Electrical conductivity
ORP	Oxidation-reduction potential
DO	Dissolved oxygen
NH_4^+	Ammonium
NO_3^-	Nitrate
NO_2^-	Nitrite
PO_4^{3-}	Phosphate
SO_4^{2-}	Sulfate

Fe^{2+}	Iron
Cu^{2+}	Copper
MoO_4^{2-}	Molybdate
Mn^{2+}	Manganese
Zn^{2+}	Zinc
Co^{2+}	Cobalt
BO_3^{3-}	Orthoborate
Mg^{2+}	Magnesium
Ca^{2+}	Calcium
Na^{+}	Sodium
K^{+}	Potassium
MP-AES	Microwave plasma atomic emission spectroscopy
S	Adsorption amount (mg/g)
C_{init}	Initial concentration (mg/L)
C_{eq}	Equilibrium concentration (mg/L)
V	Solution volume (mL)
M	Soil mass (g)
K_F	Freundlich partitioning coefficient (L/Kg)
C	Solution concentration (mg/L)
K_L	Langmuir partitioning coefficient (L/Kg)
N	Affinity degree
ADE	Advection – dispersion equation
Θ	Volumetric water content
V	Advection velocity
D_{ij}	Dispersion cartesian domain
Q_s	Bio-chemical reacting factor per unit area
D_m	Diffusion coefficient
α_L	Longitudinal dispersivities
α_T	Transverse dispersivities
m_{PK}	Particle mass load
P	Total displacement location for random particle
Z	Normal distribution function
K(θ)	Hydraulic conductivity
$C_{dk}(i)$	Dissolved solute mass concentration
N_p	Particle quantities per cell
D_v	Cell volume

M_{sk}	Adsorbed mass
$F^k(i)$	Mass exchange coefficient
P_s	Soil bulk density
N	Porosity
K_d	Adsorption distribution coefficient
FEFLOW	Finite element subsurface flow system
RMS	Root mean square error
Θ_r	Residual water content
αVG	Van-Genuchten factor for vertical unsaturated flow
n_{VG}	Van-Genuchten saturation exponent
AUC	Area under breakthrough curve

1. Introduction

1.1. Background

Global water scarcity seriously challenges human societies (Bdour, 2007). A limited freshwater supply cannot concur with the rapid demand mounting (Wild et al., 2010). Due to extreme weather patterns and water scarcity, various factors play a role, such as groundwater and surface water contamination, unequal distribution of water resources, and frequent droughts (Asano and Cotruvo, 2004). A growing population and urbanization put more pressure on water resources due to the need to produce food (Corcoran, 2010). In addition to urbanization, industrial growth can cause a significant negative impact on surface water by contaminating it with organic compounds (Schmidt and Brauch, 2008). Further, excessive groundwater pumping beyond its natural replenishment rate causes groundwater levels to decline and resources depleted (Abel et al., 2013). As urban water supply coverage expands, the proportion of wastewater requiring collection and treatment will increase, making up 75%-85% of the water supply (Scott et al., 2004). To address these issues, an urgent need exists for artificial water storage solutions with appropriate facilities (Díaz-Cruz and Barceló, 2008). Wastewater can serve as a water resource, significantly reducing the utilization of the natural valuable resources, especially for non-potable reuse (Drewes and Khan, 2011).

Numerous communities worldwide in arid and semi-arid areas have turned to reclaimed wastewater as a critical source for their water alternatives supply (Guizani et al., 2011). In water-scarce regions of southern Africa and the Middle East, wastewater has evolved into a precious resource employed for agriculture, groundwater replenishment, and urban uses after undergoing a refining treatment process (Bdour, 2007). Asano et al. (2007) state that water reuse is a supplementary water source available year-round in urban areas for diverse purposes. Water reuse is commonly used to manage water resources (Guizani et al., 2011). It offers numerous advantages, including safeguarding water resources, preventing coastal pollution, recovering nutrients for agriculture, enhancing river water flow, reducing wastewater treatment costs, and promoting groundwater recharge (Huertas et al., 2008). Water reuse applications cover various uses, such as agricultural irrigation, landscape irrigation, groundwater recharge, industrial reuse, environmental and recreational purposes, non-potable urban services, and indirect or direct potable reuse (Huertas et al., 2008). Quanrud et al. (2003) noted that several countries have recognized indirect potable reuse systems that infiltrate reclaimed water and delay its reuse through aquifer storage.

The utilization of land for treating and disposing of wastewater has been documented since as early as 2600 BC during the Minoan Civilization (Angelakis and Spyridakis, 1996). Wastewater land application provides environmental, economic, and social advantages in addressing municipal wastewater treatment and disposal, including ensuring reliable wastewater treatment to meet water quality standards for intended reuse, protecting public health, and gaining community acceptance (Duan et al., 2010). It serves three primary purposes: 1) ensuring reliable wastewater treatment, 2) protecting public health, and 3) gaining community acceptance. However, it is crucial to thoroughly examine chemical, geological, geochemical, public health parameters, and land-use ecology before reusing treated wastewater to ensure safe water reuse (Kalavrouziotis and Apostolopoulos, 2007). The quality of wastewater effluent infiltrated during land-based water treatment improves through filtration, adsorption, chemical and biodegradation in the aerated unsaturated zone, and dispersion and dilution in the underlying aquifer (Nema et al., 2001). Soil aquifer treatment (SAT) is a land treatment method that involves soil and aquifer in wastewater renovation and is part of managed aquifer recharge (MAR) processes, along with riverbank filtration (RBF) and artificial recharge and recovery (ARR), used in drinking water augmentation projects that can produce potable water from water sources influenced by wastewater (Rauch-Williams et al., 2010). These wastewater land application systems can help alleviate pressure on freshwater resources in arid and semi-arid areas (Heidarpour et al., 2007). MAR involves intentionally recharging water into aquifers for future recovery or environmental benefits (Dillon et al., 2010). Utilizing Soil Aquifer Treatment (SAT) methodologies in conjunction with Managed Aquifer Recharge (MAR) principles, which advocate for using recycled or reclaimed water, can ultimately lead to favorable outcomes by tackling water shortages and environmental challenges. Treated wastewater can be channeled into the aquifer as a steady water source instead of being released directly into surface water bodies, facilitating a cohesive management approach with other water supply methods and mitigating the overall strain on resources.

1.2. The need for research

The majority of municipal wastewater, constituting 99.9%, is water, offering an opportunity for collection, treatment, and reuse, supporting integrated urban water management (Pescod, 1992). However, developing nations encounter challenges in wastewater treatment due to inadequate facilities, power instability, and a lack of skilled personnel (Horan, 1989). Traditional methods are financially impractical for these countries, leading to untreated wastewater discharge and water quality degradation (Hussain et al., 2007). This poses significant public health risks, necessitating cost-effective and eco-friendly technologies for efficient effluent polishing. Soil Aquifer Treatment (SAT) emerges

as a promising solution, providing reliable treatment and producing acceptable quality treated wastewater (Casanova et al., 2016).

In developing countries, wastewater treatment faces hurdles like inadequate facilities, power instability, and a lack of skilled personnel (Abel, 2014). Traditional methods are financially prohibitive, resulting in untreated or poorly treated wastewater discharge, posing water quality and public health risks. To address these challenges, eco-friendly, low-energy, and cost-effective technologies like SAT are crucial for effluent treatment (Sharma and Kennedy, 2017). SAT, treating primary effluent (PE) from wastewater treatment plants (WWTPs), offers economic benefits with lower investment and reduced energy and chemical usage (Drewes and Khan, 2011). The effectiveness of SAT for pollutant removal is established, but knowledge gaps exist regarding water quality parameters and climatic conditions' impact (Guillemoto et al., 2022). Additionally, experiences from developed countries may not be directly applicable to developing nations, and information on the fate of organic micro-pollutants in SAT with various wastewater types is lacking (Fox, 2020). This study aims to address these gaps, simulating WWTP effluents with synthetic wastewater in lab-scale SAT experiments. The objective is to investigate specific soil types of impact on water quality improvement through SAT methodologies. The research findings will aid real-scale SAT-MAR structure management, enhancing this water purification technique's effectiveness. The study evaluates SAT efficiency in removing contaminants and assesses its potential for use in developing countries, considering factors like hydraulic loading rate, infiltration conditions, soil type, redox conditions, and physical and biological mechanisms.

1.3. Research aim and objectives

The aim of this research is to enhance the conditions of wastewater discharge areas by utilizing Soil Aquifer Treatment (SAT) and Managed Aquifer Recharge (MAR) systems. These techniques are complementary water treatment processes that can mitigate water scarcity and environmental issues. To apply SAT effectively, it is crucial to understand the decontamination capacities of the soil and aquifer media, which act as filters. In this regard, various soil characterization and soil-column experiments were carried out in a laboratory setting to gain insight into these capacities. The outcomes of the study contribute to a better understanding of SAT-MAR systems and their potential to improve water quality and environmental conditions.

The primary goal of this research encompasses several specific objectives aimed at understanding and optimizing the soil aquifer treatment (SAT) system for synthetic wastewater pollutant attenuation. These objectives include:

1. Examining the influence of soil type, hydraulic loading rate and infiltration conditions on the attenuation of pollutants such as nitrogen species, phosphate, sulfate, major cations, and metals during soil filtration.
2. Analyzing the impact of operational conditions (continuous drying and rewetting cycles) on pollutant attenuation in an SAT system.
3. Assessing the effects of pH, dissolved oxygen, oxidation-reduction potential conditions, and conductivity variations on pollutant removal in an SAT system.

Through these objectives, the research aims to enhance the understanding of SAT systems and improve their overall efficiency in treating synthetic wastewater pollutants.

1.4. Thesis structure

This thesis comprises 5 chapters, each targeting specific research objectives. It includes an introduction, summary and 3 additional sections addressing various aspects of the soil aquifer treatment system.

Chapter 2 investigates the influence of soil types on the efficiency of SAT system in removing pollutants from synthetic wastewater. This chapter provides guidelines for designing soil filtrate media and presents a thorough examination of the outcomes from soil characterization, soil-column, and batch experiments using natural soil. The key focus is on removing various pollutants, including nitrogen compounds, phosphate, sulfate, major cations, and heavy metals.

Chapter 3 analyzes how hydraulic loading rate and infiltration conditions affect the effectiveness of SAT in removing various synthetic wastewater pollutants. The pollutants include nitrogen species, phosphate, sulfate, major cations, and heavy metals.

Chapter 4 aims to investigate the influence of operating conditions, specifically wetting and drying cycles, on the reduction of synthetic wastewater pollutants, including nitrogen species, phosphate, sulfate, major cations, and heavy metals, in the SAT system process.

2 Comparative Investigation and Performance Evaluation of Different Soil Types in Enhancing Pollutants Removal from Synthetic Wastewater in Soil Aquifer Treatment System

2.1. Introduction

Soil assessments are necessary to select suitable soil types, optimizing SAT performance and pollutant removal. By considering these soil-related factors and optimizing the system design, SAT can effectively remove pollutants from wastewater and protect groundwater quality (Dillon et al., 2020). Therefore, A comprehensive understanding of soil characteristics, and structures is essential for designing effective SAT systems that can effectively remove pollutants from infiltrated wastewater. This chapter aims to compare and evaluate the performance of two different soil types in enhancing pollutants removal and characterizing the pollutants behavior from synthetic wastewater in the SAT system. The investigation will involve a systematic assessment of various soil properties, such as grain size distribution, soil texture determination, porosity, organic matter content, and adsorption capacity, to understand their influence on the infiltrated pollutants treatment efficiency through SAT system.

2.2. Materials and methods

The methodology employed to investigate how two distinct soil types enhance pollutant removal and reveal their behavior within SAT systems is facilitated by Figure 2-1, which presents a visual representation of the study methods in a detailed flowchart. This flowchart guides through the complexities of the experimental design and the specific steps undertaken to unlock the potential of different soil types in improving pollutant removal.

A synthetic wastewater effluent was carefully prepared in the laboratory to simulate the characteristics of real-world wastewater sources. It contained a well-balanced mix of organic and inorganic compounds such as organic matter, nitrogen compounds, phosphorus, heavy metals, and various nutrients, replicating the complexity of actual wastewater (van Loosdrecht et al., 2016). This synthetic effluent allowed for controlled experiments, with adjustable pollutant levels, to accurately assess pollutant removal efficiencies. The specific chemical composition of this laboratory-made synthetic wastewater is detailed in Table 2-1.

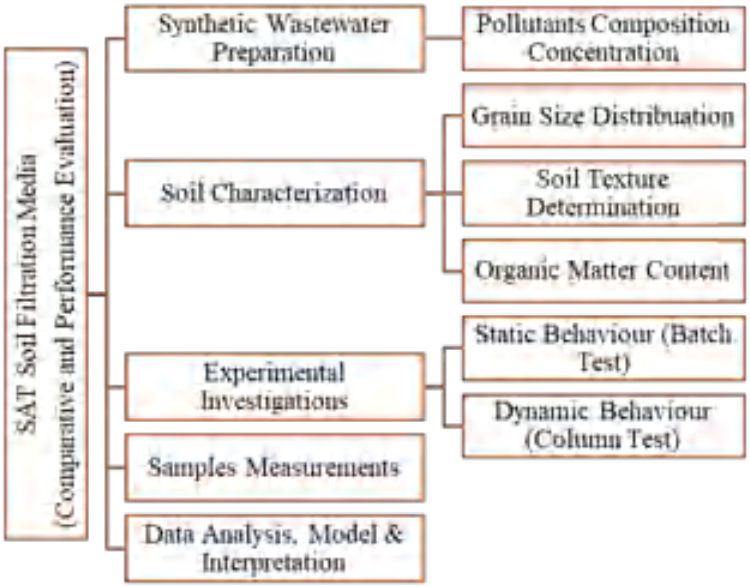

Figure 2-1: Study methodology flowchart

Table 2-1: Synthetic wastewater effluent chemical composition

Chemicals	Mass (mg/1L)	Chemicals	Mass (mg/1L)
$CH_3COONa.3H_2O$	130	H_3BO_3	150
NH_4Cl	100	$CuSO_4.5H_2O$	150
KH_2PO_4	175	KI	150
$MgSO_4 \cdot 7H_2O$	100	$MnSO_4.4H_2O$	150
$CaCl_2 \cdot 2H_2O$	15	$(NH_4)6Mo_7O_{24}.4H_2O$	50
$NaHCO_3$	200	$ZnSO_4.7H_2O$	150
KCl	35	$CoCl_2.6\ H_2O$	150
EDTA	500	Yeast extract	200
$FeCl_3.6H_2O$	150	Peptone	200

In the laboratory investigations of the SAT system, two soil filtrate medias were selected, each with distinct characteristics. Sand, known for its coarse texture and high permeability, facilitates efficient water infiltration and drainage, enhancing the SAT system's hydraulic performance (Trussell et al., 2018). Sandy loam, on the other hand, is chosen for its intermediate texture, striking a balance between water retention and permeability (Sharma and Kennedy, 2017). Both sand and sandy loam's porosity is crucial for water and contaminant retention, promoting improved treatment efficiency within the SAT system (Fox, 2020). Additionally, the organic matter content in soil filtrate media influences biological activity and pollutant degradation potential (Essandoh et al., 2013). Sandy loam, with slightly higher organic matter content than sand, may support increased microbial activity and organic degradable pollutants removal. Through meticulous soil characterization, including grain size distribution, texture analysis, and organic matter assessment, gain insights into the physical and chemical properties of these soil types which can impact the overall performance of the SAT system regarding pollutants removal efficiency. The grain size distribution curves depicted in figures 2-2 demonstrate notable

differences between the sand and sandy loam soils. In the case of the sand soil, it displays a predominantly coarse texture, with a significant proportion of large-sized particles. Conversely, the sandy loam soil exhibits a more even distribution of sand, silt, and clay particles, suggesting a finer texture composition.

The selection of sand and sandy loam soils was based on their common use in SAT systems and their contrasting physical and chemical properties. The soil samples were standardized, lab-prepared soil samples to ensure consistency in fundamental processes. Sand represents a coarser, more permeable soil type, while sandy loam offers higher organic matter content and finer texture, potentially affecting adsorption capacities differently. Also, sand and sandy loam soils, are the common geological structure reflecting the top and shallow soils found in my home land. Preliminary tests included detailed characterization of their physical and chemical properties, such as particle size distribution, organic matter content, porosity, bulk density, and pH, to confirm their suitability for the study.

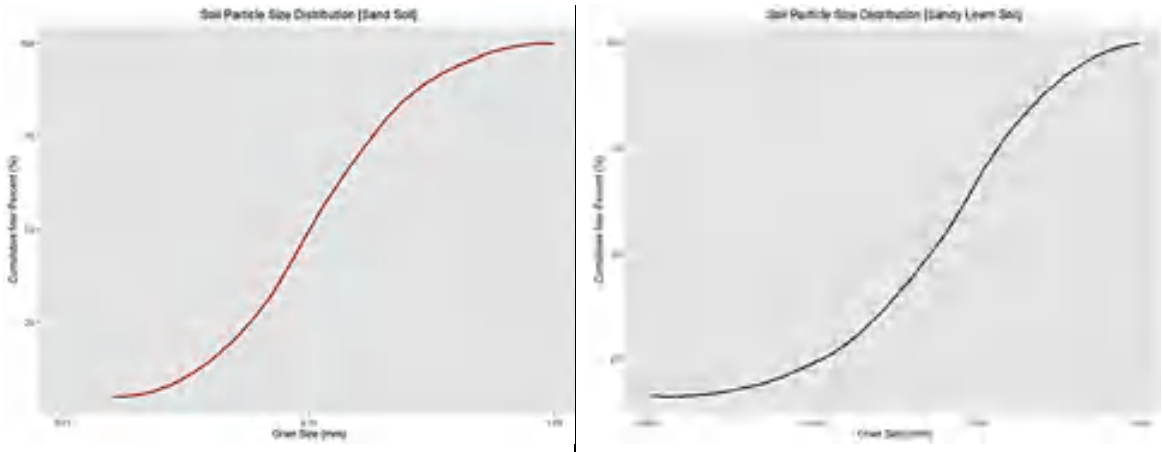

Sand soil | Sandy loam soil

Figure 2-2: Sand and sandy loam soils particle size distribution pattern

In Figure 2-3, the soil texture triangle categorizes the sand soil as predominantly sandy, with a higher concentration of sand particles. In contrast, the sandy loam soil is classified as loam, signifying a well-balanced combination of sand, silt, and clay particles.

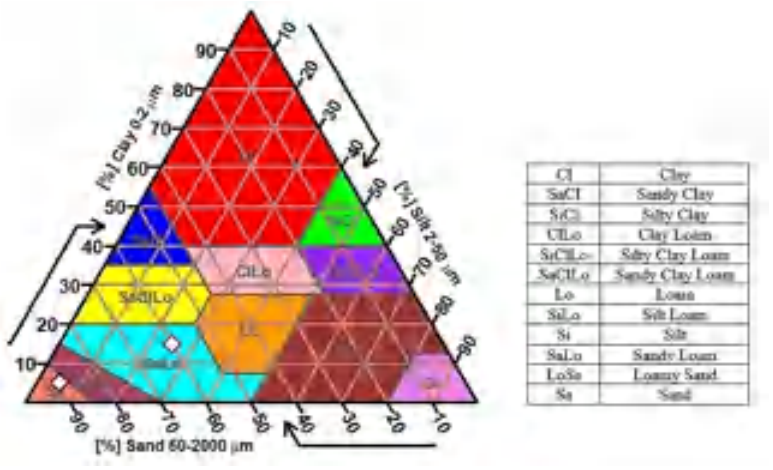

Figure 2-3: Soil texture triangle classification for sand and sandy loam soils

Additionally, Table 2-2 provides a comprehensive summary of essential soil parameters, such as organic matter content, porosity, bulk density, and pH. These parameters are instrumental in defining the physical and chemical attributes of both sand and sandy loam soils, thereby impacting their suitability and performance within the SAT system.

Table 2-2 Sand and sandy loam parameters and characterizations

Parameter	Sand soil	Sandy Loam soil
Organic matter content (%)	0.7	1.20
Dry bulk density (g/cm^3)	1.48	1.54
Porosity	0.43	0.33
pH	6.8	7.6

The comparison between the sand and sandy loam soils reveals distinct differences. The sand soil has lower organic matter content, resulting in reduced microbial activity and adsorption capacity, while the sandy loam soil has higher organic matter content, fostering increased microbial activity, adsorption, and nutrient cycling. In terms of porosity, the sand soil has more macroscopic pores, promoting efficient water infiltration and drainage, whereas the sandy loam soil maintains a balanced porosity, allowing for both water retention and movement. Furthermore, the sand soil has lower bulk density, indicating a looser structure, while the sandy loam soil exhibits slightly higher bulk density, suggesting a more compacted structure. In terms of pH, the sand and sandy loam soils tend to be slightly neutral pH level.

The measurement of soil parameters was preprocessed in the lab by collecting soil samples as lab ready prepared soil samples by drying them in the oven to remove the moisture, then grinding the dried samples to a consistent particle size for sand and sandy loam. Organic matter content is measured using the Loss on Ignition (LOI) Method, which involves heating a sample to a high temperature to burn off organic matter. The weight loss before and after heating estimates organic matter content. The pH was measured by

creating a slurry by mixing sand with distilled water in a 1:2 ratio. The pH electrode was immersed into the slurry and allowed to stabilize. Dry bulk density and porosity are measured by using the core method, which involves taking cylindrical core samples of known volume and weight and then calculating the dry bulk density using the formula (Chaudhari et al., 2013):

$$Bulk\ density = \frac{Dry\ weight}{Volume} \quad (1)$$

$$Porosity = 1 - \frac{Bulk\ density}{Particle\ density} \quad (2)$$

The experimental investigations involved assessing the static and dynamic behaviors of sand and sandy loam soils through batch tests and dynamic column setups. In the static batch behavior tests, soil samples mixed with synthetic wastewater were used to rapidly assess pollutant removal potential. These tests aided in identifying the most suitable soil type for cost-effective pollutant removal and provided data for calibrating and validating mathematical models in SAT system design. In this test, a batch polypropylene tube with 50 mL used with controlled amount of synthetic wastewater is mixed with a predetermined amount of soil sample with dose ratio 1:10 (3g soil : 30ml solution). The soil-wastewater mixture is allowed to incubate and mix for a specified period (4 hours), during which physical, chemical, and biological processes occur to reach the equilibrium and saturation phase between soil solid particles and wastewater pollutants concentrations under isotherm investigations. Batch tests allow for a controlled and systematic evaluation of the soil's ability to retain, transform, and degrade contaminants, thus serving as an important tool for assessing the overall performance of soils in the SAT system. In contrast, dynamic column behavior tests were conducted to evaluate the performance of sand and sandy loam soils in a lab-scale SAT system. These experiments involved using 40 cm glass columns with a 3 cm inner diameter filled with soil samples up to a depth of 30 cm. Synthetic wastewater was continuously applied at an infiltration rate of 0.50 mL/min over 5 experimental days, mirroring real-world conditions with a total infiltrated wastewater volume of 250 mL/day. Effluent samples (15ml/40min) were collected and analyzed for various pollutant concentrations, providing valuable insights into pollutant removal efficiency. The tests monitored how pollutants progressed over time in the soil columns, offering an assessment of treatment effectiveness. Furthermore, the experiments evaluated the ability of sand and sandy loam soils to remove different contaminants, helping determine their suitability for SAT systems. Additionally, it's worth noting that all experimental investigations for both static and dynamic conditions, involving both batch and column tests, were repeated 3 times to ensure a high level of accuracy in the experimental results.

To assess pollutant concentrations in the laboratory SAT system experiments, various sample measurement instruments were utilized to track changes in these concentrations. The HACH DR3900 spectrophotometer was employed to measure the concentrations of NH_4^+, NO_3^-, NO_2^-, PO_4^{3-}, and SO_4^{2-}. Additionally, the MP-AES (microwave plasma atomic emission spectroscopy) was used to measure the concentrations of Fe^{2+}, Cu^{2+}, MoO_4^{2-}, Mn^{+2}, Zn^{2+}, Co^{2+}, and BO_3^{3-}. These measurements provided insights into the concentration dynamics within the system, enabling a comprehensive assessment of the performance and efficiency of both the sand and sandy loam soils in the lab-scale SAT experiments.

The isothermal adsorption models are employed to study the adsorption process and the various stages of a batch reaction. The isothermal adsorption was investigated by altering the initial concentration of the adsorbate in a series of experiments until equilibrium achieved. The resulting data was then modeled using the Freundlich and Langmuir isothermal models to determine the adsorption capacity and parameters with fits the adsorption process, offering a deeper understanding of this phenomenon (Gharbia et al., 2022). The adsorption amount S (mg/g) which express the amount of the pollutants adsorbed by soils can be calculated as:

$$S = \frac{(C_{init} - C_{eq}) * V}{M * 1000} \quad (3)$$

Where: C_{init} and C_{eq} expressed to the initial concentration and equilibrium concentration of pollutants (mg/L), V is the solution volume (mL), and M (g) is the soil mass.

The Freundlich model is applied to characterize the adsorption isotherm mechanisms, which can be modeled as:

$$S = K_f \, C^{1/N} \quad (4)$$

While the Langmuir adsorption isotherm can be modeled as:

$$S = \frac{K_L * S_{max} * C}{1 + K_L * C} \quad (5)$$

Where: S is the adsorption amount (mg/g), C is the solution concentration (mg/L), K_f, and K_L are partitioning coefficients according to the Freundlich and Langmuir model (L/kg), which are used to measure the affinity of the pollutants in soil, and N is a dimensionless reaction.

In the context of column configurations, the effectiveness of the setup is commonly assessed using a breakthrough curve. Breakthrough curves provide insights into the total mass adsorbed by the adsorbent, denoted as qtotal, under specific conditions over time (t) (Fernandez et al., 2023). This is calculated using Equation (6):

$$q_{total} = \frac{QA}{1000} = \frac{Q}{1000} \int_0^{t_{total}} C_{ad} \, dt \quad (6)$$

Where: Q represent the flow rate (mL/min), A the area under the curve, t the total duration of running (min), C_{ad} the concentration (mg/L).

The experimental procedures were iteratively conducted three times to enhance the reliability and confidence in the obtained results. Subsequently, confidence intervals were calculated for each of the three experimental replications using t-test analysis, illustrating the mean and 95% confidence intervals. A comparative analysis was performed to identify the experimental replication characterized by a high mean and lower confidence interval values, signifying greater accuracy and confidence in the experimental outcomes. The graphical representation of these confidence intervals is provided in Annex 2.

2.1. Results and discussions

2.1.1. Static batch behavior

The adsorption capacity examining for sand and sandy loam soils, aiming to understand their ability to capture and immobilize contaminants in wastewater (Ambaye et al., 2021). This investigation was conducted through batch tests to evaluate isothermal adsorption efficiency, under equilibrium between solid soil particles and pollutant ions (Xu et al., 2022). Various factors, including soil texture, surface area, and composition, influenced the soils' capacity to adsorb and retain specific pollutants (Huang et al., 2020). The Freundlich and Langmuir models employed to analyze the isothermal adsorption behavior of these soils, shedding light on the adsorption mechanisms, and predicting their adsorption capacities and parameters (Yang et al., 2023). These models were used to fit the experimental data and derive parameters describing the adsorption characteristics of both sand and sandy loam soils. The Freundlich model, which assumes a heterogeneous adsorption surface, which suggests the presence of multiple adsorption sites with varying affinities for the pollutants (Koopal et al., 2020). The Freundlich model was applied to both soil types to compare their adsorption capacities and pollutant affinities (as shown in figure 2-4). Additionally, the Langmuir model, based on monolayer adsorption on a homogeneous surface, was used to assess the maximum adsorption capacity and the equilibrium binding affinity of the pollutants. The Langmuir model provided information about the maximum adsorption capacity and the strength of adsorption bonds, indicating the formation of a monolayer coverage on the adsorbent surfaces (Al-Ghouti and Da'ana, 2020). This model was also applied to both sand and sandy loam soils to compare their adsorption capacities and pollutant affinities (as shown in table 2-3). Furthermore, both the Freundlich and Langmuir models provided various model parameters for the sand and sandy loam soils. These parameters include the Freundlich constant (K_F), the Freundlich exponent (n), the Langmuir constant (K_L), and the maximum adsorption capacity (Q_{max}). These values serve to indicate the adsorption capacity and the intensity of the adsorption process for each soil

type. They are presented in table 2-3, along with the correlation factor (R2) to assess the accuracy and level of fit between the experimental data and the modeled results.

Figure 2-4: Freundlich and Langmuir isothermal models for synthetic wastewater pollutants in sand and sandy loam soils

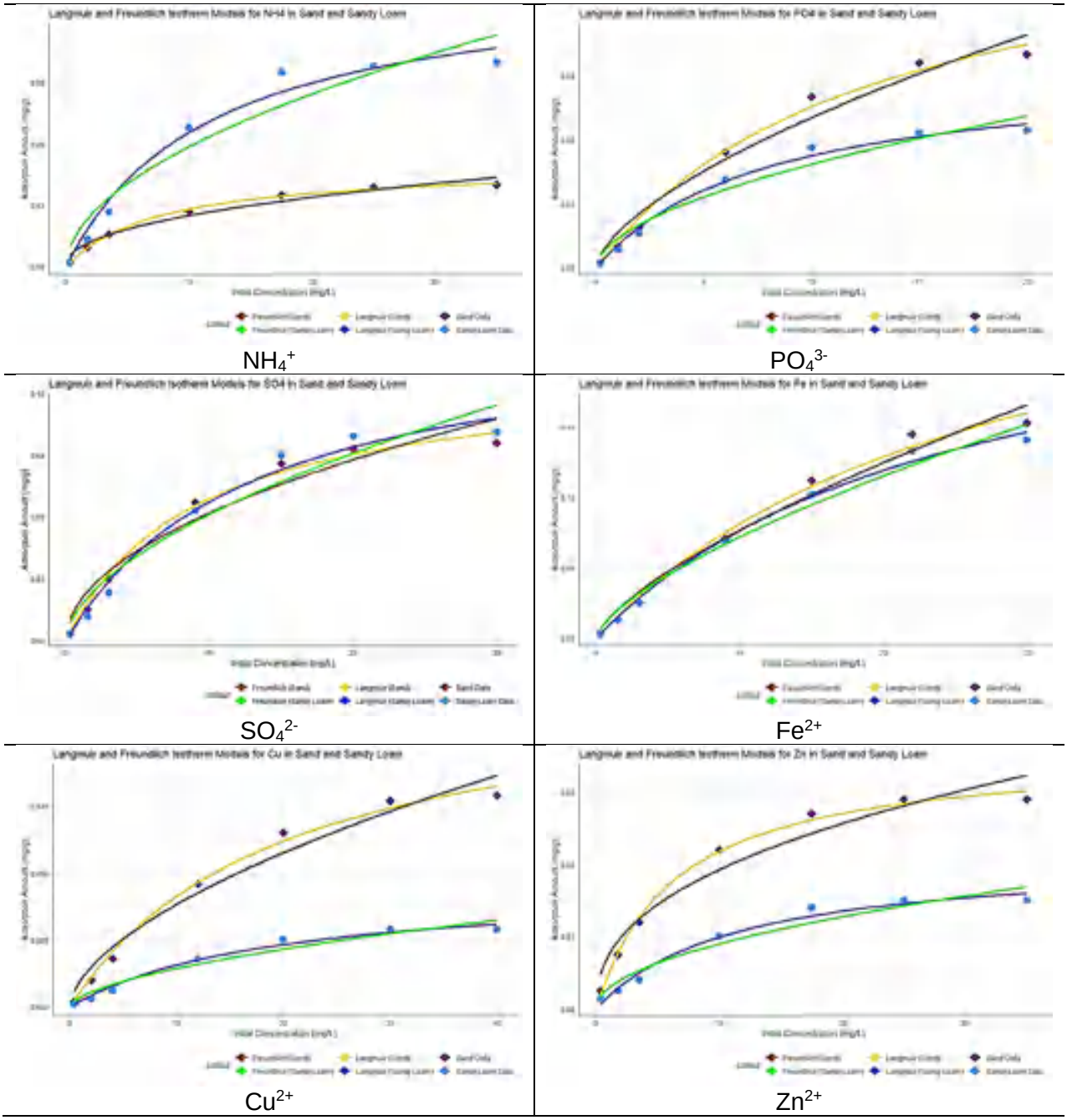

NH_4^+ PO_4^{3-}

SO_4^{2-} Fe^{2+}

Cu^{2+} Zn^{2+}

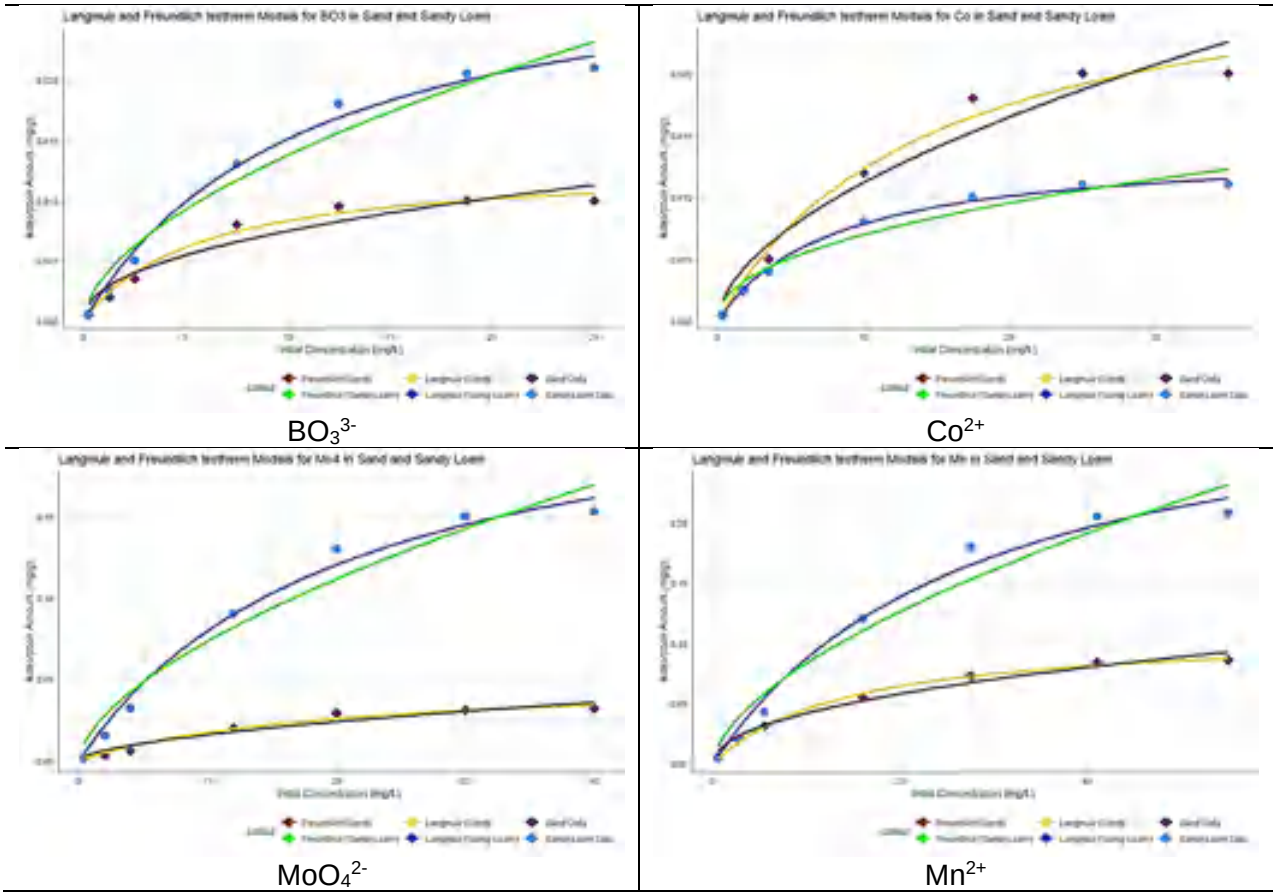

BO_3^{3-} Co^{2+}

MoO_4^{2-} Mn^{2+}

Table 2-3: The Freundlich and Langmuir adsorption parameters for sand and sandy loam soils

	Sand						Sandy Loam					
	K_F	N	R^2	K_L	Q_{max}	R^2	K_F	N	R^2	K_L	Q_{max}	R^2
NH_4^+	0.009	0.44	0.97	0.132	0.05	0.99	0.017	0.53	0.93	0.085	0.15	0.98
PO_4^{3-}	0.02	0.64	0.97	0.08	0.171	0.99	0.014	0.55	0.97	0.13	0.094	0.99
SO_4^{2-}	0.019	0.50	0.95	0.11	0.131	0.99	0.017	0.57	0.94	0.08	0.16	0.98
Zn^{2+}	0.003	0.41	0.95	0.16	0.021	0.99	0.007	0.50	0.94	0.09	0.04	0.98
Fe^{2+}	0.015	0.70	0.98	0.036	0.27	0.99	0.02	0.68	0.98	0.04	0.31	0.99
Cu^{2+}	0.01	0.59	0.97	0.05	0.052	0.99	0.004	0.59	0.95	0.05	0.123	0.99
BO_3^{3-}	0.003	0.45	0.93	0.18	0.013	0.99	0.004	0.57	0.96	0.09	0.032	0.99
Co^{2+}	0.002	0.56	0.95	0.07	0.014	0.98	0.004	0.45	0.95	0.13	0.03	0.99
MoO_4^{2-}	0.004	0.59	0.94	0.05	0.05	0.97	0.02	0.60	0.96	0.05	0.26	0.99
Mn^{2+}	0.014	0.46	0.98	0.07	0.11	0.99	0.02	0.60	0.95	0.04	0.33	0.98

The Freundlich and Langmuir models were used to analyze the adsorption behavior of sand and sandy loam soils for various pollutants. The Freundlich model's parameters, K_F and n, offer insights into adsorption behavior. All Freundlich models had correlation factors (r^2) exceeding 0.90, indicating good fit between experimental and model data. A higher K_F

value implies greater adsorption capacity. Sand exhibited higher K_F values for SO_4^{2-}, and Cu^{2+} pollutants, while sandy loam exhibited higher K_F values for others, suggesting that sandy loam is more efficient in removing certain pollutants compared to sand. The parameter n represents adsorption intensity, with differences noted between the soils for various pollutants with higher intensity for sandy loam comparing with sand. Overall, based on the Freundlich model, sandy loam appears to have a greater capacity for removing pollutants compared to sand. The Langmuir model parameters, K_L and Q_{max}, were used to assess adsorption affinity and maximum adsorption capacity. All Langmuir models had r^2 values over 0.90, indicating a strong fit. A higher Q_{max} value indicates greater adsorption capacity. Sand had higher Q_{max} values for PO_4^{3-}, while sandy loam had higher values for others that indicates for sandy loam is more efficient in removal pollutants comparing with sand. K_L values revealed the affinity of pollutants for each soil type with higher affinity for sandy loam comparing with sand. In general, based on the Langmuir model, sandy loam appears to possess a greater capacity for removing pollutants compared to sand. When comparing the Freundlich and Langmuir models based on R^2 values for synthetic wastewater pollutants, the Langmuir models displayed higher values and better alignment with the experimental results. Overall, these models effectively characterized adsorption behavior, offering insights into surface energies, adsorption capacities, and the formation of monolayer coverage.

2.1.2. Dynamic column behavior

The dynamic column experiments offer significant insights into the performance of sand and sandy loam soils in removing pollutants in the SAT systems. These results reveal how contaminants break through and emphasize differences in removal efficiencies between the two soil types. By examining the breakthrough curves, we can evaluate the retention capacities and adsorption behaviors of various pollutants in each soil medium by measuring the area under the curves to determine the total amount of pollutant removed (Zhang et al., 2022). This information is essential for assessing the effectiveness of soil filtration in eliminating specific contaminants and for optimizing the design and operation of the SAT systems. The column experiments enable the observation of breakthrough points, assessment of breakthrough times, and quantification of pollutant removal for different contaminants (Biel-Maeso et al., 2021).

Figure 2-5 displays the breakthrough curves for infiltrated NH_4^+, NO_2^-, and NO_3^-over 5-days experimental period for both sand and sandy loam.

Upon analysis of the breakthrough curves, the area under the curves (AUC) was calculated to quantify the total removal of NH_4^+ for each soil type. Remarkably, the results reveal that sandy loam exhibited a more efficient removal of NH_4^+ compared to sand. The

total amount removed in sand 19 mg with removal rate 27%, while Sandy Loam demonstrated a higher removal level with total removal amount 43.17 mg and rate 61.68%.

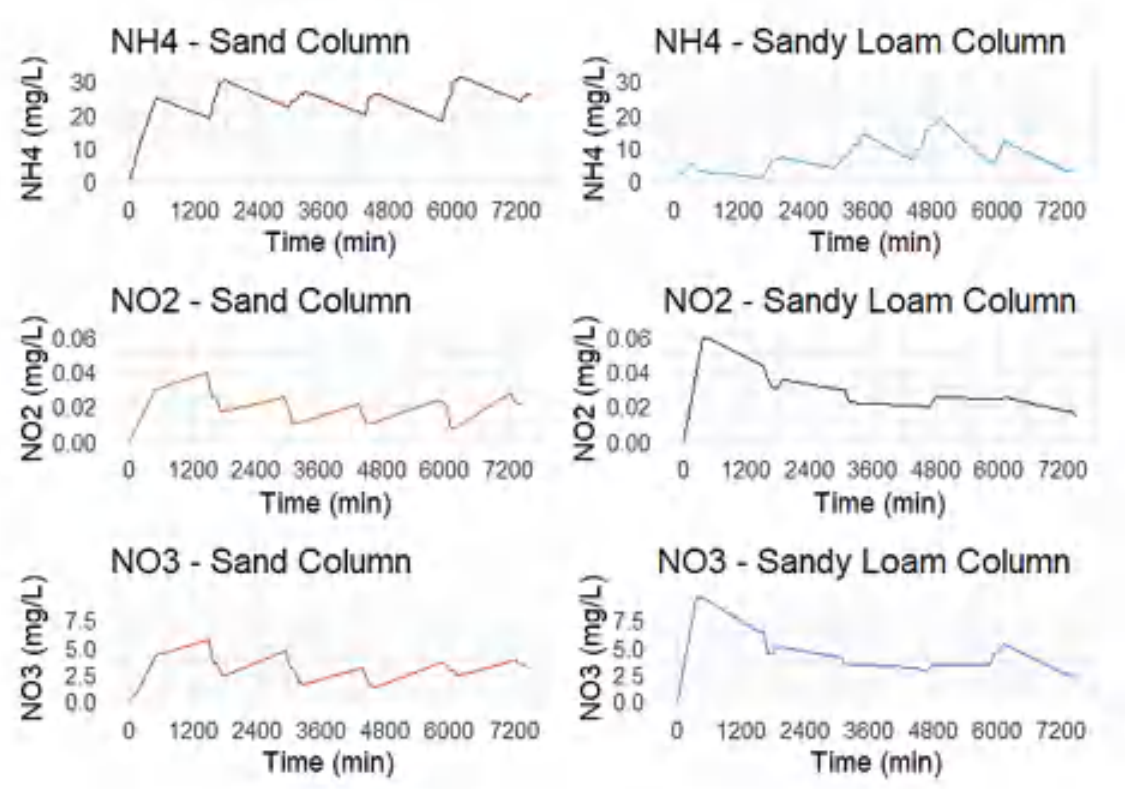

Figure 2-5: Breakthrough curves for infiltrated NH_4^+ in sand and sandy loam soils (Initial concentration NH_4^+35 mg/L)

In Figures 2-5, the breakthrough curves illustrate the removal of NO_2^- in both sand and sandy loam. The concentration of NO_2^- was generated through the infiltration process from nitrification oxidation for NH_4^+. It's noteworthy that the initial concentration for NO_2^- in the infiltrated wastewater is 0 mg/L. Upon calculating the area under the BTCs, the results indicate that Sandy Loam removed more NO_2^- compared to Sand. Specifically, the AUC for Sand is 146.63 mg-min/L, while Sandy Loam demonstrated a higher AUC of 216.96 mg-min/L.

In Figures 2-5, the breakthrough curves depict the removal of NO_3^- in both sand and sandy loam. The concentration of NO_3^- was generated through the infiltration process from nitrification oxidation for NH_4^+. It's worth noting that the initial concentration for NO_3^- in the infiltrated wastewater is 0 mg/L. After calculating the area under the breakthrough curves (AUC), the results indicate that Sand can retained more NO_3^- compared to Sandy loam. Specifically, the AUC for Sand is 22707.93 mg-min/L, while Sandy Loam exhibited a higher AUC of 33625.52 mg-min/L.

In Figures 2-6, the breakthrough curves illustrate the removal of PO_4^{3-} in both sand and sandy loam. The initial concentration for PO_4^{3-} in the infiltrated wastewater is 20 mg/L.

After calculating the area under the breakthrough curves (AUC), the results indicate that Sandy loam removed more PO_4^{3-} compared to Sand. Specifically, the removal % for Sand is 7%, while Sandy Loam showed a higher removal 11.5%.

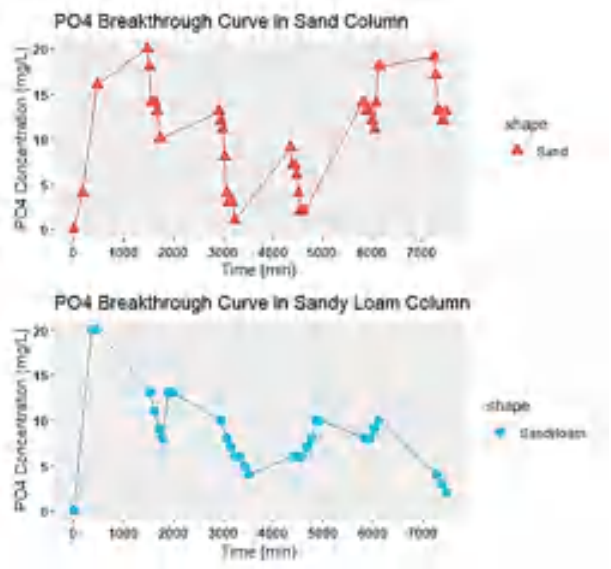

Figure 2-6 Breakthrough curves for infiltrated PO_4^{3-} in sand and sandy loam soils (Initial concentration 20 mg/L)

In Figures 2-7, the breakthrough curves illustrate the removal of SO_4^{2-} in both sand and sandy loam. The initial concentration for SO_4^{2-} in the infiltrated wastewater is 20 mg/L. After calculating the area under the breakthrough curves (AUC), the results indicate that Sand removed more SO_4^{2-} compared to Sandy loam. Specifically, the removal % for Sand is 56.5%, while Sandy Loam demonstrated a substantially lower 25%.

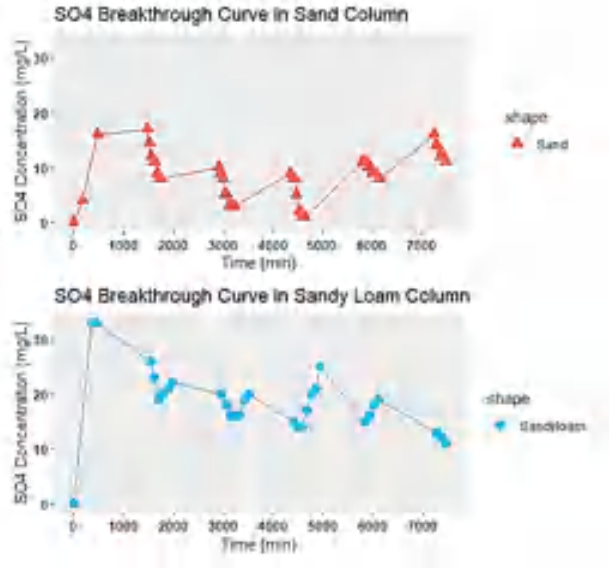

Figure 2-7 Breakthrough curves for infiltrated SO_4^{2-} in sand and sandy loam soils (Initial concentration 40 mg/L)

In Figure 2-8, the breakthrough curves illustrate the removal of Fe^{2+} in both sand and sandy loam. After calculating the area under the breakthrough curves (AUC), the results

reveal that Sand removed more Fe^{2+} compared to Sandy loam. Specifically, the removal % for Sand is 99%, while Sandy Loam demonstrated a lower removal 98%.

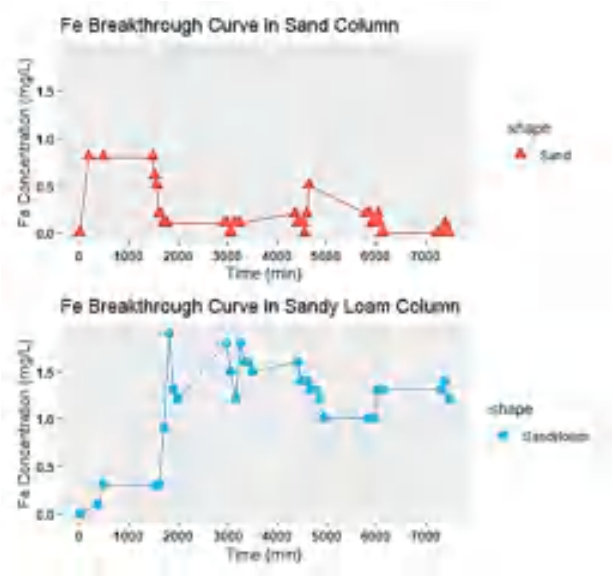

Figure 2-8 Breakthrough curves for infiltrated Fe^{2+} in sand and sandy loam soils (Initial concentration 30 mg/L)

In Figure 2-9, the breakthrough curves illustrate the removal of Cu^{2+} in both sand and sandy loam. After calculating the area under the breakthrough curves (AUC), the results indicate that Sandy loam removed more Cu^{2+} compared to Sand. Specifically, the removal % for Sand is 30.5%, while Sandy Loam demonstrated a comparatively higher 66.7%.

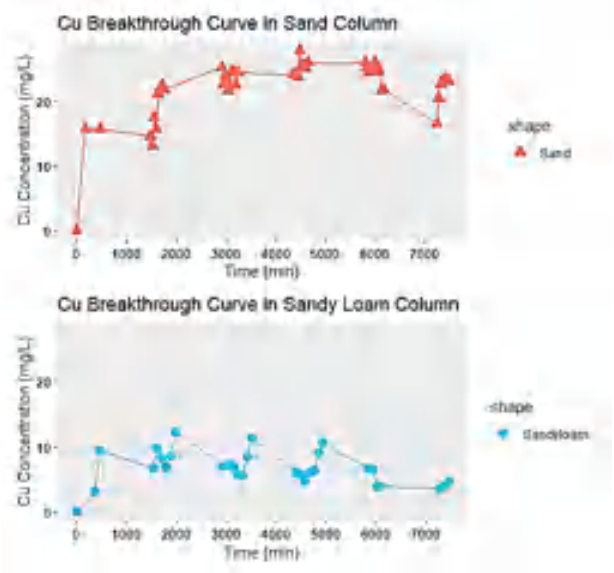

Figure 2-9 Breakthrough curves for infiltrated Cu^{2+} in sand and sandy loam soils (Initial concentration 30 mg/L)

In Figure 2-10, the breakthrough curves illustrate the removal of Mn^{2+} in both sand and sandy loam. After calculating the area under the breakthrough curves (AUC), the results reveal that Sandy loam removed more Mn^{2+} compared to Sand. Specifically, the removal % for Sand is 31.2%, while Sandy Loam demonstrated a significantly higher of 82.9%.

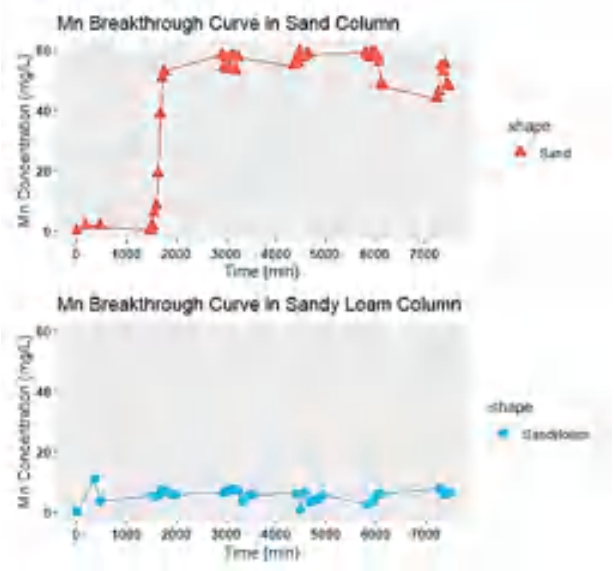

Figure 2-10: Breakthrough curves for infiltrated Mn^{2+} in sand and sandy loam soils (Initial concentration 60 mg/L)

In Figure 2-11, the breakthrough curves illustrate the removal of MoO_4^{2-} in both sand and sandy loam. After calculating the area under the breakthrough curves (AUC), the results indicate that Sandy loam removed more MoO_4^{2-} compared to Sand. Specifically, the removal % for Sand is 18.5%, while Sandy Loam demonstrated a higher removal of 37.6%.

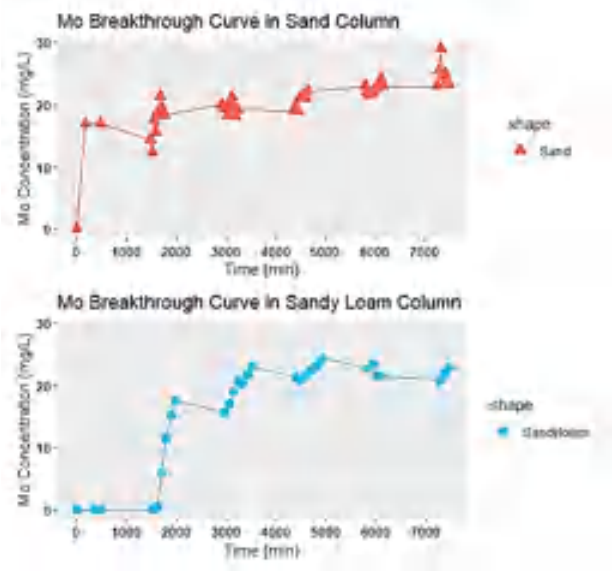

Figure 2-11: Breakthrough curves for infiltrated MoO_4^{2-} in sand and sandy loam soils (Initial concentration 25 mg/L)

In Figure 2-12, the breakthrough curves illustrate the removal of Zn^{2+} in both sand and sandy loam. The area under the breakthrough curves (AUC), indicate that Sandy loam removed more Zn^{2+} compared to Sand. Specifically, the removal % for Sand is 13.6%, while Sandy Loam demonstrated a comparatively higher removal of 48.5%.

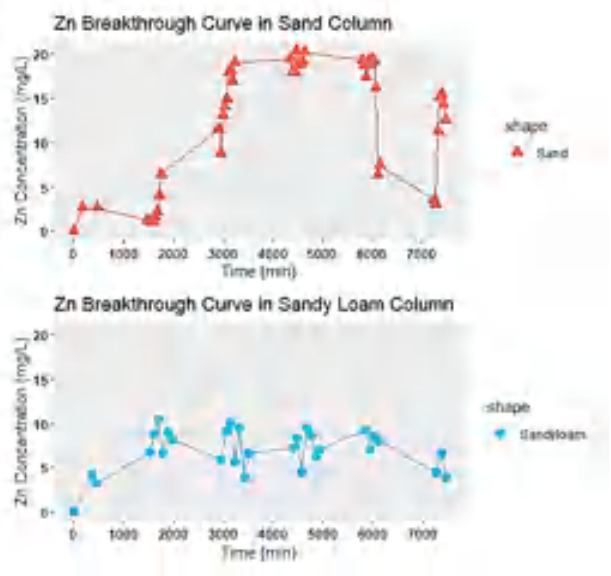

Figure 2-12: Breakthrough curves for infiltrated Zn^{2+} in sand and sandy loam soils (Initial concentration 20 mg/L)

In Figure 2-13, the breakthrough curves illustrate the removal of Co^{2+} in both sand and sandy loam. After calculating the area under the breakthrough curves (AUC), the results reveal that Sandy loam removed more Co^{2+} compared to Sand. Specifically, the removal % for Sand is 28.3%, while Sandy Loam demonstrated a significantly higher removal of 85.2%.

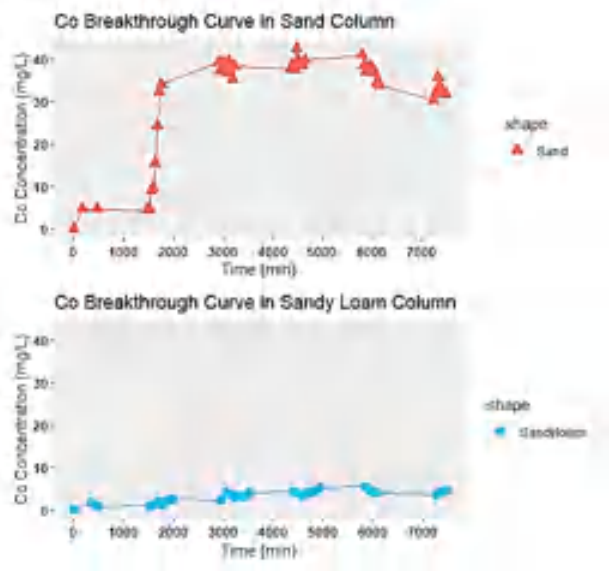

Figure 2-13: Breakthrough curves for infiltrated Co^{2+} in sand and sandy loam soils (Initial concentration 40 mg/L)

In Figure 2-14, the breakthrough curves illustrate the removal of BO_3^{3-} in both sand and sandy loam. After calculating the area under the breakthrough curves (AUC), the results indicate that Sandy loam removed more BO_3^{3-} compared to Sand. Specifically, the removal % for Sand is 17%, while Sandy Loam demonstrated a slightly higher removal of 22.8%.

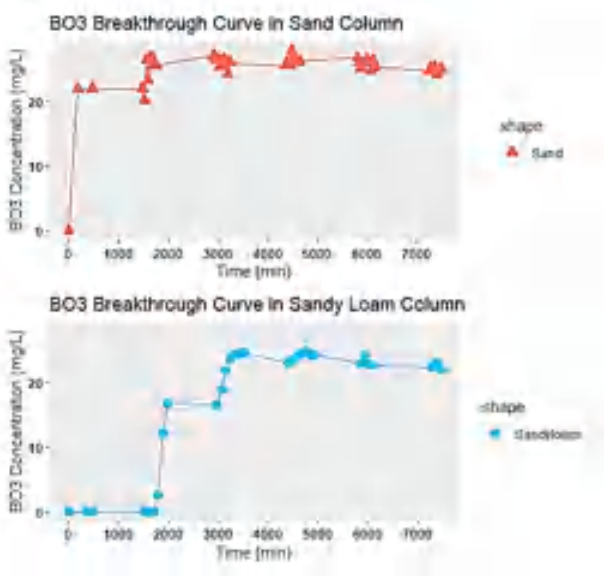

Figure 2-14: Breakthrough curves for infiltrated BO_3^{3-} in sand and sandy loam soils (Initial concentration 25 mg/L)

The breakthrough curve analysis reveals significant variations in the removal efficiency of various pollutants by sand and sandy loam soils within the SAT systems. Sand exhibited higher efficiency in removing NO_2^-, NO_3^-, SO_4^{2-}, and Fe^{2+},compared to sandy loam. Sandy loam showed higher efficiency in removing NH_4^+, PO_4^{3-}, Cu^{2+}, Mn^{2+}, MoO_4^{2-}, Zn^{2+}, Co^{2+}, and BO_3^{3-} compared to sand. The calculated area under the breakthrough curves (AUC) for each pollutant provides a comprehensive measure of the total removal amounts, encompassing adsorption, ion exchange, and biogeochemical reactions occurring in the soil interactions with pollutants. Across various pollutants, Sand consistently exhibited higher AUC values, underscoring its effectiveness in the removal of contaminants through these intricate soil processes.

The discrepancy between the results of batch and dynamic column tests regarding the pollutant removal efficiency of sandy loam and sand soils are typical in environmental research (Bibiano-Cruz et al., 2016). These variations arise from the complexities inherent in natural systems and the distinct conditions created by each testing method (Qiu et al., 2019). Sandy loam soil demonstrates superior pollutant removal in a controlled, static setting (batch test), potentially due to its composition, which fosters effective adsorption or chemical reactions facilitating pollutant elimination. Conversely, sand soil exhibits greater pollutant retention in dynamic column tests, suggesting its proficiency in filtering or retaining pollutants over time, particularly in scenarios simulating real-world substance movement through the soil.

2.2. Conclusion

The comparative investigation between sand and sandy loam soils in the soil aquifer treatment (SAT) systems revealed significant variations in their performance and pollutant removal efficiencies. The findings demonstrated that both soil types exhibited distinct

advantages and limitations in treating different pollutants. The analysis of static adsorption behavior using Freundlich, and Langmuir isothermal models revealed distinct characteristics of sand and sandy loam soils in pollutant removal. Freundlich models indicated that sandy loam exhibited higher adsorption capacity for certain pollutants, while sand excelled in others. Langmuir models reinforced these findings, with sandy loam demonstrating greater efficiency in removing pollutants overall. The comparison of Freundlich and Langmuir models favored the latter, emphasizing their effectiveness in characterizing adsorption behavior. The dynamic breakthrough curve analysis further highlighted the variations in removal efficiency, with sand being more efficient for specific pollutants, as evidenced by higher AUC values. In contrast, sandy loam showed higher efficiency for other pollutants. Concentration levels in sandy loam were generally lower for NH_4^+, PO_4^{3-}, Cu^{2+}, Mn^{2+}, MoO_4^{2-}, Zn^{2+}, Co^{2+}, and BO_3^{3-}, while sand had lower concentrations for NO_2^-, NO_3^-, SO_4^{2-}, and Fe^{2+}. These differences underscore the diverse capabilities of the two soil types in adsorbing and retaining pollutants, as supported by visual analyses. These findings emphasize the importance of selecting the appropriate soil media based on the specific pollutants of concern in SAT system design and operation. Overall, a comprehensive understanding of the soil characteristics and their influence on pollutants removal is crucial for optimizing SAT performance and ensuring effective wastewater treatment.

3 Understanding the Role of Infiltration Rate on Contaminants Fate and Transport in Soil Aquifer Treatment System: Experimental, Modeling, and Statistical Analysis Approaches

3.1 Introduction

The infiltration rate significantly affects the overall efficiency of pollutants removal processes in SAT systems. Therefore, the primary objective of this study is to elucidate the role of infiltration rate in contaminant fate and transport in soil aquifer treatment systems. The study will adopt a multidisciplinary approach, incorporating experimental investigations, modeling techniques, and statistical analysis. By combining these complementary approaches, I aim to provide a comprehensive and detailed understanding of how varying infiltration rates impact contaminants removal and transport processes from synthetic wastewater effluents through soil aquifer treatment system.

3.2 Materials and methods

The comprehensive investigation for the influence of infiltration rate on contaminant behavior in SAT systems. Synthetic wastewater and sand media were used to simulate real-world conditions and maintain controlled experiments. The methodology included selecting parameters such as infiltration rates (0.50 and 10 mL/min) and contaminant composition, preparing synthetic wastewater with precise chemical compositions as displayed in table 3-1, and characterizing suitable sand media as shown in table 3-2 to set up the experimental conditions.

Table 3-1 The chemical composition for the synthetic wastewater effluents

Chemicals	Mass (mg/1L)	Chemicals	Mass (mg/1L)
$CH_3COONa.3H_2O$	130	H_3BO_3	2.65
NH_4Cl	100	$CuSO_4.5H_2O$	15
KH_2PO_4	175	KI	15
$MgSO_4 \cdot 7H_2O$	100	$MnSO_4.4H_2O$	15
$CaCl_2 \cdot 2H_2O$	15	$(NH_4)6Mo_7O_{24}.4H_2O$	5
$NaHCO_3$	200	$ZnSO_4.7H_2O$	15
KCl	35	$CoCl_2.6\ H_2O$	15
EDTA	500	Yeast extract	200
$FeCl_3.6H_2O$	15	Peptone	200

Table 3-2 Sand media properties and characterization

Parameter	Sand soil
Particle size (mm)	0.075 – 0.500
Organic matter content (%)	0.7
Dry bulk density (g/cm^3)	1.48
Porosity	0.43
Permeability (m/d)	1.445

A lab-scale of 40 cm glass columns depth with 3 cm inner diameter were used and packed with the sand media up to 30 cm to create a controlled environment for the experiments. The infiltration rate experiments were conducted by applying different infiltration rates (0.50, and 10) mL/min, ranging from low to high. The infiltration rate was monitored and controlled throughout the experiments to ensure consistency and accuracy by using peristaltic pump to save a constant infiltration rate. The hydraulic loading rate was adjusted as 250mL/d for each infiltration rates with 2 days of experimental duration time. Sampling and analysis were performed at regular intervals to collect effluent samples from the system. These samples were analyzed for contaminant concentrations and physicochemical parameters such as pH, DO, and ORP. The experimental procedures were iteratively conducted three times to enhance the reliability and confidence in the obtained results. Subsequently, confidence intervals were calculated for each of the three experimental replications using t-test analysis, illustrating the mean and 95% confidence intervals. A comparative analysis was performed to identify the experimental replication characterized by a high mean and lower confidence interval values, signifying greater accuracy and confidence in the experimental outcomes. The graphical representation of these confidence intervals is provided in Annex 2.

Numerical modeling and 2-D simulation profiles were employed using FEFLOW v7 to simulate the fate and transport of contaminants in the SAT system under various infiltration rates. This software allowed for the creation of a numerical model representing the system's physical characteristics and behavior, generating modeling for pollutants breakthrough curves and concentration profiles. The simulation results were validated against experimental data, contributing to the calibration and refinement of the numerical model for accuracy check. The 2-D simulation and numerical modeling of pollutant transport were conducted using the random walk modeling technique, a mesh-free approach for tracking contaminants in porous media (Liang and Xuefei, 2014). This method, inspired by statistical physics, involves tracking the movement of individual particles through porous media using sequences of elementary displacements of similar time step durations. These displacements occur independently and without correlation. The cumulative migration of a solute particle is considered to result from numerous statistically independent elementary displacements. The overall displacement of solute particles follows a probability distribution resembling a normal distribution, which serves as an indicator of contaminant cloud movement (Bear, 2018). In addition, the normal distribution tendency of solute particle locations is a representation of how particle concentration spreads within a cloud plume of contaminant particles originating from a specific location and transported under consistent average flow conditions. Yang et al. (2020) have demonstrated that the random walk

modeling approach exhibits high reliability, especially in scenarios with high pollution gradients. This technique holds several advantages: it is inherently conservative, capable of accurately resolving concentration gradients, and efficient when contaminant clouds occupy a limited spatial domain within the computational framework (Bear, 2018). The simulation for tracking contaminants employs the random walk method and is based on the 2-D advection-dispersion/diffusion equation (ADE). It models the movement of synthetic wastewater pollutants in unsaturated sand, integrating water flow using Richard's equation and addressing pollutant transport requirements (Shu et al., 2023). The transport of pollutant solutes in unsaturated soil is influenced by mass transfer and degradative reactions, driven by advection under gravitational potential and capillary diffusivity. In unsaturated soil, capillary diffusivity is the dominant factor, surpassing dispersion and molecular diffusion forces (Winiarski et al., 2013). Equations 1 and 2 represent the integration of Richard's equation with the ADE to model pollutants transport through unsaturated soil.

$$\frac{\partial \theta C}{\partial t} = -V_x \frac{\partial \theta C}{\partial x} - V_y \frac{\partial \theta C}{\partial y} + \frac{\partial \theta}{\partial x}\left[D_{xx} \frac{\partial C}{\partial x} + D_{xy} \frac{\partial C}{\partial y}\right] + \frac{\partial \theta}{\partial y}\left[D_{yx} \frac{\partial C}{\partial x} + D_{yy} \frac{\partial C}{\partial y}\right] + q_s \quad (1)$$

$$D_{ij} = [\alpha_T |V| + D_m]\delta_{ij} + [\alpha_L - \alpha_T] \frac{V_i V_j}{|V|} \quad (2)$$

Where: θ is a volumetric water content related to unsaturated flow flux (cm^3/cm^3); C is the mass concentration (mg/L); t is time; V is the advection velocity; D_{ij} is the dispersion – diffusion term characterizes the spreading and mixing rate in a cartesian domain; q_s is the source factor due to the contaminated releasing or bio-chemical reacting per unit area by describing it with positive or negative signs however, the positive sign is indicating to the pollutants released whilst the negative mark is meaning to contaminants drag; Dm is the diffusion coefficient; α_L, α_T are the longitudinal and transverse dispersivities, to equilibrium the solute mass with water content, the model framework is split into regular cells of steady depth, $\delta_x = \delta_y$ while the quantity of the particles presents the θ water volumetric content (Bear, 2018).

The random walk method balances the water flux in the unsaturated soil by randomly movable particles based on the volumetric water content. This balanced movement provides a reperformance to the transported solute by realizing the mass load for every particle, m_{pk} (k is the solute term). However, the total displacement location for random particle (p) can be calculated under the advective and dispersive conditions (Bücker-Gittel et al., 2003):

$$\Delta x = \frac{\partial D}{\partial x} \Delta t + Z\sqrt{2D\Delta t} \quad (3)$$

$$\Delta y = \left[\frac{\partial D}{\partial y} - \frac{K(\theta)}{\theta}\right] \Delta t + Z\sqrt{2D\Delta t} \quad (4)$$

Z: normally distribution term function with zero average and unit variation, and K (θ) is the hydraulic conductivity. The dissolved solute mass concentration C_{dk} (i) is specified by summation of the mass loadings for each solute:

$$C_d{}^k = \frac{\sum_{p=1}^{N_p} m_p{}^k}{\theta dV} \quad (5)$$

Where: N_p is the particle quantities per cell, d_V is the cell volume (cm^3), i indicate the cell function, and k is the solute term.

While a particle transports in the fluid mobile phase and carries the concentration of solute mass from one cell location to another. Due to particle mobility, it interchanges the concentration mass with a solid immobile. This exchange happens between individual particles and a particular cell. Under the assumption of linear adsorption behavior with equilibrium statuses, two packs can reach a cell with the dissolved m_{dk} (mg) and the adsorbed masses m_{sk} (mg):

$$m_d{}^k(i) = \sum_{p=1}^{N_p} m_p{}^k \quad (6)$$

$$m_s{}^k\,(i) = f^k\,(i)\, m_d{}^k\,(i) \quad (7)$$

The mass exchange coefficient f^k (i), also called a retardation adsorption coefficient given by:

$$f^k\,(i) = K_d\,\rho_s\,\frac{1-n}{\theta} \quad (8)$$

Where ρ_s (g/cm^3) is the soil bulk density, n is the porosity of the framework, K_d (L/kg) is the adsorption distribution term coefficient, and f^k(i) is the exchange coefficient as adsorbed or desorbed mass in every location in time and depth for the dissolved mass. The particle mass should be upgraded at every step related to that mass exchange. At the same time, the interaction between particles and cell permanently changes the particle mass or the cell concentration (Cata and Mohrlok, 2006).

FEFLOW version 7 software utilizes in an analytical approach to model the transport of synthetic wastewater pollutants through unsaturated sand using the random walk method. Model accuracy is assessed through the root mean square (RMS) of the transport model. A two-dimensional numerical domain is created to simulate pollutant transport, considering advection and dispersion processes and accounting for various factors. This simulation approach offers valuable insights into pollutant behavior in unsaturated sand environments, contributing to a better understanding of transport mechanisms and the development of effective remediation strategies. The simulation process employs a rectangular cross-section domain with specific boundary conditions for simulating pollutant transport through unsaturated sand. The lateral boundaries are set as no-flow boundaries, while the upper and bottom boundaries represent inflow and outflow conditions, considering advection-dispersion motion, linear adsorption, and first-order decay reactions. Various

parameters related to sand characteristics are considered, including saturated hydraulic conductivity, volumetric water content (θ_{sat}), and residual water content (θ_r), with θ_{sat} set at 0.43 and θ_r at 0.038. Vertical unsaturated infiltration flow is modeled using the Van-Genuchten factors, with α_{vG} at 0.145 1/cm (air entry value) and n_{vG} at 2.70 (saturation exponent). These parameters play a crucial role in accurately representing unsaturated flow behavior. By integrating these factors and solute mass transport parameters, the simulation provides insights into pollutant movement in unsaturated sand media.

Finally, statistical analysis including the t-test, was performed, and visualized using R programming to assess differences in removal efficiencies and breakthrough curves across different infiltration rates, providing comprehensive insights into the impact of infiltration rates on contaminant removal in the SAT system. Therefore, a systematic approach methodology employed in this study involved carefully selecting infiltration rates, designing synthetic wastewater, conducting experiments, collecting data, and performing statistical and modeling analysis to investigate the role effect of infiltration rates on the behavior of contaminants through SAT systems.

3.3 Results and discussion

The study's results offer valuable insights into how infiltration rates affect the behavior of contaminants in the SAT systems. By combining experimental investigations, numerical modeling, and statistical analysis, the study achieved a comprehensive understanding of system performance under different infiltration rate conditions. These finding results provide a deeper understanding of contaminant dynamics, including removal efficiencies, breakthrough curves, and concentration profiles, shedding light on the influence of infiltration rates. Ultimately, the obtained results contribute to enhancing the design and operation of SAT systems for more efficient contaminants removal.

3.3.1 Experimental approach results

Lab-scale column experiments for simulating a SAT system provided significant insights into its performance under varying infiltration rates. The investigation of the breakthrough behavior for various synthetic wastewater pollutants in the SAT system under two different infiltration rates (0.50 mL/min and 10 mL/min) provide a comprehensive understanding of the transport and fate of infiltrated synthetic wastewater pollutants in the SAT system. These breakthrough curves offer valuable insights into the temporal variations in pollutant concentrations and their removal efficiencies throughout the experimental duration.

The breakthrough curve of NH_4^+, NO_2^-, NO_3^- with time scale under two different infiltration rates of 0.50 mL/min and 10 mL/min is shown in figure 3-1. The breakthrough

curves can gain a better understanding of how the infiltration rate influences the removal and behavior of NH_4^+, NO_2^-, NO_3^-.

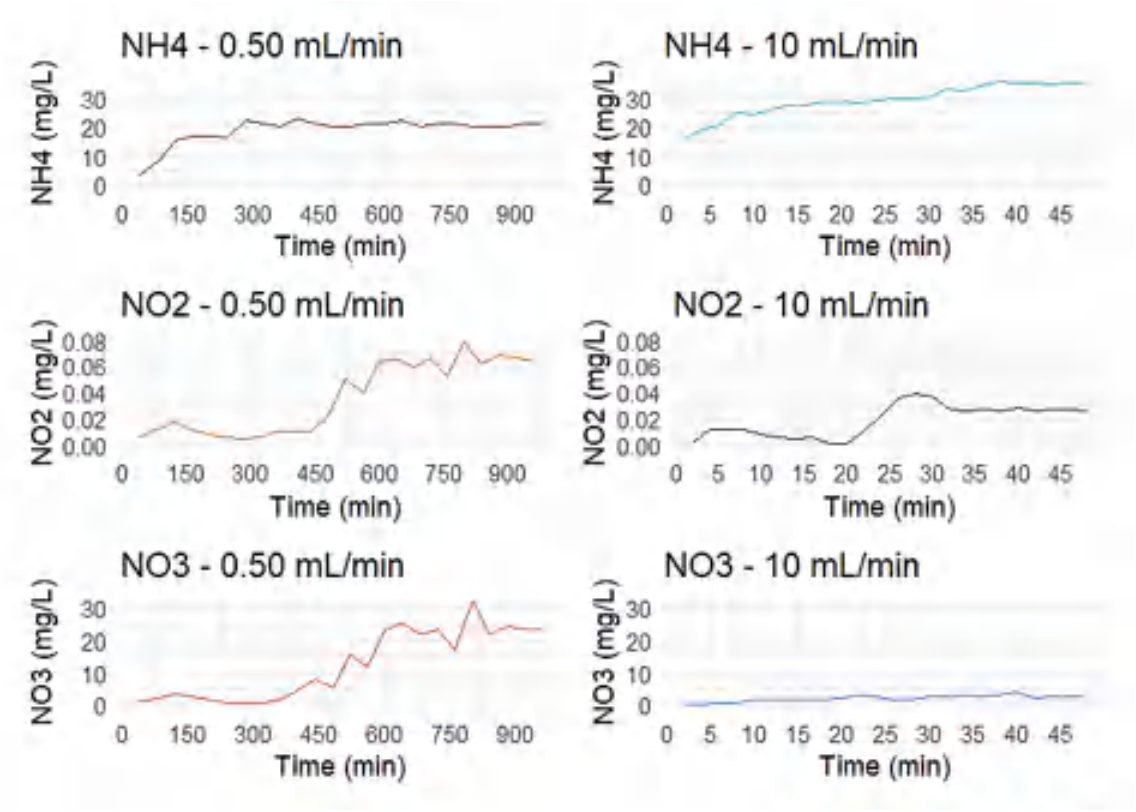

Figure 3-1: Breakthrough curves with time scale for NH_4^+, NO_2^-, NO_3^- (Initial concentration of NH_4^+ 35mg/L)

NH_4^+ breakthrough curves in SAT systems reveal insights into pollutant fate and transport. Comparing the curves at two different infiltration rates (0.50 mL/min and 10 mL/min) provides an understanding of flow rate's impact on NH_4^+ behavior and removal capacity. At 10 mL/min, the NH_4^+ breakthrough curve showed a rapid concentration increase, suggesting faster releasing and lower pollutant removal efficiency. In contrast, the 0.50 mL/min curve displayed gradual concentration increase with no significant breakthrough, indicating slower transport and stronger adsorption and retention processes. The total un-uptake amount of NH_4^+ by calculate the area under the BTCs in the sand column over 0.50 mL/min was 8.78 mg with removal rate 49.8%, while under 10 mL/min, it was 13.53 mg with removal rate 22.7%, demonstrating the efficiency of 0.50 mL/min in NH_4^+ removal due to enhanced adsorption and biodegradation processes, leading to a more effective removal of NH_4^+.

The longer contact time provided by the 0.50 mL/min infiltration rate allows for a more prolonged interaction between NH_4^+ and the soil matrix. This extended exposure facilitates greater opportunities for NH_4^+ molecules to interact with the adsorption sites on the soil particles, increasing the likelihood of adsorption and reducing the concentration of

NH_4^+ in the effluent. Additionally, the slower flow rate can promote enhanced microbial activity and biodegradation processes leading to increased NH_4^+ removal through biological transformation processes. These findings align with Levintal et al. (2023) and Ak and Gunduz (2014).

Both NO_3^- and NO_2^- are formed as a result of the biodegradation of NH_4^+ under nitrification process during the experiments. It's important to note that there are no initial concentrations for NO_3^- and NO_2^- since they are generated during the course of the nitrification byproducts. The breakthrough curves for NO_3^- and NO_2^- in the SAT system show distinct behaviors at two different infiltration flow rates. At 0.50 mL/min, NO_3^- and NO_2^- concentrations increase over time with fluctuations, indicating their production and accumulation in the system. In contrast, at 10 mL/min, the concentrations are lower, suggesting less production capacity from NH_4^+ biodegradation based on reduced retention in the system.

The total amount of NO_3^- un-uptake in the sand column under 0.50 mL/min infiltration rate was 5.7 mg, indicating a substantial removal of NO_3^- through adsorption and other processes. In contrast, the total amount of NO_3^- un-uptake under 10 mL/min infiltration rate was significantly lower at 0.89 mg, suggesting effective removal at the higher infiltration rate. Similarly, the total amount of NO_2^- un-uptake in the sand column under 0.50 mL/min infiltration rate was 0.017 mg, reflecting efficient removal. However, the total un-uptake amount of NO_2^- adsorbed under 10 mL/min infiltration rate was much lower at 0.0086 mg, indicating that the higher flow rate led to increased removal efficiency. Generally, The BTCs results indicate that the 0.50 mL/min infiltration rate is more effective in removing NO_3^- and NO_2^- from the infiltrated wastewater, with longer contact times and more efficient removal mechanisms, including adsorption and potential biological processes which aligns with Ak and Gunduz (2014).

The breakthrough curves of PO_4^{3-} with time scale under two different infiltration rates 0.50 mL/min and 10 mL/min are shown in figure 3-2.

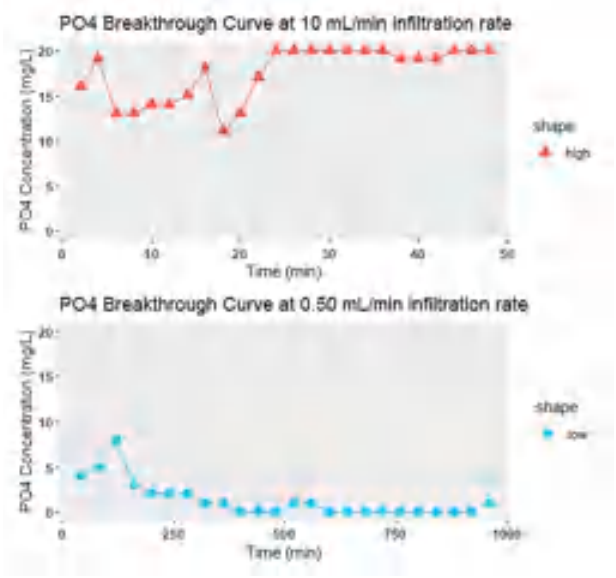

Figure 3-2: Breakthrough curves with time scale for PO_4^{3-} (Initial concentration 20 mg/L)

The breakthrough curves for PO_4^{3-} in the SAT system reveal distinct behavior at two different infiltration rates. At 0.5 mL/min, the PO_4^{3-} breakthrough curve exhibits a decreasing trend, indicating high removal and retention processes within the system. The concentration initially increases, peaks at 8 mg/L, decreases to 0 mg/L, and slightly increases to 1 mg/L. This suggests effective removal of PO_4^{3-} through adsorption, precipitation, and biogeochemical reactions. Conversely, at a flow rate of 10 mL/min, the PO_4^{3-} breakthrough curve shows an increasing trend with significant fluctuations, suggesting lower removal performance. The concentration rises to 19 mg/L, drops to 11 mg/L, and returns to the initial concentration of 20 mg/L, indicating less efficient removal compared to the lower flow rate.

The total amounts of PO_4^{3-} adsorbed in the sand column confirm these trends, with significantly higher removal at 0.5 mL/min compared to 10 mL/min. Due to the total amount of PO_4^{3-} un-uptake in the sand column under 0.50 mL/min infiltration rate was 0.57 mg with removal rate 94.3%, indicating a substantial removal of PO_4^{3-} through adsorption and other biogeochemical reactions. In contrast, the total un-uptake amount of PO_4^{3-} under 10 mL/min infiltration rate was significantly higher at 8.04 mg with removal rate 19.6%, suggesting less effective removal at the higher flow rate. This is due to the longer contact time, enhanced microbial activity, and favorable biogeochemical reactions at the lower flow rate, which collectively contribute to the higher removal efficiency of PO_4^{3-} which aligns with Ak and Gunduz (2014) and Abel et al. (2012).

The breakthrough curves of SO_4^{2-} with time scale under two different infiltration flow rates: 0.50 mL/min and 10 mL/min are shown in figure 3-3.

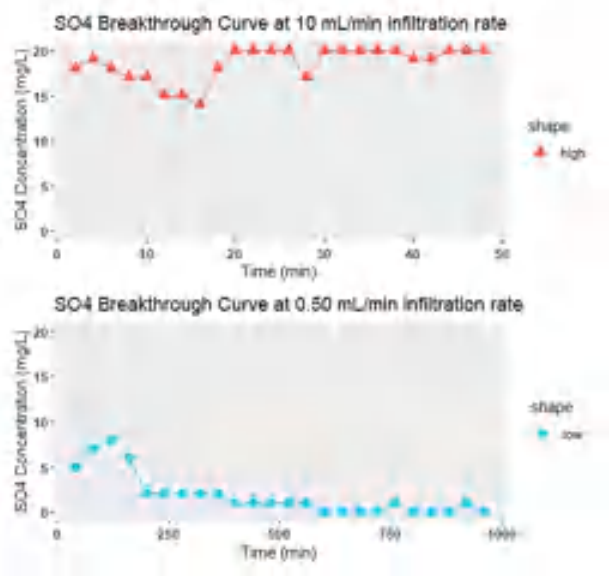

Figure 3-3: Breakthrough curves with time scale for SO_4^{2-} (Initial concentration 20 mg/L)

At 0.5 mL/min infiltration rate, the SO_4^{2-} breakthrough curve initially increases to a peak of 8 mg/L, followed by a sharp decline to 2 mg/L. The curve then stabilizes at 0 mg/L, indicating effective removal of SO_4^{2-}. In contrast, at a flow rate of 10 mL/min, the initial concentration is higher (18 mg/L) and gradually decreases, but there's an unexpected jump to 20 mg/L, stabilizing at this level. This suggests lower removal efficiency for SO_4^{2-} at the higher flow rate. The total un-uptake amounts of SO_4^{2-} in the sand column support these trends, with significantly higher removal at 0.5 mL/min (0.81 mg with removal rate 92%) compared to 10 mL/min (8.54 mg with removal rate 14.6%). The longer contact time, favorable conditions for biogeochemical processes, and reducing conditions based on lower ORP and low DO levels to be anaerobic condition (Bao et al., 2021) at 0.5 mL/min contribute to higher removal efficiency through adsorption and microbial sulfate reduction which align with Ghorbel et al. (2016).

The breakthrough curves of Fe^{2+} with time scale under two different infiltration flow rates: 0.50 mL/min and 10 mL/min are shown in figure 3-4.

At 0.5 mL/min infiltration rate, the Fe^{2+} breakthrough curve initially decreased gradually, indicating removal. However, there were subsequent increases in concentration, suggesting release or desorption of Fe^{2+}. This may be due to the convert the condition in the system to reduction based on lower ORP and lower DO level as aerobic conditions that help in presence the Fe^{2+} concentration. The differences in the curve are attributed to factors like contact time, infiltration rate, reducing conditions, oxygen availability, pH, and ion composition in the system.

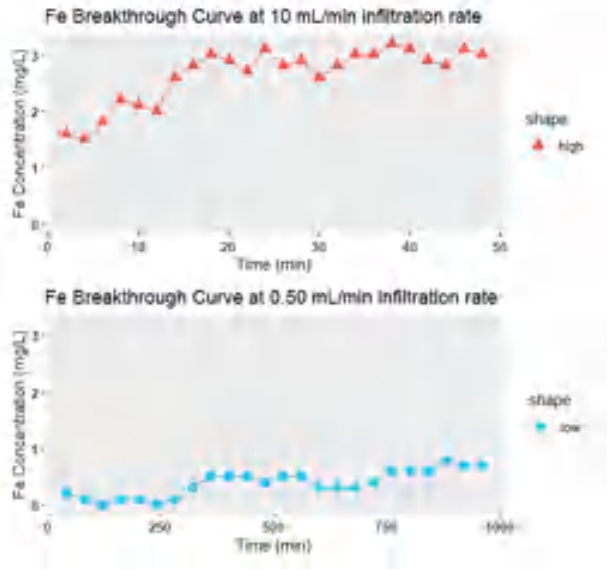

Figure 3-4: Breakthrough curves with time scale for Fe^{2+} (Initial concentration 3 mg/L)

The total amount of Fe^{2+} adsorbed in the sand column was significantly higher at the 0.5 mL/min infiltration rate (0.173 mg with removal rate 88.5%) compared to the 10 mL/min infiltration rate (1.22 mg with removal rate 18.7%). This indicates that the slower infiltration rate allows for more effective Fe^{2+} removal through processes like adsorption, precipitation, and redox reactions (Gorski et al., 2016).

The breakthrough curves of Cu^{2+} with time scale under two different infiltration flow rates: 0.50 mL/min and 10 mL/min are shown in figure 3-5.

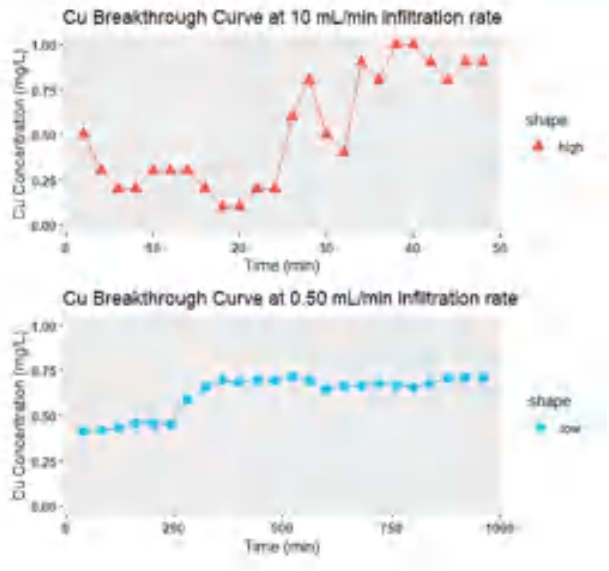

Figure 3-5: Breakthrough curves with time scale for Cu^{2+} (Initial concentration 3.8 mg/L)

At 0.5 mL/min, the Cu^{2+} breakthrough curve shows a gradual increase in concentration, reaching a stable level of 0.7 mg/L. This indicates efficient Cu^{2+} removal with a high adsorption capacity for Cu^{2+} ions. The curve has an s-shaped pattern, reflecting a slow initial breakthrough followed by a more rapid increase. This efficient removal at 0.5

mL/min is due to favorable adsorption conditions and removal of Cu^{2+}. In contrast, the Cu^{2+} breakthrough curve at 10 mL/min displays unstable and fluctuating behavior. It starts at 0.5 mg/L, decreases to 0.1 mg/L, experiences sudden concentration jumps to 0.8 mg/L and 0.5 mg/L, and finally returns to the initial concentration of 1 mg/L. This erratic behavior suggests less efficient and predictable Cu^{2+} removal at 10 mL/min. The higher infiltration rate reduces contact time, leading to decreased adsorption and removal of Cu^{2+} ions. The total amount of Cu^{2+} adsorbed in the sand column was significantly higher at the 0.5 mL/min infiltration rate (1.58 mg, removal rate 84%) compared to the 10 mL/min infiltration rate (1.36 mg, removal rate 72%), as represented by the area under the breakthrough curves. This underlines the importance of infiltration rate in Cu^{2+} removal efficiency. The slower flow rate of 0.5 mL/min allows for longer contact time and, consequently, more effective adsorption and removal of Cu^{2+} ions, resulting in higher removal efficiency (Bourliva et al., 2018).

The breakthrough curves of Mn^{2+} with time scale under two different infiltration rates 0.50 mL/min and 10 mL/min are shown in figure 3-6.

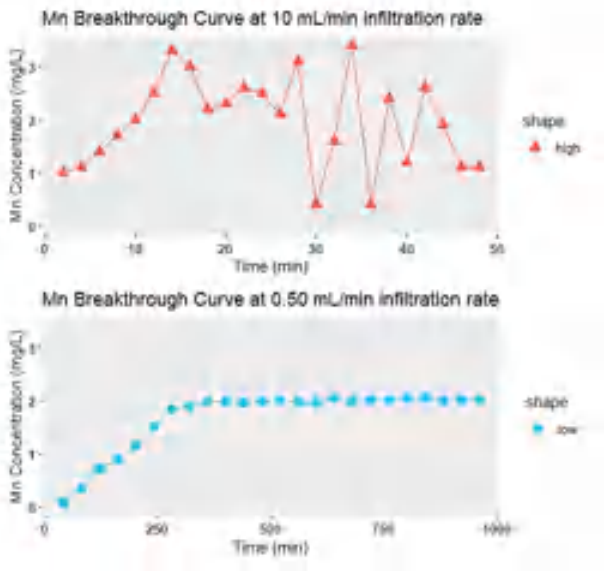

Figure 3-6: Breakthrough curves with time scale for Mn^{2+}(Initial concentration 3.7 mg/L)

The Mn^{2+} breakthrough curves in the SAT system exhibit distinct patterns at infiltration rates of 0.5 mL/min and 10 mL/min. At 0.5 mL/min, the Mn^{2+} breakthrough curve shows a steady increase, reaching a stable concentration of 2 mg/L. The s-shaped pattern indicates a gradual increase followed by a constant plateau, indicating efficient Mn^{2+} removal. The system demonstrates a high capacity for Mn^{2+} adsorption and retention at this infiltration rate. Conversely, the Mn^{2+} breakthrough curve at 10 mL/min displays erratic and fluctuating behavior. Starting at 1 mg/L, it increases to 3 mg/L, decreases to 2 mg/L, briefly stabilizes, drops to 0.5 mg/L, rapidly increases back to 3 mg/L, and drops to 0.5 mg/L again. This behavior suggests less efficient and consistent Mn^{2+} removal at 10 mL/min due to the higher infiltration rate, reducing contact time for effective adsorption and retention. The total

amount of Mn^{2+} adsorbed in the sand column was significantly higher at the 0.5 mL/min infiltration rate (0.79 mg, removal rate 47.3%) compared to the 10 mL/min infiltration rate (0.92 mg, removal rate 38.7%), as represented by the area under the breakthrough curves. This underscores the substantial impact of infiltration rate on Mn^{2+} removal efficiency. The slower infiltration rate of 0.5 mL/min allows for longer contact time, promoting better adsorption and geochemical reactions of Mn^{2+} ions. In contrast, the higher infiltration rate of 10 mL/min limits interaction between Mn^{2+} and the soil media, resulting in less efficient removal and more fluctuating breakthrough behavior (An et al., 2020).

The breakthrough curves of MoO_4^{2-} with time scale under two different infiltration rates 0.50 mL/min and 10 mL/min are shown in figure 3-7.

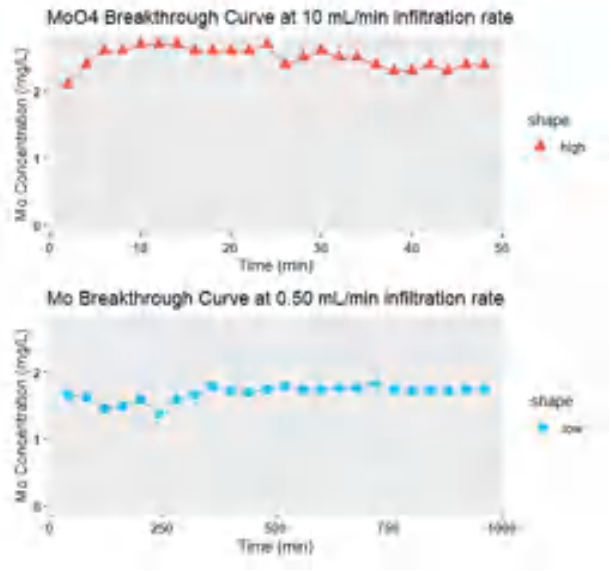

Figure 3-7: Breakthrough curves with time scale for MoO_4^{2-} (Initial concentration 2.5 mg/L)

The MoO_4^{2-} breakthrough curves in the SAT system display different behaviors based on the infiltration rate, with distinctions noted between 0.5 mL/min and 10 mL/min. At 0.5 mL/min, the MoO_4^{2-} breakthrough curve follows a complex pattern. Starting at 1.7 mg/L, the curve gradually decreases to 1.5 mg/L, increases to 1.6 mg/L, drops to 1.4 mg/L, and then exhibits an s-shaped pattern, stabilizing at 1.8 mg/L. This indicates a moderate capacity for MoO_4^{2-} adsorption and retention by the soil media, with fluctuations suggesting dynamic interactions between MoO_4^{2-} and the soil media. In contrast, the 10 mL/min infiltration rate results in a different trend. Starting at 2.1 mg/L, the curve increases to a peak of 2.7 mg/L, higher than the initial concentration. This suggests that the higher infiltration rate limits interaction between MoO_4^{2-} and the soil matrix, leading to less efficient removal. Subsequently, the curve stabilizes around 2.6 mg/L, drops to 2.4 mg/L, and exhibits minor variations but remains relatively stable around 2.3 mg/L. The breakthrough curves imply that the efficiency of MoO_4^{2-} removal is infiltration rate-dependent. The total amount of MoO_4^{2-} adsorbed in the sand column was significantly higher at 0.5 mL/min (0.77 mg,

removal rate 38.4%) than at 10 mL/min (1.15 mg, removal rate 8%), as represented by the area under the breakthrough curves. The higher concentration levels of MoO_4^{2-} at 10 mL/min can be attributed to shorter contact time and disruption of the equilibrium between MoO_4^{2-} and the soil media. When the infiltration rate is high, less time is available for equilibrium between adsorbed and dissolved MoO_4^{2-}, leading to desorption from soil particles. Conversely, the lower infiltration rate provides favorable conditions for MoO_4^{2-} adsorption. Initially, there may be desorption, but as the experiment progresses, a new equilibrium establishes between MoO_4^{2-} in the infiltrated wastewater and the adsorbed MoO_4^{2-} on the soil particles. This contributes to the observed s-shaped pattern in the breakthrough curve. Generally, the slower infiltration rate of 0.5 mL/min allows for longer contact time, facilitating adsorption and retention of MoO_4^{2-}, resulting in a stabilized pattern with high removal capacity. In contrast, the higher infiltration rate of 10 mL/min restricts interaction time, leading to less efficient removal and higher concentrations in the breakthrough curve.

The breakthrough curves of Zn^{2+} with time scale under two different infiltration rates 0.50 mL/min and 10 mL/min are shown in figure 3-8.

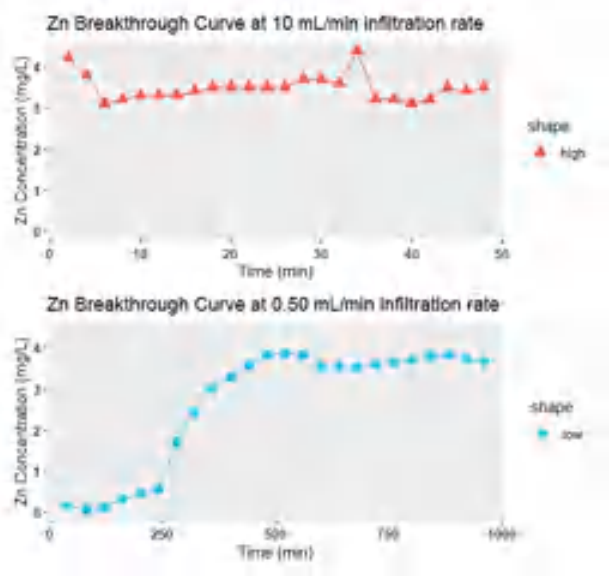

Figure 3-8: Breakthrough curves with time scale for Zn^{2+} (Initial concentration 3.5 mg/L)

The Zn^{2+} breakthrough curves at different infiltration rates exhibit distinct behaviors. At a infiltration rate of 0.5 mL/min, the curve follows an s-shaped pattern, starting from an initial concentration of 0 mg/L and gradually increasing to 4 mg/L. It then remains relatively stable, indicating effective Zn^{2+} adsorption and retention with high removal efficiency at this infiltration rate. Conversely, at 10 mL/min, the breakthrough curve shows more variability. It starts from a higher concentration of 4.20 mg/L and undergoes fluctuations throughout the experiment. The curve initially drops to 3.10 mg/L, increases slightly to 3.3 mg/L, further increases gradually to 3.6 mg/L, experiences a sudden jump to 4.4 mg/L, and then rapidly

drops to 3.1 mg/L, followed by another increase to 3.4 mg/L. This fluctuating behavior suggests that the soil media is less effective in adsorbing and retaining Zn^{2+} at this higher infiltration rate, resulting in lower removal efficiency compared to the 0.5 mL/min infiltration rate. The results indicate that the lower infiltration rate of 0.5 mL/min is more efficient in removing Zn^{2+} from the synthetic wastewater. The longer contact time allows for better adsorption and retention of Zn^{2+}, resulting in a more consistent and stable breakthrough curve with a higher removal efficiency (Chauhan et al., 2022). The total amount of Zn^{2+} adsorbed in the sand column was significantly higher at 0.5 mL/min (1.23 mg, removal rate 38.5%) than at 10 mL/min (1.6 mg, removal rate 20%), as represented by the area under the breakthrough curves.

The breakthrough curves of Co^{2+} with time scale under two different infiltration rates 0.50 mL/min and 10 mL/min are shown in figure 3-9.

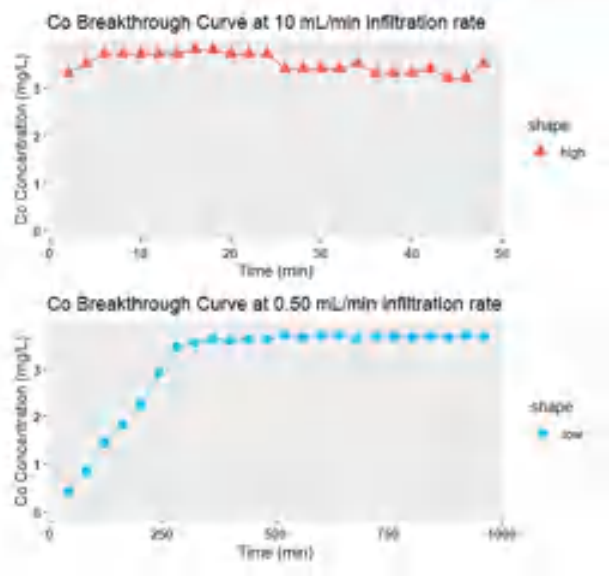

Figure 3-9: Breakthrough curves with time scale for Co^{2+} (Initial concentration 3.7 mg/L)

At 0.5 mL/min infiltration rate, the curve follows an s-shaped pattern, starting from concentration of 0.5 mg/L and gradually increasing until it reaches the target concentration of 3.5 mg/L. Once it reaches the target, the curve remains stable, indicating effective adsorption and retention of Co^{2+} with high removal efficiency at this infiltration rate. In contrast, at infiltration rate of 10 mL/min, the breakthrough curve begins with a higher concentration of 3.3 mg/L. It gradually increases to 3.7 mg/L and remains stable for a period. However, there are subsequent fluctuations, with the concentration reaching 3.8 mg/L, slightly decreasing to 3.7 mg/L, and further dropping to 3.4 mg/L before gradually decreasing to 3.3 mg/L. Interestingly, there is a sudden jump to 3.5 mg/L at the end of the experiment. The higher Co^{2+} concentration levels observed during the 10 mL/min infiltration rate can be attributed to factors such as reduced contact time between infiltrated wastewater and soil matrix, potential limited adsorption sites on soil particles, and the

presence of competing ions in the wastewater. Additionally, the rapid percolation of infiltrated wastewater under higher infiltration rates may cause desorption or release of previously adsorbed Co^{2+} from the soil media, contributing to the higher effluent concentrations. The total amount of Co^{2+} adsorbed in the sand column was significantly higher at 0.5 mL/min (1.47 mg, removal rate 16%) than at 10 mL/min (1.62 mg, removal rate 7.5%), as represented by the area under the breakthrough curves. These findings suggest that the lower infiltration rate of 0.5 mL/min is more efficient in removing Co^{2+} from the synthetic wastewater. This is evident in the stable and consistent breakthrough curve, indicating effective adsorption and retention of Co^{2+}. In contrast, the higher infiltration rate of 10 mL/min results in more fluctuations, suggesting reduced adsorption and retention capacity and lower overall removal efficiency.

The breakthrough curves of BO_3^{3-} with time scale under two different infiltration rates 0.50 mL/min and 10 mL/min are shown in figure 3-10.

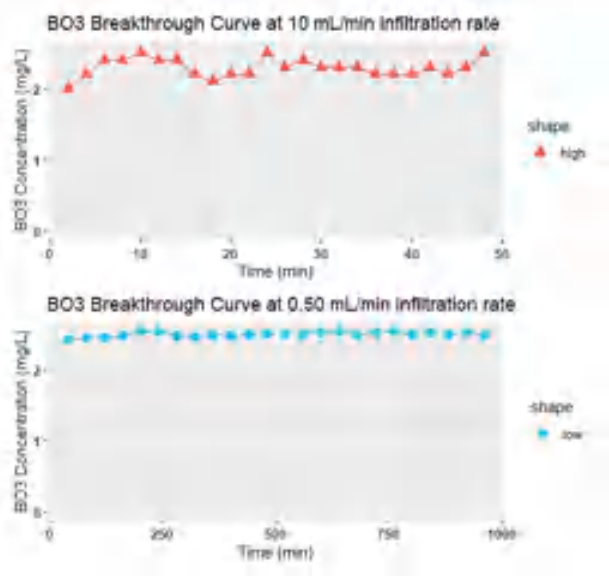

Figure 3-10: Breakthrough curves with time scale for BO_3^{3-} (Initial concentration 2.5 mg/L)

At 0.5 mL/min, the breakthrough curve exhibits fluctuations, suggesting dynamic interactions between the infiltrated wastewater and the soil media. The concentration increase followed by a drop and subsequent increase could be due to processes like adsorption, desorption, and biogeochemical complexation occurring between BO_3^{3-} and the soil particles. However, the concentration eventually stabilizes at the desired level, indicating some removal efficiency. In contrast, at 10 mL/min, the breakthrough curve displays more pronounced concentration fluctuations, indicating a less efficient removal process for BO_3^{3-} compared to the 0.5 mL/min infiltration rate. The fluctuations might result from limited adsorption capacity, increased transport through the soil media, or competition from other ions in the infiltrated wastewater. The final jump in concentration at the experiment's end may indicate breakthrough, where the soil media's removal capacity

becomes saturated, resulting in higher effluent concentrations. The total amount of BO_3^{3-} adsorbed in the sand column was significantly lower at 0.5 mL/min (1.15 mg, removal rate 8%) compared to 10 mL/min (1.05 mg, removal rate 16%), as represented by the area under the breakthrough curves. Overall, the results suggest that the 0.5 mL/min infiltration rate provides a more stable and performance of BO_3^{3-} but the higher infiltration rate of 10 mL/min demonstrates greater variability and potential in achieving effective BO_3^{3-} removal from synthetic wastewater.

3.3.2 Modeling and simulation approach results

The modeling process generates breakthrough curves, representing pollutant concentrations over time as they move through sand media in the SAT system under different infiltration rates. To verify model accuracy, these modeled curves are calibrated and compared to experimental results. The alignment between model predictions and actual measurements, assessed using the root mean square (RMS) value, determines model performance. A lower RMS value signifies a closer match, indicating greater accuracy in representing pollutant behavior. Calibration of breakthrough curves with experimental data and RMS calculations allows to evaluate the model's reliability in capturing pollutant transport dynamics and optimizing the pollutant transport parameters with the concentration dynamics through the depth profile.

The modeling of the infiltrated synthetic wastewater pollutants transported through the SAT system at an infiltration rate of 0.50 mL/min. figure 3-11 displays the breakthrough curves for pollutants during their infiltration into the sand media. These curves aim to evaluate the impact of the 0.50 mL/min infiltration rate on pollutant transport within the SAT system.

Figure 3-11: Breakthrough curves modeling for infiltrated pollutants at 0.50 mL/min rate

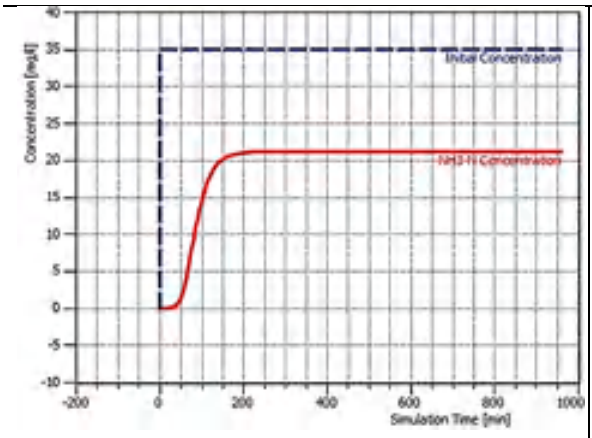

NH_4^+ - Initial concentration 35 mg/L

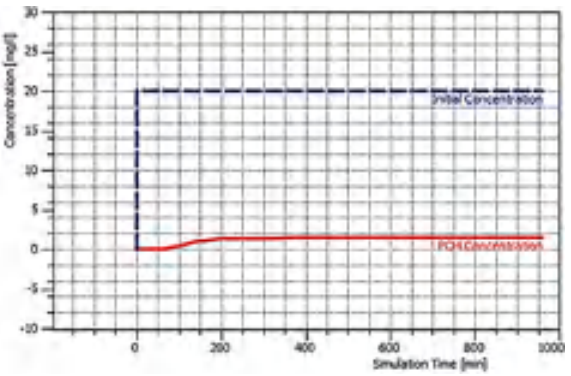

PO_4^{3-} - Initial concentration 20 mg/L

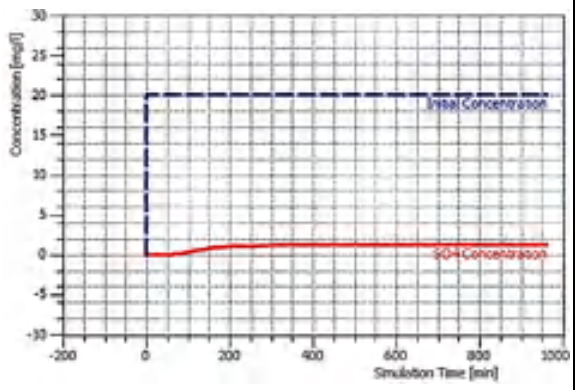

SO_4^{2-} - Initial concentration 20 mg/L

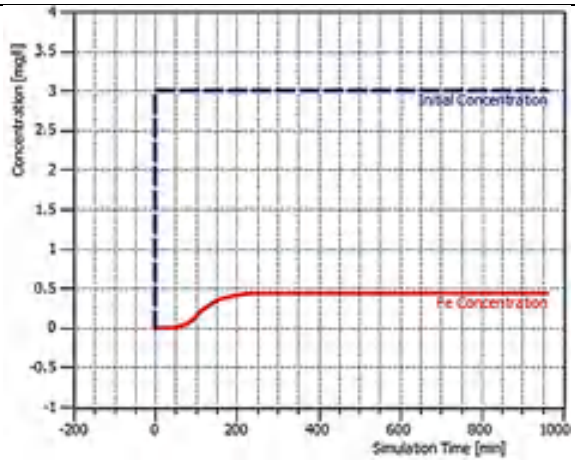

Fe^{2+} - Initial concentration 3 mg/L

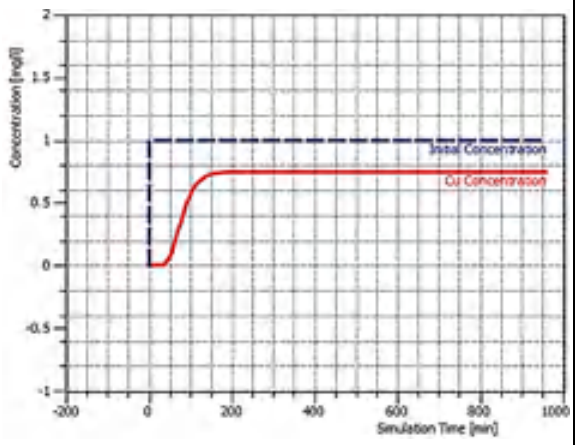

Cu^{2+} - Initial concentration 3.8 mg/L

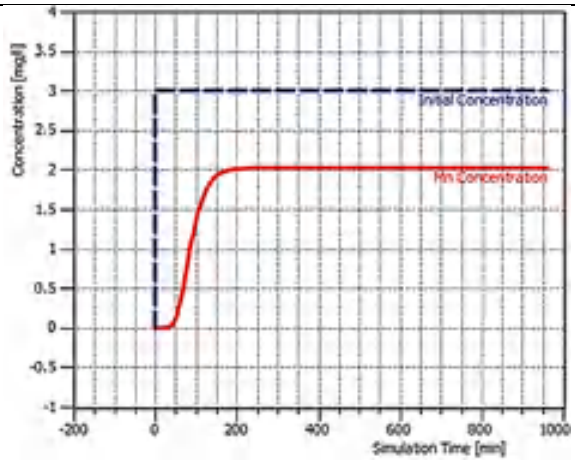

Mn^{2+} - Initial concentration 3.7 mg/L

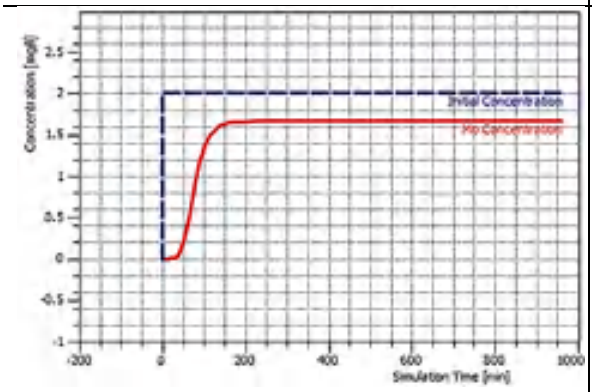

MoO_4^{2-} - Initial concentration 2.5 mg/L

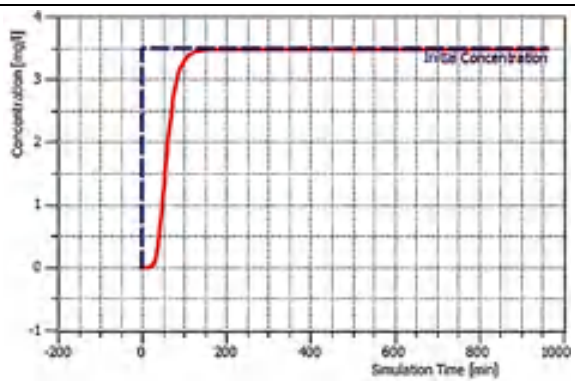

Co^{2+} - Initial concentration 3.7 mg/L

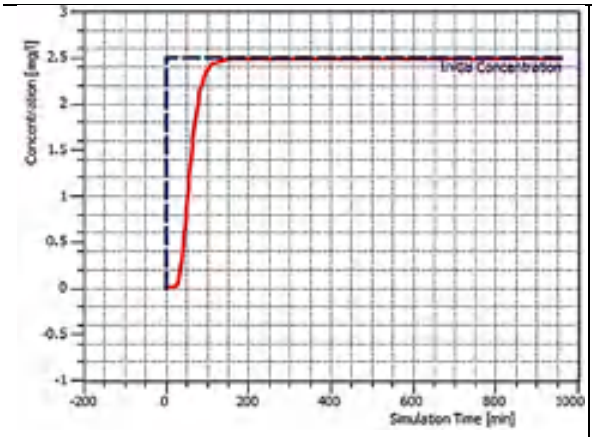

BO_3^{3-} - Initial concentration 2.5 mg/L

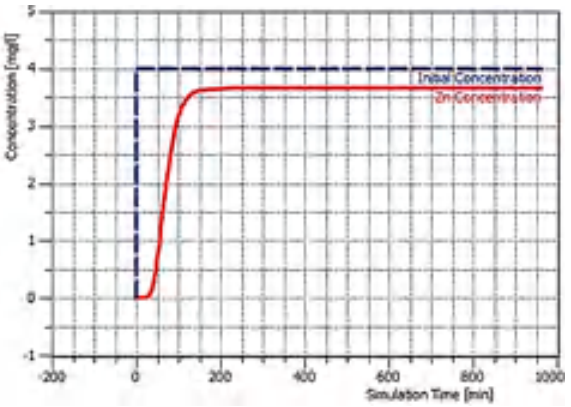

Zn^{2+} - Initial concentration 3.5 mg/L

The calibration process is vital for ensuring the accuracy and reliability of the model. It involves comparing the modeled breakthrough curves with experimental data for synthetic wastewater pollutants as shown in Annex 3.

In the context of simulating process initiates with an infiltration rate of 10 mL/min. Figure 3-12 displays the breakthrough curves for synthetic wastewater pollutants as they infiltrate the sand media, assessing the impact of the 10 mL/min infiltration rate on pollutant transport within the SAT system.

Figure 3-12: Breakthrough curves modeling for infiltrated pollutants at 10 mL/min rate

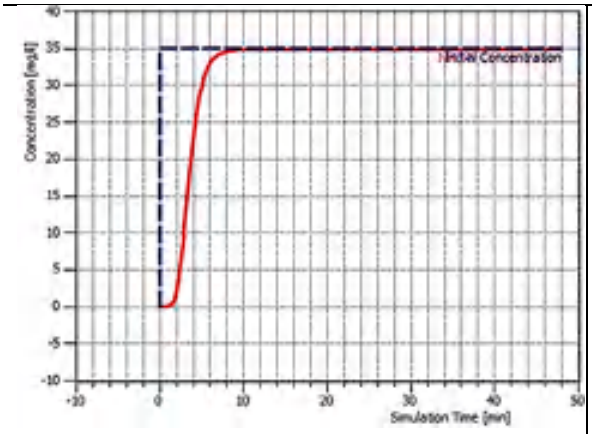

NH_4^+ - Initial concentration 35 mg/L

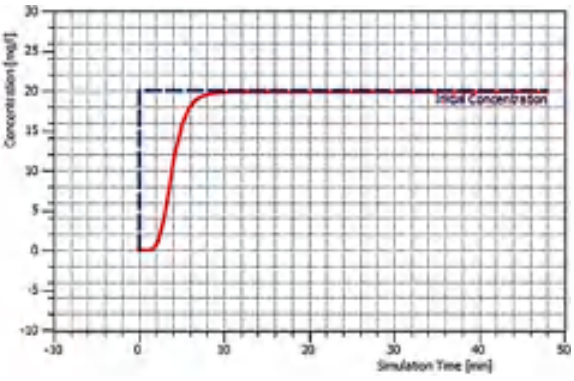

PO_4^{3-} - Initial concentration 20 mg/L

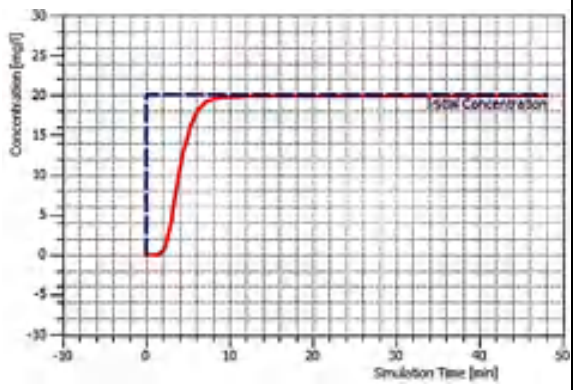

SO_4^{2-} - Initial concentration 20 mg/L

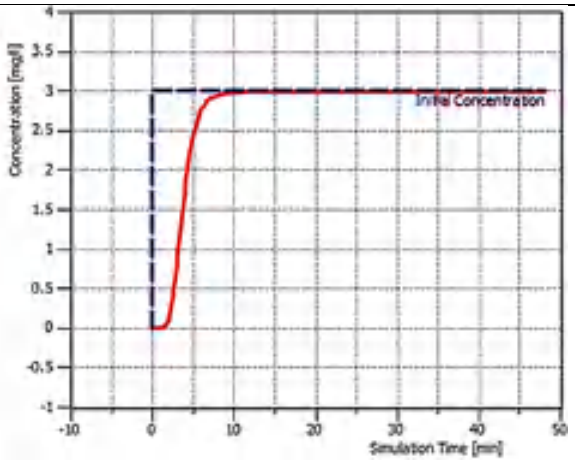

Fe^{2+} - Initial concentration 3 mg/L

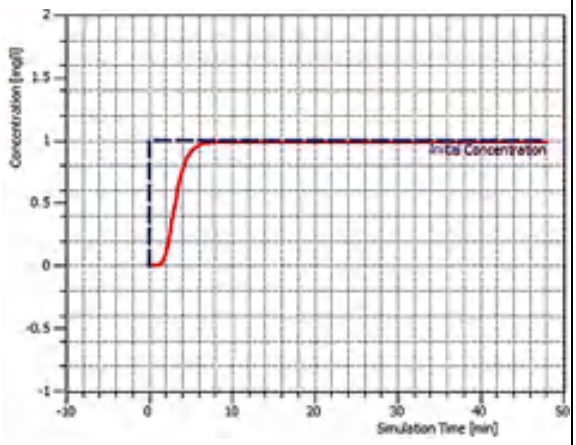

Cu^{2+} - Initial concentration 3.8 mg/L

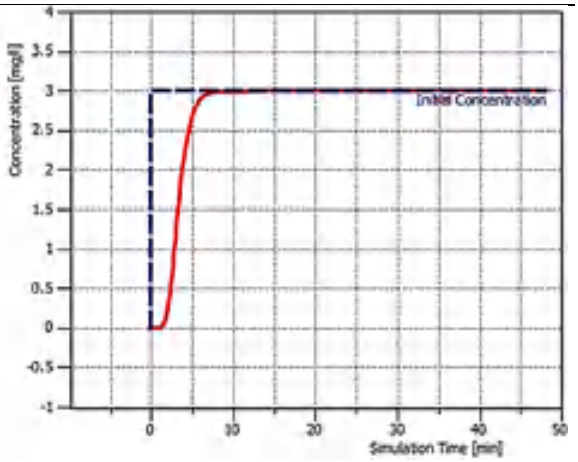

Mn^{2+} - Initial concentration 3.7 mg/L

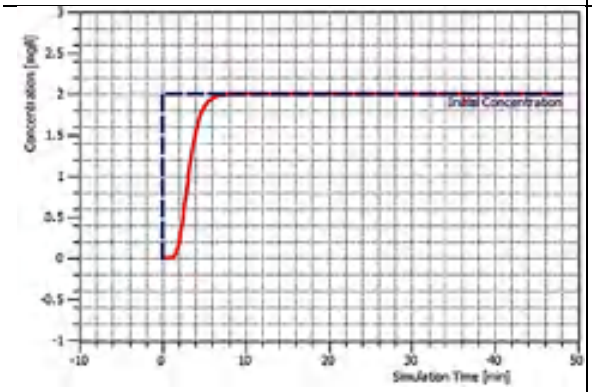

MoO_4^{2-} - Initial concentration 2.5 mg/L

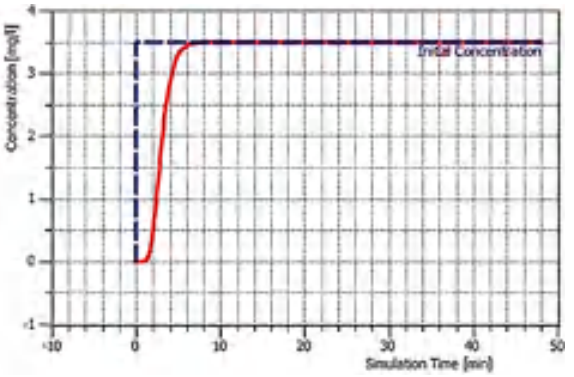

Co^{2+} - Initial concentration 3.7 mg/L

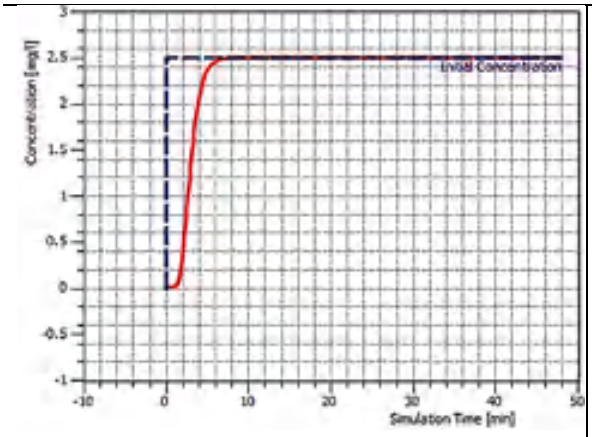

BO_3^{3-} - Initial concentration 2.5 mg/L

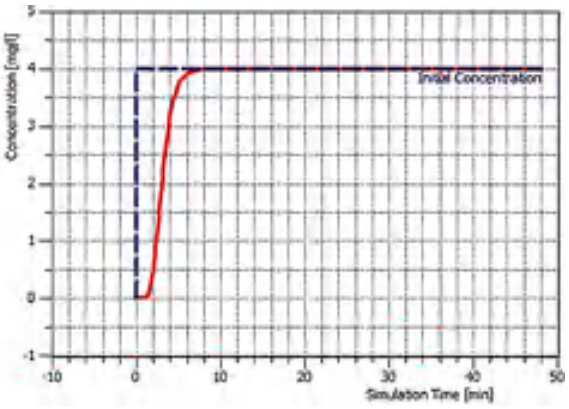

Zn^{2+} - Initial concentration 3.5 mg/L

Calibration of the modeling breakthrough curves with the experimental data is a crucial step to ensure the accuracy and reliability of the model as shown in Annex 3. Under the 10 mL/min infiltration rate, the calibration curve for synthetic wastewater pollutants shows a high degree of alignment between modeling and experimental data. The RMS values, measuring the overall deviation between model predictions and experimental data, are all below 0.10 for every pollutant. This signifies that the model effectively represents the behavior and transport of pollutants within the SAT system at the 10 mL/min infiltration rate. The calibration process ensures that model parameters and assumptions are appropriately adjusted to match model predictions with experimental measurements.

Comparing the two infiltration rates, 10 mL/min and 0.5 mL/min, in terms of breakthrough curves modeling and concentration distribution simulation over the column depth reveals significant differences in pollutant transport. At the higher infiltration rate of 10 mL/min, pollutants move more rapidly due to increased water velocity, leading to faster advection and transport through the soil media. This results in shorter breakthrough times, meaning pollutants reach the outflow point more quickly compared to the 0.5 mL/min infiltration rate. Additionally, simulations show that at the higher infiltration rate, pollutants tend to penetrate deeper into the sand column, potentially reaching greater depths. In contrast, at the lower infiltration rate of 0.5 mL/min, pollutant movement is slower, with longer breakthrough times and more gradual transport. The concentration distribution over the column depth may exhibit a slower decrease in pollutant concentration as they diffuse more slowly within the sand as shown in Annex 3.

The transport parameters, such as adsorption, reaction rate, and molecular diffusion coefficient, provide insights into pollutant behavior. Table 3-3 presents these parameters for infiltration rates of 0.5 mL/min and 10 mL/min, highlighting differences in pollutant transport behavior between the two infiltration rates.

Table 3-3 Pollutants transport parameters in sand media for infiltration flow rates of 0.50 mL/min and 10 mL/min.

Pollutant	Rate (mL/min)	K_d	Reaction rate (1/S)	D_m (m^2/s)	α_L (cm)	α_T (cm)
NH_4^+	0.50	2.30	$2.57*10^{-4}$	$0.16*10^{-9}$	2.8	1.34
	10	0.21	$0.12*10^{-4}$	3.3*10-9	3.1	1.55
PO_4^{3-}	0.50	3.20	$3.17*10^{-4}$	0.8*10-9	2.75	1.30
	10	0.29	$0.11*10^{-4}$	12*10-9	2.95	1.52
SO_4^{2-}	0.50	3.36	$3.28*10^{-4}$	$0.6*10^{-9}$	2.75	1.31
	10	0.31	$0.21*10^{-4}$	9*10-9	3.2	1.42
Fe^{2+}	0.50	2.78	$2.5*10^{-4}$	$2.3*10^{-9}$	2.95	1.4
	10	0.22	$0.18*10^{-4}$	26*10-9	2.99	1.55
Cu^{2+}	0.50	1.40	$0.58*10^{-4}$	$1.3*10^{-9}$	2.95	1.42
	10	0.1	$0.04*10^{-4}$	19*10-9	3.1	1.66
MoO_4^{2-}	0.50	1.28	$0.39*10^{-4}$	$7.2*10^{-9}$	2.90	1.4
	10	0.1	$0.04*10^{-4}$	44*10-9	3.5	1.62
Mn^{2+}	0.50	1.60	$0.72*10^{-4}$	$1.9*10^{-9}$	2.95	1.5
	10	0.11	$0.055*10^{-4}$	38*10-9	2.99	1.6
Zn^{2+}	0.50	1.09	$0.21*10^{-4}$	$7.6*10^{-9}$	2.85	1.5
	10	0.10	$0.04*10^{-4}$	39*10-9	2.96	1.62
Co^{2+}	0.50	0.80	$0.02*10^{-4}$	$1.8*10^{-9}$	2.73	1.5
	10	0.2	$0.005*10^{-4}$	31*10-9	2.86	1.61
BO_3^{3-}	0.50	0.80	$0.02*10^{-4}$	$0.7*10^{-9}$	2.74	1.5
	10	0.2	$0.005*10^{-4}$	8*10-9	2.91	1.67

These parameters are essential for pollutant transport models, contributing to a better understanding of transport mechanisms and the evaluation of the SAT system effectiveness for pollutant removal. When comparing pollutant transport parameters between infiltration rates of 0.50 mL/min and 10 mL/min, several trends are observed for synthetic wastewater pollutants (NH_4^+, PO_4^{3-}, SO_4^{2-}, Fe^{2+}, Cu^{2+}, MoO_4^{2-}, Mn^{2+}, Zn^{2+}, Co^{2+}, and BO_3^{3-}). At 0.50 mL/min, these pollutants show higher adsorption factors (K_d), indicating a stronger tendency to attach to the sand media, leading to lower concentrations in the liquid phase. Moreover, reaction rates are generally higher at 0.50 mL/min, suggesting increased the reaction kinetics due to extended contact time, facilitating more rapid transformations or degradation. The higher adsorbed species mass at 0.50 mL/min indicates efficient pollutant removal through adsorption. In contrast, at 10 mL/min, the dissolved species mass is generally higher, indicating a reduced efficiency of adsorption and a higher effluent pollutant concentration in the liquid phase.

These finding results underscore how infiltration rate impacts pollutant transport mechanisms. A lower infiltration rate (0.50 mL/min) encourages stronger retention with adsorption and reactions, which lead to lower pollutant concentrations in the liquid phase. Conversely, a higher infiltration rate (10 mL/min) shortens the contact time between pollutants and the sand matrix media, resulting in reduced adsorption and higher pollutant concentrations in the liquid phase.

3.3.3 Statistical approach results

The statistical analysis of pollutant concentrations for two infiltration rates (0.50 mL/min and 10 mL/min). A t-test was employed to assess the variations in pollutant concentrations between these two scenarios. The t-test is a common statistical method for comparing two groups and determining if there are significant differences. By comparing mean pollutant concentrations at these infiltration rates, the t-test helps identify statistically significant differences in pollutant removal effectiveness. This approach provides quantitative insights into how different infiltration rates impact pollutants removal and fate under infiltration rates.

For NH_4^+:Two-Sample t-test revealed a highly significant difference in NH_4^+ concentrations between the 0.50 mL/min and 10 mL/min infiltration rates, with a very low p-value (6.158e-09). The negative t-value (-7.163) and the 95 percent confidence interval (-13.393 to -7.513) indicate that NH_4^+ concentrations were significantly lower at the 0.50 mL/min infiltration rate (mean of approximately 18.79) compared to the 10 mL/min rate (mean of approximately 29.24). This suggests that the higher infiltration rate of 10 mL/min is associated with increased NH_4^+ concentrations, emphasizing the impact of infiltration rates on pollutant. Figure 3-13 presents the box plot comparisons of NH_4^+ concentrations under the infiltration rates (0.50 mL/min and 10 mL/min).

For NO_3^-: Two-Sample t-test results indicate a statistically significant difference in NO_3^- concentrations between the two infiltration rates (0.50 mL/min and 10 mL/min), with a low p-value of 7.855e-05. The positive t-value (4.775) and the 95 percent confidence interval (5.88 to 14.87) suggest that NO_3^- concentrations were significantly higher at the 0.50 mL/min infiltration rate (mean of approximately 12.29) compared to the 10 mL/min rate (mean of approximately 1.92). This highlights a substantial disparity in NO_3^- concentration levels between the two infiltration scenarios. Figure 3-13 presents the box plot comparisons of NO_3^- concentrations under the infiltration rates (0.50 mL/min and 10 mL/min).

For NO_2^-: Two-Sample t-test results indicate a statistically significant difference in NO_2^- concentrations between the two infiltration rates (0.50 mL/min and 10 mL/min), with a p-value of 0.0074. The positive t-value (2.86) and the 95 percent confidence interval (0.0050 to 0.0298) suggest that NO_2^- concentrations were significantly higher at the 0.50 mL/min infiltration rate (mean of approximately 0.0359) compared to the 10 mL/min rate (mean of approximately 0.0185). This finding demonstrates a notable difference in NO_2^- concentration levels between the two infiltration scenarios, with higher levels observed at the 0.50 mL/min rate. Figure 3-13 presents the box plot comparisons of NO_2^- concentrations under the infiltration rates (0.50 mL/min and 10 mL/min).

For PO_4^{3-}: Two-Sample t-test results reveal an extremely significant difference in PO_4^{3-} concentrations between the two infiltration rates (0.50 mL/min and 10 mL/min), with a p-value of less than 2.2e-16. The very negative t-value (-22.024) and the 95 percent confidence interval (-17.696 to -14.721) indicate that PO_4^{3-} concentrations were significantly lower at the 0.50 mL/min infiltration rate (mean of approximately 1.29) compared to the 10 mL/min rate (mean of approximately 17.50). This finding demonstrates a substantial contrast in PO_4^{3-} concentration levels between the two infiltration scenarios, with considerably lower levels at the 0.50 mL/min rate. Figure 3-13 presents the box plot comparisons of PO_4^{3-} concentrations under the infiltration rates (0.50 mL/min and 10 mL/min).

For SO_4^{2-}: Two-Sample t-test results show an extremely significant difference in SO_4^{2-} concentrations between the two infiltration rates (0.50 mL/min and 10 mL/min), with a p-value of less than 2.2e-16. The highly negative t-value (-27.64) and the 95 percent confidence interval (-18.02 to -15.57) indicate that SO_4^{2-} concentrations were substantially lower at the 0.50 mL/min infiltration rate (mean of approximately 1.792) compared to the 10 mL/min rate (mean of approximately 18.583). This analysis highlights a substantial disparity in SO_4^{2-} concentration levels between the two infiltration scenarios, with markedly lower levels at the 0.50 mL/min rate. Figure 3-13 presents the box plot comparisons of SO_4^{2-} concentrations under the infiltration rates (0.50 mL/min and 10 mL/min).

For Fe^{2+}: Two-Sample t-test results indicate a highly significant difference in Fe^{2+} concentrations between the two infiltration rates (0.50 mL/min and 10 mL/min), with a p-value of less than 2.2e-16. The strongly negative t-value (-20.10) and the 95 percent confidence interval (-2.496 to -2.037) reveal that Fe^{2+} concentrations were considerably lower at the 0.50 mL/min infiltration rate (mean of approximately 0.38) compared to the 10 mL/min rate (mean of approximately 2.65). This analysis underscores a substantial disparity in Fe^{2+} concentration levels between the two infiltration scenarios, with notably lower levels at the 0.50 mL/min rate. Figure 3-13 presents the box plot comparisons of Fe^{2+} concentrations under the infiltration rates (0.50 mL/min and 10 mL/min).

For Cu^{2+}: Two-Sample t-test results for Cu^{2+} concentrations indicate no statistically significant difference between the two infiltration rates (0.50 mL/min and 10 mL/min), with a p-value of 0.153, suggesting that Cu^{2+} concentrations are not significantly different between the two scenarios. The t-value is 1.47, and the 95 percent confidence interval ranges from -0.040 to 0.243, implying that there is no substantial variation in Cu^{2+} concentration levels between the two infiltration rates. The means of Cu^{2+} concentrations at the low (0.618) and high (0.517) infiltration rates are quite close, further supporting the lack

of a significant difference between them. Figure 3-13 presents the box plot comparisons of Cu^{2+} concentrations under the infiltration rates (0.50 mL/min and 10 mL/min).

For Mn^{2+}: Two-Sample t-test results for Mn^{2+} concentrations show no statistically significant difference between the two infiltration rates (0.50 mL/min and 10 mL/min), as indicated by a p-value of 0.214. This suggests that Mn^{2+} concentrations do not significantly differ between the two scenarios. The t-value is -1.262, and the 95 percent confidence interval ranges from -0.699 to 0.162, indicating that there is no substantial variation in Mn^{2+} concentration levels between the two infiltration rates. The means of Mn^{2+} concentrations at the low (1.69) and high (1.95) infiltration rates are relatively close, further supporting the lack of a significant difference between them. Figure 3-13 presents the box plot comparisons of Mn^{2+} concentrations under the infiltration rates (0.50 mL/min and 10 mL/min).

For MoO_4^{2-}: Two-Sample t-test results for MoO_4^{2-} concentrations indicate a statistically significant difference between the two infiltration rates (0.50 mL/min and 10 mL/min) with a very low p-value (< 2.2e-16). This suggests that MoO_4^{2-} concentrations significantly vary between the two scenarios. The t-value is -20.653, and the 95 percent confidence interval ranges from -0.89 to -0.73, emphasizing the substantial difference in MoO_4^{2-} concentration levels. The mean MoO_4^{2-} concentration at the low infiltration rate (1.68) is notably lower than that at the high infiltration rate (2.49), confirming the significant difference in MoO_4^{2-} concentrations between the two infiltration rates. Figure 3-13 presents the box plot comparisons of MoO_4^{2-} concentrations under the infiltration rates (0.50 mL/min and 10 mL/min).

For Zn^{2+}: Two-Sample t-test results for Zn^{2+} concentrations indicate a statistically significant difference between the two infiltration rates (0.50 mL/min and 10 mL/min) with a p-value of 0.012. This suggests that Zn^{2+} concentrations significantly vary between the two scenarios. The t-value is -2.69, and the 95 percent confidence interval ranges from -1.5 to -0.19, indicating a notable difference in Zn^{2+} concentration levels. The mean Zn^{2+} concentration at the low infiltration rate (2.65) is lower than that at the high infiltration rate (3.48), confirming the significant difference in Zn^{2+} concentrations between the two infiltration rates. Figure 3-13 presents the box plot comparisons of Zn^{2+} concentrations under the infiltration rates (0.50 mL/min and 10 mL/min).

For Co^{2+}: Two-Sample t-test results for Co^{2+} concentrations reveal a p-value of 0.081, suggesting that there is no statistically significant difference in Co^{2+} concentrations between the two infiltration rates (0.50 mL/min and 10 mL/min). The t-value is -1.82, and the 95 percent confidence interval spans from -0.80 to 0.05, indicating that the Co^{2+}

concentration means are quite similar. The mean Co^{2+} concentration at the low infiltration rate is 3.14, while it is slightly higher at 3.51 for the high infiltration rate. However, the p-value suggests that this difference is not statistically significant. Figure 3-13 presents the box plot comparisons of Co^{2+} concentrations under the infiltration rates (0.50 mL/min and 10 mL/min).

For BO_3^{3-}: Two-Sample t-test results for BO_3^{3-} concentrations indicate a highly significant difference with a very low p-value of 5.785e-08. The t-value is 7.53, and the 95 percent confidence interval ranges from 0.15 to 0.26. These results suggest that there is a statistically significant difference in BO_3^{3-} concentrations between the two infiltration rates (0.50 mL/min and 10 mL/min). The mean BO_3^{3-} concentration at the low infiltration rate is 2.49, while it is slightly lower at 2.29 for the high infiltration rate. This difference in means is statistically significant, indicating that BO_3^{3-} concentrations vary significantly between the two infiltration rates. Figure 3-13 presents the box plot comparisons of BO_3^{3-} concentrations under the infiltration rates (0.50 mL/min and 10 mL/min).

Figure 3-13: Box plot comparison of pollutant concentrations between infiltration rates

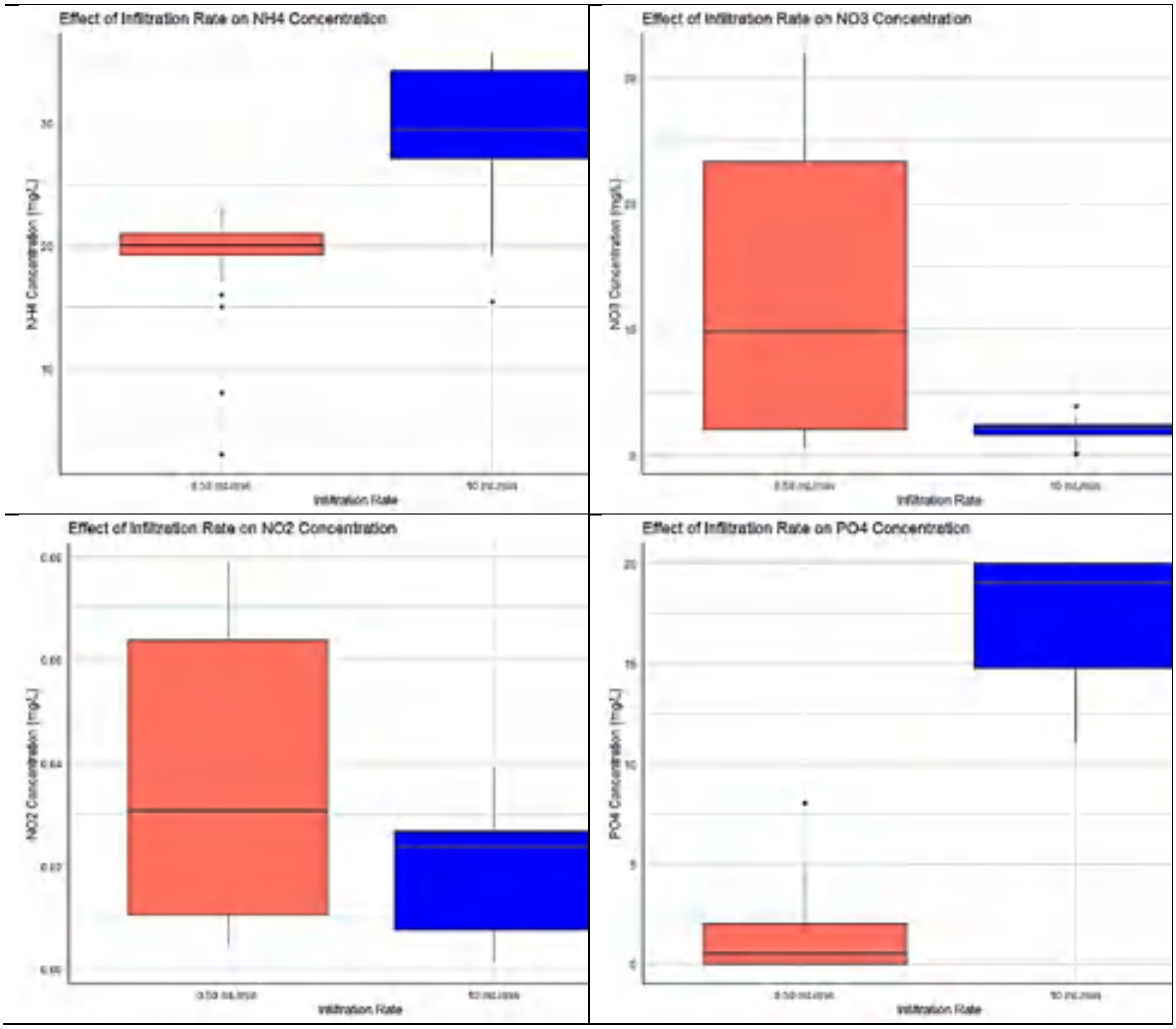

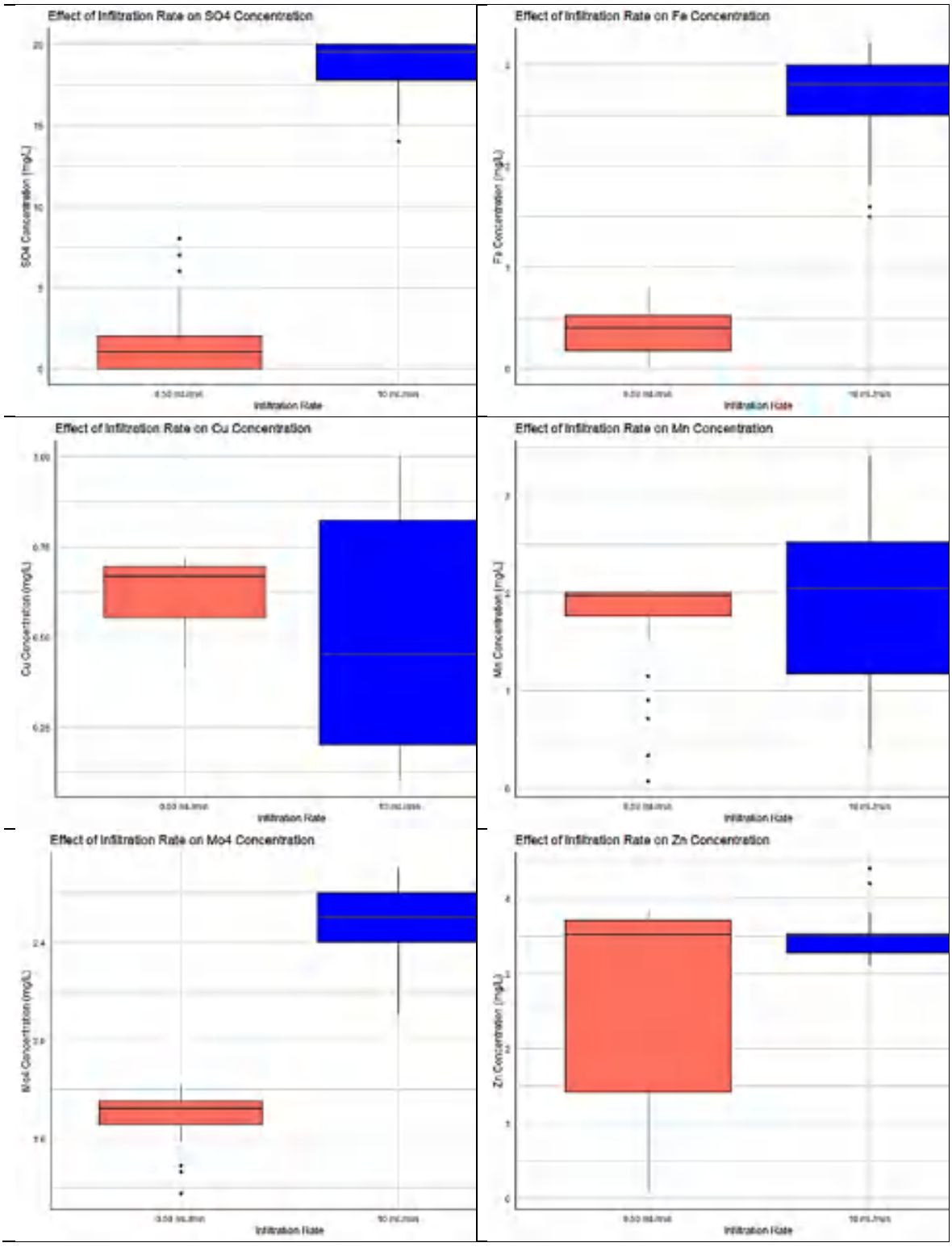
Effect of Infiltration Rate on SO4 Concentration
SO4 Concentration (mg/L)
Infiltration Rate
Effect of Infiltration Rate on Fe Concentration
Fe Concentration (mg/L)
Infiltration Rate
Effect of Infiltration Rate on Cu Concentration
Cu Concentration (mg/L)
Infiltration Rate
Effect of Infiltration Rate on Mn Concentration
Mn Concentration (mg/L)
Infiltration Rate
Effect of Infiltration Rate on Mo4 Concentration
Mo4 Concentration (mg/L)
Infiltration Rate
Effect of Infiltration Rate on Zn Concentration
Zn Concentration (mg/L)
Infiltration Rate

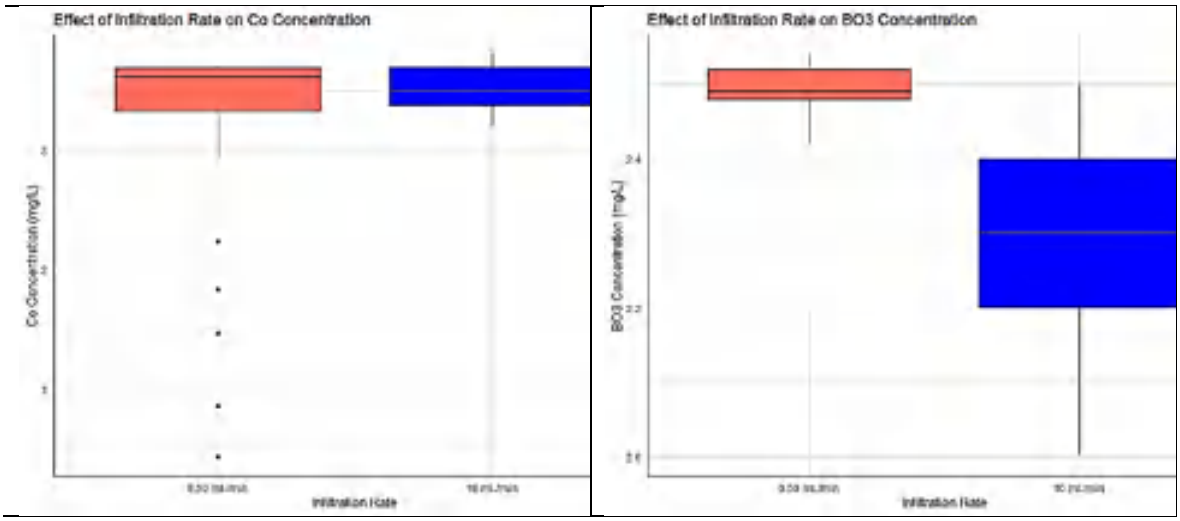

3.4 Conclusion

The comparison between the infiltration rates scenarios of 0.5 mL/min and 10 mL/min, based on the experimental, modelling, and statistical results, provides valuable insights into the behavior and removal efficiency of various pollutants. Experimental Results: The experimental breakthrough curves revealed distinct trends for different pollutants under the two infiltration rates. At 0.50 mL/min as slow infiltration rate demonstrated higher removal efficiency for all synthetic wastewater pollutants (NH_4^+, NO_3^-, NO_2^-, PO_4^{3-}, SO_4^{2-}, Fe^{2+}, Cu^{2+}, Mn^{2+}, MoO_4^{2-}, Zn^{2+}, Co^{2+}, and BO_3^{3-}). This indicates that the lower infiltration rate allows for longer contact time between the pollutants and the soil media, enhancing adsorption, and biogeochemical reaction that enhance the removal capacity comparing with high infiltration rate 10 mL/min. Modelling Results: The modelling of breakthrough curves and 2-D spatial concentration distributions further supported the experimental findings. The simulations captured the behavior of pollutants over time and their distribution within the soil media depth. The modelling results confirmed the observed trends, highlighting the pollutants transport through time and depth profiles at the higher infiltration rate of 10 mL/min compared to the 0.5 mL/min infiltration rate. Statistical Analysis: The t-test analyses were conducted to statistically compare the two infiltration rates scenarios. The obtained p-values indicated the significance of the differences in pollutant removal between the infiltration rates. Specifically, NO_3^-, NO_2^-, Cu^{2+}, and BO_3^{3-} showed significantly higher removal at the 10 mL/min infiltration rate, while NH_4^+, PO_4^{3-}, SO_4^{2-}, Fe^{2+}, Mn^{2+}, MoO_4^{2-}, Zn^{2+}, and Co^{2+} exhibited better removal at 0.50 mL/min infiltration rate. These statistical analyses provided robust evidence to support the experimental and modelling results. In summary, the comparison between the infiltration rates scenarios revealed varying removal efficiencies for different pollutants. The slower infiltration rate of 0.5 mL/min favored for almost of infiltrated synthetic wastewater pollutants retired to longer contact and retention time which increase the interactions between pollutants and sand matrix that increase the adsorption

capacity, microbial activity, equilibrium conditions, and geochemical reactions causing to increasing the removal capacity for these pollutants through the SAT systems.

4. Quantifying the influence of dynamic pulsed of wetting and drying on the transformation and fate of synthetic wastewater pollutants in soil aquifer treatment system

4.1. Introduction

The dynamics of drying and wetting cycles have a significant influence on the behavior, transformation, and removal efficiency of synthetic wastewater pollutants in soil aquifer treatment systems. The redistribution of pollutants, changes in microbial activity, availability of oxygen, alterations in soil structure and porosity, adsorption-desorption processes, and leaching and transport dynamics all contribute to the overall performance of the system. Understanding these effects is vital for designing and optimizing SAT systems to achieve effective pollutant removal and protect water resources. Therefore, investigating the influence of continuous short-term durations of wetting and drying on the behavior and fate of synthetic wastewater pollutants in SAT systems will provide valuable insights for improving system performance and ensuring sustainable water management.

4.2. Materials and methods

A lab-scale glass column with a 3 cm inner diameter and 40 cm depth was utilized to simulate soil aquifer treatment system by incorporating sand soil as the filtration media up to 30 cm of depth in a controlled laboratory setting. Synthetic wastewater with a range of pollutants was introduced into the column through a peristaltic pump as shown in table 4-1, following a controlled infiltration rate of 0.5 mL/min. The total daily amount of infiltrated synthetic wastewater was 200 mL/day, and this amount was into a wetting period of 8 hours and a drying period of 16 hours. This wetting and drying cycle was repeated continuously of 4 days. Throughout the experiment, samples were collected at regular intervals to measure the concentration of pollutants, including NH_4^+, NO_2^-, NO_3^-, PO_4^{3-}, SO_4^{2-}, Fe^{2+}, Cu^{2+}, Mn^{2+}, MoO_4^{2-}, Zn^{2+}, Co^{2+}, and BO_3^{3-}. Additionally, physiochemical parameters such as soil water content, pH, dissolved oxygen (DO), and oxidation-reduction potential (ORP) were measured for each collected sample. The experimental procedures were replicated three times to enhance the precision and reliability of the experimental outcomes. In conjunction with these measurements, a comprehensive series of statistical analyses were conducted to explore the relationships and interactions between pollutant concentrations and the varying wet and dry conditions. All plots, statistical analyses, and visualizations were executed using the R programming language. The experimental procedures were iteratively conducted three times to enhance the reliability and confidence in the obtained results. Subsequently, confidence intervals were calculated for each of the three experimental replications using t-test analysis, illustrating the mean and 95% confidence intervals. A comparative analysis was performed to identify the experimental replication

characterized by a high mean and lower confidence interval values, signifying greater accuracy and confidence in the experimental outcomes. The graphical representation of these confidence intervals is provided in Annex 2.

Table 4-1 The chemical composition for the synthetic wastewater effluent

Chemical Composition	Mass (mg/1L)	Chemical Composition	Mass (mg/1L)
$CH_3COONa.3H_2O$	130	H_3BO_3	15
NH_4Cl	100	$CuSO_4.5H_2O$	15
KH_2PO_4	175	KI	15
$MgSO_4 \cdot 7H_2O$	100	$MnSO_4.4H_2O$	15
$CaCl_2 \cdot 2H_2O$	15	$(NH_4)6Mo_7O_{24}.4H_2O$	5
$NaHCO_3$	200	$ZnSO_4.7H_2O$	15
KCl	35	$CoCl_2.6\ H_2O$	15
EDTA	500	Yeast extract	200
$FeCl_3.6H_2O$	15	Peptone	200

In addition to pollutant concentrations measurements, several physicochemical parameters such as soil water content (WC%), pH, dissolved oxygen (DO), and oxidation-reduction potential (ORP) were determined for each sample collected as shown in figure 4-1, 4-2, 4-3, 4-4. These parameters were selected to investigate how drying and wetting conditions influenced pollutant behavior and removal efficiency.

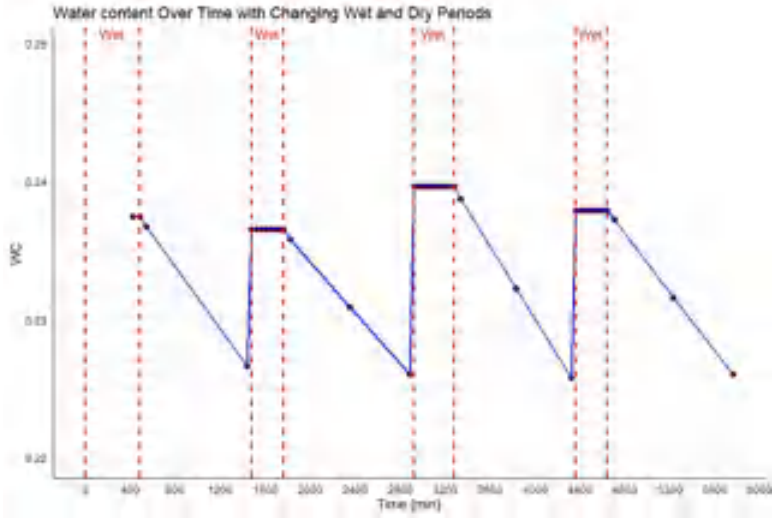

Figure 4-1 Water content during wet and dry periods in the sand column of the SAT system

The water content (WC), representing the moisture content in the soil filtration media, plays a pivotal role in the behavior of synthetic wastewater pollutants within the soil aquifer treatment system. During the wetting phase, as synthetic wastewater infiltrates the system, WC% increases, enhancing the transport and interaction between pollutants and the soil matrix. Conversely, in the drying phase, WC% decreases, restricting pollutant mobility. Figure 4-1 illustrates the dynamic shifts in WC during wet and dry periods. On the

first day, the wetting phase elevated WC% to 23.75%, followed by a decline to 22.66% during the subsequent drying phase. This pattern continued in a similar trend on the second, third, and fourth days, reflecting the cyclic nature of wetting and drying. These fluctuations have significant implications for pollutant behavior, affecting processes like diffusion, adsorption, and microbial activity within the soil aquifer treatment system, thereby influencing pollutant transformation and removal. The observed WC% changes emulate natural hydrological cycles, mirroring the environment's dynamic processes.

During the wet and dry periods in the sand column of the soil aquifer treatment system, the pH, DO, and ORP values exhibited varying patterns, as shown in Figure 4-2.

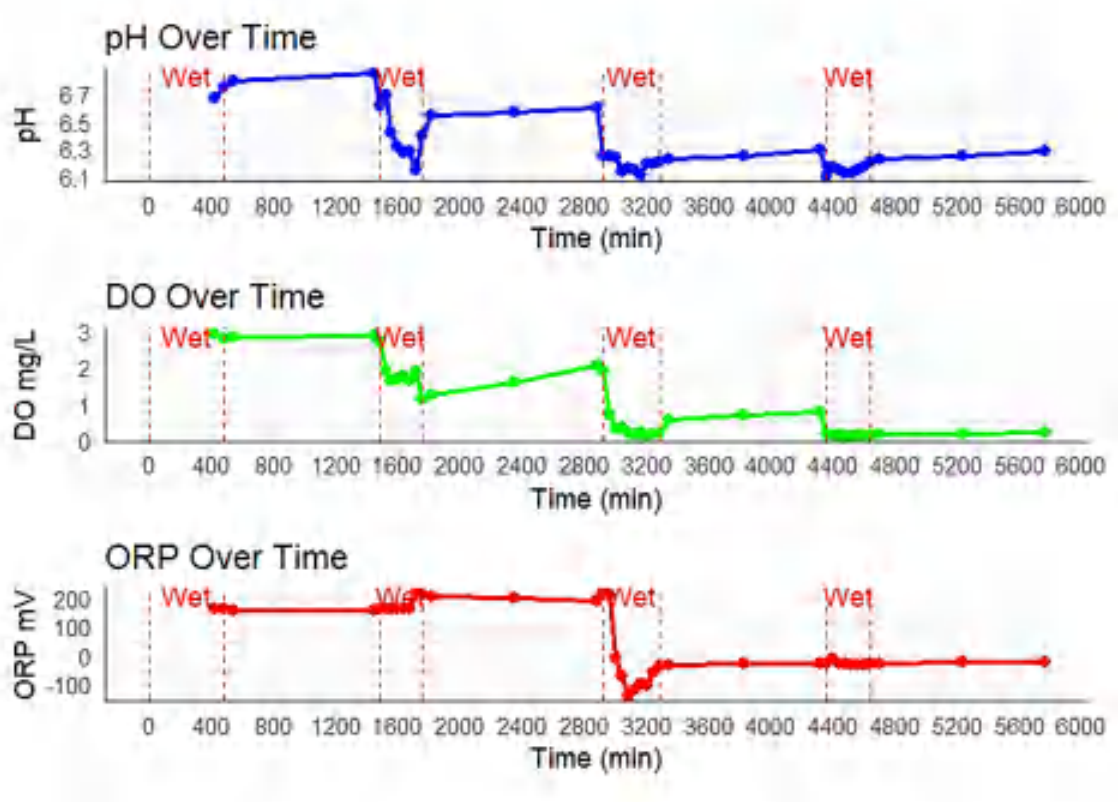

Figure 4-2 pH, DO, and ORP level during wet and dry periods in the sand column of the SAT system

Figure 4-2 illustrates the pH variations in the sand column of the soil aquifer treatment system during wet and dry periods. Initially, the pH of the sand infiltrate media was 6.85, while the synthetic wastewater had a pH of 6.5. On the first day, the pH dropped slightly to 6.75 during the wetting phase, potentially due to acidic components in the synthetic wastewater and microbial activity. As the system transitioned to the drying period, the pH increased to 6.85, possibly resulting from the evaporation of water, concentrating alkaline compounds. A similar pattern of pH changes continued on the second, third, and fourth days, reflecting the dynamic nature of the system. These fluctuations are influenced

by factors like acidic components in the wastewater, microbial activity, dilution effects, and mineral dissolution and precipitation. The observed pH shifts highlight the complex interplay of chemical and physical processes within the system, influenced by the synthetic wastewater composition, sand media characteristics, and environmental conditions.

Dissolved oxygen (DO) represents the amount of oxygen present in the wastewater. It is an essential factor for the activity of aerobic microorganisms responsible for biodegradation and removal of organic pollutants. The changes observed in the dissolved oxygen (DO) concentrations during the wet and dry periods in figure 4-2 can be attributed to several factors related to microbial activity and the physicochemical processes occurring in the sand column. The dynamics of dissolved oxygen (DO) concentration in the synthetic wastewater infiltrated sand column during wet and dry periods reveal a complex interplay of factors. Initially, during the wetting period, the DO concentration was 2.91 mg/L on the first day, gradually declining to 2.78 mg/L by the wet phase's end. This decrease can be attributed to microbial respiration and the oxygen consumption by microorganisms within the sand column. These microorganisms metabolize organic matter, leading to a reduction in DO levels. In contrast, during the subsequent dry period, the DO concentration increased to 2.81 mg/L at the beginning of the drying phase, gradually rising to 2.86 mg/L by the end. This increase in DO during drying is due to limited water availability, allowing for enhanced oxygen transfer and replenishment. As water content decreases, the improved surface area for gas exchange promotes oxygen diffusion into the system.

On the second, third, and fourth days, a similar pattern was observed: DO concentration dropped during the wetting period, reaching lows attributed to increased microbial activity and organic matter degradation. During the subsequent dry period, DO concentration exhibited a gradual increase due to enhanced oxygen transfer as water content decreased and the system became less saturated. The fluctuations in DO levels are a result of factors such as oxygen consumption during wetting, limited oxygen transfer during wetting, oxygen replenishment during drying, and microbial activity.

Oxidation-reduction potential (ORP) measures the electron transfer potential of a solution and provides an indication of the redox conditions. ORP influences the oxidation and reduction reactions that occur during the degradation and transformation of pollutants. During the wetting period, the ORP may change due to the presence of different oxidizing or reducing agents in the synthetic wastewater. These variations in ORP can impact the rates of pollutant degradation and transformation. The changes observed in the oxidation-reduction potential (ORP) values during the wet and dry periods, as shown in Figure 4-2, reflect the redox reactions and the shifting balance between oxidizing and reducing

conditions in the sand column. The oxidation-reduction potential (ORP) within the sand column exhibited dynamic changes during wet and dry periods, reflecting the interplay of multiple factors. On the first and second days, during the wetting phase, indicating towards more oxidizing conditions due to enhanced oxygen availability and oxidation reactions. In the dry period, ORP decreased.

The third day presented complex ORP changes. During wetting, ORP initially increased, then suddenly dropped to -13.6 mV, signifying a significant shift towards reducing conditions. This sharp decrease resulted from oxygen depletion and the presence of reduced species, likely stemming from microbial activity. Oxygen consumption by microorganisms can exceed supply, prompting anaerobic respiration and the accumulation of reduced compounds, leading to the highly reducing environment. During drying, ORP gradually increased, suggesting a transition towards less reducing conditions. On the fourth day, ORP remained stable during wetting, indicating persistent reducing conditions. In the subsequent drying period, ORP gradually increased, marking a shift towards less reducing conditions.

These ORP changes are influenced by factors such as oxygen availability, microbial activity, and the presence of organic matter. Wetting brings in dissolved oxygen from the infiltrated wastewater, increasing oxygen availability and leading to more oxidizing conditions. Microbial activity and organic matter breakdown then contribute to decreasing ORP during wetting. In the drying phase, limited oxygen leads to more reducing conditions as aerobic microbial activity wanes. Microbial activity and the interplay between oxidation and reduction reactions are key determinants of ORP dynamics during wet and dry periods.

The physiochemical parameters (pH, DO, and ORP) are used as wet/dry conditions factors which are considered as the main changeable parameters for the whole system under continuous changing of dry and wet periods. a logistic regression model used to explore the significant of these parameters. The logistic regression model was constructed to assess the sufficiency of physiochemical parameters, namely pH, ORP (oxidation-reduction potential), and DO (dissolved oxygen), in describing the wet and dry conditions and their impact on pollutant removal capacity. The coefficients for the model are as follows: pH with p-value = 0.0134, ORP: with p-value = 0.0499, and DO with p-value = 0.0388, which indicate to statistically significant effects on the wet and dry conditions and their influence on pollutant removal capacity. pH, DO, and ORP seem to be important predictors to significantly impact the condition represented by wet/dry periods.

4.3. Results and discussions

The wet and dry cycles in soil aquifer treatment systems have a significant impact on the removal and behavior of pollutants. By correlating and examining the relationship between wetting and drying factors (pH, DO, and ORP) and the changing concentrations of pollutants, we can gain a better understanding of the mechanisms driving pollutants removal during wet and dry cycles.

4.3.1. Ammonium (NH_4^+) interplay with wet and dry conditions

The breakthrough curve for NH_4^+ through the sand column during the wet and dry time over a 4-day column experiment with initial concentration 35 mg/L is shown in figure 4-3.

Figure 4-3 Breakthrough curve of NH_4^+ concentration performance in the sand column of the SAT system during wet and dry periods

Figure 4-3 outlines the NH_4^+ concentration changes in a sand column wastewater treatment system over a four-day period, involving alternating wet and dry cycles. Notable patterns include NH_4^+ concentration increases during wetting periods, attributed to ammonium release from synthetic wastewater, followed by slightly decreases during drying periods, likely due to increased adsorption onto sand particles, and potential microbial processes. The overall findings indicate the effective removal of NH_4^+ from the wastewater, with the sand column successfully adsorbing and degrading a substantial portion of the initial NH_4^+ concentration, which commenced at 35 mg/L. The removal mechanisms involved physical adsorption onto sand particles and potential microbial processes leading to NH_4^+ degradation or transformation.

To analyze the interaction between NH_4^+ concentration and the wetting and drying conditions, we examined the relationship, correlations and factorial interactions between NH_4^+ concentration and wet/dry key factors as pH, dissolved oxygen (DO), and oxidation-reduction potential (ORP) during both wet and dry times. The regression model revealed

significant relationships between NH_4^+ concentration and these factors, with respective p-values of 0.000053 for DO, 0.000031 for ORP, 0.01014 for pH, and 0.0575 for the wet/dry status. Additionally, the overall model was highly significant with a p-value of 1.64e-11, suggesting that the combined influence of these factors on NH_4^+ concentration is substantial. This analysis provides valuable insights into the complex relationships between NH_4^+ and the wet/dry variables during wet and dry periods, indicating their collective impact on NH_4^+ dynamics. The correlation analysis revealed strong negative relationships between NH_4^+ concentration and key wet/dry factors: -0.87 with DO, -0.47 with ORP, and -0.86 with pH. These findings signify that as DO, ORP, and pH values fluctuate during wet and dry conditions, NH_4^+ concentration experiences corresponding changes in the opposite direction. The high negative correlations emphasize the significant influence of these factors on NH_4^+ dynamics, underscoring their pivotal roles in shaping NH_4^+ behavior within the system and demonstrating the intricate interplay between environmental variables and pollutant concentration.

To analyze the factorial interaction between NH_4^+ concentration and the wetting and drying conditions, the interaction relationships trend examined between NH_4^+ concentration and key parameters such as pH, dissolved oxygen (DO), and oxidation-reduction potential (ORP) during both wet and dry times as shown in figure 4-4.

The factorial interaction analysis based on the regression model highlights the intricate relationships between NH_4^+ concentration and wet/dry parameters, specifically DO, pH, and ORP during both wet and dry periods. The results indicate that as DO, pH, and ORP increase during wet and dry times, there is a corresponding decrease in NH_4^+ concentration. This finding aligns with the correlation analysis, which demonstrated strong negative correlations between NH_4^+ and these parameters. The alignment between the observed decrease in NH_4^+ concentration with increasing DO, pH, and ORP also corresponds to the requirements for nitrification degradation in which NH_4^+ is converted into nitrite (NO_2^-) and then nitrate (NO_3^-), which ultimately results in the removal of ammonium from the system (Gharbia et al., 2024). This process is highly dependent on the availability of dissolved oxygen (DO), pH, and oxidation-reduction potential (ORP) (Zeng et al., 2018). Adequate DO levels support the activity of nitrifying bacteria, while specific pH conditions and ORP values are conducive to their growth and nitrification activity (Li et al., 2019). Together, these results confirm that the increase in DO, pH, and ORP exerts a controlling effect on reducing NH_4^+ concentration, emphasizing the significant influence of these environmental factors on NH_4^+ dynamics within the system (Gharbia et al., 2024).

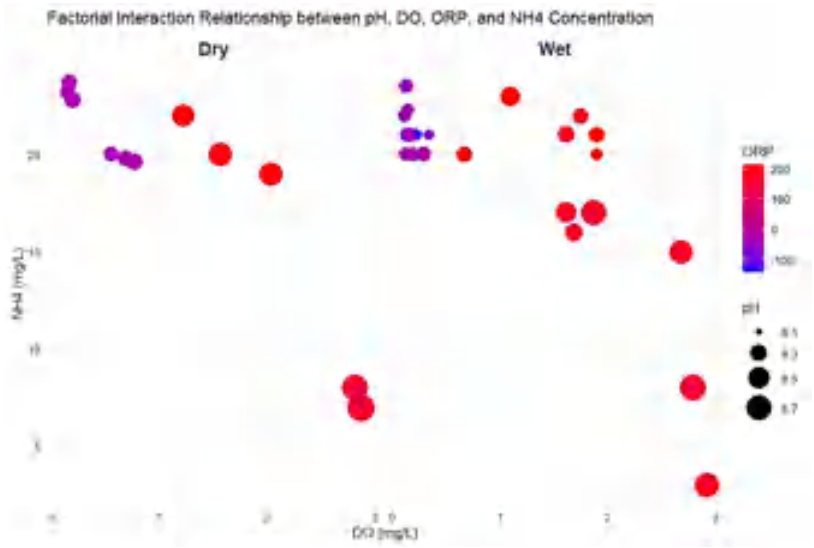

Figure 4-4 Factorial interaction relationships between NH_4^+ and wet/dry parameters

To summarize the effect of wet and dry periods on the NH_4^+ concentration the box plot used to visualize the favorable period for NH_4^+ removal conditions as shown in figure 4-5. The box plot analysis aimed to understand the impact of wet and dry periods on NH_4^+ concentration. The results show that there is a small difference in mean NH_4^+ concentration between wet and dry times, with the dry period exhibiting slightly lower values. This suggests that NH_4^+ removal conditions are favorable during the dry period which is aligns with Abel (2014), (Gharbia et al., 2024)and Ma et al. (2023) . In summary, the dry period is associated with a slightly lower NH_4^+ concentration, implying better NH_4^+ removal during this time compared to the wet period.

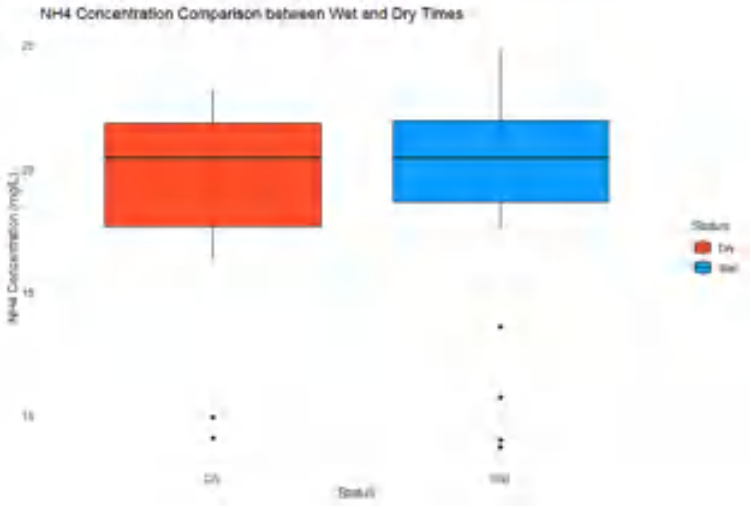

Figure 4-5 Box plot for NH_4^+ concentration during wet and dry periods

4.3.2. Nitrite (NO_2^-) interplay with wet and dry conditions

The breakthrough curve for NO_2^- through the sand column during the wet and dry time periods over a 4-day experiment with initial concentration 0 mg/L is shown in figure 4-6.

Figure 4-6 Breakthrough curve of NO_2^- concentration performance in the sand column of the SAT system during wet and dry periods

The experimental results illustrate the formation and behavior of NO_2^- as a byproduct of NH_4^+ oxidation through the nitrification process. Breakthrough curves (BTCs) for NO_2^- during the wet and dry periods of the 4-day column experiment reveal specific patterns. On the first day, the NO_2^- concentration increased from 0.006 mg/L to 0.012 mg/L during the wet period, remaining constant at 0.012 mg/L in the dry period. The second day exhibited fluctuations, with an initial increase to 0.018 mg/L, followed by a decrease to 0.012 mg/L and a gradual decline to 0.006 mg/L. Similar fluctuations were observed on the third day, with a stable NO_2^- concentration of 0.08 mg/L. The fourth day saw consistent NO_2^- concentrations of 0.064 mg/L during both wet and dry periods. These results indicate that nitrification in the sand column led to NO_2^- generation from NH_4^+ oxidation, with varying concentrations during wet and dry periods. The stable concentrations imply a relatively consistent nitrification process, shedding light on NH_4^+ behavior and NO_2^- formation in the soil aquifer treatment system.

In analysis of the interaction between NO_2^- concentration and wetting and drying conditions, the explored of the relationships, correlations, and factorial interactions between NO_2^- concentration and key factors, including pH, dissolved oxygen (DO), and oxidation-reduction potential (ORP), during both wet and dry periods. The regression model revealed significant relationships, with a p-value of 0.00000012 for ORP, indicating a strong influence. The p-values for DO, Wet/dry status, and the overall model were 0.0871, 0.0082, and 9.711e-16, respectively. These findings suggest that ORP and Wet/dry status have substantial impacts on NO_2^- concentration, highlighting their importance in understanding the behavior of NO_2^- under varying wet and dry conditions. In the correlation analysis between NO_2^- concentration and wet/dry factors, the results indicate the following correlation coefficients: a strong negative correlation of -0.89 with dissolved oxygen (DO),

a very strong negative correlation of -0.97 with oxidation-reduction potential (ORP), and a moderate negative correlation of -0.72 with pH. These coefficients suggest that DO and ORP have a significant inverse relationship with NO_2^- concentration, while the correlation with pH is moderately negative, indicating its influence on NO_2^- behavior under wet and dry conditions.

To analyze the factorial interaction between NO_2^- concentration and the wetting and drying conditions, the interaction relationships trend examined between NO_2^- concentration and key parameters such as pH, dissolved oxygen (DO), and oxidation-reduction potential (ORP) during both wet and dry times as shown in figure 4-7.

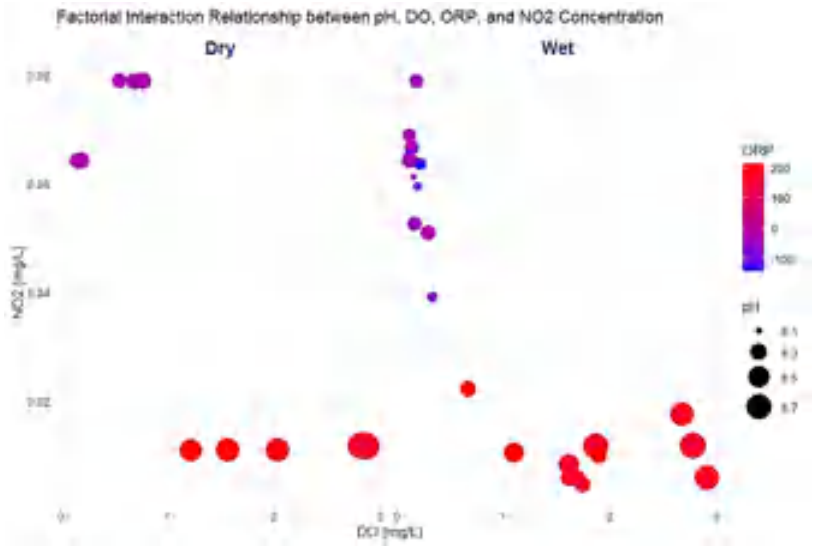

Figure 4-7 Factorial interaction relationships between NO_2^- and wet/dry parameters

The factorial interaction relationships derived from the regression model between NO_2^- concentration and wet/dry parameters reveal the dynamic interactions between NO_2^- and key factors, including dissolved oxygen (DO), pH, and oxidation-reduction potential (ORP), during wet and dry periods. The general trend observed is that as DO, pH, and ORP increase during both wet and dry times, the NO_2^- concentration decreases. This observation aligns with the negative correlations established in the correlation analysis, indicating that these factors exert control over NO_2^- concentration. Additionally, the findings are consistent with the nitrification process, where NO_2^- serves as an intermediate product in the conversion of NH_4^+ to NO_3^- (Li et al., 2019). As NO_2^- is produced from the nitrification of NH_4^+, the decrease in NO_2^- concentration is indicative of ongoing nitrification, supporting the notion that NO_2^- is a transitional stage in the oxidation of NH_4^+.

To summarize the effect of wet and dry periods on the NO_2^- concentration the box plot used to visualize the favorable period for NO_2^- removal conditions shown in figure 4-8.

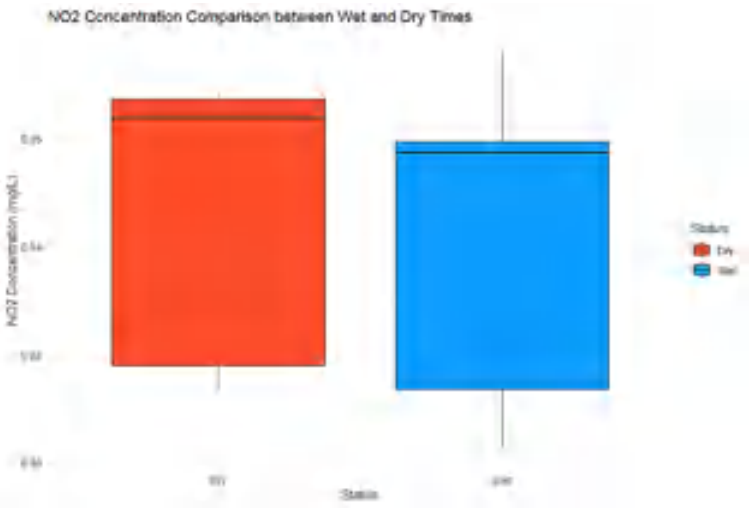

Figure 4-8 Box plot for NO_2^- concentration during wet and dry periods

The box plot analysis aimed at assessing the impact of wet and dry periods on NO_2^- concentration reveals that, in general, the mean NO_2^- concentration during the wet periods is lower than during the dry periods. This finding aligns with the observed behavior of NH_4^+ concentration, where wet periods are associated with higher NH_4^+ levels, leading to limited nitrification and consequently lower NO_2^- concentrations during those times. The lower NO_2^- concentrations in the wet periods suggest that nitrification, the process responsible for the conversion of NH_4^+ to NO_2^-, is more active during the dry periods when NH_4^+ concentrations are lower which is aligns with Selvakumar and Ganesan (2015). This highlights the favorable conditions for NO_2^- removal during dry periods, which is consistent with the understanding that NO_2^- is an intermediate product in the nitrification process.

4.3.3. Nitrate (NO_3^-) interplay with wet and dry conditions

The breakthrough curve for NO_3^- through the sand column during the wet and dry time periods over a 4-day experiment with initial concentration 0 mg/L is shown in figure 4-9.

During the experimental period, the concentration of NO_3^- displayed varying trends. On the first day, it gradually increased to 4 mg/L during both wet and dry periods, indicating active nitrification and the accumulation of NO_3^-. However, on the second day during the wet period, the concentration decreased to 1 mg/L, suggesting a slower nitrification rate compared to the first day. This trend continued during the dry period, indicating ongoing nitrification. The third day saw a similar pattern, with NO_3^- concentration increasing during the wet period to 15 mg/L but then suddenly dropping to 1 mg/L toward the end of the wet time. This fluctuation might be attributed to changes in microbial activity or environmental conditions affecting the nitrification process. The fourth day showed stable NO_3^- concentration at 1 mg/L throughout both wet and dry periods. Nitrification, the oxidation process converting NO_2^- to NO_3^-, relies on aerobic conditions with adequate oxygen supply. Reduced oxygen levels, reflected by low ORP values and oxygen content below 0.5 mg/L,

can hinder nitrification activity. Additionally, under reduced oxygen conditions, denitrifying bacteria can facilitate the conversion of NO_3^- to N_2 gas through denitrification that help in decreasing the concentration of NO_3^- from the third day until to the end of the experimental process. Hence, in the presence of limited oxygen and anaerobic conditions, both reduced nitrification and denitrification processes can lead to a decrease in NO_3^- concentration, explaining the observed fluctuations in the third-day data.

Figure 4-9 Breakthrough curve of NO_3^- concentration performance in the sand column of the SAT system during wet and dry periods

The regression analysis examining the relationship between NO_3^- concentration and wetting and drying conditions, along with associated factors (pH, DO, and ORP). The p-values for the relationships between NO_3^- concentration and the tested variables, along with the correlation coefficients, indicate the statistical significance and the strength of these associations. The relationship between NO_3^- concentration and DO showed a p-value of 0.1231, signifying no significant connection, with a weak positive correlation (r = 0.20). The relationship with ORP yielded a p-value of 0.0786, also indicating no significant correlation, with a moderate positive correlation (r = 0.63). The relationship with pH had a p-value of 0.2847, implying no significant association, and a weak positive correlation (r = 0.34). Lastly, the relationship between NO_3^- concentration and Wet/dry status had a p-value of 0.4872. The overall model's p-value was 0.373, revealing that the variations in NO_3^- concentration during wet and dry periods were not strongly influenced by these factors, although some weak to moderate positive correlations were observed.

To analyze the factorial interaction between NO_3^- concentration and the wetting and drying conditions, the interaction relationships trend examined between NO_3^- concentration and key parameters such as pH, dissolved oxygen (DO), and oxidation-reduction potential (ORP) during both wet and dry times as shown in figure 4-10.

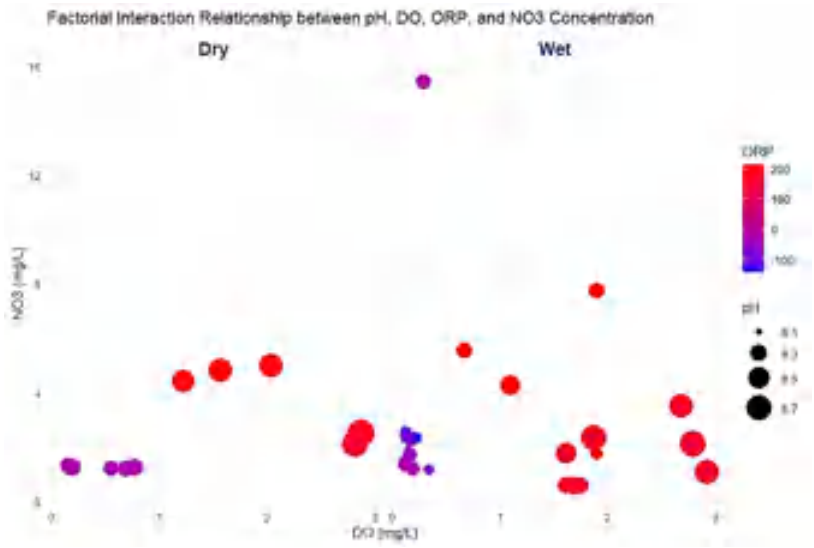

Figure 4-10 Factorial interaction relationships between NO_3^- and wet/dry parameters

The factorial interaction relationships between NO_3^- concentration and wet/dry parameters, as determined by the regression model, highlight the roles these factors play during wet and dry periods. There's a general trend where increasing DO, pH, and ORP during both wet and dry times correspond to an increase in NO_3^- concentration. This observation aligns with the positive correlation found in the correlation analysis, indicating that these factors have a positive influence on NO_3^- concentration. This behavior can be attributed to nitrification processes converting NH_4^+ to NO_3^-, where NO_3^- represents the final oxidization product (Gharbia et al., 2024). Conversely, the decrease in NO_3^- concentration is associated with denitrification, which is influenced by decreasing DO and ORP levels, as both are indicative of reduced oxygen availability in the system (Li et al., 2019). Denitrification leads to the reduction of NO_3^- to N_2 gas, contributing to a decrease in NO_3^- concentration (Gharbia et al., 2024).

To summarize the effect of wet and dry periods on the NO_3^- concentration the box plot used to visualize the favorable period for NO_3^- removal conditions shown in figure 4-11.

The box plot analysis used to assess the impact of wet and dry periods on NO_3^- concentration revealed that the mean NO_3^- concentration during dry times was generally lower than that during wet times which is aligns with Ma et al. (2023), and Sallwey et al. (2020). This suggests that dry periods are more favorable for NO_3^- removal conditions.

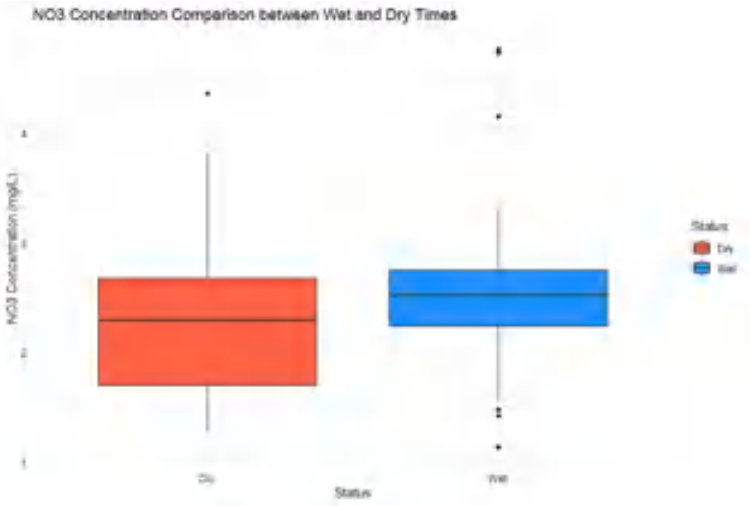

Figure 4-11 Box plot for NO_3^- concentration during wet and dry periods

4.3.4. Phosphate (PO_4^{3-}) interplay with wet and dry conditions

The breakthrough curve for PO_4^{3-} through the sand column during the wet and dry time periods over a 4-day column experiment with initial concentration 20 mg/L is shown in figure 4-12.

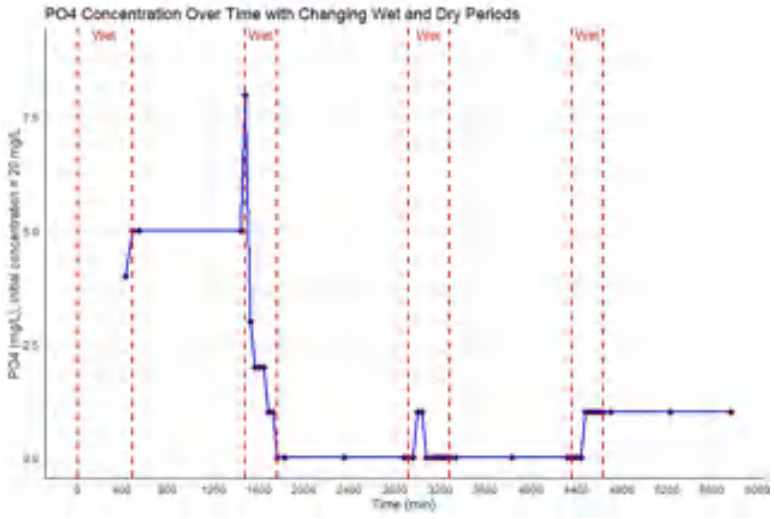

Figure 4-12 Breakthrough curve of PO_4^{3-} concentration performance in the sand column of the SAT system during wet and dry periods

The breakthrough curve (BTC) for PO_4^{3-} demonstrates a consistently high removal capacity of PO_4^{3-} from the synthetic wastewater in the sand column. Throughout the four days of the experiment, the sand column effectively reduced PO_4^{3-} concentrations. On the first day, the concentration gradually increased during the wet period, remaining stable in the dry period, showcasing the sand's strong adsorption capacity for PO_4^{3-}. On the second day, a temporary concentration spike during the wet time, followed by a decrease to 0 mg/L in the dry period, suggested efficient removal. On the third day, PO_4^{3-} concentrations stayed at 0 mg/L during both wet and dry periods, indicating continuous effective removal. Day four

saw a slight increase to 1 mg/L during the wet time, which was maintained in the dry period, likely due to some limitations in removal capacity at higher concentrations. Overall, these results confirm the sand column's exceptional ability to remove PO_4^{3-} under various wet and dry conditions, relying on adsorption and other removal mechanisms to achieve low or negligible PO_4^{3-} concentrations in the outflow.

In the analysis of the interaction between PO_4^{3-} concentration and wetting and drying conditions, including pH, DO, and ORP, the regression model revealed the relationships, the analysis of the interaction between PO_4^{3-} concentration and wetting and drying conditions, including pH, DO, and ORP, revealed significant relationships. The relationship between PO_4^{3-} concentration and DO had a p-value of 0.00253, indicating a statistically significant relationship. The relationship between PO_4^{3-} concentration and ORP also showed significance, with a p-value of 0.00208. The connection between PO_4^{3-} concentration and pH had a p-value of 0.03276, suggesting a significant relationship but with a slightly higher p-value. The relationship between PO_4^{3-} concentration and Wet/dry status was also significant, with a p-value of 0.02919. The overall model had a very low p-value of 1.796e-08, confirming that the interactions between PO_4^{3-} concentration and these factors significantly influenced the results, reflecting their combined impact on the removal of PO_4^{3-}. In the correlation analysis between PO_4^{3-} concentration and wet/dry factors, the correlations were strong, with a correlation coefficient (r) of 0.871 between PO_4^{3-} concentration and DO, 0.489 between PO_4^{3-} concentration and ORP, and 0.840 between PO_4^{3-} concentration and pH, emphasizing their substantial influence on PO_4^{3-} removal from the system.

To analyze the factorial interaction between PO_4^{3-} concentration and the wetting and drying conditions, the interaction relationships trend examined between PO_4^{3-} concentration and key parameters such as pH, dissolved oxygen (DO), and oxidation-reduction potential (ORP) during both wet and dry times as shown in figure 4-13.

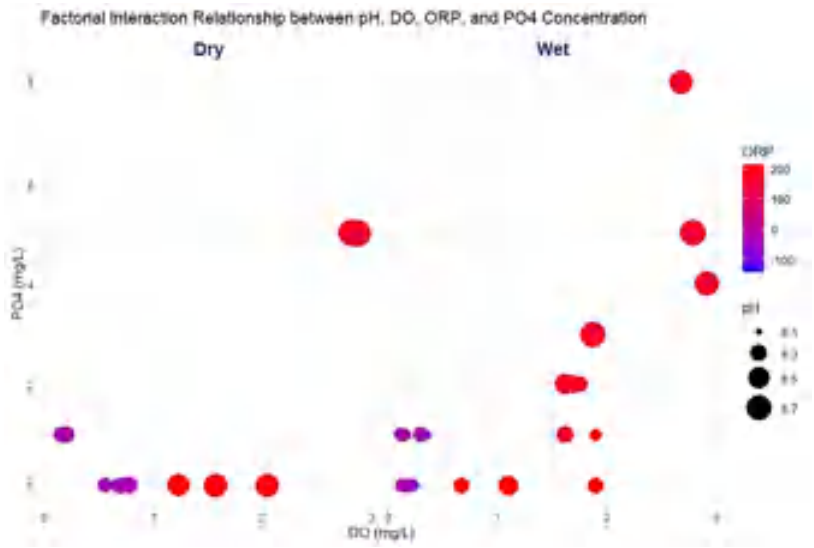

Figure 4-13 Factorial interaction relationships between PO_4^{3-} and wet/dry parameters

The factorial interaction relationships based on the regression model highlighted the roles of PO_4^{3-} in relation to DO, pH, and ORP during wet and dry times. It was observed that an increase in DO, pH, and ORP during both wet and dry conditions led to an increase in PO_4^{3-} concentration. This trend aligned with the positive correlations revealed in the correlation analysis, further emphasizing the influential roles of these factors in controlling PO_4^{3-} concentrations. Additionally, the likelihood of PO_4^{3-} precipitating with cations such as Fe^{2+} or Ca^{2+} contributed to the increased removal capacity for PO_4^{3-} (Liu, 2017). This interaction and the potential precipitation processes played a significant role in the removal of PO_4^{3-} from the system, further corroborating the positive influence of these factors on PO_4^{3-} removal (Gharbia et al., 2024).

To summarize the effect of wet and dry periods on the PO_4^{3-} concentration the box plot visualize the favorable period for PO_4^{3-} removal conditions shown in figure 4-14.

The analysis of wet and dry periods' effects on PO_4^{3-} concentrations, as visualized by box plots, revealed that, in general, the mean PO_4^{3-} concentration during dry times was lower than during wet times which is align with Wang et al. (2016). This indicates that dry periods were more favorable for the removal of PO_4^{3-} from the system. The observations align with the high removal capacity for PO_4^{3-} and the influence of factors such as DO, pH, ORP, and potential precipitation processes, emphasizing the effectiveness of the sand column in reducing PO_4^{3-} concentrations, particularly during dry conditions (Gharbia et al., 2024).

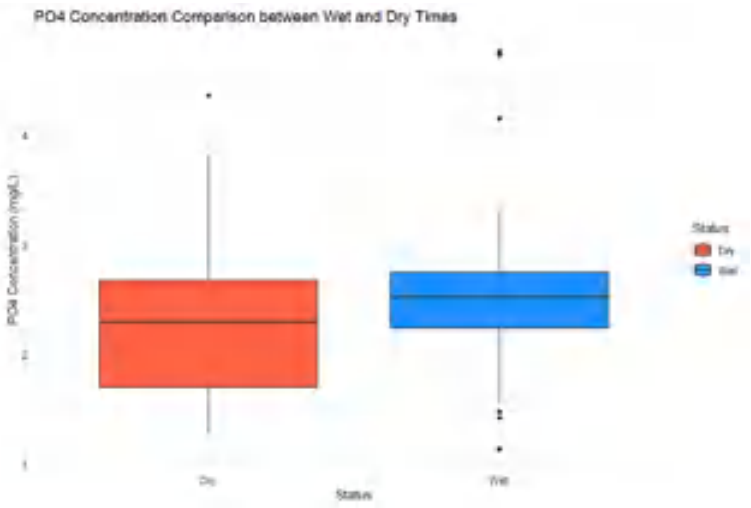

Figure 4-14 Box plot for PO_4^{3-} concentration during wet and dry periods

4.3.5. Sulfate (SO_4^{2-}) interplay with wet and dry conditions

The breakthrough curve for SO_4^{2-} through the sand column during the wet and dry time periods over a 4-day column experiment with initial concentration 30 mg/L is shown in figure 4-15.

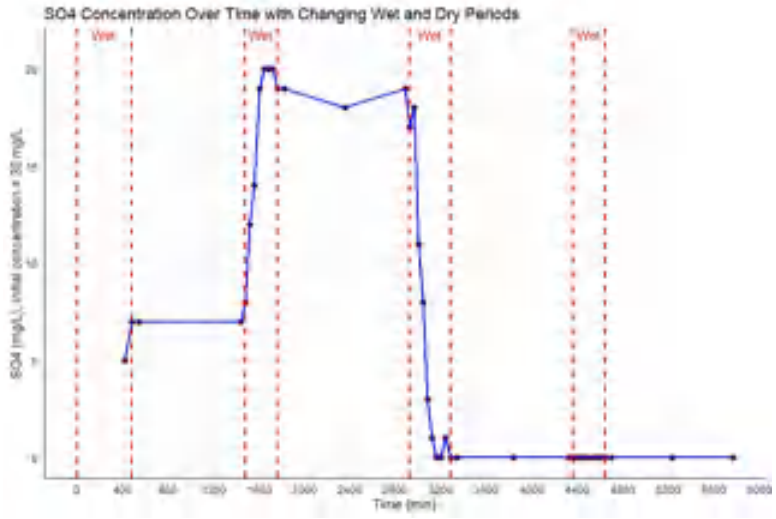

Figure 4-15 Breakthrough curve of SO_4^{2-} concentration performance in the sand column of the SAT system during wet and dry periods

In the analysis of SO_4^{2-} concentration in the outflow, it was observed that during the wet time, the concentration initially started at 5 mg/L and gradually increased to 6 mg/L, indicating the sand column's ability to retain and remove SO_4^{2-}. This removal capacity was sustained during the dry period, with a stable concentration of 6 mg/L. On the second day, the concentration increased to 20 mg/L during the wet time, likely due to the sand column reaching its retention limit. However, during the subsequent dry period, the concentration gradually decreased to 17 mg/L, suggesting additional removal mechanisms. On the third day, a significant removal of SO_4^{2-} occurred during the wet period, with the concentration

dropping to 0 mg/L, possibly due to microbial sulfate reduction and chemical reactions based on the reduction environment phase according to ORP. This low concentration was maintained throughout the remaining days, indicating the effective and sustained removal capacity of the sand column.

The analysis of the interaction between SO_4^{2-} concentration and wetting and drying conditions, as well as pH, DO, and ORP, revealed the following results: The relationship between SO_4^{2-} concentration and DO showed a high p-value of 0.836, indicating no statistically significant association. However, the relationship between SO_4^{2-} concentration and ORP had a very low p-value of 3.19e-09, indicating a highly significant correlation. The connection between SO_4^{2-} concentration and pH had a p-value of 0.0844, suggesting a potential relationship but with a slightly higher p-value. The relationship between SO_4^{2-} concentration and Wet/dry status had a p-value of 0.7534, indicating no significant relationship. The overall model demonstrated a very low p-value of 5.238e-11, confirming that the interactions between SO_4^{2-} concentration and these factors significantly influenced the results, reflecting their combined impact on SO_4^{2-} removal. In the correlation analysis between SO_4^{2-} concentration and wet/dry factors, the correlations were as follows: The correlation between SO_4^{2-} concentration and DO was 0.66, indicating a moderate positive correlation. The correlation between SO_4^{2-} concentration and ORP was 0.96, signifying a strong positive correlation. The correlation between SO_4^{2-} concentration and pH was 0.43, indicating a moderate positive correlation. These correlation values suggest positive associations between SO_4^{2-} concentration and these factors during the wet and dry periods, with ORP showing a particularly strong positive correlation with SO_4^{2-} concentration.

To analyze the factorial interaction between SO_4^{2-} concentration and the wetting and drying conditions, the interaction relationships trend examined between SO_4^{2-} concentration and key parameters such as pH, dissolved oxygen (DO), and oxidation-reduction potential (ORP) during both wet and dry times as shown in figure 4-16.

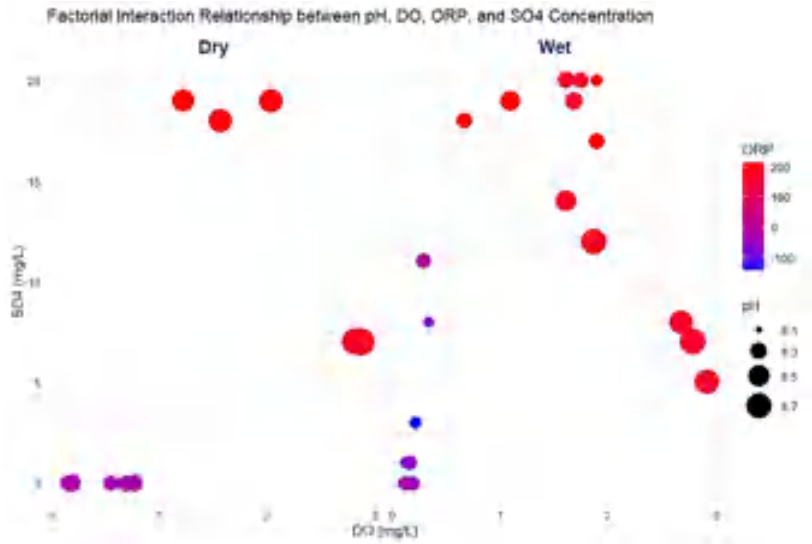

Figure 4-16 Factorial interaction relationships between SO_4^{2-} and wet/dry parameters

The factorial interaction relationships between SO_4^{2-} concentration and wet/dry parameters, as determined by the regression model, revealed that increasing DO, pH, and ORP during both wet and dry times had the effect of increasing the SO_4^{2-} concentration. This finding aligns with the positive correlation observed in the correlation analysis, indicating that these factors have a positive influence on SO_4^{2-} concentration. Additionally, the probability of SO_4^{2-} reduction, facilitated by lower ORP values (below zero mV), may contribute to the increased removal capacity for SO_4^{2-} (Dong et al., 2023). This reduction process involves the conversion of SO_4^{2-} to sulfide (S^{2-}) through sulfate reduction, occurring under anaerobic respiration conditions (Yu et al., 2016). Overall, these mechanisms contribute to the observed increase in SO_4^{2-} concentration with higher DO, pH, and ORP values during both wet and dry periods (Gharbia et al., 2024).

To summarize the effect of wet and dry periods on the SO_4^{2-} concentration the box plot used to visualize the favorable period for SO_4^{2-} removal conditions as shown in figure 4-17.

The box plot analysis, designed to visualize the impact of wet and dry periods on SO_4^{2-} concentration, reveals that the mean SO_4^{2-} concentration during dry times is generally lower than during wet times which is aligns with Estop-Aragonés et al. (2013). This observation suggests that the dry period is more favorable for SO_4^{2-} removal conditions, as it results in lower SO_4^{2-} concentrations.

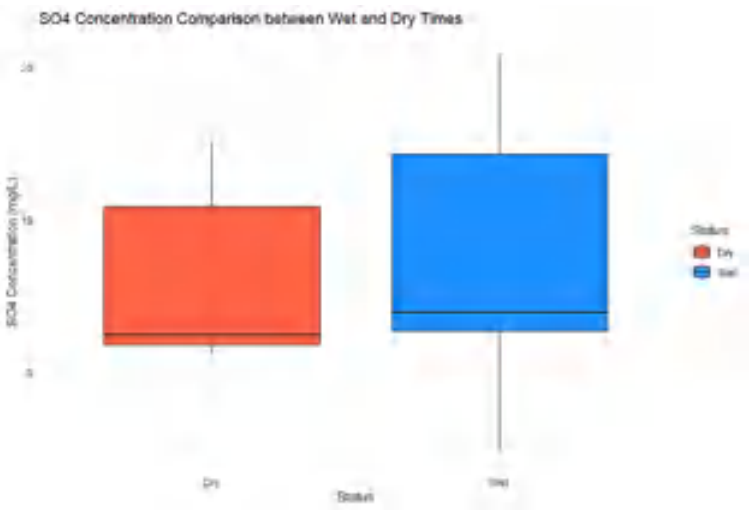

Figure 4-17 Box plot for SO_4^{2-} concentration during wet and dry periods

4.3.6. Iron (Fe^{2+}) interplay with wet and dry conditions

The breakthrough curve for Fe^{2+} through the sand column during the wet and dry time periods over a 4-day column experiment with initial concentration 3 mg/L is shown in figure 4-18.

Figure 4-18 Breakthrough curve of Fe^{2+} concentration performance in the sand column of the SAT system during wet and dry periods

The experiment began with an initial Fe^{2+} concentration of 3 mg/L in the infiltrated synthetic wastewater, and by the end of the study, it reached a saturation level of 0.7 mg/L, illustrating substantial removal of Fe^{2+} during both wet and dry periods. Importantly, there was no significant disparity in Fe^{2+} removal performance between wet and dry conditions, underscoring the sand column system's consistent effectiveness in eliminating Fe^{2+} regardless of moisture levels. Over the course of the study, the Fe^{2+} concentration exhibited variations. On the first day, it gradually decreased from 0.2 mg/L to 0.1 mg/L and remained steady during the dry period. The second day saw an increase to 0.5 mg/L during wetting,

maintaining this level during the dry period. However, the start of the third day witnessed a sudden drop to 0.3 mg/L, which remained constant until the end of the wet period. During the dry phase of the third day, the Fe^{2+} concentration incrementally rose to 0.6 mg/L. On the fourth day, Fe^{2+} concentration gradually increased to 0.8 mg/L during wetting and remained stable during the dry period. These results affirm the sand column's efficient Fe^{2+} removal capacity, with observed concentration fluctuations likely arising from factors like influent Fe^{2+} availability, sand column adsorption capacity, and chemical or biological transformations within the system.

The regression analysis examining the relationship between Fe^{2+} concentration and wetting and drying conditions, including pH, DO, and ORP, revealed that the relationship between Fe^{2+} concentration and DO had a low p-value of 0.00137, indicating a statistically significant association. Similarly, the relationship between Fe^{2+} concentration and ORP had a significant p-value of 0.040, indicating a significant relationship. The relationship between Fe^{2+} concentration and pH was also significant with a p-value of 0.037, while the relationship between Fe^{2+} concentration and Wet/dry status was also significant, with a p-value of 0.00655. The overall model had a very low p-value of 5.165e-08, confirming that the interactions between Fe^{2+} concentration and these factors significantly influenced the results, reflecting their combined impact on the removal of Fe^{2+} from the system. In the correlation analysis between Fe^{2+} concentration and wet/dry factors, the correlations were found to be as follows: The correlation coefficient (r) between Fe^{2+} concentration and DO was -0.91, indicating a strong negative correlation. The correlation coefficient between Fe^{2+} concentration and ORP was -0.72, signifying a moderate negative correlation. The correlation coefficient between Fe^{2+} concentration and pH was -0.76, indicating a moderate negative correlation. These correlation values suggest that there were strong negative associations between Fe^{2+} concentration and these factors during the wet and dry periods.

To analyze the factorial interaction between Fe^{2+} concentration and the wetting and drying conditions, the interaction relationships trend examined between Fe^{2+} concentration and key parameters such as pH, dissolved oxygen (DO), and oxidation-reduction potential (ORP) during both wet and dry times as shown in figure 4-19.

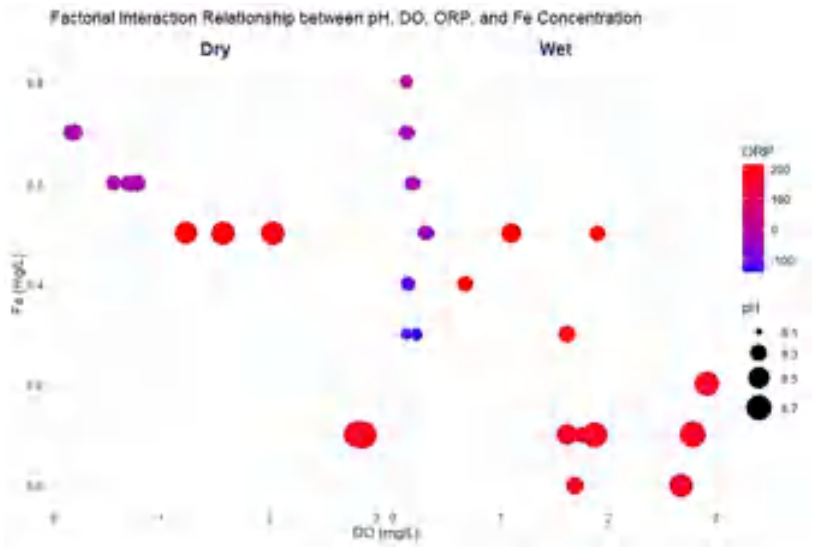

Figure 4-19 Factorial interaction relationships between Fe^{2+} and wet/dry parameters

The factorial interaction relationships between Fe^{2+} concentration and wet/dry parameters, based on the regression model, reveal that increasing levels of DO, pH, and ORP during wet and dry periods contribute to a decrease in Fe^{2+} concentration. This observation aligns with the correlation analysis, indicating a negative correlation between these factors and Fe^{2+} concentration. These findings are consistent with geochemical reactions, where higher ORP and increased DO facilitate the conversion of Fe^{2+} to Fe^{3+}, enhancing Fe^{2+} removal capacity (Quang et al., 2022). Additionally, the rise in pH aids in precipitating Fe^{2+}, further reducing Fe^{2+} concentration within the system (Wen et al., 2022). Overall, these factors collectively influence the effective removal of Fe^{2+} from the infiltrated wastewater.

To summarize the effect of wet and dry periods on the Fe^{2+} concentration the box plot used to visualize the favorable period for Fe^{2+} removal conditions as shown in figure 4-20.

The box plot analysis of the wet and dry periods' effect on Fe^{2+} concentration indicates that, generally, the wet period results in lower concentrations of Fe^{2+} compared to the dry period which is aligns with Zhang et al. (2018). This suggests that the wet conditions are more favorable for the removal of Fe^{2+} from the system.

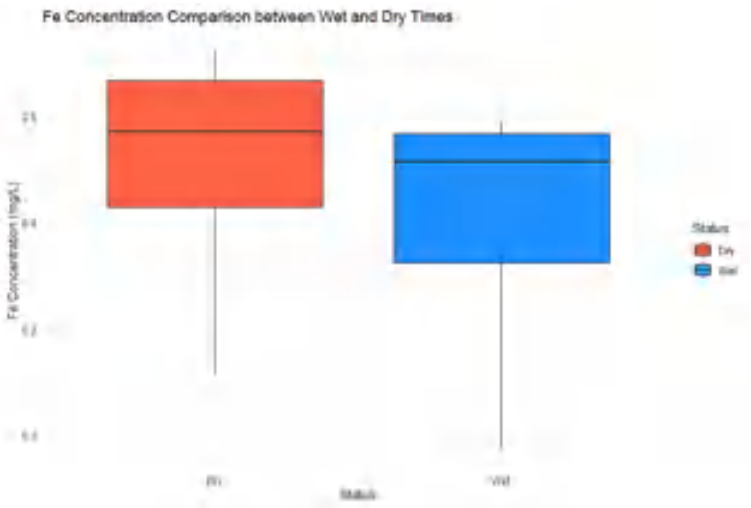

Figure 4-20 Box plot for Fe^{2+} concentration during wet and dry periods

4.3.7. Copper (Cu^{2+}) interplay with wet and dry conditions

The breakthrough curve for Cu^{2+} through the sand column during the wet and dry time periods over a 4-day column experiment with initial concentration 1 mg/L is shown in figure 4-21.

Figure 4-21 Breakthrough curve of Cu^{2+} concentration performance in the sand column of the SAT system during wet and dry periods

The Cu^{2+} breakthrough curve (BTC) exhibits an S-shaped pattern, indicating a substantial removal capacity for Cu^{2+} in both wet and dry periods. The initial Cu^{2+} concentration was 1 mg/L, and it reached a saturation level of 0.7 mg/L by the experiment's end, showcasing effective Cu^{2+} removal by the sand column, unaffected by wet or dry conditions. There's no significant difference in Cu^{2+} removal performance between these conditions. During the wet time, Cu^{2+} concentration gradually increased, peaking at 0.70 mg/L. In the dry period, the concentration remained stable at 0.70 mg/L, indicating a dynamic equilibrium between removal and release processes. These findings underscore

the sand column's consistent and effective Cu^{2+} removal capacity, with stable concentrations during dry periods, ensuring long-term stability in Cu^{2+} removal.

In the analysis of the interaction between Cu^{2+} concentration and wetting and drying conditions, as well as key factors including pH, DO, and ORP during both wet and dry periods, the regression model revealed significant relationships. The association between Cu^{2+} concentration and DO had a low p-value of 0.000127, indicating a statistically significant relationship. The relationship between Cu^{2+} concentration and ORP also had a low p-value of 0.000229, suggesting a significant correlation. The connection between Cu^{2+} concentration and pH had a p-value of 0.002834, indicating a significant relationship but with a slightly higher p-value. The relationship between Cu^{2+} concentration and Wet/dry status was also significant, with a p-value of 0.002526. The overall model had a very low p-value of 2.58e-12, confirming that the interactions between Cu^{2+} concentration and these factors significantly influenced the results, reflecting their combined impact on Cu^{2+} removal from the system. In the correlation analysis between Cu^{2+} concentration and wet/dry factors, the correlations were found to be strong, with a strong negative correlation with DO (-0.89), a moderate negative correlation with ORP (-0.53), and a strong negative correlation with pH (-0.86). These correlation values suggest that there were strong negative associations between Cu^{2+} concentration and these factors during the wet and dry periods, with DO, ORP, and pH showing substantial negative correlations with Cu^{2+} concentration.

To analyze the factorial interaction between Cu^{2+} concentration and the wetting and drying conditions, the interaction relationships trend examined between Cu^{2+} concentration and key parameters such as pH, dissolved oxygen (DO), and oxidation-reduction potential (ORP) during both wet and dry times as shown in figure 4-22.

The regression model examining the interaction between Cu^{2+} concentration and wet/dry conditions, along with the key factors of pH, DO, and ORP, revealed significant relationships. The increased levels of DO, pH, and ORP during wet and dry periods led to a decrease in Cu^{2+} concentration. This observation aligns with the negative correlation demonstrated in the correlation analysis, indicating the strength of these associations. Additionally, these findings are consistent with geochemical reactions, higher pH levels contribute to the precipitation of Cu^{2+} (Benslimane et al., 2020), further reducing its concentration in the system.

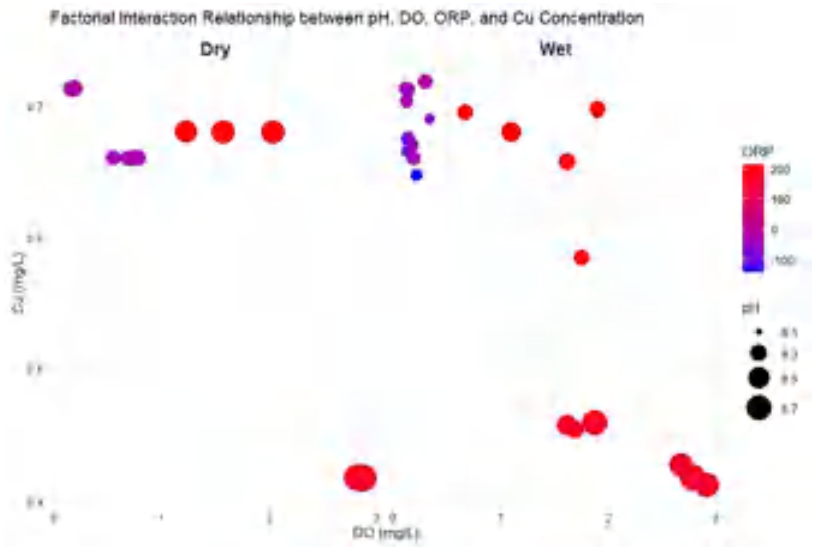

Figure 4-22 Factorial interaction relationships between Cu^{2+} and wet/dry parameters

To summarize the effect of wet and dry periods on the Cu^{2+} concentration the box plot used to visualize the favorable period for Cu^{2+} removal conditions as shown in figure 4-23.

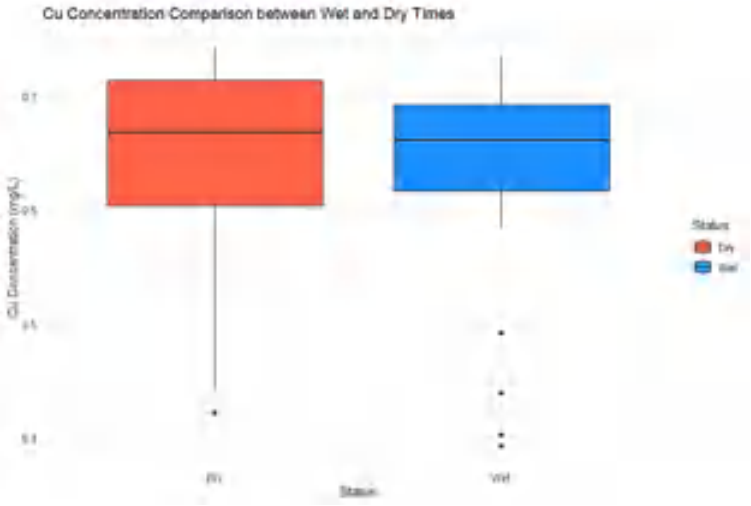

Figure 4-23 Box plot for Cu^{2+} concentration during wet and dry periods

The analysis of Cu^{2+} concentration's response to wet and dry periods, as depicted in the box plot, suggests that the wet time is associated with lower Cu^{2+} concentrations compared to the dry time which is aligns with Blecken et al. (2009). This indicates that Cu^{2+} removal conditions are generally more favorable during wet periods, as observed by the lower mean concentrations of Cu^{2+} during these times.

4.3.8. Manganese (Mn^{2+}) interplay with wet and dry conditions

The breakthrough curve for Mn^{2+} through the sand column during the wet and dry periods over a 4-day column experiment with initial concentration 3 mg/L is shown in figure 4-24.

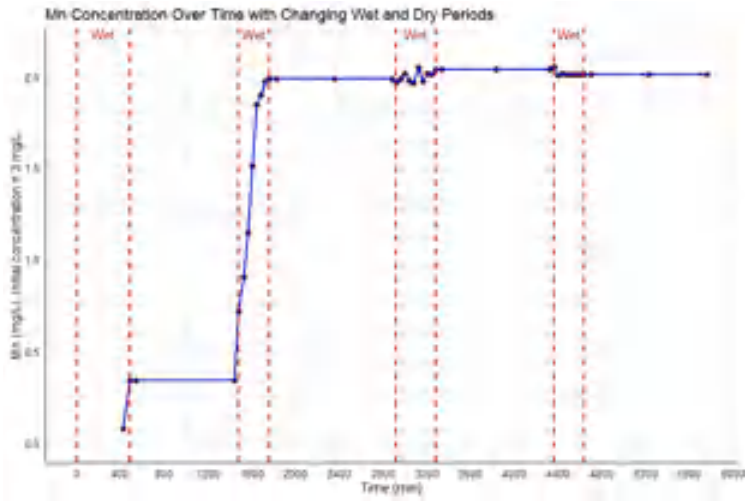

Figure 4-24 Breakthrough curve of Mn^{2+} concentration performance in the sand column of the SAT system during wet and dry periods

The analysis of breakthrough curve (BTC) results illustrates the transport behavior of Mn^{2+} through the sand column in both wet and dry conditions. The BTC curve exhibits an S-shape, indicating a substantial removal capacity for Mn^{2+} during both periods. Starting with an initial concentration of 3 mg/L in the influent synthetic wastewater, the Mn^{2+} concentration gradually increased, ultimately reaching a saturation level of 2 mg/L by the end of the experiment. This outcome reflects effective Mn^{2+} removal from the system, irrespective of whether it occurred during wet or dry conditions. The consistent performance between wet and dry conditions implies that the sand column's Mn^{2+} removal mechanism remains unaffected by the presence or absence of water. The sand column demonstrates efficient retention and removal of Mn^{2+} in both scenarios. This removal capacity can be attributed to factors such as the sand column's surface chemistry, porosity, and potential chemical reactions, including precipitation and co-precipitation with other minerals present in the sand.

In the analysis of the interaction between Mn^{2+} concentration and wetting and drying conditions, as well as key factors including pH, DO, and ORP during both wet and dry periods, the regression model revealed the following relationships: The association between Mn^{2+} concentration and DO had a very low p-value of 0.000067, indicating a statistically significant relationship. The relationship between Mn^{2+} concentration and ORP also had a very low p-value of 0.0000051, signifying a highly significant correlation. The connection between Mn^{2+} concentration and pH had a p-value of 0.0000051, suggesting a significant relationship. The relationship between Mn^{2+} concentration and Wet/dry status was also significant, with a p-value of 0.000191. The overall model had an extremely low p-value of 1.791e-15, confirming that the interactions between Mn^{2+} concentration and these factors significantly influenced the results, reflecting their combined impact on Mn^{2+} removal from

the system. In the correlation analysis between Mn^{2+} concentration and wet/dry factors, the correlations were found to be as follows: The correlation coefficient (r) between Mn^{2+} concentration and DO was -0.86, indicating a strong negative correlation. The correlation coefficient between Mn^{2+} concentration and ORP was -0.51, signifying a moderate negative correlation. The correlation coefficient between Mn^{2+} concentration and pH was -0.89, indicating a strong negative correlation. These correlation values suggest that there were strong negative associations between Mn^{2+} concentration and these factors during the wet and dry periods, with DO, ORP, and pH showing substantial negative correlations with Mn^{2+} concentration.

To analyze the factorial interaction between Mn^{2+} concentration and the wetting and drying conditions, the interaction relationships trend examined between Mn^{2+} concentration and key parameters such as pH, dissolved oxygen (DO), and oxidation-reduction potential (ORP) during both wet and dry times as shown in figure 4-25.

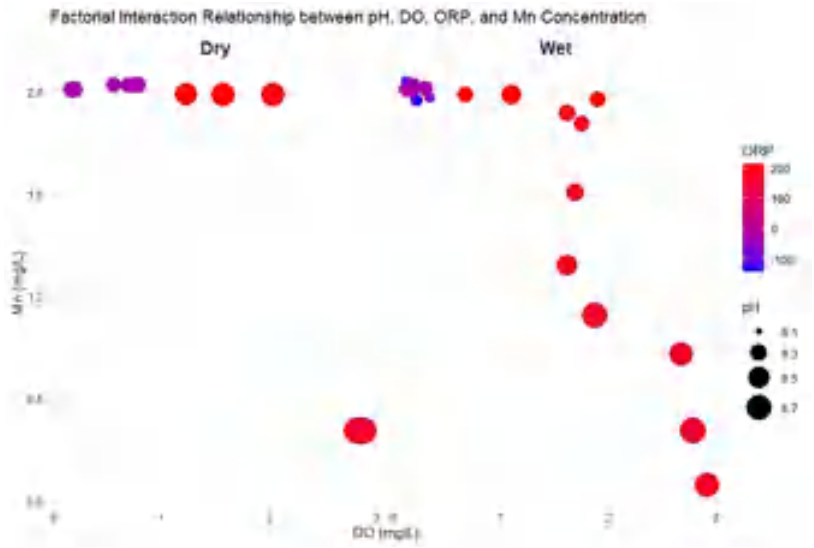

Figure 4-25 Factorial interaction relationships between Mn^{2+} and wet/dry parameters

The factorial interaction relationships between Mn^{2+} and wet/dry parameters, based on the regression model, reveal that the increase in DO, pH, and ORP during wet and dry conditions leads to a decrease in Mn^{2+} concentration. This observation aligns with the correlation analysis, indicating negative correlations between these factors and Mn^{2+} concentration. Additionally, this is consistent with geochemical reactions, where the probability of Mn^{2+} oxidation to Mn^{4+} increases with higher ORP and elevated DO (Chen et al., 2019), enhancing the removal capacity for Mn^{2+} by converting it to Mn^{4+} and eventually to MnO_2 (Chen et al., 2022). Moreover, the rise in pH assists in precipitating Mn^{2+} as $Mn(OH)_2$, further reducing Mn^{2+} concentration in the system.

To summarize the effect of wet and dry periods on the Mn^{2+} concentration the box plot used to visualize the favorable period for Mn^{2+} removal conditions as shown in figure 4-26.

The box plot analysis aimed at visualizing the impact of wet and dry periods on Mn^{2+} concentration reveals that, in general, the mean Mn^{2+} concentration during wet periods is lower compared to dry periods. This suggests that wet periods are more favorable for the removal of Mn^{2+} from the system which is aligns with Zhang et al. (2018). The data indicates that Mn^{2+} concentration is effectively reduced during wet conditions, making it the preferable period for Mn^{2+} removal.

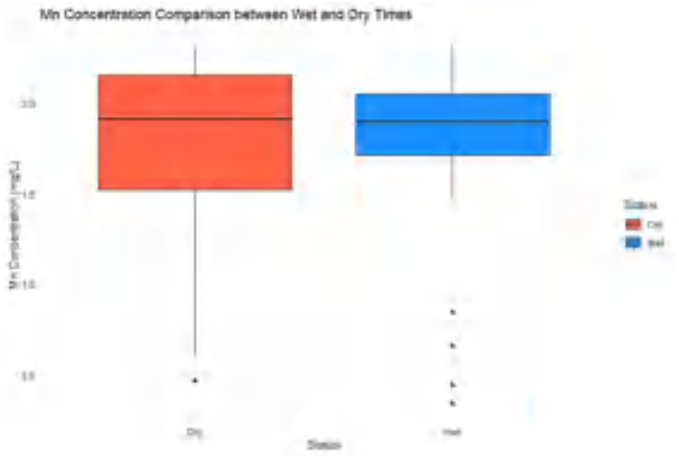

Figure 4-26 Box plot for Mn^{2+} concentration during wet and dry periods

4.3.9. Molybdate (MoO_4^{2-}) interplay with wet and dry conditions

The breakthrough curve for MoO_4^{2-} through the sand column during the wet and dry periods over a 4-day column experiment, initial concentration 2 mg/L shown in figure 4-27.

The analysis of MoO_4^{2-} transport through the sand column provides valuable insights into its removal under wet and dry conditions. Notable findings include the following: Removal Consistency there is no significant difference in MoO_4^{2-} removal performance between wet and dry conditions, indicating consistent removal mechanisms. Initial and Saturation Levels the initial MoO_4^{2-} concentration was 2 mg/L, reaching a saturation concentration of 1.8 mg/L by the experiment's end. This highlights the sand column's substantial removal capacity. Concentration Variations MoO_4^{2-} concentration decreased during wet periods and remained stable during dry periods, suggesting effective retention by the sand column. Flocculation and Fluctuations some fluctuations and flocculation occurred in MoO_4^{2-} concentration, likely due to chemical changes, precipitation, adsorption, and interactions with the sand column. In summary, the sand column demonstrates a removal capacity for MoO_4^{2-}. Decreased concentration during wet periods implies

adsorption and precipitation, while stability during dry periods suggests continued effectiveness in MoO_4^{2-} retention, even without water flow.

Figure 4-27 Breakthrough curve of MoO_4^{2-} concentration performance in the sand column of the SAT system during wet and dry periods

The regression analysis assessing the connection between MoO_4^{2-} concentration and wetting and drying conditions, pH, DO, and ORP during both wet and dry periods unveiled the following associations: The relationship between MoO_4^{2-} concentration and DO exhibited a statistically significant association with a p-value of 0.0154, while the relationship with ORP suggested a potentially significant link with a p-value of 0.0566. The association with pH was significant, indicated by a p-value of 0.0407, and the link with Wet/dry status suggested potential significance with a p-value of 0.0518. The overall model displayed a very low p-value of 0.0002543, confirming the collective impact of these factors on MoO_4^{2-} removal, despite some individual relationships having slightly higher p-values. Moreover, the correlation analysis demonstrated strong negative correlations between MoO_4^{2-} concentration and DO (-0.96), ORP (-0.78), and pH (-0.84) during both wet and dry periods. These findings imply that these factors play a role in MoO_4^{2-} transport and removal, indicating that the correlations are more robust than the regression model suggests.

To analyze the factorial interaction between MoO_4^{2-} concentration and the wetting and drying conditions, the interaction relationships trend examined between Mo_4O^{2-} concentration and key parameters such as pH, dissolved oxygen (DO), and oxidation-reduction potential (ORP) during both wet and dry times as shown in figure 4-28.

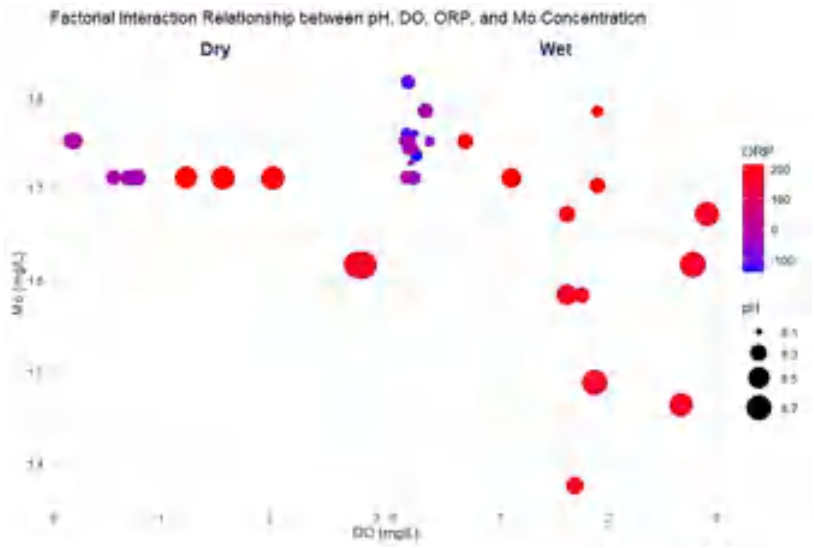

Figure 4-28 Factorial interaction relationships between MoO_4^{2-} and wet/dry parameters

The factorial interaction relationships between MoO_4^{2-} and wet/dry conditions based on the regression model highlight the interplay of MoO_4^{2-} with key factors, including DO, pH, and ORP during both wet and dry periods. The results indicate that increasing DO, pH, and ORP during wet and dry times leads to a decrease in MoO_4^{2-} concentration. This aligns with the correlation analysis that demonstrated strong negative correlations between these factors and MoO_4^{2-} concentration. The decrease in MoO_4^{2-} concentration can also be attributed to geochemical reactions, with higher ORP and DO promoting the conversion of MoO_4^{2-} to Mo^{5+} under aerobic conditions, where higher ORP values are typically observed, resulting in lower MoO_4^{2-} concentrations (Liu et al., 2023). Furthermore, an increase in pH contributes to reduced MoO_4^{2-} concentration, as Mo(VI) is more soluble in acidic solutions than in alkaline ones (Li et al., 2023). Hence, higher pH values lead to lower MoO_4^{2-} concentrations in the system.

To summarize the effect of wet and dry on the MoO_4^{2-} concentration the box plot used to visualize the favorable period for MoO_4^{2-} removal conditions as shown in figure 4-29.

The analysis of the effect of wet and dry periods on MoO_4^{2-} concentration, as represented by the box plot, reveals that the wet periods generally result in lower MoO_4^{2-} concentrations compared to dry periods. The difference between the mean values for MoO_4^{2-} concentration in wet and dry times indicates that the wet conditions favor the removal of MoO_4^{2-}. This suggests that the presence of water during wet periods enhances the processes that lead to reduced MoO_4^{2-} concentrations in the system.

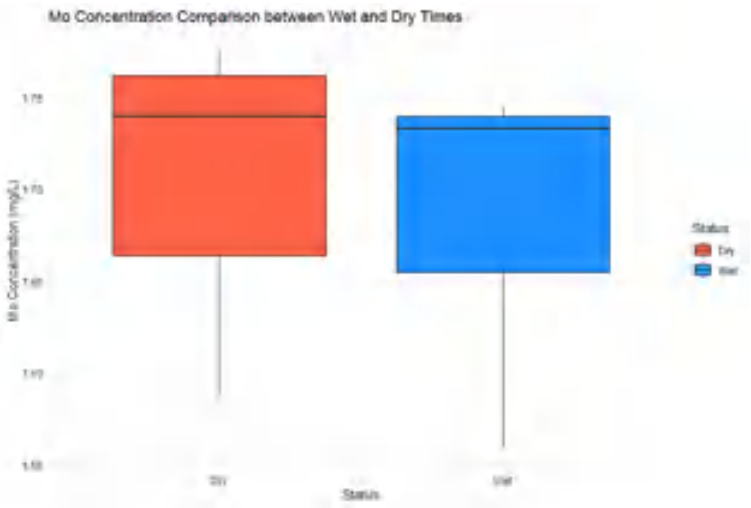

Figure 4-29 Box plot for MoO_4^{2-} concentration during wet and dry periods

4.3.10. Zinc (Zn^{2+}) interplay with wet and dry conditions

The breakthrough curve for Zn^{2+} through the sand column during the wet and dry periods over a 4-day column experiment with initial concentration 2.5 mg/L is shown in figure 4-30.

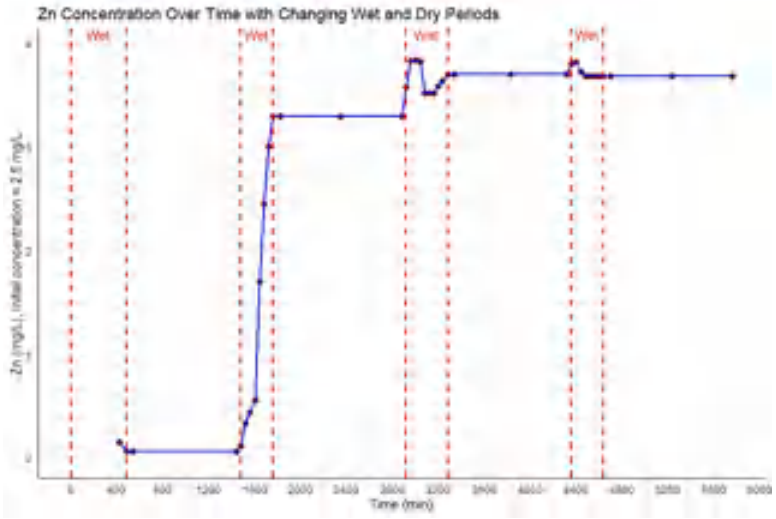

Figure 4-30 Breakthrough curve of Zn^{2+} concentration performance in the sand column of the SAT system during wet and dry periods

The results from the transport of Zn^{2+} through the sand column indicate several key findings about its removal under wet and dry conditions. The S-shaped BTC curve suggests a continuous removal capacity for Zn^{2+} throughout the experiment. The saturation concentration of Zn^{2+} at 3.5 mg/L exceeded the initial infiltrated concentration of 2.5 mg/L, indicating saturation of the sand column with Zn^{2+} ions over time. During wet periods, the concentration of Zn^{2+} increased and reached the saturation concentration, indicating higher transport and accumulation of Zn^{2+} under wet conditions. In contrast, during dry periods, Zn^{2+} concentration remained stable, indicating reduced desorption and removal processes.

The initial concentration overshoot during wet periods can be attributed to saturation-induced release and competitive interactions with other pollutants. These findings shed light on Zn^{2+} behavior in the sand column and its fate in environmental systems.

In the analysis of the interaction between Zn^{2+} concentration and wetting and drying conditions, as well as key factors including pH, DO, and ORP during both wet and dry periods, the regression model unveiled significant relationships between Zn^{2+} concentration and these factors. Specifically, the relationship between Zn^{2+} concentration and DO exhibited a low p-value of 0.000213, signifying a statistically significant association. The relationship with ORP also indicated significance with a p-value of 0.010386, albeit slightly higher. Similarly, the connection between Zn^{2+} concentration and pH revealed a significant relationship with a p-value of 0.005063. The impact of Wet/dry status on Zn^{2+} concentration was also found to be significant, supported by a p-value of 0.001244. The overall model demonstrated the collective and highly significant influence of these factors on Zn^{2+} removal with an extremely low p-value of 7.014e-13. Furthermore, the correlation analysis highlighted strong negative associations between Zn^{2+} concentration and the wet/dry factors, with DO exhibiting a correlation coefficient (r) of -0.93, indicating a strong negative correlation, ORP showing a moderate negative correlation with a coefficient of -0.64, and pH displaying a strong negative correlation with a coefficient of -0.87. These correlations indicate the pivotal role of DO, ORP, and pH in influencing the transport and removal of Zn^{2+} from the system, aligning with the regression model results.

To analyze the factorial interaction between Zn^{2+} concentration and the wetting and drying conditions, the interaction relationships trend examined between Zn^{2+} concentration and key parameters such as pH, dissolved oxygen (DO), and oxidation-reduction potential (ORP) during both wet and dry times as shown in figure 4-31.

The factorial interaction relationships between Zn^{2+} and wet/dry parameters, as revealed by the regression model, provide insights into the dynamic roles of Zn^{2+} and key environmental factors during wet and dry conditions. Notably, the increase in DO, pH, and ORP during both wet and dry periods contributes to a decrease in Zn^{2+} concentration, a trend supported by the negative correlations observed in the correlation analysis. This suggests that DO, pH, and ORP play a crucial role in controlling Zn^{2+} concentrations in the system. The geochemical reactions further support this behavior, indicating that as ORP increases, Zn^{2+} becomes less soluble, favoring its removal. Additionally, the increase in pH aids in decreasing Zn^{2+} concentration, as Zn^{2+} is more soluble in acidic conditions (Kumordzi et al., 2016). Consequently, these findings underscore the interconnected influence of

environmental factors and geochemical reactions in the transport and removal of Zn^{2+} from the system under varying wet and dry conditions.

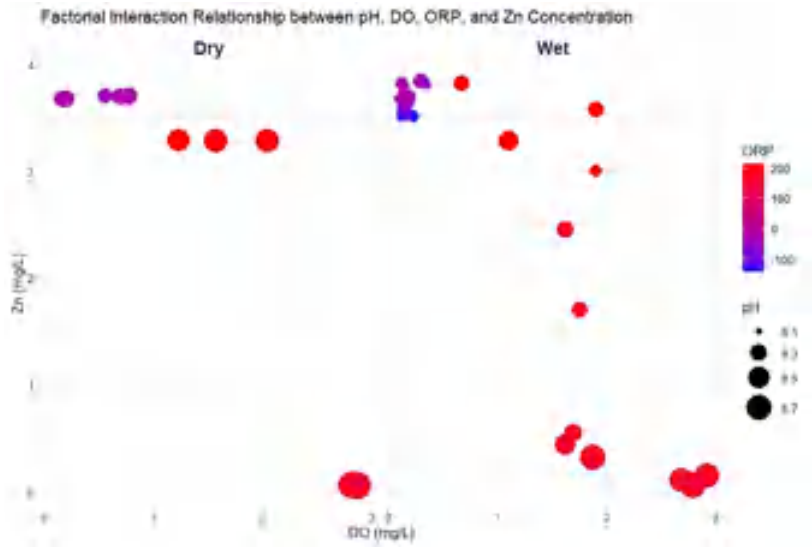

Figure 4-31 Factorial interaction relationships between Zn^{2+} and wet/dry parameters

To summarize the effect of wet and dry periods on the Zn^{2+} concentration the box plot used to visualize the favorable period for Zn^{2+} removal conditions as shown in figure 4-32.

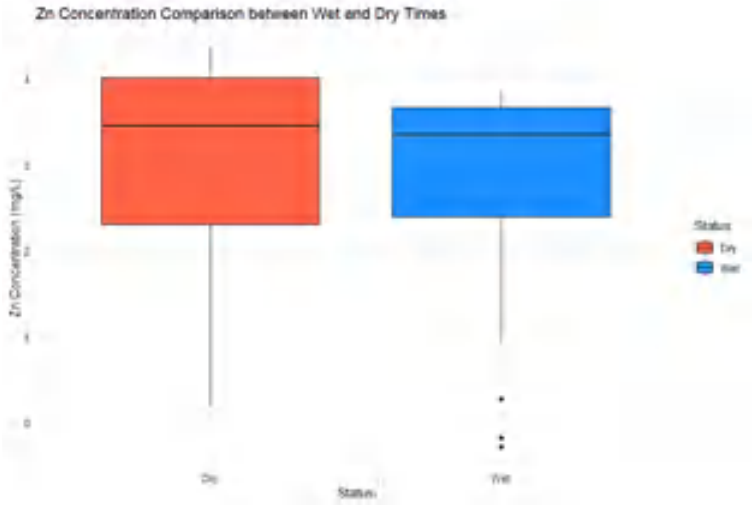

Figure 4-32 Box plot for Zn^{2+} concentration during wet and dry periods

The analysis of Zn^{2+} concentration under wet and dry conditions, visualized using box plots, highlights the impact of these conditions on Zn^{2+} removal. The box plots demonstrate that, in general, the mean values for Zn^{2+} concentration are lower during wet times compared to dry times. This suggests that wet conditions favor a lower concentration of Zn^{2+} and are a more favorable period for Zn^{2+} removal. The difference in mean values between wet and dry periods further emphasizes the influence of these conditions on Zn^{2+} concentrations, with wet times exhibiting better Zn^{2+} removal performance.

4.3.11. Cobalt (Co^{2+}) interplay with wet and dry conditions

The breakthrough curve for Co^{2+} through the sand column during the wet and dry time periods over a 4-day column experiment with initial concentration 3.5 mg/L is shown in figure 4-33.

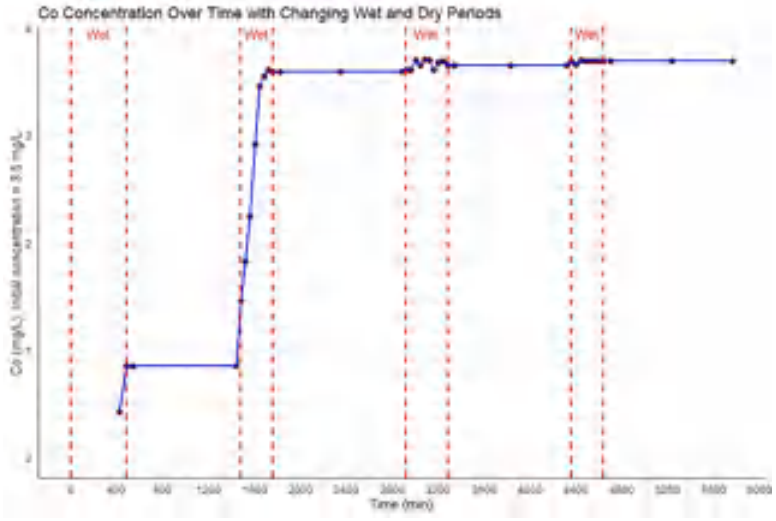

Figure 4-33 Breakthrough curve of Co^{2+} concentration performance in the sand column of the SAT system during wet and dry periods

The results from the transport of Co^{2+} through the sand column highlight key insights into its removal under wet and dry conditions. The BTC curve analysis indicates efficient Co^{2+} removal, with an S-shaped curve demonstrating removal capacity during both wet and dry periods. The initial infiltrated concentration and saturation concentration of Co^{2+} were both 3.5 mg/L, indicating equilibrium between adsorption and desorption processes. During wet conditions, Co^{2+} concentration gradually increased, likely due to improved contact between Co^{2+} ions and sand particles, facilitating adsorption. Wet conditions may also promote Co^{2+} ion leaching from the sand column. Conversely, during dry periods, Co^{2+} concentration remained stable, indicating sustained equilibrium between adsorption and desorption processes even without water flow. This suggests minimal release or desorption of Co^{2+} from the sand column during dry times.

In the analysis of the interaction between Co^{2+} concentration and wetting and drying conditions, along with key factors including pH, DO, and ORP during both wet and dry periods, the regression model revealed the following relationships: The association between Co^{2+} concentration and DO had a very low p-value of 0.0000904, indicating a statistically significant relationship. The relationship between Co^{2+} concentration and ORP also had a very low p-value of 0.00000601, signifying a highly significant correlation. The connection between Co^{2+} concentration and pH had a p-value of 0.0000034, suggesting a significant relationship. The relationship between Co^{2+} concentration and Wet/dry status was also

significant, with a p-value of 0.000337. The overall model had an extremely low p-value of 1.527e-15, confirming that the interactions between Co^{2+} concentration and these factors significantly influenced the results, reflecting their combined impact on Co^{2+} removal from the system. In the correlation analysis between Co^{2+} concentration and wet/dry factors, the correlations were found to be as follows: The correlation coefficient (r) between Co^{2+} concentration and DO was -0.86, indicating a strong negative correlation. The correlation coefficient between Co^{2+} concentration and ORP was -0.50, signifying a moderate negative correlation. The correlation coefficient between Co^{2+} concentration and pH was -0.89, indicating a strong negative correlation. These correlation values suggest that there were strong negative associations between Co^{2+} concentration and these factors during both wet and dry periods, with DO, ORP, and pH showing substantial negative correlations with Co^{2+} concentration. These findings reinforce the significance of these factors in influencing the transport and removal of Co^{2+} in the system.

To analyze the factorial interaction between Co^{2+} concentration and the wetting and drying conditions, the interaction relationships trend examined between Co^{2+} concentration and key parameters such as pH, dissolved oxygen (DO), and oxidation-reduction potential (ORP) during both wet and dry times as shown in figure 4-34.

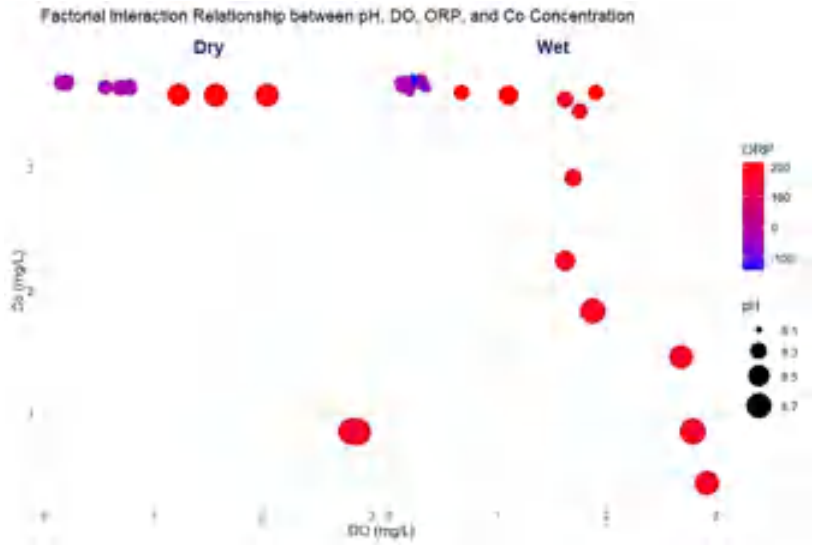

Figure 4-34 Factorial interaction relationships between Co^{2+} and wet/dry parameters

The factorial interaction relationships between Co^{2+} and wet/dry parameters, based on the regression model, highlight the interactions between Co^{2+} and key factors like DO, pH, and ORP during wet and dry periods. The results indicate that increasing DO, pH, and ORP during both wet and dry times leads to a decrease in Co^{2+} concentration, in line with the negative correlations found in the correlation analysis. These findings are further supported by geochemical reactions. Co^{2+} tends to be more soluble in reducing and anoxic environments than in oxidizing and oxic environments. Higher ORP and increased DO

levels enhance the removal capacity for Co^{2+}, leading to lower concentrations (Dabbagh et al., 2016). Additionally, the increase in pH helps reduce Co^{2+} concentration as Co^{2+} is more soluble in acidic solutions compared to alkaline ones (Adibmehr and Faghihian, 2019). Overall, these results suggest that variations in DO, pH, and ORP significantly influence the transport and removal of Co^{2+} from the system, with their combined effect leading to decreased Co^{2+} concentrations.

To summarize the effect of wet and dry periods on the Co^{2+} concentration the box plot used to visualize the favorable period for Co^{2+} removal conditions as shown in figure 4-35.

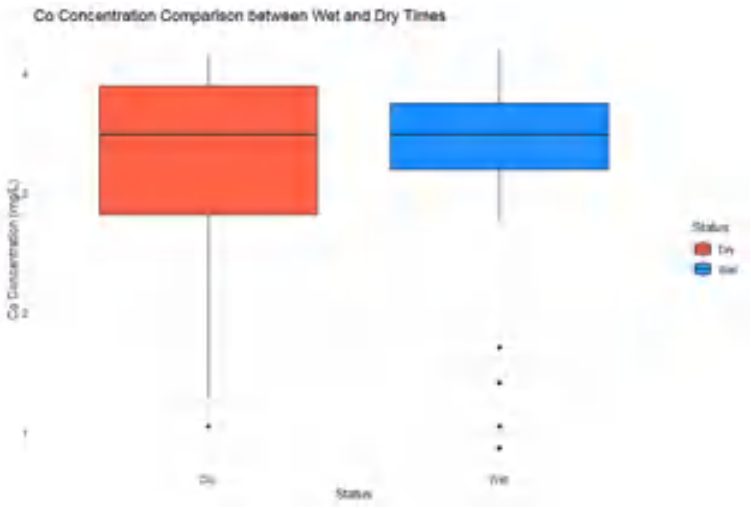

Figure 4-35 Box plot for Co^{2+} concentration during wet and dry periods

The effect of wet and dry periods on Co^{2+} concentration, as visualized through box plots, reveals that there is a relatively small difference between the mean values of Co^{2+} concentration in wet and dry times. However, it is evident that the wet period tends to have slightly lower Co^{2+} concentrations compared to the dry period, indicating that wet conditions are somewhat more favorable for Co^{2+} removal.

4.3.12. Borate (BO_3^{3-}) interplay with wet and dry conditions

The breakthrough curve for BO_3^{3-} through the sand column during the wet and dry time periods over a 4-day column experiment with initial concentration 2.5 mg/L is shown in figure 4-36.

Figure 4-36 Breakthrough curve of BO_3^{3-} concentration performance in the sand column of the SAT system during wet and dry periods

The breakthrough curve (BTC) analysis reveals the transport behavior of BO_3^{3-} through the sand column under wet and dry conditions. The BTC pattern for BO_3^{3-} concentration exhibits a flocculation pattern. Initially, the infiltrated BO_3^{3-} concentration was 2.5 mg/L, and it reached an average saturation concentration of 2.5 mg/L, indicating that the sand column has a limited capacity to retain and remove BO_3^{3-} ions from the solution. During the wet period, the BO_3^{3-} concentration shows development and exhibits peaks, reaching a maximum of 2.54 mg/L. These peaks likely result from processes such as leaching, dissolution, and mobilization of BO_3^{3-} ions from the sand column during wet conditions. Factors like increased water flow and contact with fresh solution contribute to higher concentrations. Conversely, the BO_3^{3-} concentration remains stable during the dry period, indicating minimal leaching or release. These findings suggest that wet conditions enhance BO_3^{3-} ion mobility, resulting in higher concentrations, while dry conditions minimize leaching, maintaining stable BO_3^{3-} concentrations. The flocculation pattern and concentration peaks during wet conditions likely involve complex interactions between BO_3^{3-} adsorption, precipitation, and desorption processes in the sand column.

The interaction between BO_3^{3-} concentration and wetting, drying conditions, as well as key factors of pH, DO, and ORP during wet and dry periods, the regression model revealed the following relationships: The relationship between BO_3^{3-} concentration and DO had a p-value of 0.049, indicating a statistically significant association. The relationship between BO_3^{3-} concentration and ORP had a p-value of 0.039, suggesting a significant relationship. The connection between BO_3^{3-} concentration and pH had a p-value of 0.029, indicating a significant relationship. The relationship between BO_3^{3-} concentration and Wet/dry status had a p-value of 0.0596, suggesting a potentially significant relationship. The overall model had a low p-value of 0.000105, confirming that the interactions between BO_3^{3-}

concentration and these factors significantly influenced the results, reflecting their combined impact on BO_3^{3-} removal from the system. In the correlation analysis between BO_3^{3-} concentration and wet/dry factors: The correlation coefficient (r) between BO_3^{3-} concentration and DO was -0.94, indicating a strong negative correlation. The correlation coefficient between BO_3^{3-} concentration and ORP was -0.67, signifying a moderate negative correlation. The correlation coefficient between BO_3^{3-} concentration and pH was -0.95, indicating a strong negative correlation. These correlation values reveal strong negative associations between BO_3^{3-} concentration and these factors during the wet and dry periods. While the regression model results for individual relationships had relatively higher p-values, the overall model demonstrated significant interactions between BO_3^{3-} concentration and these factors, indicating their combined influence on BO_3^{3-} removal.

To analyze the factorial interaction between BO_3^{3-} concentration and the wetting and drying, the interaction relationships trend examined between BO_3^{3-} concentration and key parameters such as pH, DO, and ORP during wet and dry times as shown in figure 4-37.

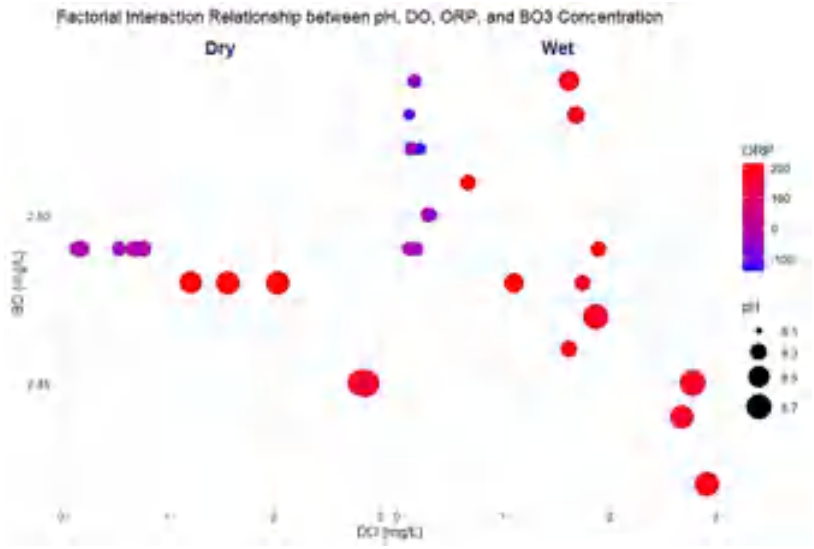

Figure 4-37 Factorial interaction relationships between BO_3^{3-} and wet/dry parameters

The factorial interaction relationships based on the regression model highlight the interactions between BO_3^{3-} concentration and key factors like dissolved oxygen (DO), pH, and oxidation-reduction potential (ORP) during both wet and dry periods. It was observed that increasing DO, pH, and ORP during both wet and dry times had a consistent effect, leading to a decrease in BO_3^{3-} concentration. This trend aligns with the findings of the correlation analysis, which indicated strong negative correlations between BO_3^{3-} concentration and these factors. The observed interactions and correlations collectively suggest that elevated levels of DO, higher pH, and increased ORP contribute to reducing the concentration of BO_3^{3-} in the system during both wet and dry conditions (Tokatli et al., 2014), emphasizing their influential roles in BO_3^{3-} removal and transport dynamics.

To summarize the effect of wet and dry periods on the BO_3^{3-} concentration the box plot used to visualize the favorable period for BO_3^{3-} removal conditions as shown in figure 4-38.

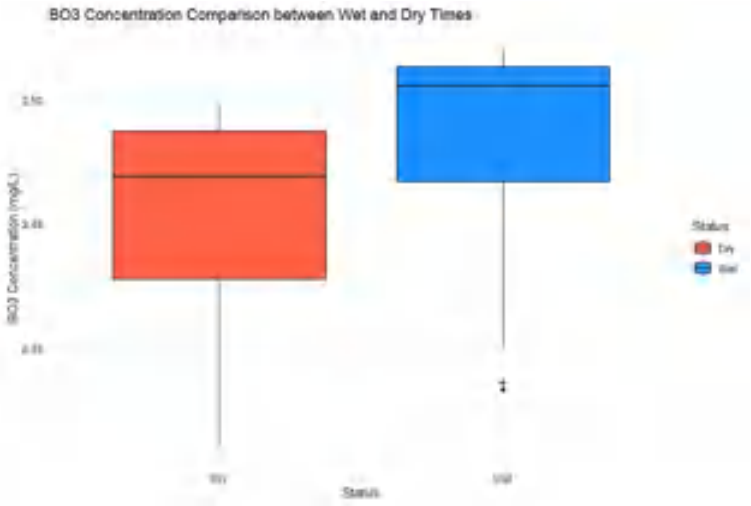

Figure 4-38 Box plot for BO_3^{3-} concentration during wet and dry periods

The box plot analysis designed to visualize the impact of wet and dry periods on BO_3^{3-} concentration revealed that, in general, the dry time resulted in lower BO_3^{3-} concentrations. This suggests that the dry conditions favor the removal of BO_3^{3-}, leading to reduced concentrations compared to wet periods.

4.4. Conclusion

Wetting and drying cycles within a soil aquifer treatment system exert significant influence over the performance and elimination of infiltrated wastewater pollutants within the sand column. These cycles facilitate the removal of pollutants through physical filtration, adsorption, and biological degradation during wet periods, whereas the drying phases promote the retention and immobilization of pollutants, leading to a further reduction in their concentration. The cyclic nature of wetting and drying profoundly impacts the transport and fate of pollutants within the sand column, influencing their movement, solubility, and sorption capacity. Depending on their properties and environmental conditions, these cycles can induce the release, retention, or transformation of pollutants. Moreover, wetting and drying cycles significantly impact microbial activity and the degradation of pollutants. Wet periods support thriving microbial populations engaged in biodegradation processes, while drying periods may limit microbial activity while enhancing the persistence of certain microbial communities. The variability in treatment performance within the sand column arises due to fluctuations in wetting and drying cycles. The efficiency of pollutant removal fluctuates, influenced by factors like pH, dissolved oxygen (DO) levels, and oxidation-reduction potential (ORP) conditions. Long-term exposure to these cycles also alters the physical

structure of the sand, affecting parameters like porosity, permeability, and adsorption capacity.

The comprehensive laboratory investigations simulated soil aquifer treatment systems during wet and dry cycles with robust statistical analysis, revealed notable variations, factorial relationships, and correlations among various pollutants and wet/dry conditions, specifically pH, DO, and ORP fluctuations. Ammonium (NH_4^+) exhibited increased concentrations during wetting, with more effective removal during drying phases, primarily through adsorption and potential microbial processes. Conversely, Nitrite (NO_2^-) showed lower concentrations during wet periods, indicating limited nitrification due to higher NH_4^+ levels, with more presence during dry periods. Nitrate (NO_3^-) and sulfate (SO_4^{2-}) concentrations varied, influenced by factors like DO, pH, and ORP, lacking distinct removal trends based on wet/dry periods. Phosphate (PO_4^{3-}) concentrations increased with rising DO, pH, and ORP in both wet and dry periods, yet removal was more favorable during dry phases, aligning with lower mean PO_4^{3-} concentrations. Furthermore, the analysis of metal ions like Iron (Fe^{2+}), Copper (Cu^{2+}), Manganese (Mn^{2+}), Molybdate (MoO_4^{2-}), Zinc (Zn^{2+}), and Cobalt (Co^{2+}) underscored their varied responses to wet and dry conditions and environmental factors. Each ion exhibited specific correlations with DO, ORP, and pH, influencing their removal within the simulated system. Wet periods generally favored lower concentrations of these metal ions, highlighting enhanced removal potential during water presence. Additionally, the nuanced behaviors observed in Borate (BO_3^{3-}) within wet and dry conditions further emphasize the complex dynamics at play. Borate concentrations displayed removal during dry periods and exhibited associations with DO, ORP, and pH.

Overall, wetting and drying cycles play a critical role in the fate, transport, transformation and treatment of infiltrated wastewater pollutants in the sand column, highlighting the importance of considering these cycles in system optimization, design and operation.

5. New Scientific Results

Thesis 1. Comparative soil types in pollutant removal for SAT systems

I used two methods in comparing the performance of sand and sandy loam soils in removing pollutants, while also assessing the scalability of the results based on SAT system considerations. The first method involved the isothermal adsorption technique, which was used to study the static and equilibrium conditions between infiltrated pollutants and the soil particle matrix. The second method simulated real-world SAT systems through dynamic column investigations. All laboratory investigations aimed to quantify the effect of the infiltrate media and soil selection on SAT system performance.

The comparative analysis of soil adsorption performance using Freundlich and Langmuir isothermal models provided new insights in to the adsorption processes relevant to SAT systems, particularly regarding the adsorption characteristics and pollutant affinities of sand and sandy loam soils. Freundlich accommodates heterogeneous surfaces, while Langmuir provides insights into monolayer adsorption, covering a broad spectrum of adsorption behaviors. The findings revealed that sandy loam generally has a higher adsorption capacity for pollutants due to its higher organic matter content and greater pollutant affinity intensity.

Dynamic column experiments simulating real-world scenarios of partially treated wastewater infiltration revealed significant differences in the removal efficiencies of various pollutants between sand and sandy loam soils. These differences are attributed to variations in soil characteristics such as texture, structure, porosity, pH, and organic matter content. Sandy loam demonstrated superior removal capabilities for pollutants such as NH_4^+, PO_4^{3-}, Cu^{2+}, Mn^{2+}, MoO_4^{2-}, Zn^{2+}, Co^{2+}, and BO_3^{3-}, with removal rates substantially higher than those observed in sand. However, sand exhibited greater efficiency in removing NO_2^-, NO_3^-, SO_4^{2-}, and Fe^{2+}.

The area under breakthrough curve (AUC) calculations highlighted the dynamic pollutant removal performance of sand and sandy loam soils in real-world scenarios. This method demonstrates its utility in evaluating the performance of SAT systems, providing a practical measurable index for assessing SAT performance based on specific soil types and pollutant profiles.

Thesis 2. Infiltration rate impact on pollutants transport in SAT systems

The infiltration rate significantly influences the transport, retention and removal of various pollutants. A lower infiltration rate (0.5 mL/min) enhances pollutant removal by increasing contact time with the sand medium particles matrix, facilitating higher adsorption

and more efficient biogeochemical reactions due to prolonged interaction between pollutants and the microbial community within the system. In contrast, a higher infiltration rate (10 mL/min) reduces contact time, resulting in less effective pollutant removal and higher effluent concentrations.

Understanding how different pollutants respond to changes in infiltration rate reveals significant variations in their removal efficiencies. Pollutants such as NH_4^+, PO_4^{3-}, SO_4^{2-}, Fe^{2+}, Mn^{2+}, MoO_4^{2-}, Zn^{2+}, Cu^{2+} and Co^{2+} exhibit significantly better removal at the slower infiltration rate due to enhanced adsorption and microbial degradation interactions. However, pollutants such as NO_3^-, NO_2^-, and BO_3^{3-} show higher removal at the higher infiltration rate likely due to reduced production rates, particularly for nitrogen species. These findings suggest that specific conditions tailored to the pollutant profile may optimize removal processes.

The two-dimensional spatial concentration distributions and breakthrough curve modeling, developed using random walk technique, represent an innovative approach that effectively simulates particle dispersion and advection in porous media. This method demonstrates high efficiency and accuracy, particularly under conditions with steep pollutant gradients, making it a valuable tool for modeling dynamic contaminant transport plumes in SAT systems. The developed models calibrated with experimental observations by accurately capturing pollutant behavior over time and depth. These models reinforce experimental results and provide a visual representation of pollutant transport dynamics while characterizing key transport parameters. Capillary diffusivity, which drives solute movement in unsaturated soils, surpasses molecular diffusion and dispersion in dominance, especially under low infiltration rates where it enhances adsorption and retention.

The statistical analysis using t-tests provides quantitative evidence of the impact of infiltration rate on pollutant removal. The p-values reveal statistically significant differences in pollutant concentrations between the two infiltration rates, validating the experimental and modeling results.

Thesis 3. Impact of pulsed wetting and drying on pollutant fate in SAT systems

The impact of wetting and drying cycles on the overall performance of the SAT system as a nature cyclic based on seasonal and operational variation, these conditions leads to fluctuations in pollutant removal efficiency, affecting treatment performance and the physical properties of the filtrate media.

The use of robust statistical analysis, including logistic regression models, correlation trends and factorial interaction analysis as an innovation framework to validate and track the geochemical interactions, provides a detailed understanding of the

relationships between pollutants and climatical and operational factors. This approach offers new perspectives on how these factors collectively impact pollutant behavior and treatment efficacy.

pH, Dissolved Oxygen (DO), and Oxidation-Reduction Potential (ORP) factors interact with wetting and drying cycles to influence pollutant removal. Strong correlations and interactions between these factors and pollutant concentrations highlight their pivotal role in the treatment process.

Nitrogen species (NH_4^+, NO_2^-, and NO_3^-) exhibit dynamic behaviors during wet and dry periods in the SAT system. NH_4^+ concentrations increase during wet periods due to enhanced leaching but are more effectively removed during dry phases through adsorption and nitrification potential microbial processes, highlighting the critical role of drying in improving NH_4^+ removal efficiency. In contrast, NO_2^- concentrations are lower during wet periods due to limited nitrification, while NO_3^- concentrations show varied responses influenced by DO, pH, and ORP, underscoring the differential behavior of nitrogen species under fluctuating wetting conditions.

Increased PO_4^{3-} concentrations during wet periods, associated with higher DO, pH, and ORP interactions, and more effective removal during dry periods due to immobilization and geochemical reactions, highlight the importance of wet/dry conditions in phosphate management. Meanwhile, The variability in SO_4^{2-} concentrations during wetting and drying cycles, influenced by wet/dry factors such as pH and ORP, provides new insights into the complexities of sulfate dynamics in SAT systems.

Fe^{2+}, Cu^{2+}, Mn^{2+}, MoO_4^{2-}, Zn^{2+}, and Co^{2+} specific patterns in the transport and removal of these metal ions, with wet conditions generally favoring lower concentrations. Each metal ion exhibits distinct correlations with DO, ORP, and pH influencing the oxidation or precipitation of these metals, indicating their unique responses to wet/dry conditions. In contrast, BO_3^{3-} concentrations display a distinct fluctuation pattern, with higher levels during wet periods due to leaching and dissolution. This finding suggests complex interactions between BO_3^{3-} adsorption, precipitation, and desorption processes.

6. Summary

Comparative Investigation and Performance Evaluation of Different Soil Types in Enhancing Pollutants Removal from Synthetic Wastewater in Soil Aquifer Treatment System

This chapter present comprehensive analysis, combining static adsorption studies and dynamic column experiments, offers a novel and detailed understanding of the performance of SAT systems using sand and sandy loam soils for significantly contribute to the understanding of how different soil types perform in SAT systems and offer practical insights for optimizing the design and operation of these systems based on specific environmental conditions and pollutant profiles. The ability to correlate the adsorption capacity with real-world pollutant retention and removal efficiency provides a robust framework for designing and improving SAT systems to achieve more effective wastewater treatment.

The comparative use of Freundlich and Langmuir isothermal models provided new insights into the adsorption characteristics of sand and sandy loam soils. The findings revealed that sandy loam generally has a higher adsorption capacity for certain pollutants, while sand excels in others. The preferential fit of the Langmuir model for sandy loam pollutants further emphasizes its effectiveness in characterizing adsorption behavior, contributing to the optimization of SAT systems based on soil type.

The dynamic column experiments revealed significant differences in the removal efficiencies of various pollutants between sand and sandy loam soils. Sandy loam demonstrated superior removal capabilities for pollutants such as NH_4^+, PO_4^{3-}, Cu^{2+}, Mn^{2+}, MoO_4^{2-}, Zn^{2+}, Co^{2+}, and BO_3^{3-}, with removal rates substantially higher than those observed in sand. Conversely, sand exhibited greater efficiency in removing NO_2^-, NO_3^-, SO_4^{2-}, and Fe^{2+}. This differential behavior underscores the need for a tailored approach in selecting soil media based on the specific pollutants present in SAT systems. Moreover, the application of breakthrough curve analysis to quantify the area under the curve (AUC) provided a comprehensive measure of the total pollutant removal. This approach allowed for the detailed assessment of the retention capacities and adsorption behaviors of the soils, revealing the intricate processes governing pollutant removal in SAT systems. The AUC calculations highlighted the dynamic performance of sand and sandy loam soils in real-world scenarios, demonstrating the utility of this method in evaluating and optimizing SAT system designs.

Understanding the Role of Infiltration Flow Rate on Contaminants Fate and Transport in Soil Aquifer Treatment System: Experimental, Modeling, and Statistical Analysis Approaches

This chapter elucidates the role of infiltration rate in pollutant removal within SAT systems. It combines experimental data, modeling insights, and statistical analysis to present a comprehensive understanding of how varying infiltration rates impact pollutant behavior and removal efficiency.

Infiltration rate significantly affects the transport and removal of various pollutants. A lower infiltration rate (0.5 mL/min) enhances pollutant removal through increased contact time with the sand media, leading to higher adsorption and more efficient biogeochemical reactions. In contrast, a higher infiltration rate (10 mL/min) reduces contact time, resulting in less effective pollutant removal and higher effluent concentrations. By identifying how different pollutants respond to changes in infiltration rate. NH_4^+, PO_4^{3-}, SO_4^{2-}, Fe^{2+}, Mn^{2+}, MoO_4^{2-}, Zn^{2+}, and Co^{2+} these pollutants show significantly better removal at the lower infiltration rate. However, NO_3^-, NO_2^-, Cu^{2+}, and BO_3^{3-} these pollutants exhibit higher removal at the higher infiltration rate, suggesting that specific conditions may benefit their removal.

The detailed experimental breakthrough curves demonstrate clear trends in pollutant removal efficiency under different infiltration rates. The findings confirm that a slower infiltration rate generally leads to better removal due to extended contact time.

The 2-D spatial concentration distributions and breakthrough curve modeling support the experimental observations. Models effectively capture pollutant behavior over time and depth, reinforcing the experimental results and providing a visual representation of pollutant transport dynamics.

The statistical analysis using t-tests provides quantitative evidence of the impact of infiltration rate on pollutant removal. The p-values reveal statistically significant differences in pollutant concentrations between the two infiltration rates, validating the experimental and modeling results.

The chapter findings highlight the importance of customizing infiltration rates based on specific pollutants to optimize removal efficiency. This approach allows for tailored SAT system operation, potentially improving treatment performance for diverse wastewater compositions.

Quantifying the influence of dynamic pulsed of wetting and drying on the transformation and fate of synthetic wastewater pollutants in soil aquifer treatment system

This chapter explains the complex interactions between wetting and drying cycles and pollutant dynamics in SAT systems. The findings contribute to a deeper understanding of pollutant removal processes and offer valuable insights for optimizing system design and operation.

The impact of wetting and drying cycles on the overall performance of the SAT system as a nature cyclic based on seasonal variation, these conditions leads to fluctuations in pollutant removal efficiency, affecting treatment performance and the physical properties of the sand column.

The use of robust statistical analysis, including logistic regression models, correlation studies and factorial interaction trends, provides a detailed understanding of the relationships between pollutants and environmental factors. This approach offers new perspectives on how these factors collectively impact pollutant behavior and treatment efficacy.

pH, Dissolved Oxygen (DO), and Oxidation-Reduction Potential (ORP) factors interact with wetting and drying cycles to influence pollutant removal. Strong correlations and interactions between these factors and pollutant concentrations highlight their pivotal role in the treatment process.

NH_4^+ concentrations increase during wet periods due to enhanced leaching but are more effectively removed during dry periods through adsorption and potential microbial processes. This highlights the critical role of drying phases in improving NH_4^+ removal efficiency.

NO_2^- concentrations are lower during wet periods due to limited nitrification, whereas NO_3^- concentrations show varied responses influenced by DO, pH, and ORP. This underscores the differential behavior of nitrogen species under varying wetting conditions.

Variability in SO_4^{2-} concentrations with respect to wet and dry cycles and their association with environmental factors such as pH and ORP provides new insights into the complexities of sulfate dynamics in SAT systems.

Increased PO_4^{3-} concentrations with higher DO, pH, and ORP, and more effective removal during dry periods, illustrate the importance of environmental conditions in phosphate management.

Fe^{2+}, Cu^{2+}, Mn^{2+}, MoO_4^{2-}, Zn^{2+}, and Co^{2+} specific patterns in the transport and removal of these metal ions, with wet conditions generally favoring lower concentrations. Each metal ion exhibits distinct correlations with DO, ORP, and pH, indicating their unique responses to environmental conditions.

A unique flocculation pattern in BO_3^{3-} concentrations, with higher levels during wet periods due to leaching and dissolution. This finding suggests complex interactions between BO_3^{3-} adsorption, precipitation, and desorption processes.

In summary, wetting and drying cycles emerge as critical determinants in the fate, transport, and treatment of infiltrated wastewater pollutants in the sand column. Recognizing and incorporating these cycles into system design and operation protocols is paramount for achieving and maintaining optimal system efficiency.

Publication list from the MTMT platform

1. Abdalkarim S.Gharbia (**Gharbia Abdalkarim** S.) **UM/FESE/Institute of Water Resources and Environmental Management** ; Balázs Zákányi (**Zákányi Balázs Zsolt** Hidrogeológia) **UM/FESE/Institute of Water Resources and Environmental Management** ; Márton Tóth (**Tóth Márton** Hidrogeológia) **UM/FESE/Institute of Water Resources and Environmental Management**

   Impact of sand media continuous drying and rewetting cyclic on nutrients transformation performance from reclaimed wastewater effluent at soil aquifer treatment

   SCIENTIFIC REPORTS (2045-2322 2045-2322): **14** 1 Paper 8065. (2024)
   Language: English | DOI Other URL
   Journal subject: Scopus - Multidisciplinary Rank: D1
   Szociológiai Tudományos Bizottság HASSELIX SZTB [1901-] A nemzetközi Regionális Tudományok Bizottsága HASSELIX RTB [1901-] B nemzetközi
   Publication: 34778630 | Published Core | **Journal Article (Article)** | Scientific | kézi felvitel

2. Abdalkarim S. Gharbia (**Gharbia Abdalkarim** S.) **UM/FESE/Mikoviny Sámuel Doctoral School of Earth Sciences** ; Balázs Zákányi (**Zákányi Balázs Zsolt** Hidrogeológia) **UM/FESE/Institute of Water Resources and Environmental Management** ; Márton Tóth (**Tóth Márton** Hidrogeológia) **UM/FESE/Institute of Water Resources and Environmental Management**

   OPTIMIZING PHOSPHATEREMOVAL BY MANIPULATING MANGANESE AND COBALTLEVELS IN SOIL AQUIFER TREATMENT SYSTEM

   MULTIDISZCIPLINÁRIS TUDOMÁNYOK: A MISKOLCI EGYETEM KÖZLEMÉNYE (2062-9737 2786-1465): **13** 3 pp 65-73 (2023)
   Language: English | DOI REAL Other URL
   Number of cited publications: 1
   Publication: 34444469 | Published Core Citing | **Journal Article (Article)** | Scientific | kézi felvitel

3. Abdalkarim S. Gharbia (**Gharbia Abdalkarim** S.) **UM/FESE/Mikoviny Sámuel Doctoral School of Earth Sciences** ; Viktória Mikita (**Mikita Viktória** Hidrogeológia) **UM/FESE/Környezetgazdálkodási Intézet** ; Balázs

Zákányi (**Zákányi Balázs Zsolt** Hidrogeológia) **UM/FESE/Környezetgazdálkodási Intézet** ; Márton Tóth (**Tóth Márton** Hidrogeológia) **UM/FESE/Környezetgazdálkodási Intézet**

IMPACTS OF SHORT-TERM CONTINUOUS DRYING AND REWETTING CYCLES ON NITRATE (NO3-) AND PHOSPHATE (PO43-) BEHAVIOR IN SOIL AQUIFER TREATMENT OF INFILTRATED WASTEWATER

In: URBAN WATER 2023
Conference: Czech Republic 2023.03.28. - 2023.03.31.
Velké Bílovice: URBAN WATER 2023, pp 256-263 (2023)
Language: English | Book link(s): ISBN: 9788086020976
Publication: 34431515 | Published Book: 34431511 Core | **Chapter in Book (Conference paper)** | Scientific | kézi felvitel

4. Gharbia Abdalkarim S (**Gharbia Abdalkarim** S.) **UM/FESE/Környezetgazdálkodási Intézet** ; Zakanyi Balazs (**Zákányi Balázs Zsolt** Hidrogeológia) **UM/FESE/Környezetgazdálkodási Intézet** ; Toth Marton (**Tóth Márton** Hidrogeológia) **UM/FESE/Környezetgazdálkodási Intézet**

   Manganese and cobalt metals interrelations with ammonium performance in soil aquifer treatment

   MATEC WEB OF CONFERENCES (2261-236X): **385** Paper 01008. 6 p. (2023)
   Language: English | DOI
   Publication: 34401639 | Published Core | **Journal Article (Conference paper in journal)** | Scientific | RIS-Egyéb

5. Abdalkarim S. Gharbia (**Gharbia Abdalkarim** S.) **UM/FESE/Környezetgazdálkodási Intézet; UM/FESE/Mikoviny Sámuel Doctoral School of Earth Sciences** ; Salem S. Gharbia ; Balázs Zákányi (**Zákányi Balázs Zsolt** Hidrogeológia) **UM/FESE/Környezetgazdálkodási Intézet** ; Márton Tóth (**Tóth Márton** Hidrogeológia) **UM/FESE/Környezetgazdálkodási Intézet** ; Peter Szucs (**Szűcs Péter** Hidrogeológia, kúthidraulika) **UM/FESE/Környezetgazdálkodási Intézet**

   Groundwater Quality Evaluation for Irrigation Suitable Using Geostatistical Algorithms

DESALINATION AND WATER TREATMENT (1944-3994 1944-3986): 24 p. (2022)
Language: English | Preprint DOI
Journal subject: Scopus - Ocean Engineering Rank: Q3
Journal subject: Scopus - Pollution Rank: Q3
Journal subject: Scopus - Water Science and Technology Rank: Q3
HAS Section of Agricultural Sciences (IV.) HASSASIV A
Citing papers: 2 | Independent citation: 2 | Self citation: 0 | Unknown citation: 0 | Number of citations with DOI: 1
Publication: 32801367 | Published Core | **Journal Article (Article)** | Scientific | kézi felvitel

6. Gharbia Abdelkarim S. (**Gharbia Abdalkarim** S.) **UM/FESE/Környezetgazdálkodási Intézet** ; Zákányi Balázs (**Zákányi Balázs Zsolt** Hidrogeológia) **UM/FESE/Környezetgazdálkodási Intézet** ; Tóth Márton (**Tóth Márton** Hidrogeológia) **UM/FESE/Környezetgazdálkodási Intézet**

   Equilibrium Adsorption Modeling for Ternary Multi-Metals in the Clay Soil

   In: Szabó Norbert Péter (**Szabó Norbert Péter** Mélyfúrási geofizika) **UM/FESE/Geofizikai és Térinformatikai Intézet** ; Virág Zoltán (**Virág Zoltán István** Gépészeti tudományok) **UM/FESE/Bányászati és Geotechnikai Intézet** (eds.)
   Új eredmények a műszaki föld- és környezettudományban 2022
   Miskolc-Egyetemváros: University of Miskolc, Faculty of Earth Sciences and Engineering, pp 291-298 (2022)
   Language: English | Teljes dokumentum Book link(s): ISBN: 9789633582695 MIDRA
   Publication: 33317800 | Admin approved Book: 33300465 Core | **Chapter in Book (Study)** | Scientific | kézi felvitel

7. Tóth Márton (**Tóth Márton** Hidrogeológia) **UM/FESE/Környezetgazdálkodási Intézet** ; Kovács Balázs (**Kovács Balázs** Hidrogeológia) **UM/FESE/Környezetgazdálkodási Intézet** ; Czinkota Imre (**Czinkota Imre** Talajkémia) ; Gharbia Abdelkarim S.Szász Noémi (**Gharbia Abdalkarim** S.) **UM/FESE/Környezetgazdálkodási Intézet** ; Székely István (**Székely István** Hidrogeológia) **UM/FESE/Környezetgazdálkodási Intézet**

   Investigation of Selective Dynamic Adsorption of Scandium on CH Collector

In: Szabó Norbert Péter (**Szabó Norbert Péter** Mélyfúrási geofizika) **UM/FESE/Geofizikai és Térinformatikai Intézet** ; Virág Zoltán (**Virág Zoltán István** Gépészeti tudományok) **UM/FESE/Bányászati és Geotechnikai Intézet** (eds.)
Új eredmények a műszaki föld- és környezettudományban 2022
Miskolc-Egyetemváros: University of Miskolc, Faculty of Earth Sciences and Engineering, pp 299-304 (2022)
Language: English | Book link(s): ISBN: 9789633582695 MIDRA
Publication: 33317847 | Admin approved Book: 33300465 Core | **Chapter in Book (Study)** | Scientific | kézi felvitel

8. Abdalkarim S. Gharbia (**Gharbia Abdalkarim** S.) **UM/FESE/Környezetgazdálkodási Intézet; UM/FESE/Mikoviny Sámuel Doctoral School of Earth Sciences** ; Balázs Zákányi (**Zákányi Balázs Zsolt** Hidrogeológia) **UM/FESE/Környezetgazdálkodási Intézet** ; Márton Tóth (**Tóth Márton** Hidrogeológia) **UM/FESE/Környezetgazdálkodási Intézet**

   Experimental and numerical study for the adsorption behavior of Cu(II) and Mn(II) in quartz sand

   SUSTAINABLE WATER RESOURCES MANAGEMENT (2363-5037 2363-5045): **8** 5 Paper 126. 9 p. (2022)
   Language: English | DOI WoS Scopus Other URL
   Journal subject: Scopus - Water Science and Technology Rank: Q2
   Journal subject: Scopus - Renewable Energy, Sustainability and the Environment Rank: Q3
   Citing papers: 4 | Independent citation: 3 | Self citation: 1 | Unknown citation: 0 | Number of citations in WoS: 1 | WoS/Scopus assigned: 1 | Number of citations with DOI: 3
   Publication: 33049018 | Validated Core | **Journal Article (Article)** | Scientific | kézi felvitel

9. Abdelkarim S. Gharbia (**Gharbia Abdalkarim** S.) **UM/FESE/Környezetgazdálkodási Intézet; UM/FESE/Mikoviny Sámuel Doctoral School of Earth Sciences** ; Balázs Zákányi (**Zákányi Balázs Zsolt** Hidrogeológia) **UM/FESE/Környezetgazdálkodási Intézet** ; Márton Tóth (**Tóth Márton** Hidrogeológia) **UM/FESE/Környezetgazdálkodási Intézet**

EXPERIMENTAL AND NUMERICAL STUDIES FOR THE ADSORPTION BEHAVIOR Cu(II) AND Zn(II) IONS ON A FIXED CLAY BED

In: Szigyártó I-L ; Szikszai A (eds.)
XVII. Kárpát-medencei Környezettudományi Konferencia : konferenciakötet
Conference: Cluj-Napoca, Romania 2022.04.06. - 2022.04.09. (Sapientia Hungarian University of Transylvania)
Cluj-Napoca: Ábel Kiadó, pp 220-226 (2022) (Kárpát-Medencei Környezettudományi Konferencia 1842-9815)
Language: English | Book link(s): Kiadónál Other URL
Publication: 32787928 | Published Book: 32778734 Core | **Chapter in Book (Conference paper)** | Scientific | kézi felvitel

10. Abdalkarim S. Gharbia (**Gharbia Abdalkarim** S.) **UM/FESE/Környezetgazdálkodási Intézet; UM/FESE/Mikoviny Sámuel Doctoral School of Earth Sciences** ; Salem S. Gharbia ; Hassan Tamous ; Thaer Abushbak ; Balázs Zákányi (**Zákányi Balázs Zsolt** Hidrogeológia) **UM/FESE/Környezetgazdálkodási Intézet** ; Márton Tóth (**Tóth Márton** Hidrogeológia) **UM/FESE/Környezetgazdálkodási Intézet**

Optimization modeling for the use of antiscalants in the brackish RO desalination plants

DESALINATION AND WATER TREATMENT (1944-3994 1944-3986): **224** pp 12-20 (2021)
Language: English | DOI WoS Scopus
Journal subject: Scopus - Ocean Engineering Rank: Q3
Journal subject: Scopus - Pollution Rank: Q4
HAS Section of Agricultural Sciences (IV.) HASSASIV A
Publication: 31855120 | Validated Core | **Journal Article (Article)** | Scientific | kézi felvitel

References

ABEL, C. D., SHARMA, S. K., BUÇPAPAJ, E. & KENNEDY, M. D. 2013. Impact of hydraulic loading rate and media type on removal of bulk organic matter and nitrogen from primary effluent in a laboratory-scale soil aquifer treatment system. *Water science and technology,* 68**,** 217-226.

ABEL, C. D., SHARMA, S. K., MALOLO, Y. N., MAENG, S. K., KENNEDY, M. D. & AMY, G. L. 2012. Attenuation of bulk organic matter, nutrients (N and P), and pathogen indicators during soil passage: effect of temperature and redox conditions in simulated soil aquifer treatment (SAT). *Water, Air, & Soil Pollution,* 223**,** 5205-5220.

ABEL, C. D. T. 2014. *Soil aquifer treatment: assessment and applicability of primary effluent reuse in developing countries*, CRC Press Inc.

ADIBMEHR, Z. & FAGHIHIAN, H. 2019. Preparation of highly selective magnetic cobalt ion-imprinted polymer based on functionalized SBA-15 for removal Co2+ from aqueous solutions. *Journal of Environmental Health Science and Engineering,* 17**,** 1213-1225.

AHARONI, A., GUTTMAN, J., CIKUREL, H. & SHARMA, S. 2011. Guidelines for design, operation and maintenance of SAT (and hybrid SAT) systems. *EU SWITCH project*.

AK, M. & GUNDUZ, O. 2014. Fate of nutrients in secondary treated municipal wastewater during percolation through the soil media. *CLEAN–Soil, Air, Water,* 42**,** 1036-1043.

AL-GHOUTI, M. A. & DA'ANA, D. A. 2020. Guidelines for the use and interpretation of adsorption isotherm models: A review. *Journal of hazardous materials,* 393**,** 122383.

AL-KAISI, M. M., LAL, R., OLSON, K. R. & LOWERY, B. 2017. Fundamentals and functions of soil environment. *Soil health and intensification of agroecosytems.* Elsevier.

AMBAYE, T., VACCARI, M., VAN HULLEBUSCH, E. D., AMRANE, A. & RTIMI, S. 2021. Mechanisms and adsorption capacities of biochar for the removal of organic and inorganic pollutants from industrial wastewater. *International Journal of Environmental Science and Technology***,** 1-22.

AMY, G. & DREWES, J. 2007. Soil aquifer treatment (SAT) as a natural and sustainable wastewater reclamation/reuse technology: fate of wastewater effluent organic matter (EfOM) and trace organic compounds. *Environmental monitoring and assessment,* 129**,** 19-26.

AN, Q., MIAO, Y., ZHAO, B., LI, Z. & ZHU, S. 2020. An alkali modified biochar for enhancing Mn2+ adsorption: Performance and chemical mechanism. *Materials Chemistry and Physics,* 248**,** 122895.

ANGELAKIS, A. N. & SPYRIDAKIS, S. V. The status of water resources in Minoan times: A preliminary study. Diachronic Climatic Impacts on Water Resources: with Emphasis on the Mediterranean Region, 1996. Springer, 161-191.

ARYE, G., DROR, I. & BERKOWITZ, B. 2011. Fate and transport of carbamazepine in soil aquifer treatment (SAT) infiltration basin soils. *Chemosphere,* 82**,** 244-252.

ASANO, T., BURTON, F. & LEVERENZ, H. 2007. *Water reuse: issues, technologies, and applications*, McGraw-Hill Education.

ASANO, T. & COTRUVO, J. A. 2004. Groundwater recharge with reclaimed municipal wastewater: health and regulatory considerations. *Water research,* 38**,** 1941-1951.

BAO, S., DI, J., DONG, Y., WANG, X., XUE, L. & SUN, J. 2021. Optimization of preparation conditions of sulfate-reducing bacteria (SRB) immobilization particles strengthened by maifanite and its treatment of wastewater containing Mn2+. *Energy Sources, Part A: Recovery, Utilization, and Environmental Effects***,** 1-14.

BDOUR, A. Perspectives on sustainable wastewater treatment technologies and reuse options in the urban areas of the Mediterranean region. World Environmental and Water Resources Congress 2007: Restoring Our Natural Habitat, 2007. 1-15.

BEAR, J. 2018. *Modeling phenomena of flow and transport in porous media*, Springer.

BEKELE, E., TOZE, S., PATTERSON, B., FEGG, W., SHACKLETON, M. & HIGGINSON, S. 2013. Evaluating two infiltration gallery designs for managed aquifer recharge using secondary treated wastewater. *Journal of environmental management,* 117**,** 115-120.

BEN MOSHE, S., WEISBROD, N., BARQUERO, F., SALLWEY, J., ORGAD, O. & FURMAN, A. 2020. On the role of operational dynamics in biogeochemical efficiency of a soil aquifer treatment system. *Hydrology and Earth System Sciences,* 24**,** 417-426.

BENSLIMANE, S., BOUHIDEL, K.-E., FERFACHE, A. & FARHI, S. 2020. Mechanistic study of the synergetic inhibiting effects of Zn2+, Cu2+ and Mg2+ ions on calcium carbonate precipitation. *Water Research,* 186**,** 116323.

BENTO, L. R., CASTRO, A. J. R., MOREIRA, A. B., FERREIRA, O. P., BISINOTI, M. C. & MELO, C. A. 2019. Release of nutrients and organic carbon in different soil types from hydrochar obtained using sugarcane bagasse and vinasse. *Geoderma,* 334**,** 24-32.

BIBIANO-CRUZ, L., GARFIAS, J., SALAS-GARCÍA, J., MARTEL, R. & LLANOS, H. 2016. Batch and column test analyses for hardness removal using natural and homoionic clinoptilolite: breakthrough experiments and modeling. *Sustainable Water Resources Management,* 2**,** 183-197.

BIEL-MAESO, M., BURKE, V., GRESKOWIAK, J., MASSMANN, G., LARA-MARTIN, P. A. & CORADA-FERNANDEZ, C. 2021. Mobility of contaminants of emerging concern in soil column experiments. *Science of the Total Environment,* 762**,** 144102.

BIERLEIN, K. A. 2012. *Modeling Manganese Sorption and Surface Oxidation During Filtration.* Virginia Tech.

BLECKEN, G.-T., ZINGER, Y., DELETIĆ, A., FLETCHER, T. D. & VIKLANDER, M. 2009. Influence of intermittent wetting and drying conditions on heavy metal removal by stormwater biofilters. *Water research,* 43**,** 4590-4598.

BOURLIVA, A., SIKALIDIS, A., PAPADOPOULOU, L., BETSIOU, M., MICHAILIDIS, K., SIKALIDIS, C. & FILIPPIDIS, A. 2018. Removal of Cu2+ and Ni2+ ions from aqueous solutions by adsorption onto natural palygorskite and vermiculite. *Clay Minerals,* 53**,** 1-15.

BOUWER, H. 2000. Integrated water management: emerging issues and challenges. *Agricultural water management,* 45**,** 217-228.

BOUWER, H. 2002. Artificial recharge of groundwater: hydrogeology and engineering. *Hydrogeology journal,* 10**,** 121-142.

BÜCKER-GITTEL, M., MOHRLOK, U. & JIRKA, G. 2003. Modelling unsaturated water transport using a random walk approach. *IAHS PUBLICATION***,** 17-21.

CANDELA, L., FABREGAT, S., JOSA, A., SURIOL, J., VIGUÉS, N. & MAS, J. 2007. Assessment of soil and groundwater impacts by treated urban wastewater reuse. A case study: Application in a golf course (Girona, Spain). *Science of the total environment,* 374**,** 26-35.

CASANOVA, J., BÉCHU, E., BOUZIT, M., LEROY, P., MATON, L. & PETTENATI, M. 2008. Appui au projet de REcharge artificielle et Gestion Active des nappes Littorales (REGAL). *Rapport intermédiaire BRGM/RP–56836 RFR, Décembre,* 63.

CASANOVA, J., DEVAU, N. & PETTENATI, M. 2016. Managed aquifer recharge: an overview of issues and options. *Integrated groundwater management: Concepts, approaches and challenges***,** 413-434.

CATA, C. & MOHRLOK, U. 2006. A random-walk approach for simulating wastewater transport and transformations in the. *Calibration and Reliability in Groundwater Modelling: From Uncertainty to Decision Making***,** 255.

CHAUDHARI, P. R., AHIRE, D. V., AHIRE, V. D., CHKRAVARTY, M. & MAITY, S. 2013. Soil bulk density as related to soil texture, organic matter content and available total nutrients of Coimbatore soil. *International Journal of Scientific and Research Publications,* 3**,** 1-8.

CHAUHAN, D., KUMAR, A. & WARKAR, S. 2022. An efficient adsorbent for the removal of Zn2+ Cd2+ and Hg2+ from the real industrial effluents. *International Journal of Environmental Science and Technology,* 19**,** 1483-1494.

CHEN, L., ZHANG, J. & ZHENG, X. 2019. A laboratory study of the presence and transformation of dissolved Mn (III) across the sediment–water interface of an anoxic freshwater body. *Environmental Earth Sciences,* 78**,** 1-9.

CHEN, Y., GU, S., WU, S., MA, X., HUSSAIN, I., SUN, Z., LU, Z. & ZHANG, K. 2022. Copper activated near-full two-electron Mn4+/Mn2+ redox for mild aqueous Zn/MnO2 battery. *Chemical Engineering Journal,* 450**,** 137923.

CHOCAT, B., BERTRAND-KRAJEWSKI, J.-L. & BARRAUD, S. 2007. Eaux pluviales urbaines et rejets urbains par temps de pluie.

CORCORAN, E. 2010. *Sick water?: the central role of wastewater management in sustainable development: a rapid response assessment*, UNEP/Earthprint.

COUNCIL, N. R. 2012. *Water reuse: potential for expanding the nation's water supply through reuse of municipal wastewater*, National Academies Press.

CRITES, R. W., MIDDLEBROOKS, E. J. & BASTIAN, R. K. 2014. *Natural wastewater treatment systems*, CRC press.

CRUZ AYALA, M.-B. & TORTAJADA, C. 2023. Managed aquifer recharge in Mexico: proposals for an improved legal framework and public policies. *Water International,* 48**,** 165-183.

DABBAGH, R., ASHTIANI MOGHADDAM, Z. & GHAFOURIAN, H. 2016. Removal of cobalt (II) ion from water by adsorption using intact and modified Ficus carica leaves as low-cost natural sorbent. *Desalination and Water Treatment,* 57**,** 19890-19902.

DAHLKE, H. E., LAHUE, G. T., MAUTNER, M. R., MURPHY, N. P., PATTERSON, N. K., WATERHOUSE, H., YANG, F. & FOGLIA, L. 2018. Managed aquifer recharge as a tool to enhance sustainable groundwater management in California: examples from field and modeling studies. *Advances in chemical pollution, environmental management and protection.* Elsevier.

DE ROZARI, P. Performance efficiency of sand media amended with biochar for phosphorus removal using column filtration. IOP Conference Series: Materials Science and Engineering, 2020. IOP Publishing, 012043.

DÍAZ-CRUZ, M. S. & BARCELÓ, D. 2008. Trace organic chemicals contamination in ground water recharge. *Chemosphere,* 72**,** 333-342.

DILLON, P. 2005. Future management of aquifer recharge. *Hydrogeology journal,* 13**,** 313-316.

DILLON, P., ALLEY, W., ZHENG, Y. & VANDERZALM, J. 2022. Managed aquifer recharge: Overview and governance. IAH Special Publication.

DILLON, P., FERNÁNDEZ ESCALANTE, E., MEGDAL, S. B. & MASSMANN, G. 2020. Managed aquifer recharge for water resilience. MDPI.

DILLON, P. & LIGGETT, J. 1983. An ephemeral stream-aquifer interaction model. *Water Resources Research,* 19**,** 621-626.

DILLON, P., PAVELIC, P., PAGE, D., BERINGEN, H. & WARD, J. 2009. Managed aquifer recharge: an introduction. waterlines report series No. 13. *National Water Commission, Canberra, Australia, 65p*.

DILLON, P., PAVELIC, P., TOZE, S., RINCK-PFEIFFER, S., MARTIN, R., KNAPTON, A. & PIDSLEY, D. 2006. Role of aquifer storage in water reuse. *Desalination,* 188**,** 123-134.

DILLON, P., STUYFZAND, P., GRISCHEK, T., LLURIA, M., PYNE, R., JAIN, R., BEAR, J., SCHWARZ, J., WANG, W. & FERNANDEZ, E. 2019. Sixty years of global progress in managed aquifer recharge. *Hydrogeology journal,* 27**,** 1-30.

DILLON, P., TOZE, S., PAGE, D., VANDERZALM, J., BEKELE, E., SIDHU, J. & RINCK-PFEIFFER, S. 2010. Managed aquifer recharge: rediscovering nature as a leading edge technology. *Water science and technology,* 62**,** 2338-2345.

DONG, Y., WANG, J., GAO, Z., DI, J., WANG, D., GUO, X., HU, Z., GAO, X. & WANG, Y. 2023. Study on Growth Influencing Factors and Desulfurization Performance of Sulfate Reducing Bacteria Based on the Response Surface Methodology. *ACS omega,* 8**,** 4046-4059.

DREWES, J. & KHAN, S. 2011. Water reuse for drinking water augmentation. *Water quality and treatment***,** 16.1-16.48.

ELKAYAM, R., AHARONI, A., VAIZEL-OHAYON, D., SUED, O., KATZ, Y., NEGEV, I., MARANO, R., CYTRYN, E., SHTRASLER, L. & LEV, O. 2018. Viral and microbial pathogens, indicator microorganisms, microbial source tracking indicators, and antibiotic resistance genes in a confined managed effluent recharge system. *Journal of Environmental Engineering,* 144**,** 05017011.

ESCALANTE, E. F., SAUTO, J. S. S. & GIL, R. C. 2019. Sites and indicators of MAR as a successful tool to mitigate climate change effects in Spain. *Water,* 11**,** 1943.

ESSANDOH, H. M., TIZAOUI, C. & MOHAMED, M. H. 2013. Removal of dissolved organic carbon and nitrogen during simulated soil aquifer treatment. *Water research,* 47**,** 3559-3572.

ESSANDOH, H. M., TIZAOUI, C., MOHAMED, M. H., AMY, G. & BRDJANOVIC, D. 2011. Soil aquifer treatment of artificial wastewater under saturated conditions. *Water research,* 45**,** 4211-4226.

ESTOP-ARAGONÉS, C., KNORR, K.-H. & BLODAU, C. 2013. Belowground in situ redox dynamics and methanogenesis recovery in a degraded fen during dry-wet cycles and flooding. *Biogeosciences,* 10**,** 421-436.

EWEN, J., PARKIN, G. & O'CONNELL, P. E. 2000. SHETRAN: distributed river basin flow and transport modeling system. *Journal of hydrologic engineering,* 5**,** 250-258.

FERNÁNDEZ ESCALANTE, E. 2015. Practical management to minimize the effects of clogging in managed aquifer recharge wells at two sites in the Guadiana Basin, Spain. *Journal of Hydrologic Engineering,* 20**,** B5014002.

FERNANDEZ, R. M. D., ESTRADA, R. J. R., TOMON, T. R. B., DINGCONG JR, R. G., AMPARADO JR, R. F., CAPANGPANGAN, R. Y., MALALUAN, R. M., DUMANCAS, G. G., LUBGUBAN, A. A. & ALGUNO, A. C. 2023. Experimental Design and Breakthrough Curve Modeling of Fixed-Bed Columns Utilizing a Novel 3D Coconut-

Based Polyurethane-Activated Carbon Composite Adsorbent for Lead Sequestration. *Sustainability,* 15**,** 14344.

FICHTNER, T., GOERSMEYER, N. & STEFAN, C. 2019. Influence of soil pore system properties on the degradation rates of organic substances during soil aquifer treatment (SAT). *Applied Sciences,* 9**,** 496.

FOSTER, S., VAN STEENBERGEN, F., ZULETA, J. & GARDUÑO, H. 2010. Conjunctive use of groundwater and surface water. *GW-Mate, Strateg Overview Ser***,** 26.

FOX, P. 2001. *Soil aquifer treatment for sustainable water reuse*, American Water Works Association.

FOX, P. 2020. Soil aquifer treatment: an assessment of sustainability. *Management of aquifer recharge for sustainability.* CRC Press.

FOX, P., HOUSTON, S., WESTERHOFF, P., DREWES, J., NELLOR, M., YANKO, B., BAIRD, R., RINCON, M., ARNOLD, R. & LANSEY, K. 2001. An investigation of soil aquifer treatment for sustainable water reuse. *Research Project Summary of the National Center for Sustainable Water Supply (NCSWS), USA,* 110.

GALE, I. & DILLON, P. 2005. *Strategies for Managed Aquifer Recharge (MAR) in semi-arid areas*, UNESCO Paris.

GAO, L., WANG, B., LI, S., WU, H., WU, X., LIANG, G., GONG, D., ZHANG, X., CAI, D. & DEGRÉ, A. 2019a. Soil wet aggregate distribution and pore size distribution under different tillage systems after 16 years in the Loess Plateau of China. *Catena,* 173**,** 38-47.

GAO, Q., BLUM, K. M., GAGO-FERRERO, P., WIBERG, K., AHRENS, L. & ANDERSSON, P. L. 2019b. Impact of on-site wastewater infiltration systems on organic contaminants in groundwater and recipient waters. *Science of the Total Environment,* 651**,** 1670-1679.

GAVRIĆ, S., LEONHARDT, G., MARSALEK, J. & VIKLANDER, M. 2019. Processes improving urban stormwater quality in grass swales and filter strips: A review of research findings. *Science of the Total Environment,* 669**,** 431-447.

GHARBIA, A. S., ZÁKÁNYI, B. & TÓTH, M. 2022. Experimental and numerical study for the adsorption behavior of Cu (II) and Mn (II) in quartz sand. *Sustainable Water Resources Management,* 8**,** 1-9.

GHARBIA, A. S., ZÁKÁNYI, B. & TÓTH, M. 2024. Impact of sand media continuous drying and rewetting cyclic on nutrients transformation performance from reclaimed wastewater effluent at soil aquifer treatment. *Scientific Reports,* 14**,** 8065.

GHARBIA, S. S., AISH, A., ABUSHBAK, T., QISHAWI, G., AL-SHAWA, I., GHARBIA, A., ZELENAKOVA, M., GILL, L. & PILLA, F. 2016. Evaluation of wastewater post-treatment options for reuse purposes in the agricultural sector under rural development conditions. *Journal of Water Process Engineering,* 9**,** 111-122.

GHORBEL, L., COUDERT, L., GILBERT, Y., MERCIER, G. & BLAIS, J.-F. 2016. Assessment of sulfide production risk in soil during the infiltration of domestic wastewater treated by a sulfur-utilizing denitrification process. *Environmental Science and Pollution Research,* 23**,** 19071-19083.

GILL, L., MAC MAHON, J., KNAPPE, J. & MORRISSEY, P. 2023. Hydraulic conductivity assessment of falling head percolation tests used for the design of on-site wastewater treatment systems. *Water Research,* 236**,** 119968.

GOREN, O. 2008. *Geochemical Evolution and Manganese Mobilization in Organic Enriched Water Recharging Calcareous-Sandstone Aquifer; Clues from the Shafdan Sewage Treatment Plant*, Hebrew University.

GOREN, O., BURG, A., GAVRIELI, I., NEGEV, I., GUTTMAN, J., KRAITZER, T., KLOPPMANN, W. & LAZAR, B. 2014. Biogeochemical processes in infiltration basins and their impact on the recharging effluent, the soil aquifer treatment (SAT) system of the Shafdan plant, Israel. *Applied geochemistry,* 48**,** 58-69.

GORSKI, C. A., EDWARDS, R., SANDER, M., HOFSTETTER, T. B. & STEWART, S. M. 2016. Thermodynamic characterization of iron oxide–aqueous Fe2+ redox couples. *Environmental science & technology,* 50**,** 8538-8547.

GRESKOWIAK, J., PROMMER, H., MASSMANN, G. & NÜTZMANN, G. 2006. Modeling seasonal redox dynamics and the corresponding fate of the pharmaceutical residue phenazone during artificial recharge of groundwater. *Environmental science & technology,* 40**,** 6615-6621.

GRINSHPAN, M., FURMAN, A., DAHLKE, H. E., RAVEH, E. & WEISBROD, N. 2021. From managed aquifer recharge to soil aquifer treatment on agricultural soils: Concepts and challenges. *Agricultural Water Management,* 255**,** 106991.

GUILLEMOTO, Q., PICOT-COLBEAUX, G., VALDES, D., DEVAU, N., MATHURIN, F., PETTENATI, M., KLOPPMANN, W. & MOUCHEL, J.-M. 2022. Transfer of trace organic compounds in an operational soil-aquifer treatment system assessed through an intrinsic tracer test and transport modelling. *Science of The Total Environment,* 836**,** 155643.

GUIZANI, M., KATO, H. & FUNAMIZU, N. 2011. Assessing the removal potential of soil-aquifer treatment system (soil column) for endotoxin. *Journal of Environmental Monitoring,* 13**,** 1716-1722.

HÄNDEL, F., LIU, G., DIETRICH, P., LIEDL, R. & BUTLER JR, J. J. 2014. Numerical assessment of ASR recharge using small-diameter wells and surface basins. *Journal of Hydrology,* 517**,** 54-63.

HARTOG, N. & STUYFZAND, P. J. 2017. Water quality considerations on the rise as the use of managed aquifer recharge systems widens. MDPI.

HEIDARPOUR, M., MOSTAFAZADEH-FARD, B., KOUPAI, J. A. & MALEKIAN, R. 2007. The effects of treated wastewater on soil chemical properties using subsurface and surface irrigation methods. *Agricultural water management,* 90**,** 87-94.

HEILWEIL, V. M. & MARSTON, T. M. 2011. Assessment of managed aquifer recharge from Sand Hollow Reservoir, Washington County, Utah, updated to conditions in 2010.

HENDRICKX, J. M. & FLURY, M. 2001. Uniform and preferential flow mechanisms in the vadose zone. *Conceptual models of flow and transport in the fractured vadose zone***,** 149-187.

HORAN, N. J. 1989. *Biological wastewater treatment systems: theory and operation*, John Wiley & Sons Ltd.

HUANG, B., YUAN, Z., LI, D., ZHENG, M., NIE, X. & LIAO, Y. 2020. Effects of soil particle size on the adsorption, distribution, and migration behaviors of heavy metal (loid) s in soil: A review. *Environmental Science: Processes & Impacts,* 22**,** 1596-1615.

HUERTAS, E., SALGOT, M., HOLLENDER, J., WEBER, S., DOTT, W., KHAN, S., SCHAEFER, A., MESSALEM, R., BIS, B. & AHARONI, A. 2008. Key objectives for water reuse concepts. *Desalination,* 218**,** 120-131.

HUSSAIN, S., AZIZ, H. A., ISA, M. H., ADLAN, M. N. & ASAARI, F. A. 2007. Physico-chemical method for ammonia removal from synthetic wastewater using limestone and GAC in batch and column studies. *Bioresource technology,* 98**,** 874-880.

HUTCHISON, A., MILCZAREK, M. & BANERJEE, M. 2013. Clogging phenomena related to surface water recharge facilities. *Clogging issues associated with managed aquifer recharge methods***,** 34-49.

ICEKSON-TAL, N., AVRAHAM, O., SACK, J. & CIKUREL, H. 2003. Water reuse in Israel-the Dan Region Project: evaluation of water quality and reliability of plant's operation. *Water science and technology: water supply,* 3**,** 231-237.

IMIG, A., SZABÓ, Z., HALYTSIA, O., VRACHIOLI, M., KLEINERT, V. & REIN, A. 2022. A review on risk assessment in managed aquifer recharge. *Integrated Environmental Assessment and Management,* 18**,** 1513-1529.

KALAVROUZIOTIS, I. K. & APOSTOLOPOULOS, C. A. 2007. An integrated environmental plan for the reuse of treated wastewater effluents from WWTP in urban areas. *Building and Environment,* 42**,** 1862-1868.

KAVURI, M., BODDU, M. & ANNAMDAS, V. G. M. 2011. New methods of artificial recharge of aquifers: A review. *poster presented at the 4th International Perspective on Water Resources & the Environment (IPWE), National University of Singapore (NUS), Singapore***,** 4-6.

KAZNER, C., WINTGENS, T. & DILLON, P. 2012. *Water reclamation technologies for safe managed aquifer recharge*, IWA publishing.

KEBEDE, G., TAFESE, T., ABDA, E. M., KAMARAJ, M. & ASSEFA, F. 2021. Factors influencing the bacterial bioremediation of hydrocarbon contaminants in the soil: mechanisms and impacts. *Journal of Chemistry,* 2021**,** 1-17.

KEESSTRA, S. D., GEISSEN, V., MOSSE, K., PIIRANEN, S., SCUDIERO, E., LEISTRA, M. & VAN SCHAIK, L. 2012. Soil as a filter for groundwater quality. *Current Opinion in Environmental Sustainability,* 4**,** 507-516.

KENNEDY, K. K., MASEKA, K. J. & MBULO, M. 2018. Selected adsorbents for removal of contaminants from wastewater: towards engineering clay minerals. *Open Journal of Applied Sciences,* 8**,** 355-369.

KONSTANTINOU, C. & BISCONTIN, G. 2022. Experimental Investigation of the Effects of Porosity, Hydraulic Conductivity, Strength, and Flow Rate on Fluid Flow in Weakly Cemented Bio-Treated Sands. *Hydrology,* 9**,** 190.

KOOPAL, L., TAN, W. & AVENA, M. 2020. Equilibrium mono-and multicomponent adsorption models: From homogeneous ideal to heterogeneous non-ideal binding. *Advances in Colloid and Interface Science,* 280**,** 102138.

KUMAR, V., SHAHI, S. & SINGH, S. 2018. Bioremediation: an eco-sustainable approach for restoration of contaminated sites. *Microbial bioprospecting for sustainable development***,** 115-136.

KUMORDZI, G., MALEKSHOAR, G., YANFUL, E. K. & RAY, A. K. 2016. Solar photocatalytic degradation of Zn2+ using graphene based TiO2. *Separation and Purification Technology,* 168**,** 294-301.

KURKI, V., LIPPONEN, A. & KATKO, T. 2013. Managed aquifer recharge in community water supply: the Finnish experience and some international comparisons. *Water international,* 38**,** 774-789.

KVITSAND, H., MYRMEL, M., FIKSDAL, L. & ØSTERHUS, S. 2017. Evaluation of bank filtration as a pretreatment method for the provision of hygienically safe drinking water in Norway: results from monitoring at two full-scale sites. *Hydrogeology Journal,* 25.

LE COUSTUMER, S.-M. 2008. *Colmatage et rétention des éléments traces métalliques dans les systèmes d'infiltration des eaux pluviales.* Lyon, INSA.

LEVANTESI, C., LA MANTIA, R., MASCIOPINTO, C., BÖCKELMANN, U., AYUSO-GABELLA, M. N., SALGOT, M., TANDOI, V., VAN HOUTTE, E., WINTGENS, T. & GROHMANN, E. 2010. Quantification of pathogenic microorganisms and microbial indicators in three wastewater reclamation and managed aquifer recharge facilities in Europe. *Science of the Total Environment,* 408**,** 4923-4930.

LEVINTAL, E., HUANG, L., GARCÍA, C. P., COYOTL, A., FIDELIBUS, M. W., HORWATH, W. R., RODRIGUES, J. L. M. & DAHLKE, H. E. 2023. Nitrogen fate during agricultural managed aquifer recharge: Linking plant response, hydrologic, and geochemical processes. *Science of the Total Environment,* 864**,** 161206.

LI, J., HU, C., LIU, B. & LIU, Z. 2023. Dual pathway reduction of Mo4+ and photogenerated electrons restore catalytic sites to enhance heterogeneous peroxymonosulfate activation system. *Chemical Engineering Journal,* 452**,** 139246.

LI, M., CHENG, X. & GUO, H. 2013. Heavy metal removal by biomineralization of urease producing bacteria isolated from soil. *International Biodeterioration & Biodegradation,* 76**,** 81-85.

LI, S., MU, J., DU, Y. & WU, Z. 2019. Study and application of real-time control strategy based on DO and ORP in nitritation–denitrification SBR start-up. *Environmental technology*.

LIANG, D. & XUEFEI, W. 2014. A random walk simulation of scalar mixing in flows through submerged vegetations. *Journal of Hydrodynamics, Ser. B,* 26**,** 343-350.

LIU, M., YE, J., LIU, S., XU, X., CUI, Y., QU, J., ZHANG, Z., ZHANG, K., NIU, N. & CHEN, L. 2023. Turning Silica into Enzymes by Hydrogenation: Simultaneously Achieving Oxygen Vacancy Engineering and Tumor Adaptive Accumulation for NIR-II-Potentiated Therapy. *Advanced Functional Materials***,** 2306392.

LIU, Y. 2017. Geochemical processes and solute transport in coastal groundwater mixing zone. *HKU Theses Online (HKUTO)*.

LU, Q. M., KNUDSEN, J., ESKESEN, S., POWERS, J., SHREMP, F., SEGAR, D., STAMMAN, E. & YUCHENG, Z. 2012. *Wastewater management for coastal cities: the ocean disposal option*, Springer Science & Business Media.

MA, H., YANG, Z., PU, S. & MA, X. 2023. The Effect of Drying–Wetting Cycles on Soil Inorganic Nitrogen Transformation in Drip-Irrigated Cotton Field Soil in Northwestern China. *Applied Sciences,* 13**,** 3892.

MALOLO, Y. 2011. *Effect of temperature and redox conditions on removal of contaminents during soil aquifer treatment.* Unesco-IHE.

MANISHA, M., VERMA, K., RAMESH, N., ANIRUDHA, T., SANTRUPT, R., DAS, R., KUMAR, M. M., CHANAKYA, H. & RAO, L. 2023. Socio-economic impact assessment of large-scale recycling of treated municipal wastewater for indirect groundwater recharge. *Science of the Total Environment,* 859**,** 160207.

MASCIOPINTO, C. 2007. Biodegradation of wastewater nitrogen compounds in fractures: Laboratory tests and field observations. *Journal of contaminant hydrology,* 92**,** 230-254.

MIENIS, O. & ARYE, G. 2018. Long-term nitrogen behavior under treated wastewater infiltration basins in a soil-aquifer treatment (SAT) system. *Water research,* 134**,** 192-199.

MIOTLIŃSKI, K., BARRY, K., DILLON, P. & BRETON, M. 2010. Alice Springs SAT project hydrological and water quality monitoring report 2008-2009. CSIRO Canberra.

MORRISON, C. M., BETANCOURT, W. Q., QUINTANAR, D. R., LOPEZ, G. U., PEPPER, I. L. & GERBA, C. P. 2020. Potential indicators of virus transport and removal during soil aquifer treatment of treated wastewater effluent. *Water research,* 177**,** 115812.

MUKHERJEE, S., MUKHOPADHYAY, S., HASHIM, M. A. & SEN GUPTA, B. 2015. Contemporary environmental issues of landfill leachate: assessment and remedies. *Critical reviews in environmental science and technology,* 45**,** 472-590.

NADAV, I., ARYE, G., TARCHITZKY, J. & CHEN, Y. 2012. Enhanced infiltration regime for treated-wastewater purification in soil aquifer treatment (SAT). *Journal of hydrology,* 420**,** 275-283.

NEGEV, I., GUTTMAN, J. & KLOPPMANN, W. 2017. The use of stable water isotopes as tracers in soil aquifer treatment (SAT) and in regional water systems. *Water,* 9**,** 73.

NEGEV, I., SHECHTER, T., SHTRASLER, L., ROZENBACH, H. & LIVNE, A. 2020. The effect of soil tillage equipment on the recharge capacity of infiltration ponds. *Water,* 12**,** 541.

NEMA, P., OJHA, C., KUMAR, A. & KHANNA, P. 2001. Techno-economic evaluation of soil-aquifer treatment using primary effluent at Ahmedabad, India. *Water Research,* 35**,** 2179-2190.

OREN, O., GAVRIELI, I., BURG, A., GUTTMAN, J. & LAZAR, B. 2007. Manganese mobilization and enrichment during soil aquifer treatment (SAT) of effluents, the Dan Region Sewage Reclamation Project (Shafdan), Israel. *Environmental science & technology,* 41**,** 766-772.

PACHAURI, R. K., ALLEN, M. R., BARROS, V. R., BROOME, J., CRAMER, W., CHRIST, R., CHURCH, J. A., CLARKE, L., DAHE, Q. & DASGUPTA, P. 2014. *Climate change 2014: synthesis report. Contribution of Working Groups I, II and III to the fifth assessment report of the Intergovernmental Panel on Climate Change*, Ipcc.

PAGE, D., BEKELE, E., VANDERZALM, J. & SIDHU, J. 2018. Managed aquifer recharge (MAR) in sustainable urban water management. *Water,* 10**,** 239.

PAGE, D., MIOTLIŃSKI, K., DILLON, P., TAYLOR, R., WAKELIN, S., LEVETT, K., BARRY, K. & PAVELIC, P. 2011. Water quality requirements for sustaining aquifer storage and recovery operations in a low permeability fractured rock aquifer. *Journal of environmental management,* 92**,** 2410-2418.

PAN, W., XIONG, Y., HUANG, Q. & HUANG, G. 2017. Removal of nitrogen and COD from reclaimed water during long-term simulated soil aquifer treatment system under different hydraulic conditions. *Water,* 9**,** 786.

PAVELIC, P., DILLON, P., MUCHA, M., NAKAI, T., BARRY, K. & BESTLAND, E. 2011. Laboratory assessment of factors affecting soil clogging of soil aquifer treatment systems. *Water research,* 45**,** 3153-3163.

PAVELIC, P., DILLON, P. J., BARRY, K. E., VANDERZALM, J. L., CORRELL, R. L. & RINCK-PFEIFFER, S. M. 2007. Water quality effects on clogging rates during reclaimed water ASR in a carbonate aquifer. *Journal of Hydrology,* 334**,** 1-16.

PESCOD, M. 1992. Wastewater treatment and use in agriculture.

PYNE, R. D. G. 2005. Aquifer storage recovery: a guide to groundwater recharge through wells/R. David G. Pyne.

QIU, S., YAN, L. & JING, C. 2019. Simultaneous removal of arsenic and antimony from mining wastewater using granular TiO2: Batch and field column studies. *Journal of Environmental Sciences,* 75**,** 269-276.

QUANG, H. H. P., DINH, N. T., THI, T. N. T., BAO, L. T. N., YUVAKKUMAR, R. & NGUYEN, V.-H. 2022. Fe2+, Fe3+, Co2+ as highly efficient cocatalysts in the homogeneous

electro-Fenton process for enhanced treatment of real pharmaceutical wastewater. *Journal of Water Process Engineering,* 46**,** 102635.

QUANRUD, D. M., HAFER, J., KARPISCAK, M. M., ZHANG, J., LANSEY, K. E. & ARNOLD, R. G. 2003. Fate of organics during soil-aquifer treatment: sustainability of removals in the field. *Water Research,* 37**,** 3401-3411.

RAUCH-WILLIAMS, T., HOPPE-JONES, C. & DREWES, J. 2010. The role of organic matter in the removal of emerging trace organic chemicals during managed aquifer recharge. *Water research,* 44**,** 449-460.

RINGLEB, J., SALLWEY, J. & STEFAN, C. 2016. Assessment of managed aquifer recharge through modeling—A review. *Water,* 8**,** 579.

RITSEMA, C. & DEKKER, L. 2000. Preferential flow in water repellent sandy soils: principles and modeling implications. *Journal of Hydrology,* 231**,** 308-319.

RUSSO, J., ROMANO, F., KROC, L., SCIORTINO, F., ROVIGATTI, L. & ŠULC, P. 2022. SAT-assembly: A new approach for designing self-assembling systems. *Journal of Physics: Condensed Matter,* 34**,** 354002.

SALLWEY, J., JURADO, A., BARQUERO, F. & FAHL, J. 2020. Enhanced removal of contaminants of emerging concern through hydraulic adjustments in soil aquifer treatment. *Water,* 12**,** 2627.

SÁNCHEZ-MURILLO, R. & BIRKEL, C. 2016. Groundwater recharge mechanisms inferred from isoscapes in a complex tropical mountainous region. *Geophysical Research Letters,* 43**,** 5060-5069.

SCANLON, B. R., REEDY, R. C., FAUNT, C. C., POOL, D. & UHLMAN, K. 2016. Enhancing drought resilience with conjunctive use and managed aquifer recharge in California and Arizona. *Environmental Research Letters,* 11**,** 035013.

SCHMIDT, C. & BRAUCH, H. 2008. Characteristics of natural attenuation processes for organic micropollutant removal during riverbank filtration. *Groundwater Management in large River Basins (Eds. M. Dimkić, HJ Brauch, M. Kavanaugh)***,** 332-352.

SCOTT, C., FARUQUI, N. & RASCHID, L. 2004. Wastewater use in irrigated agriculture: coordinating the livelihood and environmental realities. International Water Management Institute (IWMI), International Development Research Centre (IDRC). *International Water Management Institute (IDRC)*.

SELVAKUMAR, T. & GANESAN, M. 2015. Water quality improvements in soil aquifer treatment (SAT) simulated soil columns. *Indian Journal of Science and Technology,* 8**,** 1-6.

SHARMA, S. K. & KENNEDY, M. D. 2017. Soil aquifer treatment for wastewater treatment and reuse. *International Biodeterioration & Biodegradation,* 119**,** 671-677.

SHU, X., WU, Y., ZHANG, X. & YU, F. 2023. Experiments and Models for Contaminant Transport in Unsaturated and Saturated Porous Media-A Review. *Chemical Engineering Research and Design*.

TOKATLI, C., KÖSE, E. & ÇIÇEK, A. 2014. Assessment of the effects of large borate deposits on surface water quality by multi statistical approaches: a case study of Seydisuyu Stream (Turkey). *Polish Journal of Environmental Studies,* 23.

TREDOUX, G., CAVÉ, L. & BISHOP, R. 2020. Long-term stormwater and wastewater infiltration into a sandy aquifer, South Africa. *Management of Aquifer Recharge for Sustainability.* CRC Press.

TREDOUX, G., GENTHE, B., STEYN, M. & GERMANIS, J. 2012. Managed aquifer recharge for potable reuse in Atlantis, South Africa. *Water reclamation technologies*

*for safe managed aquifer recharge. Eds: Christian Kazner TW, TMelin T, Dillon***,** 121-140.

TRUSSELL, B., TRUSSELL, S., QU, Y., GERRINGER, F., STANCZAK, S., VENEZIA, T., MONROY, I., BACARO, F. & TRUSSELL, R. 2018. A four-year simulation of soil aquifer treatment using columns filled with San Gabriel Valley sand. *Water research,* 144**,** 26-35.

TURKELTAUB, T., FURMAN, A., MANNHEIM, R. & WEISBROD, N. 2022. Continuous monitoring of a soil aquifer treatment system's physico-chemical conditions to optimize operational performance. *Hydrology and Earth System Sciences,* 26**,** 1565-1578.

VAN CUYK, S., SIEGRIST, R., LOGAN, A., MASSON, S., FISCHER, E. & FIGUEROA, L. 2001. Hydraulic and purification behaviors and their interactions during wastewater treatment in soil infiltration systems. *Water Research,* 35**,** 953-964.

VAN HOUTTE, E., CAUWENBERGHS, J., WEEMAES, M., THOEYE, C., KAZNER, C., WINTGENS, T. & DILLON, P. 2012. Indirect potable reuse via managed aquifer recharge in the Torreele/St-Andre project. *Water reclamation technologies for safe managed aquifer recharge. IWA, London***,** 33-33.

VAN LOOSDRECHT, M. C., NIELSEN, P. H., LOPEZ-VAZQUEZ, C. M. & BRDJANOVIC, D. 2016. *Experimental methods in wastewater treatment*, IWA publishing.

VANDERZALM, J., PAGE, D., DILLON, P., GONZALEZ, D. & PETHERAM, C. 2022. Assessing the costs of Managed Aquifer Recharge options to support agricultural development. *Agricultural Water Management,* 263**,** 107437.

WANG, K., LIN, Z. & ZHANG, R. 2016. Impact of phosphate mining and separation of mined materials on the hydrology and water environment of the Huangbai River basin, China. *Science of the Total Environment,* 543**,** 347-356.

WEI, L., WANG, K., NOGUERA, D. R., JIANG, J., OYSERMAN, B., ZHAO, N., ZHAO, Q. & CUI, F. 2016. Transformation and speciation of typical heavy metals in soil aquifer treatment system during long time recharging with secondary effluent: Depth distribution and combination. *Chemosphere,* 165**,** 100-109.

WEN, Q., MA, M., HOU, H., YU, W., GUI, G., WU, Q., XIAO, K., ZHU, Y., TAO, S. & LIANG, S. 2022. Recirculation of reject water in deep-dewatering process to influent of wastewater treatment plant and dewaterability of sludge conditioned with Fe2+/H2O2, Fe2+/Ca (ClO) 2, and Fe2+/Na2S2O8: From bench to pilot-scale study. *Environmental Research,* 203**,** 111825.

WILD, D., FRANCKE, C.-J., MENZLI, P. & SCHON, U. 2010. Water: a market of the future. *A Sustainable Asset Management (SAM) Study. SAM, Switzerland*.

WINIARSKI, T., LASSABATERE, L., ANGULO-JARAMILLO, R. & GOUTALAND, D. 2013. Characterization of the heterogeneous flow and pollutant transfer in the unsaturated zone in the fluvio-glacial deposit. *Procedia Environmental Sciences,* 19**,** 955-964.

XIAO, X.-Y., WANG, M.-W., ZHU, H.-W., GUO, Z.-H., HAN, X.-Q. & ZENG, P. 2017. Response of soil microbial activities and microbial community structure to vanadium stress. *Ecotoxicology and Environmental Safety,* 142**,** 200-206.

XU, C., FENG, Y., LI, H., WU, R., JU, J., LIU, S., YANG, Y. & WANG, B. 2022. Adsorption of heavy metal ions by iron tailings: Behavior, mechanism, evaluation and new perspectives. *Journal of Cleaner Production,* 344**,** 131065.

YANG, C., LIU, K., YANG, S., ZHU, W., TONG, L., SHI, J. & WANG, Y. 2023. Prediction of metformin adsorption on subsurface sediments based on quantitative experiment

and artificial neural network modeling. *Science of The Total Environment,* 899**,** 165666.

YANG, F., LIANG, D., WU, X. & XIAO, Y. 2020. On the application of the depth-averaged random walk method to solute transport simulations. *Journal of Hydroinformatics,* 22**,** 33-45.

YU, Z.-G., GÖTTLICHER, J., STEININGER, R. & KNORR, K.-H. 2016. Organic sulfur and organic matter redox processes contribute to electron flow in anoxic incubations of peat. *Environmental Chemistry,* 13**,** 816-825.

ZACHARA, J., BRANTLEY, S., CHOROVER, J., EWING, R., KERISIT, S., LIU, C., PERFECT, E., ROTHER, G. & STACK, A. G. 2016. Internal domains of natural porous media revealed: critical locations for transport, storage, and chemical reaction. *Environmental Science & Technology,* 50**,** 2811-2829.

ZAIDI, M., AHFIR, N.-D., ALEM, A., EL MANSOURI, B., WANG, H., TAIBI, S., DUCHEMIN, B. & MERZOUK, A. 2020. Assessment of clogging of managed aquifer recharge in a semi-arid region. *Science of the Total Environment,* 730**,** 139107.

ZENG, D., MIAO, J., WU, G. & ZHAN, X. 2018. Nitrogen removal, microbial community and electron transport in an integrated nitrification and denitrification system for ammonium-rich wastewater treatment. *International Biodeterioration & Biodegradation,* 133**,** 202-209.

ZHANG, H., XU, Y. & KANYERERE, T. 2020. A review of the managed aquifer recharge: Historical development, current situation and perspectives. *Physics and Chemistry of the Earth, Parts A/B/C,* 118**,** 102887.

ZHANG, L.-Y., YE, Y.-B., WANG, L.-J., XI, B.-D., WANG, H.-Q. & LI, Y. 2015. Nitrogen removal processes in deep subsurface wastewater infiltration systems. *Ecological Engineering,* 77**,** 275-283.

ZHANG, X., LI, H., LI, Y., GUO, F., YANG, Z. & BAI, J. 2018. Do Wet-Dry Ratio and Fe-Mn System Affect Oxidation-Reduction Potential Nonlinearly in the Subsurface Wastewater Infiltration Systems? *International Journal of Environmental Research and Public Health,* 15**,** 2790.

ZHANG, Y., WANG, F., CAO, B., YIN, H. & AL-TABBAA, A. 2022. Simultaneous removal of Pb and MTBE by mixed zeolites in fixed-bed column tests. *Journal of Environmental Sciences,* 122**,** 41-49.

Annex (1) : Managed Aquifer Recharge (Definitions, Applications, Processes, and Operations)

Introduction

Managed aquifer recharge (MAR) is a method of replenishing depleted aquifers by introducing surface water, treated wastewater, or stormwater into underground water reserves. Also, According to Dillon et al. (2010), MAR is the intentional replenishment of groundwater with water for later restoration or environmental advantage. MAR is a tool for navigating water resources that includes a wide range of water sources, replenish techniques, and handling of storage practices. It has grown to be a widely used approach for handling water resources in areas that are experiencing water shortages as a result of accelerating population explosion and global warming (Pachauri et al., 2014). The importance of the replenished water, the effects on groundwater quality, and the preservation of human health and the ecosystem should all be taken into account by MAR as a "managed" system (Ringleb et al., 2016). The term of MAR must include the concept of intentional recharging. Therefore, MAR can offer several benefits, including increasing water availability, improving water quality, reducing surface runoff, and mitigating the effects of drought (Hartog and Stuyfzand, 2017).

Moreover, MAR is often less expensive and more environmentally friendly than other water storage options, such as constructing dams and reservoirs (Dillon et al., 2009). Recharge improvement, a deliberate effort to regulate groundwater quality and quantity within the framework of the whole procedure (Gale and Dillon, 2005), is a component of managed aquifer recharge. Recharge water is able to be kept in a variety of confined and unconfined aquifer forms, including karstic and fractured rocks to unconsolidated alluvial deposits (Händel et al., 2014). Recovery is frequently accomplished via wells. However, in other instances, natural water outflow to surface water bodies is used. Recovering water can be utilized for a variety of things, including irrigation, cooling, industrial processes, drinking water, and environmental objectives (Dillon et al., 2009). Figure 1 demonstrates how MAR can be customized to a particular locale (Dillon et al., 2022).

The idea of MAR has been recognized for millennia, but natural MAR structures have only recently received widespread attention as an intentional and regulated activity. In many ways, MAR is the phrase artificial recharge's contemporary equivalent (Sánchez-Murillo and Birkel, 2016). Both of them are not interchangeable because an artificial recharge does not automatically imply a controlled procedure. The expression "artificial recharge," which was used under certain older legislation and standards, has developed

and is now gradually being replaced. MAR has been used in other nations, notably the US, Australia, Europe, and Asia, with variable degrees of effectiveness.

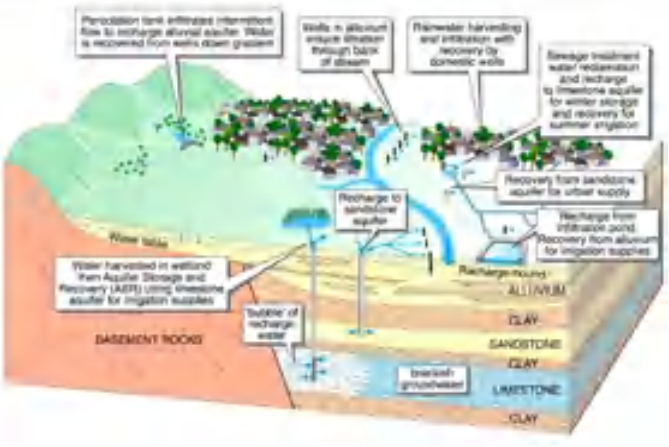

Managed aquifer recharge adaptation according to aquifer type, topography, land use, and recovery water using (Dillon et al., 2022)

Purposes of MAR

For several associated objectives, managed aquifer recharge has been effectively utilized globally (Kurki et al. (2013); Dillon et al. (2022); Dillon et al. (2019); Zhang et al. (2020)). One of these is:

- Controlling the water availability: MAR is frequently employed to manage the imbalances between demand and supply. This could happen with regard to seasonal timescales (such as recharging during rainfall periods and recovery during dry periods), interannual timescales (such as drought mitigation), or crisis usage (such as for fighting fires or replacing lost water during storms or disasters).
- Fulfilling legal responsibilities: MAR could be utilized to assist in fulfilling responsibilities related to downstream water rights or regional arrangements.
- Protecting and Restoring aquifers: MAR can be used to stop land subsidence, manage the intrusion of saltwater, and recover or stop additional groundwater level reductions.
- Keeping low flows and levels in place: MAR can be employed to keep rivers, streams, and lakes at their minimal flows.
- Flooding mitigation: Using rainwater for MAR can assist safeguard against flooding.
- The safeguarding and improvement of water purity: MAR is capable of helping regulate or upgrade the quality of surface and groundwater as well as to stop the spread of contaminants.
- Water recycling: MAR is being utilized more and more to control the recycling of treated wastewater, frequently for agriculture and potable uses.

- Ecosystem rehabilitation and security: rebuilding or preserving wetlands and safeguarding threatened species and their natural environments are a few examples of how MAR is used to benefit environments.

Sustainable Development, joint usage, and demand control are frequently linked to managed aquifer recharge (Dahlke et al., 2018).

- In the words of Page et al. (2018), the term "groundwater sustainability" refers to the development and use of groundwater resources that may be sustained eternally without having a negative impact on the environment or society. Consumption eventually needs to be monitored and controlled in order to equalize the recharge, whether natural, controlled, or accidental, for groundwater utilization to be sustainable. Imig et al. (2022) latest assessment revealed that regulators have little interest in controlling natural recharge when the usage of land is altered or incidental/unintentional recharging happens, and there was no shared methodology. Consequently, both strategies water managers utilize to affect the groundwater equilibrium over the years are regulating demand and MAR. For groundwater supplies to remain sustainable, the water's purity must also be preserved. Six environmentally and three socially sustainable criteria were specifically created for MAR systems in Dillon et al. (2022). These cutting-edge governance tools ensure residents of the fairness and transparency of legislation while safeguarding the security and quality of water supplies and environments impacted by groundwater.
- In order to maximize the combined impact and reduce any unfavorable physical, environmental, and financial consequences of depending solely on one or the other, surface water and groundwater are used in conjunction (Scanlon et al., 2016). Conjunctive usage is a method of depending more on groundwater throughout dry periods and droughts and more on surface water when it is accessible during wetter decades, especially to recharge groundwater. MAR is frequently (albeit rarely) a component in the simultaneous use of groundwater and surface water. In order to preserve water supplies and meet groundwater and surface water management goals including the safeguarding of environments, MAR enhances groundwater with accessible surface water and works in tandem with conjunction utilization of surface water and groundwater (Foster et al., 2010).
- There are several ways to control demand, involving more effective utilize, education, fiscal measures, and shifting priorities for the consumption of water (Dillon et al., 2020).

As a means to replace depleted aquifers while avoiding negative effects on irrigation communities' way of life, managed aquifer recharge, or MAR, is frequently employed in conjunction with demand control tactics. In order to preserve water supplies and achieve

management goals like protecting ecosystems, MAR improves groundwater by utilizing available surface water and works in tandem with concurrent use of surface waters and groundwater (see Figure 2).

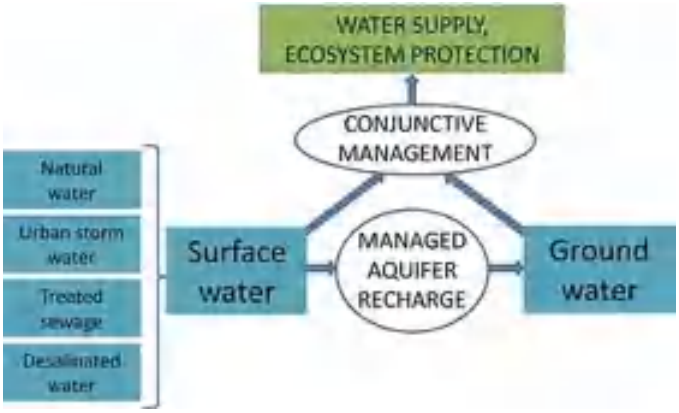

The integrated water resources management functions with managed aquifer recharge and conjunctive application (Dillon et al., 2022)

Benefits of MAR

MAR has many benefits (Dillon et al., 2022), including:

- Improving Water Quality: MAR can help enhance water quality by removing contaminants through natural filtration.
- Enhancing Groundwater Storage: MAR can help improve groundwater storage by recharging depleted aquifers.
- Increasing Water Availability: MAR can help improve water availability for domestic, agricultural, and industrial use.
- Reducing the Risk of Groundwater Depletion: MAR can help reduce the risk of groundwater depletion by replenishing depleted aquifers.

MAR Techniques:

MAR is a broad term that encompasses many different techniques for recharging aquifers (Zhang et al., 2020); (Dillon et al., 2022). Spreading methods, induced bank filtration, well, saft, and borehole recharge, in-channel modification, and rainwater and runoff collecting are some of the most popular approaches. The global geography of MAR techniques is shown in Figure 3. Through expanding water infiltration into aquifer formations, MAR innovations' main goal is to increase the availability of groundwater. In conjunction with treated wastewater, desalinated seawater, and rainfall water, it is typically included as one of the unusual water sources in integrated water management strategies. MAR is an effective way to control the amount as well as the quality of groundwater resources, ensure a secure water supply, and mitigate the negative consequences of global warming. It cannot, however, be used as part of groundwater management strategies that

depend on lowering the extraction of water and tailoring withdrawals depending on resource availability (Casanova et al., 2016).

MAR techniques distribution map around the world

Over the past 40 years, MAR has primarily been used in developed nations, including the United States and Europe becoming the most active areas in implementing these strategies (Levantesi et al., 2010). Large towns like Berlin, the suburbs of Paris, Lyon, Dunkirk, and Geneva regularly employ it to regulate rainwater by gathering surface runoff waters in infiltration ponds. However, heavy metals, hydrocarbons, and other organic compounds causing technical as well as environmental issues can be found in substantial proportions in urban stormwater runoff (Chocat et al., 2007). Nevertheless, several MAR techniques can reduce the contamination of surface water by absorbing some of the contaminated water and keeping an eye on the geo-purification and attenuate operations. As a result, MAR is capable of protecting the ecosystem by reducing the amount of pollutants in sensitive receptor medium. To reduce evaporative losses, MAR has occasionally been considered in reservoir building in Mediterranean nations. In coastal locations, MAR can switch from passive to active control of saltwater intrusion, which involves maximizing pumping and natural and artificial recharging to build a hydraulic barriers that keeps contaminants and seawater out (Casanova et al., 2008).

Infiltration techniques

The diffusion of water into the groundwater reservoir can be improved by using infiltration approaches, often with the use of filtration basins like ponds or tanks. These methods enable for natural abatement in the aquifer's unsaturated zone, which is intended to improve the purity of the recharge water. They are frequently used to build hydraulic obstacles or to replenish aquifers beneath the water table. Techniques of infiltration are very

useful because they are low-cost and simple to operate. The term "infiltration ponds" refers to a variety of facilities, including small reservoirs, dams, and various types of rainwater and sewage treatment unit management tools. Additional structures such recharge pits, drainage trenches, vegetated ditches, mound mechanisms, sand filters, and septic drain fields are included in this category. Employing these methods, the water enters the unsaturated zone before entering the aquifer. The water has the chance to be purified by soil contact in this way, which can get rid of pathogenic organisms and potentially dangerous organic and inorganic chemicals.

Infiltration ponds have a frequently used technique in MAR initiatives, particularly in areas where there is a water scarcity. Depending on the technology being employed, like infiltration ponds, percolation tanks, and soil aquifer treatment (SAT), watershed parameters such as infiltration rate are modified to fulfill the specific aims of each method (Dillon, 2005). A slower infiltration rate (with an average of 0.5 m.day-1) is advised when the purpose involves geo-purifying the intruding water. A moderately high infiltration rate (several meters per day) could be utilized when the goal is centered on boosting the water amount. In some cases, plant growth on the filtration layer can improve its capacity for cleaning water. Greens can protect the basin's surface from erosion and blockage as well as function as transporters for microorganisms that help in the breakdown of some inorganic and organic contaminants. By encouraging phytoremediation in summertime, plants can further enhance the cleansing of contaminated water. Additionally, the infiltration rate is influenced by the water's temperature; cooler water penetrates more slowly owing to its higher viscosity. Winter can dramatically reduce the amount of water that penetrates beneath a catchment. Organic debris in untreated water encourages microbial growth and can cause biofilms, which can impair permeability. In addition, based on the usage, clogging in infiltration basins can be prevented or delayed down utilizing a variety of ways (Le Coustumer, 2008).

Pre-treating the water with settling ponds or sand filters before it penetrates is one of the alternatives. Alternately, chemical substances—mostly inorganic ones—can be added to change the recharge water's chemical makeup. Using "wetting-drying" periods for operating infiltration basins is an alternative strategy that enables the decompaction and maintenance of the basin floor. While infiltration method as one of MAR applications offers many benefits, it also presents some challenges, including:

- Challenges related to the design and sizing of the infiltration basins to optimize infiltration rates while preventing clogging and sedimentation
- Challenges related to managing the quality of stormwater runoff to ensure that contaminants are removed before infiltration

- Challenges related to land acquisition and siting of infiltration basins in urban areas where land availability is limited

Direct injection techniques

The primary method used globally for injecting water into aquifers is through injection wells. Aquifer Storage and Recovery (ASR) and Aquifer Storage Transfer and Recovery (ASTR) systems are commonly installed with two main goals:

1. recharge confined or semi-confined aquifers.
2. establish hydraulic barriers.

Monitoring of the water quality is necessary to avoid any potential contamination. In situations where space is limited, injection wells might be a preferred solution since their footprint is considerably smaller than that of infiltration basins, occupying only several tens of square meters. Additionally, their wellhead protection zone is small.

Aquifer Storage and Recovery (ASR) is a method of recharging groundwater that entails extracting water out of the aquifer after it has been injected there. The ASR approach is frequently applied to aquifers with poor natural recharge rates and non-point source contamination vulnerability. As a "pocket of fresh water" in an aquifer holding non-potable water, ASR is typically employed for the periodic storage of exceptionally pure water. The benefit of this approach is that water can be saved and retrieved when it is most urgently required. Furthermore, by causing a reversal of the water movement in the well screen along with the surrounding aquifer, the alternating stages of injection and extraction in a single well assist in reducing clogging. This procedure assists in avoiding biofouling and sedimentation, which over time may reduce the system's effectiveness. Additionally, since a single well can be utilized for injection and abstraction, ASR lowers investment expenses.

In ASR, water is injected into an aquifer and later recovered by pumps from the same well. This approach is appropriate for slow-moving groundwater aquifers that are less susceptible to non-point source contamination. A "pocket of fresh water" in an aquifer that normally includes non-potable water is created via ASR, which is frequently utilized for annual water storage. When injecting and extraction stages are alternated within the same well, blockage and inverting of the water movement in the well screen are reduced, and the nearby aquifer aids in preventing clogging. ASR is a dependable and affordable form of groundwater recharge, as demonstrated by (Dillon et al., 2006), and (Pyne, 2005). To prevent pollution, it is crucial to regularly monitor the purity of the injected water. When space is at a premium and surface water is hard to come by, ASR is a practical solution. In times of drought, it is also a useful strategy for controlling the water supplies that are available. ASTR uses an alternative strategy than ASR since water is injected into one well

and recovered by pumping from another well a few hundred meters down-gradient from the injection well. The injected water is subsequently moved through the aquifer before being extracted. The aquifer's water quality needs to be somewhat excellent for this procedure to be effective. So, when the pumped water is meant for consumption by humans, ASTR is typically employed.

Filtration techniques

Riverbank filtration, also known as induced recharge. The practice of boosting water penetration from a river to its alluvial aquifer using wells situated close to the riverbank is recognized as riverbank filtration, often referred to as stimulated recharge. The level of the water can be lowered by placing a number of wells parallel to and near to the river, which results in an elevation in head among the river and the groundwater. As a result, surface water passes through the riverbank and into the aquifer, where it can be filtered and purified by the riverbank's geo-purifying capabilities. It is crucial to keep an adequate infiltration rate and regularly clean the riverbanks since the high concentration of suspended particles in surface water may swiftly clog riverbanks. Dune filtration is a different technique that requires gathering water from wells or reservoirs at a lower elevation by seeping water from ponds built in dunes (Dillon, 2005).

A variety of the local circumstances, different MAR approaches can be utilized to replenish water in metropolitan settings. While well injection methods are better suited for deeply confined aquifers, methods of infiltration may be utilized to recharge unconfined aquifers. The conceptual categorization for MAR techniques is shown in Figure 3 (Dillon, 2005). Table 1 also provides an overview, advantages, and difficulties for the typical MAR variants used globally. Despite the possible benefits of MAR, a number of issues must be resolved in order for it to be successfully implemented. The absence of knowledge and comprehension among stakeholders, particularly decision-makers, water managers, and the general public, is one of the main problems. The effective implementation of MAR may be hampered by a lack of general knowledge and involvement (Cruz Ayala and Tortajada, 2023). The accessibility as well as the quality of source water for recharge present a different challenge. The water quality of the aquifer may be negatively impacted in some areas if the available water is too salty or filthy for recharging. Before choosing an appropriate MAR approach, a thorough source water quality assessment is required (Hartog and Stuyfzand, 2017). In addition, numerous neighborhoods, especially those in developing nations, may face considerable financial difficulties because to the expense of MAR infrastructure and operation. Based on the regional hydrogeological parameters, water demand, and recharge goals, MAR's affordability should be assessed (Vanderzalm et al., 2022).

The efficiency, environmental sustainability and resilience of the recharge methods will likely be improved in the course of future MAR study and implementation. Coupling of MAR with other water management strategies, such as collecting rainfall and reusing wastewater, is one possible advancement. According to Dillon et al. (2022), combining various water sources and management techniques can result in more dependable and long-lasting water supply alternatives. The implementation of natural and hybrid MAR structures that imitate natural recharge procedures as well as a hybrid MAR method consisting of surface water spreading basins and groundwater wells to improve aquifer recharge and guarantee a sustainable water supply for the area are other potential developments (Dahlke et al., 2018).

MAR implementation can be challenging due to the need for specialized knowledge and potential environmental concerns. These include the risk of aquifer damage and fluctuating groundwater levels, which can have negative effects on dependent ecosystems and increase aquifer vulnerability to contamination. These challenges may hinder the widespread adoption of MAR as a groundwater management technique, but despite these concerns, MAR has been successfully implemented in various countries. Five essential elements were first suggested by Dillon et al. (2009) for a fruitful MAR application:

1. Demand: The project's financial scope ought to be capable to bring in sufficient revenue from the water demand to pay for all of its expenses. A good reason to invest in Managed Aquifer Recharge (MAR) in reused water projects is the decrease in treated effluent outflow into the ocean.
2. Source: To create a storage reserve that satisfies dependability and quality standards, there must be a sufficient water supply for recharge.
3. Aquifer: The recharging media ought to have enough storage and retention power.
4. Detention Storage: Ample capacity must be available for water retention in order to reach the desired recharge quantity, as well as for treatment methods following recovery, if necessary.
5. Management Capability: For managing the project successfully, sufficient expertise in hydrogeological and geotechnical elements, as well as in water storage and treatment structure, should be attained.

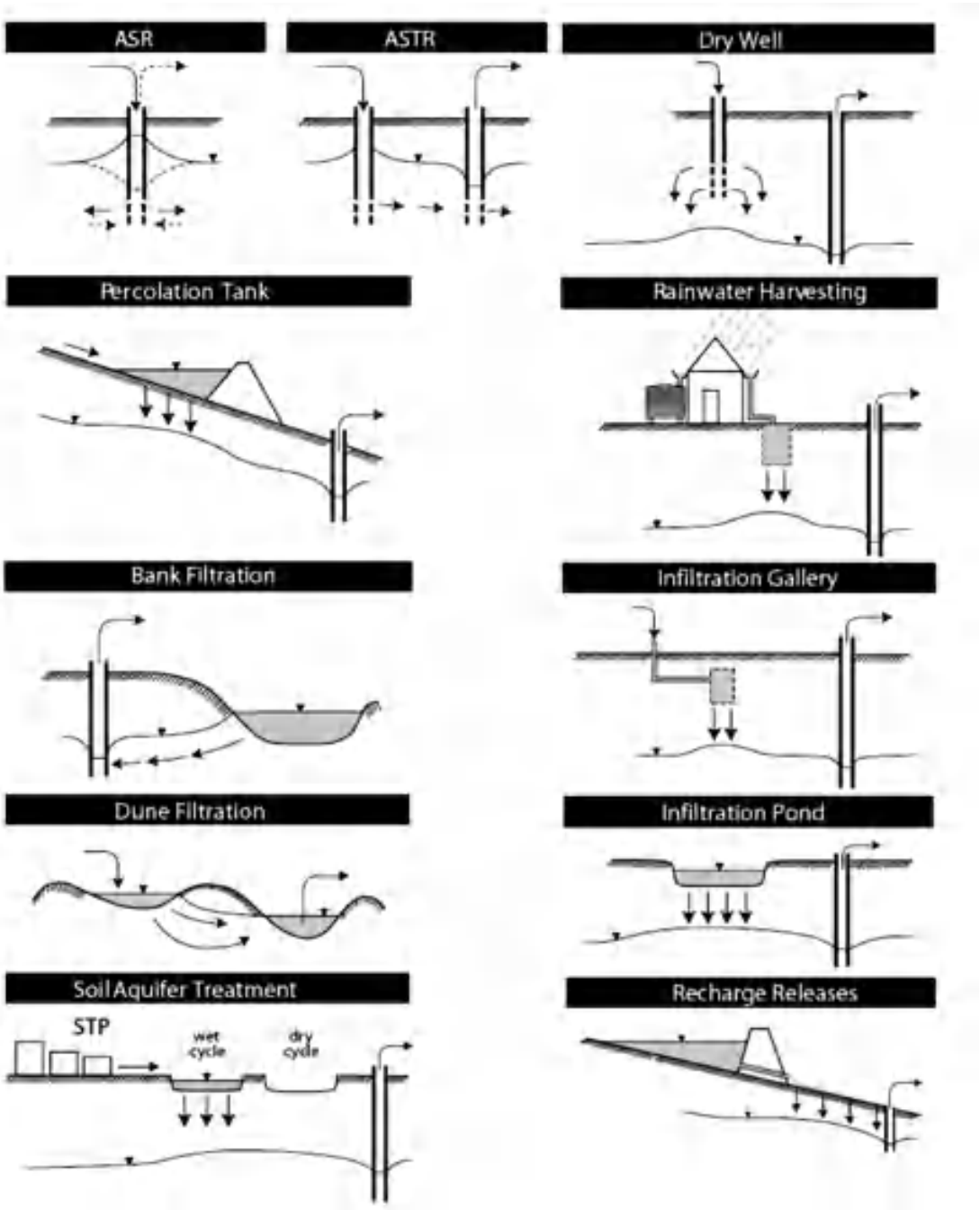

schematic characterization for common MAR methods

Common MAR applications (Zhang et al., 2020)

MAR Method	Description	Benefits and Challenges
Aquifer Storage and Recovery (ASR)	A method of preserving water that entails injecting it into a well and then drawing water out of it later.	The brackish aquifers where the emphasis is on storage rather than water treatment, while purification continues to serve an essential part, make this technology particularly effective. It is often utilized to store drinking water in the USA (Pyne, 2005), and it is additionally utilized effectively in Australia for tasks including purifying urban runoff (Page et al., 2011) and irrigating horticulture with treated sewage(Pavelic et al., 2007). In overall, better water quality is required to avoid probable well obstruction.
Aquifer Storage Transfer and Recovery (ASTR)	In order to use this technique, water must first be injected into a well for storage before being extracted from another well.	The method entails extending an aquifer's water supply's residency period beyond that of a single well in order to more effectively treat the water, mostly for viruses and micropollutants. This technique is employed in Australia for urban stormwater collecting (Kazner et al., 2012), and in overall, improved water quality is needed to prevent well clogs.
Dry wells	When the water level is deep, shallow wells are typically employed to enable high-quality water to infiltrate the unconfined aquifer at considerable depths.	It may render it possible for specific deepest aquifers, such those found in the US, to be refilled (Heilweil and Marston, 2011).

Percolation Tanks, Check Dams or Recharge Weirs	Dams built in fleeting streams keep water from flowing, allowing it to seep into the stream bed and increasing storage in unconfined aquifers. The water is then drawn from the valley below.	Increases urban rivers' natural penetration, as shown in India (Kavuri et al., 2011).
Rainwater Harvesting for Aquifer Storage	Roof runoff is redirected using this method to a well with sand or gravel, where it can seep to the water table. After that, the water is drawn from the well and gathered.	Typically employed on a lesser scale than other MAR approaches, but when used widely, as was the case in Nepal (Page et al., 2018), it can be quite effective.
Bank Filtration	In order to promote surface water to penetrate into the aquifer, this technique includes extracting groundwater from a well that is close to or below a river or lake.	When this procedure is used, the obtained water's quality improves and is more consistent, as was the case, for example, in Germany (Greskowiak et al., 2006) and Norway (Kvitsand et al., 2017)).
Infiltration Galleries	on order to replenish the unconfined aquifer, this technique includes digging underground tunnels on permeable soils that allow water to penetrate across the unsaturated zone.	In comparison to infiltration ponds, these technologies need less acreage and pose a lesser danger of blockage due to extensive algal development. For instance, this has been proven in Australia (Bekele et al., 2013).
Dune Filtration	Water is collected from wells or reservoirs that are situated at a lower height after being ingested from basins constructed on top of dunes.	This approach is used, for instance, in Belgium (Van Houtte et al., 2012), to enhance water quality and preserve an equilibrium among water supply and demand.
Infiltration Ponds	Surface water is diverted into off-stream ponds and canals in order to encourage water to	These techniques need a greater area of land than well injecting techniques and galleries, and they can be more prone to clogging because of the rapid rate of algae

	penetrate into the unconfined aquifer beneath through an unsaturated zone.	growth. They can also be harder to handle, like in South Africa (Tredoux et al., 2020).
Soil Aquifer Treatment (SAT)	Using this technique, pathogens and nutrients can be removed from the unsaturated zone by periodically sending wastewater that has been treated effluent via infiltration ponds. After spending some time in the unconfined aquifer, the recovered water is subsequently removed from wells.	As shown in the USA (Fox et al., 2001), permitting the SAT recharging basins to dry out improves management of infiltration rates and lowers the risk of severe blockage.
Recharge Releases	To store floodwater and discharge it gently into the streambed downstream, dams are built on ephemeral streams. By allowing water to penetrate into the subsurface aquifers, this technique greatly improves recharge and aids in matching the rate of infiltration.	The planned, monitored discharge of water from surface reservoirs to enable the use of both surface water and groundwater storage, as demonstrated in Australia (Dillon and Liggett, 1983).

Soil aquifer treatment system (SAT) (Definitions, Applications, Processes, and Operations)

As stated by Sharma and Kennedy (2017), soil aquifer treatment (SAT) is an environmentally friendly water preservation strategy that uses natural soil and groundwater systems to purify and buffer wastewater. As an affordable and successful solution to the problems of inadequate water supplies and water contamination in many parts of the world, SAT has attracted increased interest in recent years. The following reviewing articles will give an overview of the fundamental ideas and principles of SAT, discuss the various SAT systems and the design factors that should be taken into account, go through the advantages and difficulties of SAT, and show real-life examples of productive SAT endeavors. In the words of Sharma and Kennedy (2017), soil aquifer treatment (SAT) is a special kind of managed aquifer recharge (MAR) technique that uses treated wastewater (TWW) as an alternative source of water. Wastewater discharge is passed across soil as part of the SAT procedure, which raises its quality to an acceptable level for recharging groundwater. Therefore, SAT may be a crucial part of a system for indirect potable reuse (Amy and Drewes, 2007). Figure 1 depicts a schematic of a SAT system (Dillon et al., 2022).

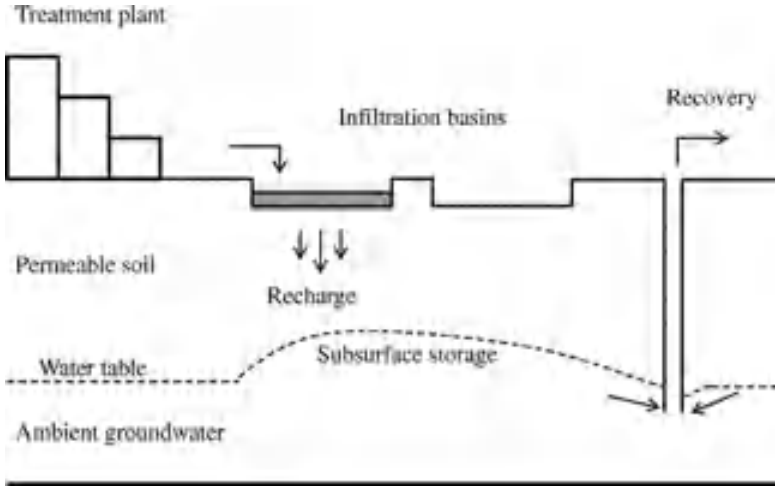

schematic design for SAT system

In line with Kazner et al. (2012), the SAT method is usually employed to additional cleanse and repurpose primary, secondary, or tertiary discharges from wastewater treatment plants (WWTPs). The typical SAT arrangement involves intermittent discharges of effluent from the WWTP, alternately between phases of flooding and drying, to enter specific infiltration basins (Dillon, 2005). The stability of the infiltration rates and aeration of the soil under the SAT basin depend on the periods of wetting and drying (Negev et al., 2020). The effluent includes physical filtration, biodegradation, adsorption, chemical precipitation, ion exchange, and dilution in the vadose zone throughout the SAT procedure to eliminate pollutants (Fox, 2001). Since larger levels of oxygen are needed for biological

treatment in the near-surface layer of the vadose zone, these processes perform best there (Icekson-Tal et al., 2003). The effluent is retrieved using extraction wells from the underlying unconfined aquifer following a residence time that ranges from a few months to a year, in both the unsaturated and saturated zone ((Dillon et al., 2009); (Oren et al., 2007)). As stated by Elkayam et al. (2018), the prolonged residence period guarantees that dangerous organisms are effectively removed, helping to disinfect the effluent. In the end, reclaimed water from SAT is able to be utilized for a variety of things, like groundwater recharging, irrigation for farming and landscaping, recreation, aquaculture, and industrial uses (Huertas et al., 2008).

The aquifer restoration technique known as SAT is used extensively all around the world (Grinshpan et al., 2021). The Dan Regional Reclamation Project (commonly referred to as Shafdan), located in Israel, is one of the biggest wastewater treatment facilities in the whole world. It is accompanied by high-effluent loading SAT establishments that can handle about 120 Mm3 of wastewater annually (Negev et al. (2020); Aharoni et al. (2011); Icekson-Tal et al. (2003)). A number of SAT stations may be found operating in the United States, which involves those in Arizona, California, Colorado, Florida, Massachusetts, Michigan, Montana, New Jersey, New York, and South Dakota (Crites et al. (2014); Sharma and Kennedy (2017)). Other nations have also implemented SAT technology, such as Spain, Belgium, South Africa, and Australia (Escalante et al. (2019); Van Houtte et al. (2012); Tredoux et al. (2012); Dillon et al. (2006)). Since SAT solutions are centered on natural processes and run through the year, they are simple to setup and provide water storage during times of low need and water extraction during times of increased demand (Aharoni et al., 2011). SAT has a number of benefits, involving:

1. Using vadose zone purification can effectively remove organics, nutrients, heavy metals, microbes, and micropollutants from recharged water (Wei et al. (2016); Aharoni et al. (2011)).
2. Creating an effective barrier that takes the place of or supplements other treatment methods, lowering the cost of wastewater treatment and water reusing overall.
3. Protecting coastal aquifers against invasion by seawater.
4. Encouraging the reuse and recycling of water.

Due to its year-round sewage recharge capability, SAT has a distinct advantage over other MAR approaches, which renders it the best option for regions where TWW is dumped into regional streams and rivers or into the ocean (Lu et al., 2012). The purity of the recharged effluent is improved in SAT because recycled water is piped using recovery wells

rather than straight from WWTPs (Bouwer (2000); Negev et al. (2017)). Additionally, it helps achieve public acceptance for environmentally friendly wastewater reuse.

Key Concepts and Principles of SAT system

SAT relies on soil and groundwater's inherent abilities to purge contaminants from wastewater and replenish groundwater supplies. The SAT technique employs mechanical filtration to eliminate suspended particles from the water, as described by Miotliński et al. (2010). Nitrification and denitrification reactions are made possible by the soil within the basin's alternating aerobic and anaerobic environments. It is possible to completely or partially eliminate pathogens, organic and inorganic nitrogen, organic carbon, phosphorus, non-aromatic organic chemicals, and trace metals as a consequence. The elimination procedure can be controlled by adjusting the wetting and drying periods, and the purity of the water at hand is crucial to its success. SAT typically involves the following processes:

- Infiltration: The first step in SAT is the infiltration of wastewater into the soil through a network of infiltration basins, trenches, or other structures. During infiltration, wastewater is distributed over a large area, allowing it to percolate slowly through the soil.
- Filtration: As wastewater moves through the soil, it is filtered by the soil matrix, which removes organic matter, pathogens, and nutrients. Soil particles and microorganisms in the soil act as a natural filter, breaking down and removing pollutants.
- Adsorption: Pollutants that are not removed by filtration can be adsorbed onto the soil particles, reducing their concentration in the wastewater.
- Biodegradation: Soil microorganisms play an important role in the biodegradation of organic matter and nutrients in wastewater. Microorganisms consume the organic matter and convert it into carbon dioxide and water.
- Chemical precipitation: the interaction of naturally occurring minerals in the soil and aquifer with the wastewater, resulting in the formation of insoluble precipitates that can remove pollutants.
- Dilution: After passing through the soil, treated wastewater recharges the underlying aquifer, replenishing groundwater resources.

SAT system benefits

1. Cost-effective: SAT is often less expensive than other water treatment technologies, particularly for small to medium sized communities.
2. Sustainable: SAT systems can be designed to be sustainable by using natural treatment processes and minimizing energy inputs.

3. Water conservation: SAT systems can be used to recharge groundwater aquifers, which can help to sustain water resources and reduce dependence on surface water supplies.
4. Improved water quality: SAT systems can remove a wide range of pollutants from wastewater, including nutrients, pathogens, and organic matter, resulting in improved water quality.
5. Flexibility: SAT systems can be designed to treat a range of wastewater types, from domestic sewage to industrial wastewater.
6. Reuse of water: SAT systems can be used to produce high-quality reclaimed water that can be used for irrigation, industrial processes, and other non-potable uses.
7. Habitat creation: SAT systems can provide habitat for a variety of plants and animals, which can support biodiversity conservation efforts.

SAT system mechanisms, operation, and processes

SAT is an efficient land-based technology used in managed aquifer recharge (MAR) techniques, according to Abel (2014) definition. Enhancing water resources and reducing the uncontrolled discharge of treated effluent into natural water bodies are its main goals. The cleanliness of water noticeably improves as a result of the physical, chemical, and biological processes that wastewater effluent goes through during the SAT operation as it permeates through various soil layers. According to Bdour (2007), SAT is a geo-purification technology in which mostly treated sewage is injected towards the aquifer over the unsaturated zone and finally mixes with the local water. In order to facilitate treated sewage's progressive penetration into the earth and eventual recharging of the aquifers, the SAT technique calls for the regular input of treated effluent into recharge basins. The aforementioned activities further improve the effluent's purity as it moves throughout the soil and aquifer (Miotliński et al., 2010). This comprehensive approach to SAT ensures the reliable restoration and utilization of water resources while minimizing the environmental impact associated with untreated wastewater discharge.

According to the natural wastewater treatment system (Crites et al., 2014), the soil and underlying aquifer have a remarkable capacity to remove contaminants and pathogens as water percolates deeper into the aquifer. This crucial process plays a significant role in minimizing potential health risks during water recovery. To ensure the desired water quality, pre-treatment of wastewater effluent can be conducted before its application in Soil Aquifer Treatment (SAT) systems. This pre-treatment can be tailored to meet regulatory standards or optimize operational efficiency (Abel, 2014). SAT systems offer flexibility in accommodating different wastewater qualities, including primary, secondary, or tertiary effluents. By incorporating appropriate pre-treatment measures, SAT enhances overall water quality and helps mitigate health hazards associated with contaminated water

sources. The combination of natural attenuation processes within the soil and aquifer, along with pre-treatment strategies, contributes to the reliable improvement of water resources in SAT applications.

According to the findings of Abel et al. (2013), an optimal soil for Soil Aquifer Treatment (SAT) systems is one that strikes a balance between high recharge rates (typically found in coarse-textured soils) and effective adsorption and removal of contaminants (commonly associated with fine-textured soils). The selected soil should possess the necessary physical and chemical properties to ensure adequate contaminant removal (Bekele et al., 2013). Therefore, SAT systems are highly site-specific, taking into account the unique characteristics of each location. In addition to soil considerations, the evaluation of SAT feasibility requires a comprehensive assessment that includes the properties of the wastewater effluent and site-specific factors (Sharma and Kennedy, 2017). Taking into account these factors ensures the successful implementation of SAT systems by optimizing contaminant removal and achieving the desired treatment outcomes.

Abel (2014) looked at a number of variables that could affect how well contaminants were removed during Soil Aquifer Treatment (SAT) utilizing main effluent. The preliminary treatment of the main effluent, the hydraulic loading rate, the variety of soil, the wetting and drying cycles, the biological activity, the temperature and redox circumstances, and other parameters were among them. According to the results, pre-treatment simply produced notable elimination rates of 90% for suspended particles, 70% for dissolved organic carbon, and 98% for phosphorus. Because of the longer contact times and improved adsorption processes made possible by lower hydraulic loading rates and the presence of fine soil particles, nitrogen was reduced. E. coli and total coliforms were eliminated through wetting and drying cycles. Temperature and redox conditions were discovered to have an impact on SAT efficiency, with the best elimination of nitrogen occurring around 15 and 25 ^{o}C (89.7% to 99%) and nitrate and phosphate extraction increasing as temperature climbed, highlighting the importance of viscosity in adsorption. It is possible that oxygenation prior to the infiltration procedure, together with wetting and drying cycles, can improve SAT performance. Aerobic circumstances also produced better pollutant clearance. Malolo (2011) further emphasized the connection between temperature and ammonia nitrogen oxidation, with soil-column tests utilizing primary effluent at a temperature of 20°C showing the highest clearance (76%) of ammonia nitrogen. The elimination of phosphorus also turned out to be affected by temperature.

It was demonstrated in a field study by Bekele et al. (2013) that the penetration of secondary treated wastewater via a 9 m-thick limestone vadose zone in a 39-month

managed aquifer recharge (MAR) led to considerable decreases in the mean concentrations of several pollutants. Particularly, the levels of phosphorus, fluoride, iron, and total organic carbon all decreased by more than 30%, 66%, 62%, and 62%, respectively. This demonstrates how well MAR works to clean wastewater and elevate water quality. Furthermore, National Research Council (2012) gives a case study of the nitrogen cycle in the Soil Aquifer Treatment (SAT), where nitrogen is converted quickly to nitrates. Nitrates are very transportable in soils beneath normal circumstances, but they can be eliminated during denitrification in anaerobic environments. Whilst trace metals, with the exception of boron, have been diminished and can precipitate in the soil, particularly under alkaline and aerobic conditions, other substances, like phosphorus, undergo reduction through sorption and precipitation. These results highlight the different ways that SAT can successfully remove impurities and enhance water quality.

The creation of minerals can be aided by microbes during an action termed bio mineralization, according to a research study conducted by Li et al. (2013). Inorganic contaminants, particularly heavy metals, can be effectively immobilized using this method under durable solid states. The principal processes by which microbes precipitate minerals were examined by scientists. Six kinds of bacteria obtained from seedling garden soil that have metal resistance were used in microcosm tests. The potential for these kinds of bacteria to be used in bioremediation led to additional characterization. It was discovered that the bacteria produced the urease enzyme, which was essential for hydrating urea. The pH of the soil rose as a consequence of this enzyme activity, and carbonate formed. As a result, the soluble heavy metal ions in the soil water began to mineralize and eventually turned into carbonates. In order to successfully reduce the amount of heavy metals in polluted soil, the study emphasizes the importance of microorganisms to promote the bio mineralization mechanism.

It was shown in an investigation by Bierlein (2012) that manganese may be efficiently eliminated by granular media filtration utilizing a procedure called as the "natural greensand effect." This process comprises the adsorption of soluble manganese onto a surface covered with manganese oxide (MnOx(s)), which is followed by the oxidation of the manganese by chlorine, which produces more manganese oxide. By taking consideration of the possibility of sorption sites and incorporating the transport and reaction processes inside the porous structure of the MnOx(s), the study aims to enhance the models already in use. The model was able to accurately represent the experimental data and predict the oxidation rate constant, which was the sole variable that needed to be determined, by taking these variables into account. This work emphasizes the significance of comprehending the fundamental mechanisms driving the removal of manganese using granular media filtration

and offers suggestions for enhancing the modeling and optimization of such treatment procedures.

In the study conducted by Goren (2008), the focus was on the aquatic geochemistry of manganese during the interaction between groundwater enriched with organic matter and calcareous-sandstone rocks. The presence of high levels of dissolved organic matter in the groundwater leads to reducing conditions in the aquifer, which are favorable for the reduction and mobilization of manganese. Through column experiments, it was observed that the retardation of manganese is significantly greater compared to other major cations when water flows through sandy sediments under suboxic conditions. The breakthrough behavior of Mn^{2+} is primarily influenced by its adsorption capacity. As a result, higher concentrations of Mn^{2+} in the inflow solution lead to earlier appearance in the outflow solutions and a steeper rise in its breakthrough curve. These findings highlight the complex behavior of manganese during groundwater interactions and emphasize the importance of considering adsorption dynamics for accurate predictions of its transport and fate in aquifers.

The efficiency of natural filtration in reducing nitrogen in wastewater applied to the soil overlaying fractured limestone in the Salento area of Southern Italy was examined in the research carried out by Masciopinto (2007). To determine the effectiveness of this natural filtration mechanism, laboratory experiments and field observations were used. Municipal wastewater effluent from treatment facilities was channeled over a number of fissures in limestone panels in a laboratory environment. The decay rates and constants for nitrogen transformation through natural filtration for both aerated and non-aerated (saturated) soil cracks have been established by tracking the amounts of different wastewater elements over time. The total amount of inorganic nitrogen removed from wastewater pumped into an aquifer in the Nard region in Salento was subsequently estimated using a modeling programmed that included the biodegradation decay rates discovered through laboratory research. The laboratory-derived nitrification and denitrification rates were verified using water samples taken from two monitoring wells situated 320 m and 500 m from the wastewater injecting site, and downstream with regard to groundwater flow.

SAT systems cannot fully replace water treatment processes due to the inherent limitations of removal mechanisms in natural environments. Various factors, which are constantly changing, contribute to the inefficiency of these processes, and not all contaminants can be effectively retained or degraded. According to the National Research Council (2012), the success of SAT systems relies on appropriate management strategies

and regular monitoring, which can help reduce treatment costs. However, the acceptance of such treatment systems by the public is crucial for their implementation. Despite advanced water treatment processes, some communities still perceive recycled water as unpleasant. This perception is not solely based on the extent of water treatment but is influenced by socio-economic, cultural, and religious factors. To address these concerns, education and community programs play a vital role in dispelling misconceptions about the safety and purity of recycled water (Bouwer, 2002). Many areas where there is a shortage of water have not made full use of SAT technology. In order to ensure greater comprehension and acceptance of SAT systems, it is vital to build public outreach initiatives that create a connection between organizations and end users (Abel, 2014).

A managed aquifer recharge (MAR) system will inevitably clog, especially when using an injection and recovery borehole approach like the aquifer storage and recovery (ASR) procedure, as stated by Fernández Escalante (2015). The likelihood of blockage is greater with this approach. Infiltration ponds frequently experience clogging, which is caused by the precipitation of substances, the entrapment of gases in the soil, the development of biofilms from algae, and the buildup and depositing of sediments. In spreading infrastructure, Hutchison et al. (2013) describe the effects of these issues, such as decreased infiltration rates, decreased soil-aquifer treatment efficacy, the requirement for routine maintenance (like basin flow ripping and draining), and, in extreme circumstances, site abandonment. The research of Zaidi et al. (2020), there are four various kinds of clogging: chemical, physical, mechanical, and biological. Chemical clogging occurs by the precipitation of elements and matrix dissolution, physical clogging is triggered by the movement of suspended particles and interstitial fines, and physical clogging is prompted by the attachment of entrained air. Careful monitoring of a number of parameters is required for effective prevention of clogging issues in MAR technologies. One strategy is to manage the injection water's quality, which entails eliminating suspended matter and making sure that the pH and dissolved oxygen levels are suitable. Despite the fact that they might not entirely address clogging caused by microbiological activity, these procedures can help to lower the likelihood of blockage. Additionally, the length of ponding intervals must be taken into account because long intervals might worsen soil blockage. However, by maintaining soil structure stability and limiting excessive organic matter buildup, wetting and drying cycles may assist to attenuate the consequences of clogging barriers (Hutchison et al., 2013).

Soil Aquifer Treatment (SAT) is an environmentally sustainable method for wastewater treatment and groundwater replenishment (Manisha et al., 2023). SAT relies on physical, chemical, and biological processes within soil, acting as a natural contaminant filter

(Sharma and Kennedy, 2017). The performance of SAT varies with the soil type used (Goren et al., 2014). Soil type is critical for efficient removal of pollutants, including suspended solids, nutrients, organic compounds, and pathogens (Abel, 2014). Different soil types have unique physical and chemical characteristics influencing pollutant removal processes (Gharbia et al., 2016). The performance of SAT systems is significantly influenced by different soil types and structures (Fichtner et al., 2019). Various factors related to soil characteristics, such as hydraulic conductivity, pore size distribution, porosity, soil organic matter (SOM), soil cation exchange capacity (CEC), adsorption and ion exchange capacities, biological activity, nutrient retention, and redox conditions, have a profound impact on treatment efficiency and overall SAT effectiveness (Al-Kaisi et al., 2017). Soil types exhibit variations in porosity and pore size, affecting water movement and contaminant behavior in the soil. Coarse-grained soils, with larger pores and higher porosity, facilitate better water movement, flow, but with reduce treatment efficiency based on reduce the retention and reaction time, while fine-grained soils, with smaller pores and lower porosity, may hinder water movement but increase treatment effectiveness (Zachara et al., 2016). Additionally, soil types with higher hydraulic conductivity, such as coarse-grained soils like sands and gravels, enable faster and more efficient wastewater infiltration, ensuring proper distribution and contact with the soil matrix (Gill et al., 2023).

Soils rich in clay minerals and organic matter have higher adsorption capacities, effectively binding and removing contaminants from wastewater, acting as natural filters, and improving water quality through adsorption and ion exchange processes (Kennedy et al., 2018). Organic matter in the soil promotes biological activity, facilitating microbial degradation of contaminants, particularly in soils with higher organic matter content, enhancing SAT system treatment efficiency (Kebede et al., 2021). Different soil types vary in their nutrient retention capacities, allowing effective removal of nutrients like nitrogen and phosphorus, which is vital for preventing groundwater contamination and maintaining ecological balance (Bento et al., 2019). Soil types can also influence redox conditions within SAT systems; well-drained soils promote aerobic conditions, while poorly drained soils create anaerobic conditions, affecting processes like denitrification for nitrogen compound removal (Ben Moshe et al., 2020). Soil characteristics, including hydraulic conductivity, adsorption capacity, biological activity, nutrient retention, porosity, pore size distribution, soil organic matter content (SOM), cation exchange capacity (CEC), and redox conditions, is essential for designing an effective SAT systems that safeguard groundwater quality (Russo et al., 2022).

Soil aquifer treatment (SAT) system is a widely recognized and sustainable approach for wastewater treatment and groundwater recharge (Gharbia et al., 2016). SAT relies on

natural soil processes to remove contaminants before they reach the aquifer (Candela et al., 2007). The infiltration rate, which determines the speed at which water penetrates the soil, significantly influences SAT systems performance, impacting the fate, transport, removal, and behavior of contaminants in the soil (Nadav et al., 2012). Additionally, the choice of infiltration rate depends on the hydraulic conductivity, porosity and permeability of filtrate media, affects the distribution and movement of contaminants in the system (Ewen et al., 2000). The infiltration rate indeed affects hydraulic conductivity, residence time, and the potential for preferential flow, all of which can influence the fate and transport of contaminants in soil media. With higher rates increasing conductivity and allowing faster water and contaminant flow. This may reduce contact time between contaminants and soil particles, potentially decreasing removal efficiencies. Conversely, lower flow rates encourage better contact and retention within the soil matrix, enhancing pollutant removal (Konstantinou and Biscontin, 2022). Flow rates also affect preferential flow and bypassing. Higher rates can create paths of least resistance, potentially allowing contaminants to bypass much of the soil, reducing removal effectiveness. Lower rates minimize preferential flow, ensuring a more uniform distribution of water and contaminants throughout the soil, enhancing pollutant removal opportunities (Ritsema and Dekker, 2000).

The fate and transport of contaminants in soil aquifer treatment systems are complex processes influenced by several factors, with the infiltration rate playing a key role (Arye et al., 2011). This infiltration rate determines the hydraulic loading and residence time within the soil (Van Cuyk et al., 2001), where higher infiltration rates increase hydraulic loading and reduce contact time with contaminants, while lower rates facilitate longer interactions (Pavelic et al., 2011). Consequently, the infiltration rate directly affects the extent of contaminant removal through processes like adsorption, desorption, precipitation, and microbial degradation (Gavrić et al., 2019). Different infiltration rates lead to distinct patterns of contaminant migration, infiltration depth, and potential leaching into the underlying aquifer (Gao et al., 2019b). Higher infiltration rates may induce faster vertical movement through preferential pathways, whereas lower rates encourage lateral spreading within the soil matrix (Hendrickx and Flury, 2001). The infiltration rate's critical role in determining the spatial distribution and extent of contaminant plumes significantly impacts overall treatment performance and potential risks to groundwater quality (Mukherjee et al., 2015). Also, infiltration rate significantly affects SAT system performance by altering residence time, which is the duration wastewater remains in contact with the soil media. Higher infiltration rates lead to shorter residence times, while lower rates extend contact times with the soil matrix. Longer residence times facilitate greater interaction between contaminants and soil particles, enhancing the potential for pollutant removal through physical, chemical, and

biological processes from filtration, adsorption, and microbial degradation activity (Essandoh et al., 2011). Additionally, higher infiltration rates may reduce contact time between contaminants and soil particles, limiting effective filtration and adsorption, while lower flow rates provide more time for these processes, increasing pollutant removal (Keesstra et al., 2012). Also, lower rates favor microbial growth and activity, enhancing pollutant degradation, whereas higher rates may hinder microbial activity due to limited contact time and nutrient availability (Guillemoto et al., 2022).

Soil aquifer treatment (SAT) systems are widely used for the treatment of wastewater, providing a natural and sustainable approach for pollutant removal before water is recharged into aquifers or reused for various purposes (Page et al., 2018). In these systems, the physical, chemical, and biological processes occurring in the soil matrix and aquifer play a crucial role in the transformation and removal of pollutants (Gharbia et al., 2016). Among the various factors that influence pollutant behavior in SAT systems, the dynamics of drying and wetting cycles have been recognized as important drivers of pollutant fate and transport (Turkeltaub et al., 2022). Understanding the effect of drying and wetting on the performance of synthetic wastewater pollutants in SAT systems is essential for optimizing system design, operation, and pollutant removal efficiency (Gharbia et al., 2024).

Drying and wetting cycles can induce the movement and redistribution of pollutants within the soil aquifer system (Morrison et al., 2020). During wetting, water infiltrates the soil, carrying pollutants deeper into the subsurface. The extent of pollutant migration depends on their solubility, sorption affinity, and the hydraulic properties of the soil (Ben Moshe et al., 2020). Conversely, during drying, water evaporates from the soil surface, potentially leading to pollutant accumulation near the surface or at specific soil horizons. This redistribution of pollutants can have implications for their long-term fate and persistence in the system (Sharma and Kennedy, 2017).

Moreover, the alternation of drying and wetting cycles creates dynamic conditions that can influence microbial activity and the biodegradation of pollutants (Essandoh et al., 2013). Wetting events provide favorable conditions for microbial growth, promoting the activity of microorganisms involved in pollutant degradation and transformation processes (Pavelic et al., 2011). The presence of moisture enhances the availability of dissolved oxygen, facilitating aerobic degradation pathways. Conversely, drying periods can limit microbial activity due to reduced moisture and oxygen availability, potentially leading to a decrease in pollutant degradation rates (Zhang et al., 2015). Furthermore, the transition from aerobic to anaerobic conditions during drying may promote different types of pollutant

transformations, such as anaerobic degradation or chemical reduction processes (Xiao et al., 2017). Drying and wetting cycles affect the availability of oxygen within the soil aquifer system, influencing the type and rate of pollutant degradation (Elkayam et al., 2018). During wetting, oxygen is replenished as water infiltrates the soil, allowing aerobic microbial degradation processes to occur. Adequate oxygen supply supports the activity of aerobic microorganisms responsible for the breakdown of organic pollutants (Kumar et al., 2018). In contrast, drying periods reduce oxygen availability in the soil, leading to anaerobic or microaerobic conditions. Under anaerobic conditions, different microbial communities may thrive, leading to distinct pollutant degradation pathways (Mienis and Arye, 2018). The transition between aerobic and anaerobic conditions during drying and wetting cycles can impact the overall efficiency of pollutant removal.

Furthermore, drying and wetting cycles can significantly influence the physical properties of the soil, including its structure, porosity, and hydraulic conductivity (Fichtner et al., 2019). Extended drying periods can lead to soil compaction, shrinkage, and the development of cracks. These changes in soil structure can have consequences for water movement and pollutant transport within the system. Compacted soils may exhibit reduced hydraulic conductivity, hindering water infiltration and potentially creating preferential flow paths for pollutants (Gao et al., 2019a). In contrast, wetting events can help restore soil structure and porosity, improving water infiltration and enhancing treatment efficiency (de Rozari, 2020). Likewise, drying and wetting cycles can affect the adsorption and desorption of pollutants onto soil particles (Gharbia et al., 2022). During wetting, pollutants may be adsorbed onto soil surfaces, reducing their mobility and enhancing their retention within the system. The presence of water films on soil particles provides sites for pollutant sorption and contributes to their removal (Russo et al., 2022). In contrast, drying periods can promote desorption processes, releasing previously adsorbed pollutants back into the aqueous phase and potentially increasing their mobility. Desorption during drying events can result from changes in soil moisture, pH, and the availability of competing ions (Dillon et al., 2022).

The cycling of wetting and drying can influence the leaching and transport of pollutants within the soil aquifer system (Trussell et al., 2018). Wetting events can mobilize pollutants, increasing the potential for downward transport and leaching into the groundwater (Gharbia et al., 2024). The degree of leaching depends on pollutant solubility, sorption affinity, and the soil's hydraulic properties (Dahlke et al., 2018). In contrast, drying periods may reduce leaching by promoting pollutant retention within the soil matrix. The establishment of preferential flow paths, such as cracks or macropores, during drying events can further impact pollutant transport, bypassing the treatment zone and potentially compromising system efficiency (Pan et al., 2017).

Annex (2): Confidence intervals analysis for the experimental replications

All experimental investigations were repeated three times to enhance the accuracy of the results. Confidence intervals were employed to compare the experimental replications, with the highest confidence interval selected for analysis, as it represents the highest level of accuracy.

Chapter (3) Comparative investigation and performance evaluation of different soil types in enhancing pollutants removal from synthetic wastewater in soil aquifer treatment system

- The static batch test investigations for sand and sandy loam
    1. Sand soil

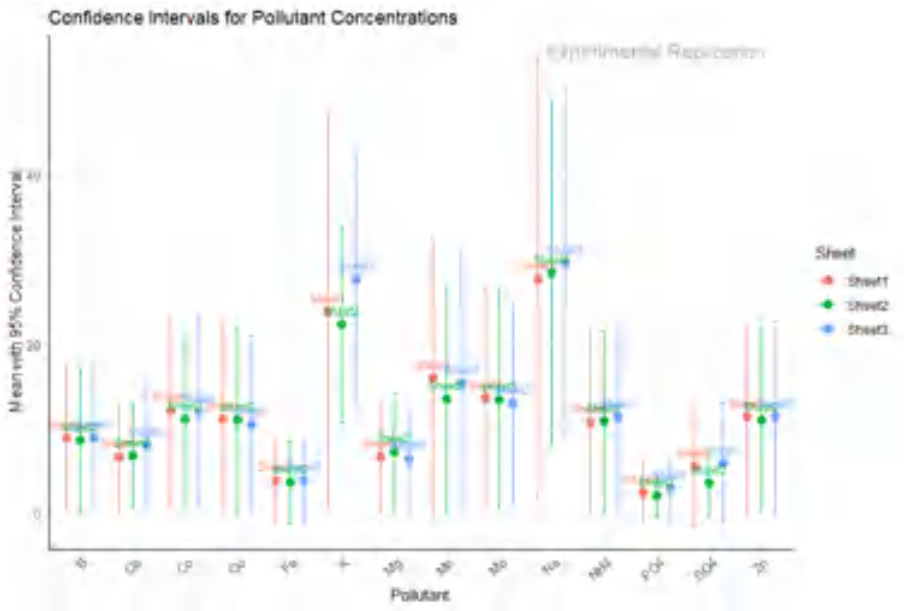

The best experimental replication with high mean and lower confidence interval is the experimental replication 3.

2. Sandy loam soil

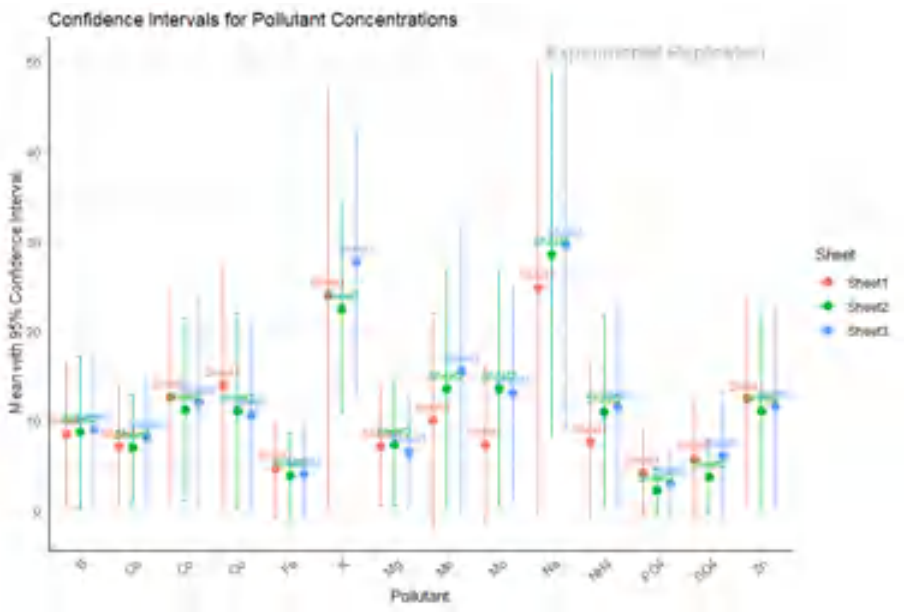

The best experimental replication with high mean and lower confidence interval is the experimental replication 2.

- The dynamic breakthrough column investigations for sand and sandy loam
    1. Sand

The best experimental replication with high mean and lower confidence interval is the experimental replication 1.

2. Sandy loam soil

The best experimental replication with high mean and lower confidence interval is the experimental replication 1.

Chapter (4) Understanding the Role of Infiltration Rate on Contaminants Fate and Transport in Soil Aquifer Treatment System: Experimental, Modeling, and Statistical Analysis Approaches

- Low infiltration rate (0.50 mL/min) through sand column

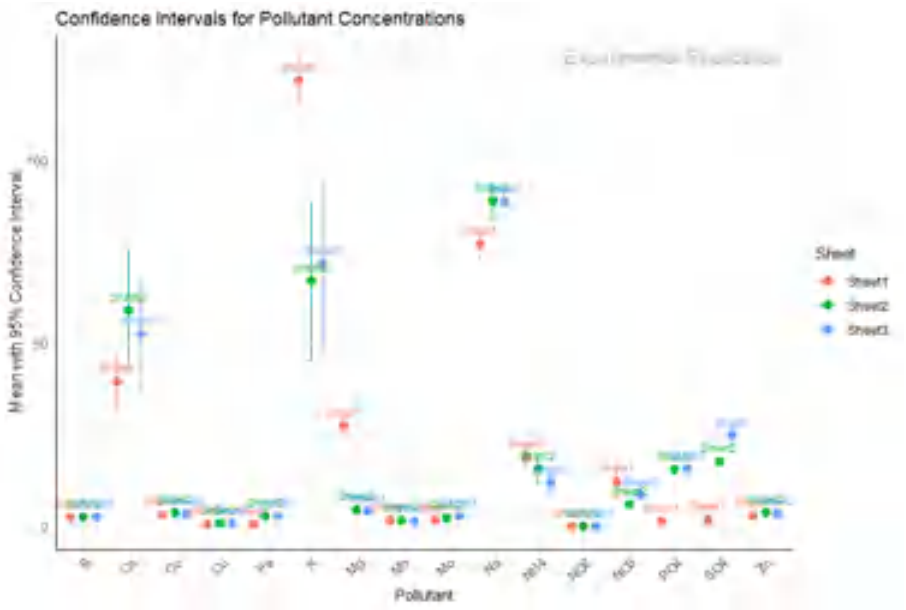

The best experimental replication with high mean and lower confidence interval is the experimental replication 1.

- High infiltration rate (10 mL/min) through sand column

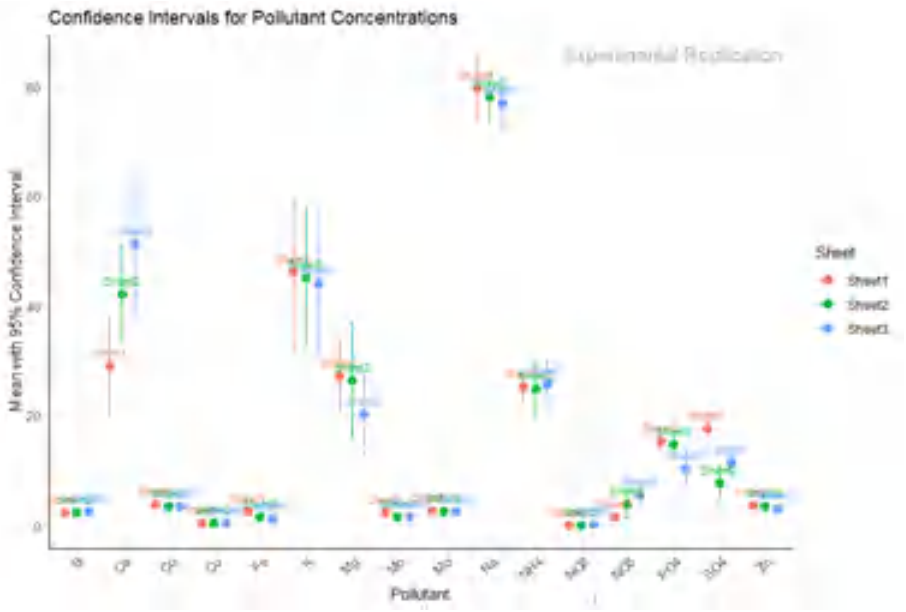

The best experimental replication with high mean and lower confidence interval is the experimental replication 1.

Chapter (5) Quantifying the influence of dynamic pulsed of wetting and drying on the transformation and fate of synthetic wastewater pollutants in soil aquifer treatment system

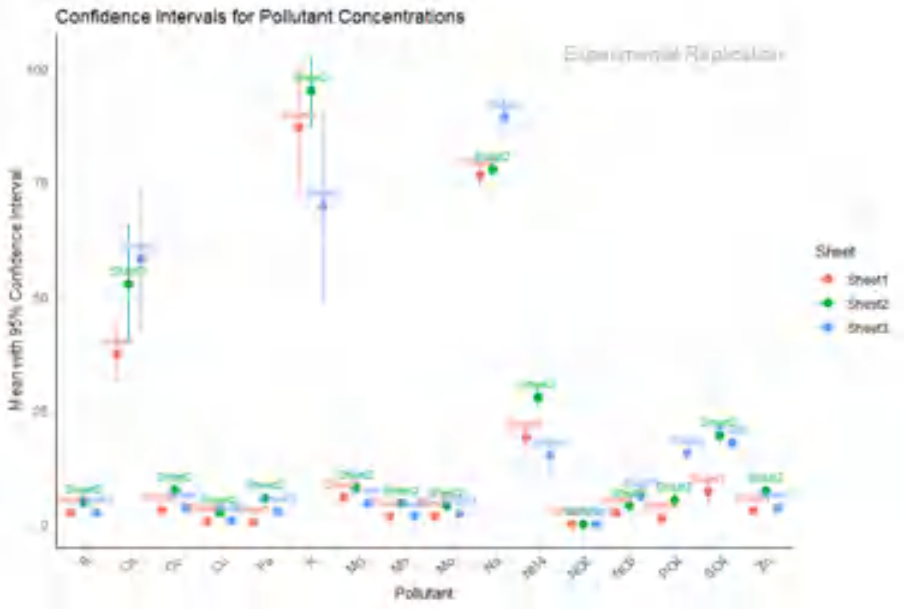

The best experimental replication with high mean and lower confidence interval is the experimental replication 2.

Chapter (6) Synergistic and Competitive Pollutant Interactions in SAT System: Impact of Synthetic Wastewater Chemical Variability

- Low concentrations level through sand column

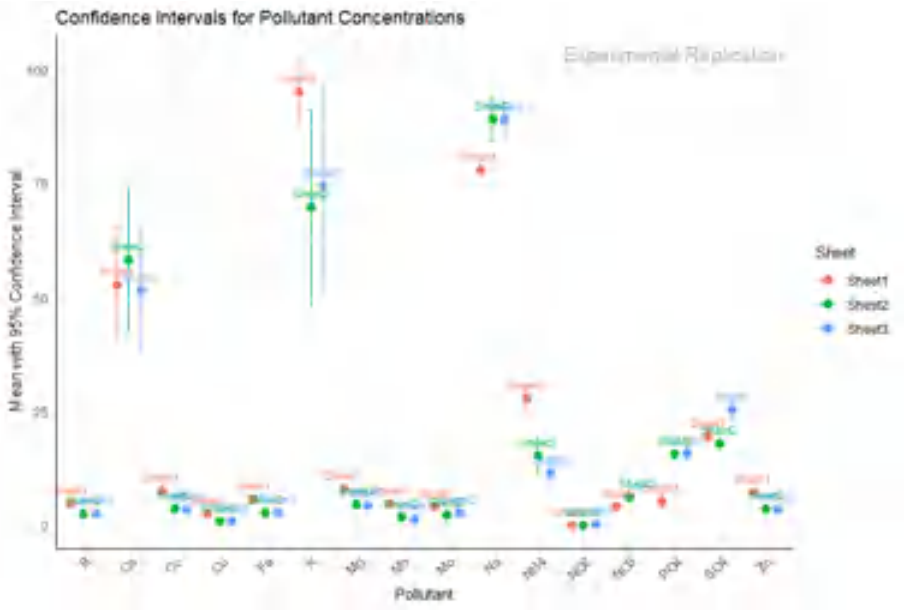

The best experimental replication with high mean and lower confidence interval is the experimental replication 1.

- High concentrations level through sand column

The best experimental replication with high mean and lower confidence interval is the experimental replication 1.

Annex (3): Spatial concentration simulation through sand column under different infiltration rate (0.50 – 10) mL/min

The Figure shows how well the model aligns with the experimental data. The Root Mean Square (RMS) values are used to quantify the differences between the two sets of curves. Lower RMS values indicate a closer match between the model and experimental data, indicating higher predictive accuracy. The calibration of synthetic wastewater pollutants under a 0.5 mL/min infiltration flow rate demonstrates a high level of agreement between the model and experimental observations. The RMS values, all below 0.50 for every pollutant, signify a close match between the modeled and experimental values, indicating accurate representation of pollutant behavior under the specified infiltration rate. This close alignment confirms the model's capability to predict pollutant concentrations accurately over time and depth with assures that model parameters and assumptions have been appropriately adjusted. This level of calibration instills confidence in the model's ability to simulate and predict pollutant transport in the SAT scenarios with similar infiltration rates.

Calibration curves for modeling pollutants breakthrough under 0.50 mL/min rate

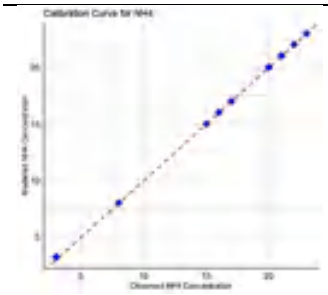	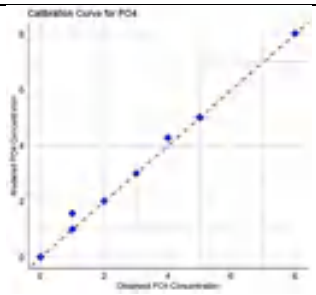	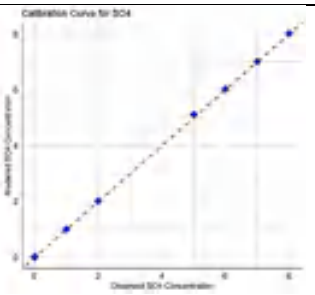	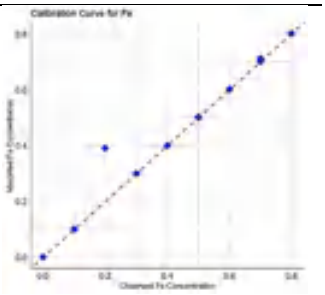
NH_4^+ - RMS = 0.062	PO_4^{3-} - RMS = 0.27	SO_4^{2-} - RMS = 0.10	Fe^{2+} - RMS = 0.19
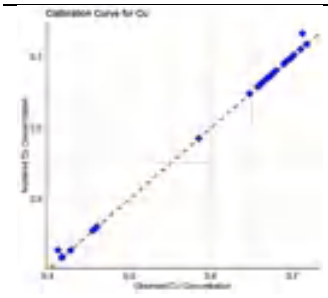	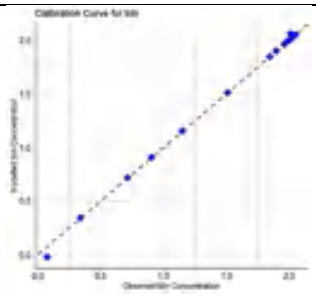	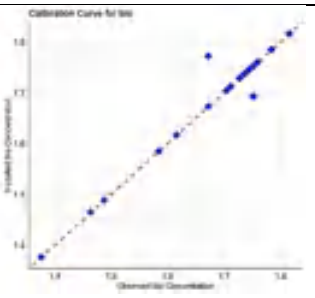	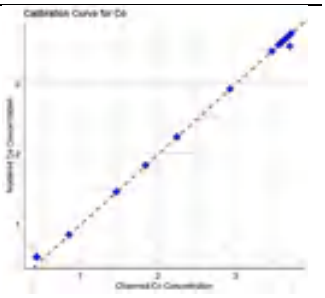
Cu^{2+} - RMS = 0.03	Mn^{2+} - RMS = 0.005	MoO_4^{2-} - RMS = 0.06	Co^{2+} - RMS = 0.16
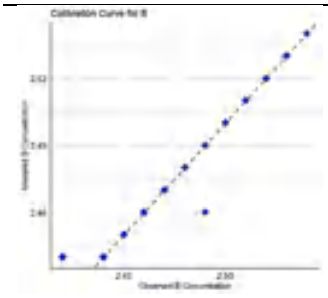	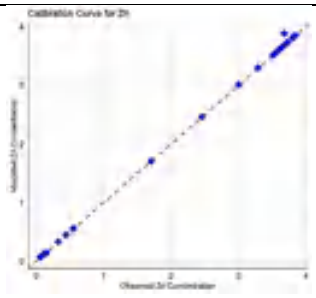		
BO_3^{3-} - RMS = 0.03	Zn^{2+} - RMS = 0.05		

Simulation results for spatial concentration distributions and changes in pollutant concentrations within the column depth at the calibrated 0.50 mL/min infiltration rate. These simulations offer valuable insights into how pollutant concentrations are distributed and vary within the sand media. Concentration gradients are observed, with higher levels near the inflow boundary and lower levels near the outflow boundary. The specific concentration profiles depend on pollutant characteristics and their interactions with the sand media. Additionally, these simulations depict how pollutant concentrations change as they pass through the sand media, capturing dynamic behaviors involving adsorption, dispersion, and decay processes. This information is crucial for comprehending how pollutants move and change within the SAT systems.

Pollutants spatial concentration over the column depth under 0.50 mL/min rate

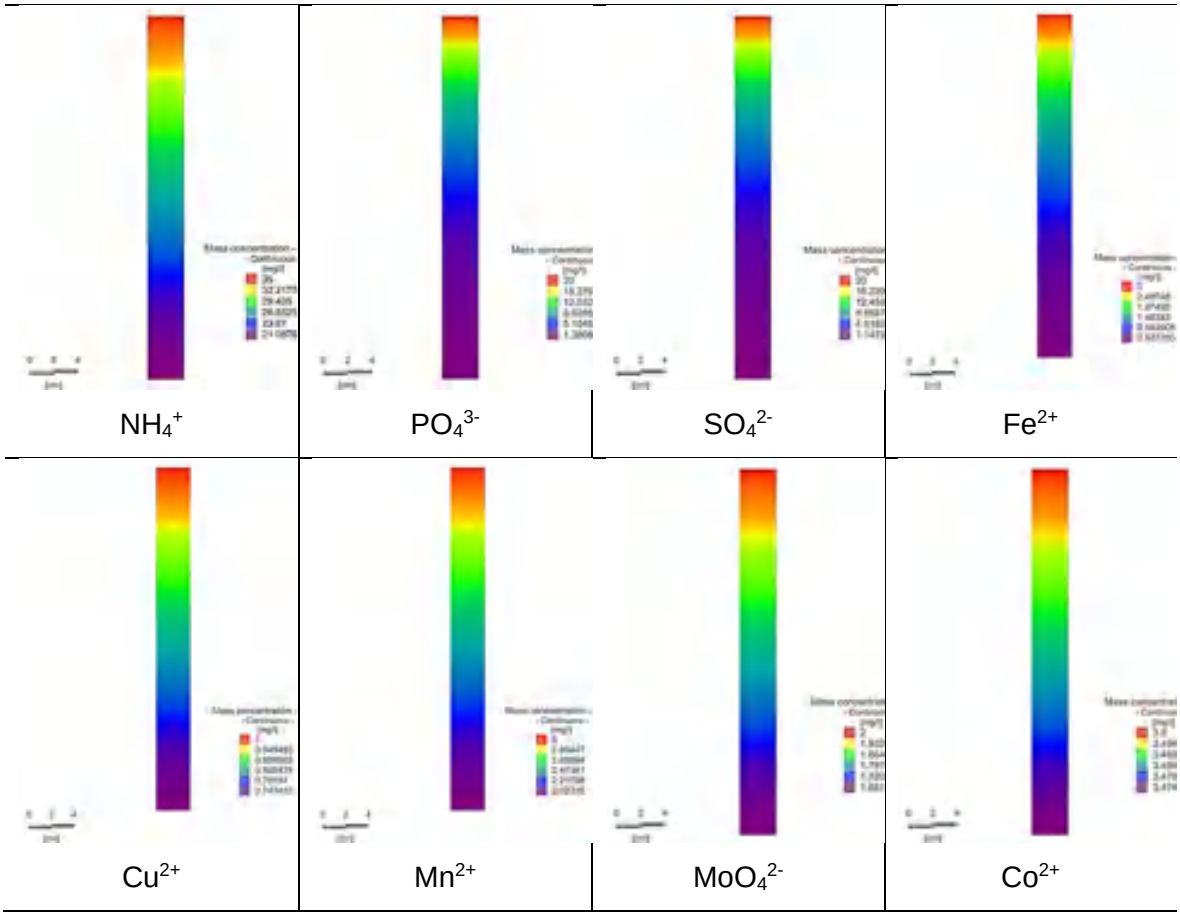

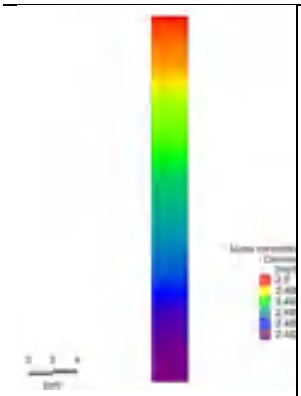	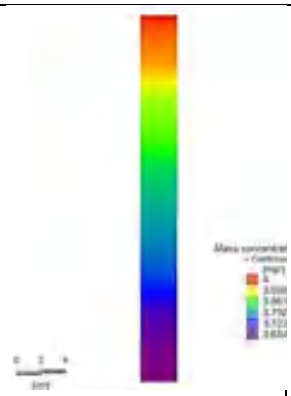		
BO_3^{3-}	Zn^{2+}		

The simulation results, including spatial concentration distributions and changes in pollutant concentrations across the column depth, under the accepted level of calibration for the 10 mL/min infiltration rate.

In figure of the calibration curves and the Root Mean Square (RMS) values for each pollutant are presented.

Calibration curves for modeling pollutants breakthrough under 10 mL/min rate

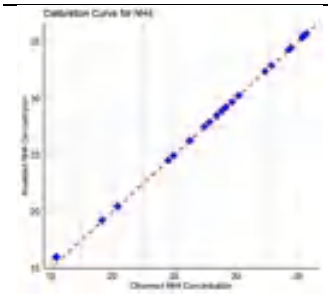	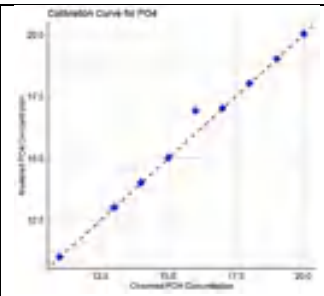	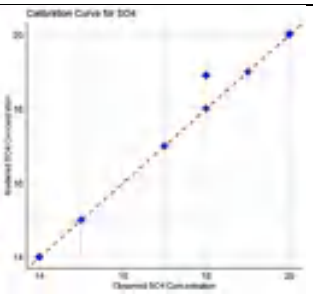	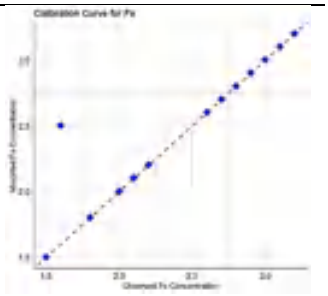
NH_4^+ - RMS = 0.001	PO_4^{3-} - RMS = 0.02	SO_4^{2-} - RMS = 0.03	Fe^{2+} - RMS = 0.02
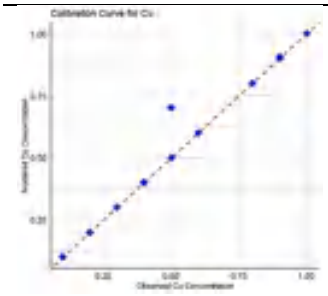	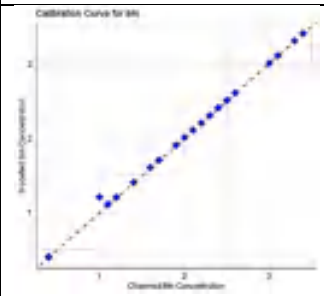	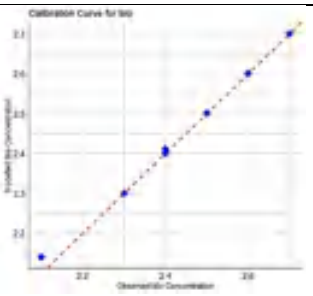	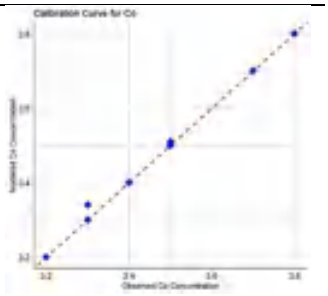
Cu^{2+} - RMS = 0.06	Mn^{2+} - RMS = 0.01	MoO_4^{2-} - RMS = 0.013	Co^{2+} - RMS = 0.014
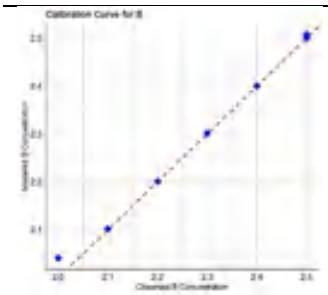	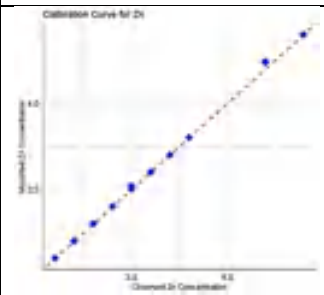		
BO_3^{3-} - RMS = 0.007	Zn^{2+} - RMS = 0.013		

Pollutants spatial concentration over the column depth under 10 mL/min rate

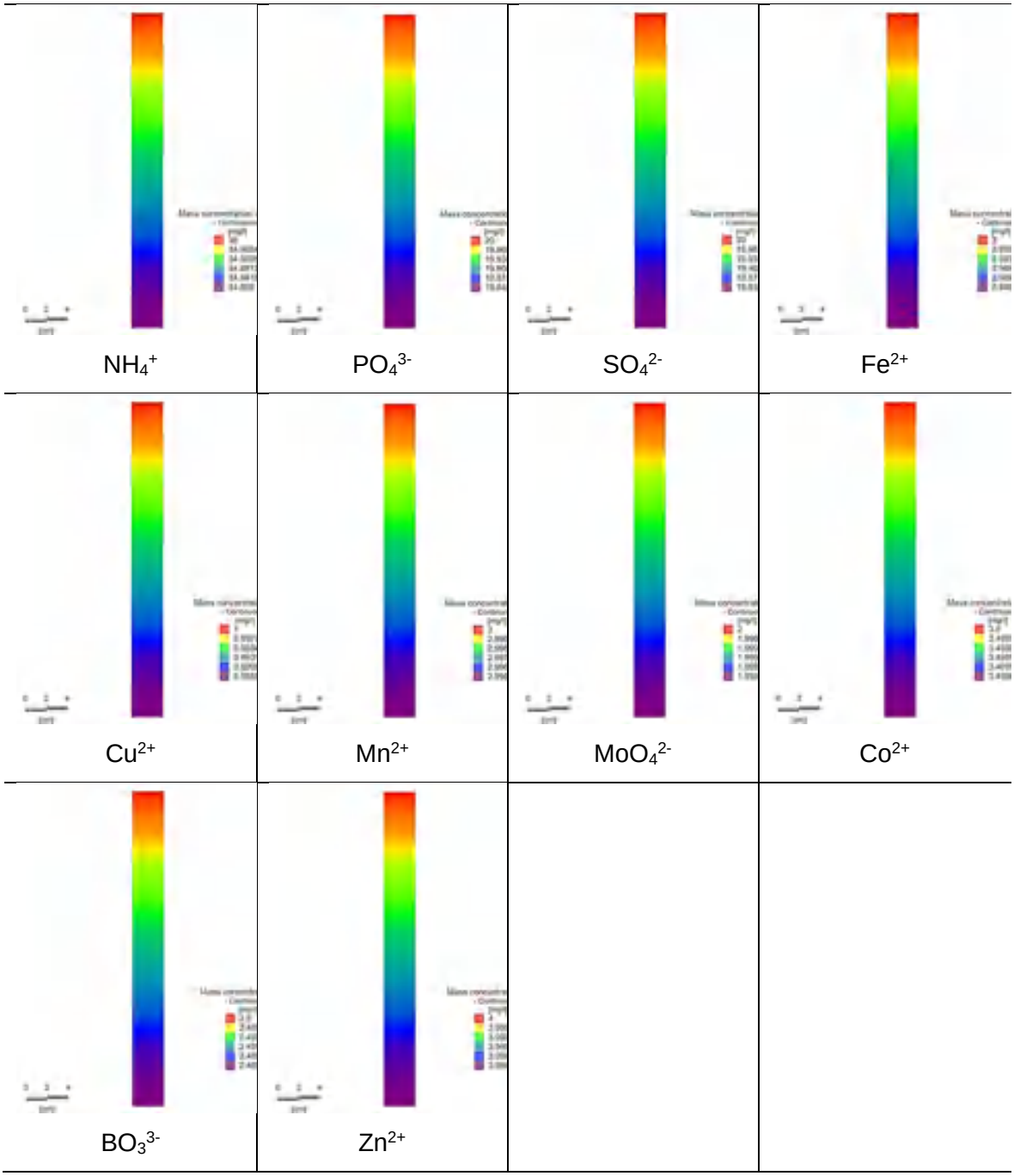

NH_4^+ PO_4^{3-} SO_4^{2-} Fe^{2+}

Cu^{2+} Mn^{2+} MoO_4^{2-} Co^{2+}

BO_3^{3-} Zn^{2+}